

An investigation of respiratory abnormalities in a male and female mouse
model of Rett Syndrome

Emma Grace Brockett
BSc (Hons)

A Thesis submitted in fulfilment of the requirements for the degree of Doctor of Philosophy to
the Institute of Neuroscience and Psychology, College of Medical, Veterinary and Life
Sciences, University of Glasgow, October 2012

Wellcome Surgical Institute, University of Glasgow,
Garscube Estate, Bearsden Road,
Glasgow, UK, G61 1QH



University
of Glasgow

Abstract

Rett Syndrome (RTT) is a severe neurodevelopmental disorder affecting 1 in 10,000 girls and is often associated with respiratory abnormalities. RTT is almost exclusively caused by loss-of-function mutations in the human *MECP2* gene. It remains unknown as to whether the respiratory abnormalities seen in RTT patients and MeCP2 deficient animals may be due to problems with respiratory rhythmogenesis or the result of an inappropriate chemosensitive response. The main aim of this thesis was to investigate the respiratory abnormalities presented in a male and female mouse model of RTT syndrome.

In a male mouse model, the endogenous *Mecp2* gene was silenced by insertion of a Lox-Stop cassette, which mimicked a number of RTT symptoms, including disordered breathing (Guy *et al.*, 2007). The *Mecp2* gene was reactivated by Tamoxifen(TM)-induced deletion of the Lox-Stop cassette. As such, the progression and development of respiratory disturbances were monitored in the early stages of MeCP2 deficiency and also assessed during and after gene reactivation. Respiratory parameters were recorded using whole body plethysmography, a non-invasive method of recording respiratory behaviour. Compared to WT, MeCP2 deficient male mice had an increased respiratory frequency and increased number of sighs prior to gene reactivation. The fact that animals were still viable suggests that neuronal development can occur in the absence of MeCP2, but signs of respiratory instability e.g. the increased number of sighs, indicate that MeCP2 may be required for neuronal maturation as the animal develops. Gene reactivation reduced respiratory frequency and the number of sighs in MeCP2 deficient mice to a level comparable with WT suggesting that TM-induced activation of *Mecp2* can reverse some of the respiratory abnormalities.

Since RTT syndrome is a predominantly female based disorder it was of benefit to observe the progression of the respiratory phenotype in a female model. Female mice which were heterozygous for the *Mecp2*-null mutation were also studied using plethysmography. It was observed that at 23 wks of age, following a period of normal development, the *Mecp2*^{+/-} mice began to display an increased number of respiratory abnormalities compared to WT animals which

suggested an inability of the respiratory network to maintain optimal function. Also, the respiratory response to hypoxia was significantly greater in *Mecp2*^{+/-} mice compared to WT, yet the hypercapnic response of the two genotypes was comparable. This indicates that the response to hypoxia and hypercapnia are mediated by two different mechanisms and that the hypoxic response may be affected by a reduction in the level of MeCP2.

Neuromodulators such as noradrenaline and serotonin are important in modulation of the respiratory pattern and the chemosensitive response. Previous research has implicated changes in bioamine content in the pathophysiology of RTT patients and MeCP2 deficient animals (Riederer *et al.*, 1985; Ide *et al.*, 2005; Viemari *et al.*, 2005; Roux *et al.*, 2010) Thus, cells expressing tyrosine hydroxylase (TH), a marker for noradrenergic cells, and cells expressing 5-HT were quantified in the brainstems of MeCP2 deficient male mice to observe how the absence and subsequent reactivation of *Mecp2* may affect noradrenergic and serotonergic cell number. Compared to WT, MeCP2 deficient mice exhibited a trend towards a decrease in the number of TH and 5-HT expressing cells in various noradrenergic and serotonergic regions of the brainstem, which may account for the development of the respiratory abnormalities in the mutant mice. It was also found that reactivation of *Mecp2* did not restore the number of MeCP2 expressing cells to WT level. MeCP2 was often found to be co-expressed with 5-HT and TH, yet many MeCP2 positive neurons were not found to be 5-HT or TH positive indicating that these MeCP2 expressing neurons may be co-localised with another as yet unidentified neuromodulator. Interestingly, reactivation of *Mecp2* appeared to occur at a greater rate in noradrenergic TH expressing neurons than 5-HT expressing neurons.

Whilst studying MeCP2 deficient male mice it was noted that some of the mutant animals began to develop rale-like rattling within the chest and also began to foam at the mouth. Much of the research in RTT syndrome focuses on the neurological aspect, whereas this phenotype indicated a problem within the lungs. Lungs of WT and MeCP2 deficient mice were removed and processed with various histological stains to highlight various aspects of the lung morphology. Comparison of WT and MeCP2 deficient tissue revealed that there was a trend towards an increase in the amount of elastin surrounding airways and an increase in the thickness of the interalveolar septum in MeCP2 deficient mice

compared to WT. An increase in interalveolar septum may interfere with ventilation and may account for the increased occurrence of sighing observed in the male MeCP2 deficient mice. These morphological changes in the lung may indicate that the respiratory abnormalities of RTT may not be solely neurological. Since changes in the morphology of the lung were clearly present in the male with evidence of increased elastin deposits surrounding the airways, investigation into the presence of pulmonary arterial hypertension (PAH) was carried out in the female model. Results indicated that there was a trend towards a higher right ventricular pressure in *Mecp2*^{+/-} animals compared to WT, along with a trend towards right ventricular hypertrophy, indices of the presence of PAH.

In conclusion, *Mecp2* has been shown *in vivo* to be involved in both the development and maintenance of neurons involved in the respiratory network, both neuromodulatory and chemosensitive, and the absence or reduction of MeCP2 is also proposed to have a novel role in the development of lung pathology in MeCP2 deficient mice.

Contents

Title Page	
Abstract	ii
Contents	v
List of Tables.....	xi
List of Figures.....	xii
List of Figures.....	xii
Acknowledgements.....	xvii
Author's Declaration	xviii
Abbreviations page	xx
Chapter 1: Introduction	28
1.1 Why Breathing is Essential	29
1.2 History of the Study of Involuntary Control	29
1.3 Location of Respiratory Neurons	31
1.4 Modulation of Respiration by Neurotransmitters	33
1.4.1 Serotonin	33
1.4.2 Noradrenaline and Dopamine	35
1.4.3 Opiates	36
1.4.4 Substance P	37
1.5 Rhythmic Breathing	37
1.6 Areas of Rhythm Generation	39
1.6.1 The Pre-Bötzinger Complex	39
1.6.2 Parafacial Respiratory Group/RTN	41
1.7 Chemosensitivity	44
1.7.1 Central Chemoreception	44
1.7.2 The Specialised and Distributed Theories of Central Chemoreception	46
1.7.3 Peripheral Chemoreception	47
1.8 Rett Syndrome.....	48
1.8.1 Genes Involved in Development of the Rett Phenotype.....	49
1.9 MECP2.....	49
1.9.1 Expression of Mecp2	51
1.9.2 MeCP2 in Development.....	51
1.9.3 Mutations of Mecp2	52
1.9.4 Animal Models of Dysfunctional Mecp2	53

1.10 Respiratory Phenotype in RTT	55
1.11 Neuromodulation and Chemosensitivity in RTT	56
1.11.1 Noradrenaline	56
1.11.2 5-HT	57
1.11.2 Brain Derived Neurotrophic Factor (BDNF)	58
1.11.3 GABA and Glutamate.....	60
1.11.4 Substance P.....	61
1.12 Mecp2 in the Periphery	61
1.13 Aims of the Thesis	62
Chapter 2: General Methods	63
2.1 Mouse models.....	64
2.1.1 Male Mouse Model.....	64
2.1.2 Female Mouse Model.....	64
2.2 Behavioural Scoring.....	65
2.3 Tamoxifen Treatment of Male Mice	68
2.4 Plethysmography	68
2.4.1 The Plethysmographic Chambers	68
2.4.2 Respiratory Analysis	71
2.6 Tissue Fixation.....	72
2.6.1 Perfusion	72
2.6.2 Paraffin Processing	73
2.7Cutting.....	74
2.7.1 Cryostat Sections.....	74
2.7.2 Microtome.....	74
2.8 Brain ICC.....	75
2.8.1 Brain Imaging and Cell counting	77
2.9 Lung Immunocytochemistry	78
2.10 Lung IHC.....	79
2.10.1 3, 3'-Diaminobenzidine (DAB) Reaction	79
2.10.2 Haematoxylin & Eosin.....	81
2.10.3 Miller's Elastin	81
2.10.4 PAS/HA (Periodic Acid, Schiff's/Haematoxylin & Aurantia).....	82
2.10.5 Masson's Trichrome Stain	82
2.10.6 Lung Imaging and Measurements	82
2.11 Pulmonary Arterial Hypertension (PAH) Analysis.....	85

2.11.1 Measurement of Right Ventricular Pressure and Systemic Pressure..	85
2.11.2 Assessing Right Ventricular Hypertrophy	85
2.11.3 Measurement of Remodelling of Small Blood Vessels	86
2.11 Statistics	86
2.11.1 Male Respiratory Data (chapter3)	86
2.11.2 Female Respiratory Data (chapter 6)	86
2.11.3 Brain ICC (chapter 4).....	86
2.11.4 Lung ICC (chapter 5)	87
2.11.5 PAH Anaylsis (chapter 6)	87
Chapter 3: Respiratory patterns of the male MeCP2 deficient mouse model.	88
3.1 Introduction	89
3.2 METHODS	91
3.2.1 Male Mouse Model.....	91
3.2.2 N numbers.....	91
3.2.3 Behavioural Scoring.....	92
3.2.4 Tamoxifen Treatment	92
3.2.5 Respiratory Measurements.....	93
3.2.6 Analysis	94
3.3 RESULTS	95
3.3.1 Behavioural Scoring.....	95
3.3.2 Raw Respiratory Traces	97
3.3.3 Respiratory Frequency	102
3.3.4 Response to Hypercapnia	106
3.3.5 Sighing	112
3.3.6 Double Breaths	117
3.3.7 Apneas	121
3.4 Discussion	123
3.4.1 Experimental Issues	123
3.4.1.1 The Male Mouse Model and Variability	123
3.4.1 Respiratory Frequency and Rhythm	124
3.4.2 Chemoreception.....	126
3.4.3 Sighing	128
3.4.4 Double Breaths	130
3.4.5 Apnea	131

Chapter 4: Immunocytochemistry (ICC) of respiratory rhythm generators and sites of neuromodulation in male mouse brain	133
4.1 Introduction.....	134
4.1.1 Rhythm Generation, Chemosensitivity and Neuromodulation	135
4.1.2 The Role of Noradrenaline (NA).....	137
4.1.3 The Role of Serotonin (5-HT).....	139
4.2 Methods.....	140
4.2.1 Fixation.....	140
4.2.2 Imaging and Quantification of TH Expressing Neurons	141
4.2.3 Imaging and Quantification of 5-HT Expressing Neurons	148
4.2.4 Imaging and Quantification of NK1 Expressing Neurons	157
4.2.5 Imaging and Quantification of Phox2b Expressing Neurons	161
4.3 Results	165
4.3.1 Tyrosine Hydroxylase (TH).....	165
4.3.2 Serotonin (5-HT)	167
4.3.3 Neurokinin-1 (NK1).....	170
4.3.4 Phox2b.....	170
4.4 Discussion	172
4.4.1 Noradrenergic Neuromodulation.....	172
4.4.2 Serotonergic Neuromodulation.....	174
4.4.3 NK1 Expression in the PreBötzinger Complex	177
4.4.4 Phox2b Expression in the RTN/pFRG	178
Chapter 5: Investigation of possible lung pathology in male mouse model of RTT syndrome.	180
5.1 Introduction	181
5.1.1 Lung Pathology in RTT patients and Mecp2 Deficient Mice	181
5.1.2 Difference in Murine and Human Lung Anatomy	182
5.1.3 BDNF and the Role of Tyrosine Kinase Receptor (TrkB) in the Lung..	184
5.2 Methods.....	186
5.2.1 Animals	186
5.2.2 Histology	187
5.2.3 Immunocytochemistry.....	188
5.2.5 Statistics.....	194
5.3 Results	194
5.3.1 Preliminary Histological Staining	194

5.3.2 Measuring Various Morphological Aspects of the Lung.....	199
5.3.3 TrkB and MeCP2 Expression	208
5.4 Discussion	215
5.4.1 Morphological Changes in MeCP2 Deficient Lungs.....	215
5.4.2 TrKB in the Lung	218
Chapter 6: Respiratory pattern of <i>Mecp2</i>^{+/-} mice and investigation of possible underlying lung pathology.	221
6.1 Introduction.....	222
6.2 Methods.....	224
6.2.1 Female Mouse Model.....	224
6.2.2 Behavioural Scoring.....	224
6.2.3 Respiratory Measurements.....	225
6.2.4 Respiratory Analysis	226
6.2.5 PAH Analysis	226
6.3 Results	227
6.3.1 Behavioural Score	227
6.3.2 Respiratory Traces of <i>Mecp2</i> ^{+/-} Animals	230
6.3.3 Quantifying Respiratory Abnormalities	234
6.3.4 PAH analysis	245
6.4 DISCUSSION.....	248
6.4.1 Behaviour.....	248
6.4.2 The Hypercapnic and Hypoxic Response of <i>Mecp2</i> ^{+/-} Mice	250
6.4.3. Respiratory Variability and Maturity of Neurons	252
6.4.4 Sighing and Double Breaths.....	253
6.4.5 Apnea	256
6.4.6 PAH.....	258
Chapter 7: Final Discussion.....	261
7.1 Behavioural Phenotype of Male and Female Model	262
7.2 MeCP2 and Maturation.....	267
7.3 MeCP2 and Neuromodulation.....	269
7.4 Chemosensitivity - Response to hypoxia and hypercapnia	273
7.5 Lung Pathology	277
Appendix 1.....	281
1L of 4% Paraformaldehyde.....	281
30% Sucrose solution.....	281

0.2M Phosphate buffer (PB)	281
0.3M Phosphate buffer saline (PBS)	281
Phosphate buffer saline + Triton X-100 (0.3%PBST)	281
0.01M Citrate Buffer	281
Tris Buffered Saline (TBS).....	282
TBS Tween (TBST).....	282
NGS/TBS/BSA solution.....	282
List of References	283

List of Tables

Table 1-1 Mouse models of MeCP2 deficiency and overexpression.....	54
Table 2-1 3 point behavioural scoring system used to monitor progression of the RTT-like phenotype.. ..	66
Table 2-2 5 point behavioural scoring system used to monitor progression of the RTT-like phenotype.. ..	67
Table 2-3 List of primary and secondary antibodies used to stain brainstem of male MeCP2 deficient and WT mice and highlight areas involved in control of respiration.	76

List of Figures

Fig 1-1 Dorsal view of brainstem illustrating the ventral respiratory columns...	31
Fig 1-2 MeCP2 as a transcriptional activator and repressor	50
Fig 2-1 Illustration of the apparatus involved in respiratory plethysmography.	70
Fig 2-2 Respiratory trace(s) highlighting the respiratory parameters	71
Fig 2-3 Respiratory traces to highlight various respiratory events	72
Fig 2-4 Illustration of how imaging and cell counting was performed within the brainstem	78
Fig 2-5 Schematic of the principle reaction in the DAB reaction.....	80
Fig 2-6 Illustration of lung tissue processing and imaging.	84
Fig 3-1 The <i>Mecp2</i> ^{tm2Bird} model of RTT syndrome.	90
Fig 3-3 Average behavioural score of <i>Stop/y</i> (n=1) and <i>Stop/y,cre</i> (n=1) mice, comparing 3 point scale (left y axis) and 5 point scale (right y axis).....	96
Fig 3-4 Respiratory traces to illustrate WT respiratory pattern pre and post TM treatment.....	98
Fig 3-5 Respiratory traces to illustrate respiratory pattern of two <i>Stop/y</i> mice pre TM.....	99
Fig 3-6 Respiratory traces to illustrate respiratory pattern of <i>Stop/y,cre</i> animal with severe respiratory phenotype	100
Fig 3-7 Respiratory traces to illustrate the respiratory pattern of a <i>Stop/y,cre</i> mouse with mild respiratory phenotype.	101
Fig 3- 8 Plot of the average respiratory frequency of <i>Stop/y</i> , <i>Stop/y, cre</i> and WT mice in normoxia (mean±SD)	104
Fig 3-9 Plot of % co var of the average respiratory frequency of <i>Stop/y</i> , <i>Stop/y, cre</i> and WT mice in normoxia (mean±SD).....	105
Fig 3-10 Plot of the average respiratory frequency of <i>Stop/y</i> , <i>Stop/y,cre</i> and WT mice 4 weeks before TM treatment (mean±SD).....	108
Fig 3-11 Plot of the average respiratory frequency of <i>Stop/y</i> , <i>Stop/y,cre</i> and WT mice before TM treatment (mean±SD).	109
Fig 3-12 Plot of the average respiratory frequency of <i>Stop/y,cre</i> and WT mice 5 weeks after TM treatment (mean±SD)	110
Fig 3-13 Plot of the average respiratory frequency of <i>Stop/y,cre</i> and WT mice 9 weeks after TM treatment (mean±SD).	111
Fig 3-14 Example of sigh taken from respiratory trace of <i>Stop/y,cre</i> mouse ...	112

Fig 3-15 Average number of sighs which occur in normoxic conditions in WT, <i>Stop/y</i> and <i>Stop/y,cre</i> mice (mean \pm SD).....	114
Fig 3-16 Average number of sighs in WT, <i>Stop/y,cre</i> and <i>Stop/y</i> mice 2 weeks prior to TM (mean \pm SD)	115
Fig 3-17 Plot to illustrate the average number of sighs which occur per 2 min trace in WT and <i>Stop/y,cre</i> +TM mice at 5 wks post TM treatment (TM+5;mean \pm SD).....	116
Fig 3-18 Example of respiratory trace containing double breath from <i>Stop/y,cre</i> animal	117
Fig 3-19 Plot to show the average number of double breaths that occur per 2 min trace in WT, <i>Stop/y,cre</i> and <i>Stop/y</i> animals, (mean \pm SD).	118
Fig 3-20 Plot to show the average number of double breaths that occur per 2 min trace in WT, <i>Stop/y,cre</i> and <i>Stop/y</i> animals (mean \pm SD)	119
Fig 3-21 Example of respiratory trace from <i>Stop/y,cre</i> animal containing apnea	121
Fig 3.22 Plot to show the average number of apneas that occur per 2 min trace in WT, <i>Stop/y,cre</i> and <i>Stop/y</i> animals	122
Fig 4-1 Diagram of midsaggital brain section to illustrate respiratory rhythm generators and sites of neuromodulation.....	135
Fig 4-2 Illustration of the position of A1/C1 region	142
Fig 4-3 Single plane confocal image of Tyrosine hydroxylase and MeCP2 expression in A1/C1 of WT, <i>Stop/y</i> , <i>Stop/y,cre</i> -TM, and <i>Stop/y,cre</i> +TM animals	143
Fig 4-4 Illustration of the position of A2/C2 region	144
Fig 4-5 Single plane confocal image of Tyrosine hydroxylase and MeCP2 expression in A2/C2 of WT, <i>Stop/y</i> , <i>Stop/y,cre</i> -TM, <i>Stop/y,cre</i> +TM and animals	145
Fig 4-6 Illustration of the position of LC	146
Fig 4-7 Single plane confocal image of Tyrosine hydroxylase and MeCP2 expression in A6/LC of WT, <i>Stop/y</i> , <i>Stop/y,cre</i> -TM, <i>stop/y,cre</i> +TM animals ...	147
Fig 4-8 Illustration of the position of Raphe Obscurus (ROb) and Raphe Pallidus (RPa) region	149
Fig 4-9 Single plane confocal image of 5-HT and MeCP2 expression in the Raphe Obscurus of WT, <i>Stop/y</i> , <i>Stop/y,cre</i> -TM, <i>stop/y,cre</i> +TM animals	150

Fig 4-10 Single plane confocal image of 5-HT expressing neurons of the Raphe pallidus/magnus of WT, <i>Stop/y</i> , <i>Stop/y,cre-TM</i> , <i>Stop/y,cre+TM</i> animals.....	151
Fig 4-11 Illustration of the position of Raphe Magnus (RMg) region.....	152
Fig 4-12 Single plane confocal image of 5-HT expressing neurons of the ventrolateral medulla of WT, <i>Stop/y</i> , <i>Stop/y,cre-TM</i> , <i>stop/y,cre+TM</i> animals.	153
Fig 4-13 Illustration of the position of raphe dorsalis (DRI) and pontine raphe nuclei (PnR) region.....	154
Fig 4-14 Single plane confocal image of 5-HT expressing neurons of the DRI of WT, <i>Stop/y</i> , <i>Stop/y,cre-TM</i> , <i>stop/y,cre+TM</i> animals	155
Fig 4-15 Single plane confocal image of 5-HT expressing neurons of the PnR/MnR of WT, <i>Stop/y</i> , <i>Stop/y,cre-TM</i> , <i>stop/y,cre+TM</i> animals	156
Fig 4-17 Single plane confocal image of NK1, MeCP2 and VLGUT2 expression within the PreBötC of WT animal	159
Fig 4-18 Single plane confocal image of NK1R and MeCP2 expression in the PreBötC of WT, <i>Stop/y</i> , <i>Stop/y,cre-TM</i> , <i>stop/y,cre+TM</i> animals.....	160
Fig 4-19 Illustration of the position of RTN/pFRG	163
Fig 4-20 Single plane confocal images of Phox2b and MeCP2 expressing neurons of the RTN/pFRG of WT and <i>Stop/y</i> animal	164
Fig 4-21 Plots to show average number of TH and MeCP2 expressing neurons in WT, <i>Stop/y,cre +TM</i> , <i>Stop/y,cre -TM</i> and <i>Stop/y</i> mice.....	166
Fig 4-22 Plots to show average number of 5-HT and MeCP2 expressing neurons in WT, <i>Stop/y,cre +TM</i> , <i>Stop/y,cre -TM</i> and <i>Stop/y</i> mice.....	169
Fig 4-23 Plots to show average number of NK1 and MeCP2 expressing neurons in the preBötC of WT, <i>Stop/y,cre +TM</i> , <i>Stop/y,cre -TM</i> and <i>Stop/y</i> mice	171
Fig 5-1 Anatomy of human trachea and lungs	183
Fig 5-2 Comparison of airway branching in mouse and human lung	183
Fig 5-3 Illustration of the measurement of bronchial epithelium of WT mouse	190
Fig 5-4 Illustration of data collection from images taken within the lung tissue for measurement of alveolar septum thickness, respiratory epithelium thickness and thickness of elastic fibres surrounding the airways	191
Fig 5-5 Illustration of the measurement of alveolar septum thickness. Light microscope image of lung tissue of WT animal stained with haematoxylin and eosin.....	192

Fig 5-6 Illustration of the measurement of the elastic fibres surrounding airways.	193
Fig 5-7 Light microscope image of H&E staining of WT and <i>Stop/y</i> lung tissue .	195
Fig 5-8 High power magnification light microscopy images of H&E stained <i>Stop/y</i> tissue	196
Fig 5-9 Masson's trichrome staining of WT and <i>Stop/y</i> lung tissue.....	197
Fig 5-10 Light microscope image of Periodic acid-schiff stain (PAS) staining of WT and <i>Stop/y</i> lung tissue	198
Fig 5-11 Light microscopy images of Masson's trichrome staining in WT, <i>Stop/y</i> , <i>Stop/y,cre-TM</i> , <i>Stop/y,cre+TM</i> and animals	200
Fig 5-12 Plots to show the average thickness of the epithelial lining of the airways in WT, <i>Stop/y,cre+TM</i> , <i>Stop/y,cre-TM</i> and <i>Stop/y</i> animals	201
Fig 5-13 Plot to illustrate the average thickness of the interalveolar septum in WT, <i>Stop/y,cre+TM</i> , <i>Stop/y,cre-TM</i> and <i>Stop/y</i> animals	202
Fig 5-14 Plot to show the average thickness of the elastin surrounding airways in WT, <i>Stop/y</i> , <i>Stop/y,cre-TM</i> and <i>Stop/y,cre+TM</i> , and animals	204
Fig 5-15 Plot to show the average thickness of the elastic fibres surrounding airways in WT, <i>Stop/y</i> , <i>Stop/y,cre-TM</i> and <i>Stop/y,cre+TM</i> animals	205
Fig 5-16 Plots comparing the aggregate behavioural score of <i>Stop/y</i> and <i>Stop/y,cre-TM</i> mice which did or did not present the rale-like breathing (RLB) phenotype	207
Fig 5-17 Single plane confocal images of TrkB and MeCP2 expression in lung of WT animals	208
Fig 5-18 Single plane confocal image of MeCP2 and TrkB staining in <i>Stop/y</i> lung	209
Fig 5-19 Single plane confocal images of MeCP2 and TrkB staining in <i>Stop/y,cre-</i> <i>TM</i> animal.....	210
Fig 5-20 Single plane confocal image of MeCP2 and TrkB staining in <i>Stop/y,cre+TM</i> mice	211
Fig 5-21 Single plane confocal images of MeCP2 and TrkB staining in <i>Stop/y,cre+TM</i> muscle layer	212
Fig 5-22 TrkB staining (DAB) of airways of WT, <i>Stop/y,cre-TM</i> , <i>Stop/y,cre+TM</i> and <i>Stop/y</i> males.....	214
Fig 6-1 Protocol for measurement of respiratory parameters of <i>Mecp2^{+/-}</i> mice	225

Fig 6-2 Plots to illustrate the average behavioural score of WT and <i>Mecp2</i> ^{+/-} mice using 3 point and 5 point scales	228
Fig 6-3 Plots to illustrate the average weight of WT and <i>Mecp2</i> ^{+/-} mice	229
Fig 6-4 Respiratory traces of 10 wk old WT (left) and <i>Mecp2</i> ^{+/-} (right) animals in normoxia, hypercapnia and hypoxia.	231
Fig 6-5 Respiratory traces of 19 wk old WT (left) and <i>Mecp2</i> ^{+/-} (right) animals in normoxia, hypercapnia and hypoxia.	232
Fig 6-6 Respiratory traces of 32 wk old WT (left) and <i>Mecp2</i> ^{+/-} (right) animals in normoxia, hypercapnia and hypoxia.	233
Fig 6-7 Plots to illustrate the average respiratory frequency of WT and <i>Mecp2</i> ^{+/-} females under each respiratory stimulus	235
Fig 6-8 Plots to illustrate the coefficient of variation of the average respiratory frequency of WT and <i>Mecp2</i> ^{+/-} females in normoxia, hypercapnia and hypoxia.	237
Fig 6-10 Average number of double breaths observed per 2min trace in WT and <i>Mecp2</i> ^{+/-} females in air and during respiratory stimulus.....	241
Fig 6-11 Average number of sighs and double breaths per 2min trace in WT and <i>Mecp2</i> ^{+/-} females in normoxia, hypercapnia and hypoxia	242
Fig 6-12 Average number of apneas observed per 2min trace in WT and <i>Mecp2</i> ^{+/-} females under each respiratory stimulus	244
Fig 6-13 Plots to illustrate the measurement of indices of pulmonary arterial hypertension in WT (n=4) and <i>Mecp2</i> ^{+/-} (n=8) mice.	246
Fig 6-14 Light microscopy images of WT and <i>Mecp2</i> ^{+/-} tissue stained with Miller's elastin stain and counterstained with Van Giesson's.....	247

Acknowledgements

Firstly I would like to thank my supervisor Dr Leanne McKay not only for giving me the opportunity to complete my PhD in her lab, but for all her support and encouragement throughout the past three years.

I'd also like to thank the staff in the spinal cord research group, in particular Robert and Christine for their endless patience to match my endless questioning!

I wish to thank David Russell, Andy Lockhart, Stuart McNally for their help and advice with regards to tissue staining and Denise Padgett for her assistance with lung tissue preparation.

Thanks also go to Margaret Nielsen for her help and advice with regards to the female PAH studies.

Many thanks to the all the staff at the Wellcome Surgical Institute for the warm welcome I received into their workplace and for the support they offered in the final months of my PhD.

I'd also like to thank all my fellow students, friends, and flatmate (Kennedy, Leroy, Mitchell, Dave, Miranda, Ash B, Wheez and many more!) for encouraging me, listening to rants, telling me to stop whining and keeping me sane! G-cube crew, I'm going to miss disco Friday!

Last but by no means least; I would like to thank my parents, brother and sister in law for all their love, encouragement, support and prayers throughout these past years.

Thanks to you all and apologies to anyone I forgot to mention!

Author's Declaration

I declare that, except where explicit reference is made to the contribution of others, this dissertation is the result of my own work and has not been submitted for any other degree at the University of Glasgow or any other institution. Portions of the work described herein have been published elsewhere as listed below.

Emma Brockett

October 2012

Published Manuscripts

Robinson L., Guy J., McKay L.C., Brockett E., Spike, R., Selfridge J., De-Souza D., Merusi C.A., Riedel G., Bird A., Cobb S. (2012) Morphological and functional abnormalities in the mouse model of Rett syndrome and their propensity for reversal by delayed activation of the *Mecp2* gene. *Brain*, **135**(Pt 9):2699-710.

Manuscripts in Preparation

Brockett E., Guy J., Bird A., McKay L.C. (2012). Observation and reversal of respiratory abnormalities of male MeCP2 deficient mice [in preparation]

Brockett E., Guy J., Bird A., McKay L.C. (2012). Progression of the respiratory phenotype in a female mouse model of Rett Syndrome [in preparation]

Brockett E., Guy J., Bird A., McKay L.C., Padgett D., Russell D. (2012). Morphological changes in the lungs of MeCP2 deficient male mice [in preparation]

Abstracts

Brockett E., Guy J., Bird A., McKay L.C. (2010). Breathing abnormalities in a mouse model of Rett syndrome. *The Integrative Mammalian Biology Symposium, University of Glasgow*.

Brockett E., Guy J., Bird A., McKay L.C. (2010). Breathing abnormalities in a mouse model of Rett syndrome. *Rett Syndrome Europe Scientific Conference, Edinburgh.*

Brockett E., Guy J., Bird A., McKay L.C. (2011). Reversal of breathing abnormalities in a mouse model of Rett syndrome. *Glasgow Neuroscience Day, University of Glasgow.*

Brockett E., Guy J., Bird A., McKay L.C. (2011). Reversal of breathing abnormalities in a mouse model of Rett syndrome. *British Neuroscience Society, Harrowgate.* (Selected for 'breaking hot topics' session oral presentation).

Brockett E., Guy J., Bird A., McKay L.C. (2012). Tyrosine hydroxylase expression in a mouse model of Rett syndrome. *The Integrative Mammalian Biology Symposium, University of Glasgow.*

Brockett E., Guy J., Bird A., McKay L.C. (2012). TH and 5-HT expression in a mouse model of Rett syndrome. *Federation of European Neuroscience, Barcelona.*

Abbreviations page

5-HT	Serotonin
5-HTT	Serotonin Transport Protein
6-OHDA	6-hydroxydopamine
A1/C1	A1 noradrenaline cells/C1 adrenaline cells
A2/C2	A2 noradrenaline cells/C2 adrenaline cells
A5	A5 noradrenaline cells
A6/LC	A6 noradrenalne cells/Locus Coeruleus
ACTH	Adrenocorticotropic hormone
AMPA	2-amino-3-(3-hydroxy-5-methyl-isoxazol-4-yl)propanoic acid
APE	Aminopropyltriethoxysilane
BALB/c	Inbred mouse strain
BDNF	Brain Derived Neurotrophic Factor
BötC	Bötzingen Complex
bpm	Breaths per minute
BSA	Bovine serum albumin
C4	Cervical spinal nerve 4
C57BL6/CBA	Inbred mouse strain
CCHS	Congenital central hypoventilation syndrome

CDKL5	Cyclin-dependent kinase-like 5
Cl ⁻	Chlorine ion
CNQX	6-cyano-7-nitroquinoxaline-2,3-dione
CNS	Central nervous system
CO ₂	Carbon dioxide
CPG	Central pattern generator
CRH	Corticosterone releasing hormone
CTb	Cholera toxin b sub unit
cVRG	Caudal ventral respiratory group
DAB	Diaminobenzidine reaction
DAMGO	[D-Ala ² , N-MePhe ⁴ , Gly-ol]-enkephalin
DAPI	4',6-diamidino-2-phenylindole
DBH	Dopamine beta hydroxylase
DNA	Deoxyribonucleic acid
DOI	5-HT _{2a} agonist
DPX	Distrene, Plasticiser, Xylene
DRG	Dorsal respiratory group
DRI	Dorsal raphe nuclues
E14.5	Embryonic day 14.5

E18	Embryonic day 18
e-pf	Embryonic parafacial oscillator
F1	First generation offspring
F2	Second generation offspring
FFA	Free fatty acids
Fkbp5	FK506 binding protein 5
FOXP1	Forkhead box G1
Fr	Respiratory frequency
GABA	Gamma-Aminobutyric acid
H&E	Haematoxylin and eosin
HBR	Herring breuer reflex
HCl	Hydrochloric Acid
HDAC1	Histone deacetylase 1
HDAC2	Histone deacetylase 2
HoxB1	Homeobox protein HoxB1
HRCT	High Resolution Computed Tomography
kDA	Kilodaltons
KF	Kölliker-fuse nucleus
KO	Knock out

Krox 20	Zinc finger protein
LC	Locus Coeruleus
L-DOPA	L-3,4-dihydroxyphenylalanine
Lmx1b	LIM homeobox transcription factor 1-beta
<i>Lmx1b f/f/p</i>	LIM homeobox transcription factor 1 beta conditional knock out
LV+S	Left ventricle plus septum
<i>Mecp2</i>	Methyl CpG binding protein 2 mouse gene
MeCP2	Methyl CpG binding protein 2 mouse protein
<i>MECP2</i>	Methyl CpG binding protein 2 human gene
MECP2	Methyl CpG binding protein 2 human protein
<i>Mecp2</i> ^{308/y}	Mouse model expressing truncated MeCP2 protein
<i>Mecp2</i> ^{flx/y}	Mouse model expressing only 50% of the WT level of MeCP2
<i>Mecp2</i> KO	<i>Mecp2</i> knock out, expresses no MeCP2
<i>Mecp2</i> ^{TG1}	Model which expresses hypomorphic MeCP2
<i>Mecp2</i> ^{-/y}	Male model which expresses no MeCP2
<i>Mecp2</i> ^{+/-}	Female model heterozygous for <i>Mecp2</i>
<i>Mecp2</i> ^{tm2Bird}	Male model in which <i>Mecp2</i> can be silenced and reactivated
mGluRs	Metabotropic glutamate receptors
mmHg	Millimetre of mercury

Mnr	Median raphe nucleus
NA	Noradrenaline
nA	Nucleus ambiguus
NaCl	Sodium Chloride
NaH ₂ PO ₄	Sodium di-hydrogen phosphate
NaHPO ₄	Di-sodium hydrogen phosphate
NaOH	Sodium Hydroxide
NGS	Normal goat serum
NK1R	Neurokinin-1 receptor
NMDA	N-Methyl-D-aspartic acid
Non-REM	Non-rapid eye movement
NT-4	Neurotrophin 4
<i>NTRK2</i>	Neurotrophic tyrosine kinase receptor type 2
nTS	Nucleus of the tractus solitarius
<i>Nurr1</i>	The Nuclear receptor related 1 protein
O ₂	Oxygen
OCT	Optimal Cutting Temperature compound
P14	Postnatal day 14
PAH	Pulmonary arterial hypertension

PVN	Paraventricular nucleus
PAS	Periodic acid Schiff stain
Pb	Barometric pressure
PBN	Parabrachial nuclei
PB	Phosphate buffer
PBS	Phosphate buffer saline
PBST	Phosphate buffer saline with Triton-x.
PCO ₂	Carbon dioxide partial pressure
PCR	Polymerase chain reaction
Pet-1	Pheochromocytoma 12 ETS factor-1
PGi	Paragigantocellular reticular nucleus
Phox2a	Paired mesoderm homeobox protein 2A
Phox2b	Paired-like homeobox 2b
PnR	Pontine raphe nucleus
PO ₂	Oxygen partial pressure
PreBötC	Pre-Bötzinger Complex
Pre-I	Pre-inspiratory
PRG	Pontine respiratory group
REM	Rapid eye movement

Riluzole	2-amino-6-(trifluoromethoxy)benzothiazole
RLB	Rale-like breathing
RMg	Raphe magnus
RNA	Ribonucleic acid
Rob	Raphe obscurus
RPa	Raphe pallidus
RTN/pFRG	Retrotrapezoid nucleus/parafacial respiratory group
RTT	Rett Syndrome
RV	Right ventricle
LV+S	Left ventricle plus septum
RVH	Right ventricular hypertrophy
RVLM	Rostroventrolateral medulla
RVP	Right ventricular pressure
rVRG	Rostral ventral respiratory group
<i>Sgk</i>	Aldosterone-induced gene
Sim-1	Single-minded homolog 1/ class E basic helix-loop-helix protein 14
Sin3A	Paired amphipathic helix protein
SO	Superior olive
sRVP	Systolic right ventricular pressure

<i>Stop/y</i>	Male MeCP2 deficient mouse in which <i>Mecp2</i> cannot be reactivated
<i>Stop/y,cre</i>	Male MeCP2 deficient mouse in which <i>Mecp2</i> can be reactivated
<i>Stop/y,cre-TM</i>	<i>Mecp2</i> was not reactivated
<i>Stop/y,cre+TM</i>	<i>Mecp2</i> was reactivated
SubP	Substance P
TBS	Tris buffered saline
TBST	Trisbuffered saline tween
TH	Tyrosine Hydroxylase
TM	Tamoxifen
TrkB	Tyrosine kinase beta
Ttot	Total breath time
TTX	Tetrodotoxin
VII	Facial nerve
VGLUT2	Vesicular glutamate transporter 2
VRC	Ventral respiratory column
VRG	Ventral respiratory group
WT	Wild type
XCI	X chromosome inactivation

Chapter 1: Introduction

1.1 Why Breathing is Essential

Respiration plays a pivotal role in the regulation of blood gases such as carbon dioxide (CO₂) and oxygen (O₂). Mammals have a relatively high metabolic rate and as such benefit from the rich supply of energy that comes from aerobic respiration. In humans, the oxygen demand can vary from 0.25 litres per minute at rest to 3-6 litres per min during exercise.

1.2 History of the Study of Involuntary Control

Respiration is subject to voluntary control, illustrated by the fact that it can be readily modulated during behaviours such as coughing, crying, laughing, and speaking. However, the fact that breathing continues in the absence of a subject's awareness indicates that there is also a large degree of involuntary control. Claudius Galen (131-201 A.D.), a physician to numerous roman emperors, noted that both gladiators and animals who were injured below the neck continued to breathe but those injured above the neck ceased to do so. Lorry (1760) illustrated that removing the cerebellum of rabbits did not abolish breathing, but destruction of the brain stem led to cessation of breathing and thus concluded that the circuitry required for control of respiration must lie within the brain stem and upper spinal cord. Attempts were made (Legallois, 1813) to unearth the areas of the brain stem that were involved in respiratory genesis by destroying various areas of the medulla. Legallois stated, *“For every time a certain portion is destroyed, be it of the brain or of the spinal cord, a function is compelled to cease suddenly, and before the time known beforehand when it would stop naturally, it is certain that this function depends upon the area destroyed. It is in this way that I have recognized that the prime motive power of respiration has its seat in that part of the medulla oblongata that gives rise to the nerves of the eighth pair [vagi]; and it is by this method that up to a certain point it will be possible to discover the use of certain parts of the brain”*.

Herring and Breuer (1868) observed breathing reflexes in response to inflation and deflation of the lungs and it soon became apparent that there were various inputs involved in the modulation of the respiratory pattern. Cajal studied the afferent and efferent projections of respiratory related nerves and went on to suggest three important brain stem nuclei: the nucleus of the solitary tract,

commissural nuclei (both of which are primary targets of pulmonary afferents) and the nucleus ambiguus which contains cranial motor neurons that innervate the upper airway muscles. Cajal proposed that respiratory neurons in the solitary tract processed signals from pulmonary afferents and a blood factor which was present in local capillaries. It was thought that this information would cause modulation of respiration via output to spinal motorneurons which would in turn innervate the diaphragm or intercostal muscles (Cajal, 1909). Lumsden (Lumsden, 1923) carried out *in vivo* experiments in the cat, also showing that respiratory rhythm is generated in the lower brain stem, and he defined certain respiratory centres including the apneustic centre in the lower pons (though to produce prolonged periods of inspiration) and the pneumotaxic centre in the rostral pons, (thought to inhibit the activity of the apneustic centre). Later studies involved taking recordings from individual medullary neurons which revealed that these neurons exhibit bursts of activity which are in phase with the breathing rhythm, (Gesell *et al.*, 1936). These results sparked off an effort to find the neurons that generate respiratory rhythm.

1.3 Location of Respiratory Neurons

The motor pattern that is produced during rhythmic breathing comes from the ventral respiratory columns (VRC's), which are composed of several rostro-caudally arranged compartments.

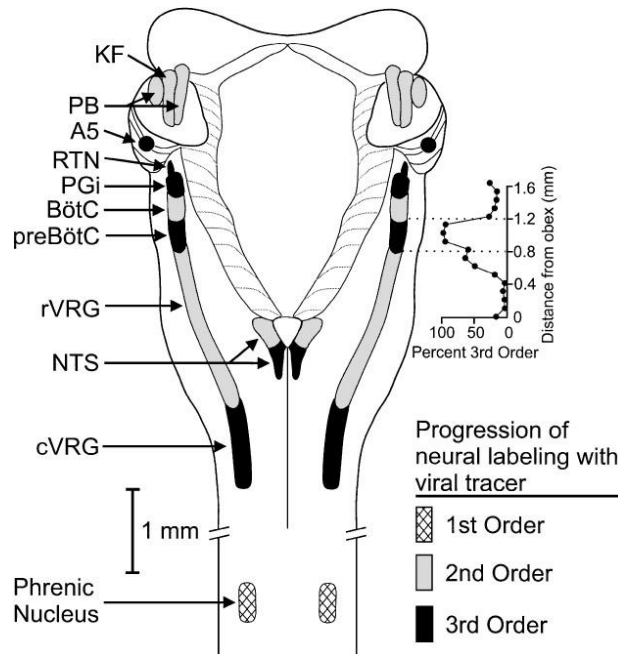


Fig 1-1 Dorsal view of brainstem illustrating the ventral respiratory columns. BötC, Bötzinger Complex; cVRG, caudal ventral respiratory group; KF, Kolliker-Fuse nucleus; NTS, nucleus tractus solitarius; PB, parabrachial nuclei; PGi, paragigantocellular reticular nucleus; preBötC, preBötzinger Complex; RTN, retrotrapezoid nucleus; rVRG, rostral ventral respiratory group. Image taken from (Rekling & Feldman, 1998).

The bötzinger complex (BötC) is situated in the rostral part of the respiratory column and contains mainly expiratory neurons, some of which are bulbospinal (meaning these neurons project from the medulla and terminate in the spinal cord) and others which are propriobulbar (neurons which project and terminate within the medulla). The BötC is also suggested to have a pivotal role in the switch between inspiratory and expiratory activity in the respiratory network (Smith *et al.*, 2009).

Caudal to the BötC lies the pre-Bötzinger complex (Smith *et al.*, 1991), defined as a group of vesicular glutamate transporter 2 (VGLUT2) positive interneurons

which also express high levels of neurokinin receptor (NK1R;(Stornetta *et al.*, 2003). The pre-Bötzinger complex (preBötC) is important in the generation of respiratory activity given that neonatal rat brainstem slices which contain the preBötC continue to produce rhythmic activity *in vitro* (Smith *et al.*, 1991). Also, destruction of the NK1R expressing neurons in the preBötC of the rat leads to disordered breathing during sleep and eventually disturbances in breathing during wakefulness (McKay *et al.*, 2005).

Caudal to the preBötC and extending down the spinal cord is the ventral respiratory group (VRG) which contains most of the premotor neurons that innervate inspiratory and expiratory motor neurons in the spinal cord. This area is further subdivided into rostral (rVRG) and caudal (cVRG) divisions. The rVRG consists primarily of inspiratory premotor neurons which innervate spinal inspiratory motor neurons i.e. the phrenic motor neurons that innervate the diaphragm and external intercostal motor neurons. The rVRG contains bilateral clusters of excitatory neurons that project to phrenic and intercostal motor neurons and shape the inspiratory motor output pattern (Bianchi *et al.*, 1995; Richter, 1996). Unlike the rVRG, the cVRG contains mainly expiratory neurons and innervates expiratory motor neurons, whose axons lie in the internal intercostal nerves and also supply abdominal muscles. As such, the cVRG is key in the expiratory phase of respiration.

Moving rostrally from the preBötC lies the retrotrapezoid nucleus/parafacial respiratory group (RTN/pFRG; (Onimaru & Homma, 2003) which contains Phox2b and VGLUT2 expressing neurons (Mulkey *et al.*, 2004; Stornetta *et al.*, 2006). Pre-I neurons within the pFRG have been shown to have rhythmic properties and may contribute to respiratory rhythm generation (Onimaru & Homma, 2003) however the function of the RTN/pFRG is still debated with some studies suggesting the area has a more prominent role in chemosensitivity (Mulkey *et al.*, 2004; Guyenet *et al.*, 2005b).

The dorsal respiratory group (DRG) is located in the nucleus of the tractus solitarius (nTS) and receives input from chemoreceptors and both mechanically and chemically sensitive neurons of the lung. It contains inspiratory neurons that project to phrenic motor neurons (Richerson, 2004) and outputs from the nTS

include projections to the parabrachial area, ventral respiratory group and spinal cord. Neurons of the nTS are not likely to be involved in respiratory rhythm generation; rather they are important in the modification of the respiratory pattern and in the augmentation of ventilation during hypoxic challenges.

The pontine respiratory group (PRG) includes the Kölliker-fuse nucleus, the parabrachial complex in the rostral dorsolateral pons and some areas in the ventrolateral pons. The role of the pons in respiration has not been fully established but *in situ* studies of perfused mouse brain stem revealed that glutamate injections in the intermediate Kölliker-fuse triggered a transient postinspiratory apnea, while injections into the margin of the Kölliker-fuse area caused bradypnea and enhanced postinspiratory activity (Stettner *et al.*, 2007). This suggests that pontine connections to the medullary circuits serve to regulate post inspiratory activity (Dutschmann & Herbert, 2006). Also, transecting the pons leads to an increase in the frequency of phrenic bursting suggesting that pontine regions may play a role in the suppression of the respiratory rhythm generator (Hilaire *et al.*, 1989).

1.4 Modulation of Respiration by Neurotransmitters

The respiratory pattern can be modified by various neurotransmitters which act at many different sites within the respiratory network.

1.4.1 Serotonin

Serotonin (5-HT) is a neurotransmitter essential in the development of the respiratory network and is critical for stable breathing and maintenance of respiratory rhythm. Pheochromocytoma 12 OAS factor-1 (Pet-1) is a transcription factor which, in the brain, is only expressed in 5-HT neurons and their precursors and is important in the control of the 5-HT neuron phenotype (Hendricks *et al.*, 1999). Pet-1 knock out mice have a 70-80% loss of 5-HT neurons in the CNS (Hendricks *et al.*, 2003) and at neonatal stages show an increased variability in respiratory output compared to WT animals. Pet-1 KO mice also fail to achieve the maturation step seen at post natal day 4.5 in the WT mice, where the breathing patterns becomes stabilised (Erickson *et al.*, 2007), data which highlight the importance of 5-HT during development. The gene *Lmx1b* is also

thought to be important in the delineation of 5-HT neurons (Ding *et al.*, 2003) and the *Lmx1b f/f/p* mouse model gives rise to animals which have no central 5-HT neurons. The animals still breathe and are viable (Zhao *et al.*, 2006; Hodges *et al.*, 2009) which indicates that 5-HT is not required for the production of the respiratory rhythm. However, *Lmx1b f/f/p* mice present severe and frequent apnea during development (Hodges *et al.*, 2009), a breathing pattern which is recovered to WT standard by the application of 5-HT_{2a} agonist DOI, (Hodges *et al.*, 2009) suggesting that 5-HT is an important respiratory neuromodulator, particularly at neonatal and developmental stages.

5-HT is also thought to be important in modulating the chemosensitive response given that *Lmx1b f/f/p* mice also exhibit a decreased ventilatory response to hypercapnia (Hodges & Richerson, 2008). 5-HT neurons are also often located close to cerebral blood vessels (Bradley *et al.*, 2002) which allows detection of changes in pH levels of the blood. Further to this, *in vitro* patch-clamp recordings of rat medullary brain slices illustrate that the midline raphe contains neurons which are intrinsically sensitive to increases in carbon dioxide (Richerson, 1995a). The firing rate of 5-HT neurons is highest in wakefulness and decreases in slow wave sleep, reaching its minimum in REM sleep (Jacobs & Fornal, 1991). This implies that 5-HT may contribute to the drive to breathe in wakefulness and the sleep-related reduction in the release of 5-HT could contribute to the decrease in ventilation that is often seen (Hodges & Richerson, 2008). 5-HT immunoreactive fibres are found in many areas associated with respiration such as respiratory motoneurons, the nTS, nucleus ambiguus, RTN and preBötC (Holtman, 1988; Voss *et al.*, 1990). Injection of the retrograde tracer cholera toxin b subunit (CTb) into the rostroventrolateral medulla (RVLM) and combined with 5-HT immunolabeling illustrates that there are many serotonergic projections from raphe nuclei to respiratory areas within the medulla (Bago *et al.*, 2002).

The respiratory response to 5-HT is varied and is thought to depend on a number of different 5-HT receptor subtypes that exist and the subsequent G-proteins with which these receptors interact (Richter *et al.*, 2003). For example, the application of DOI, a 5-HT_{2A} agonist, to mouse brainstem slices leads to an increase in fictive respiratory activity and fictive sighing recorded from the pre-

Böttinger, (Pena & Ramirez, 2002) and *in vitro* and *in vivo* studies in the rat and cat respectively, have also illustrated that exogenous application of 5-HT_{2A} receptor agonists has an excitatory effect on respiratory activity (Lalley *et al.*, 1995; Onimaru *et al.*, 1998). Contrary to this effect, application of 5-HT_{2c} agonist to the neonatal rat brainstem spinal cord prep induced a decrease in respiratory output as measured by C4 output (Onimaru *et al.*, 1998). 5-HT endogenous activation is also thought to be required to stabilise the eupneic rhythm in slices (Pena & Ramirez, 2002) as activation of 5-HT_{1A} receptors reverses apneustic breathing (Lalley *et al.*, 1994). The authors of the latter study suggest that in situations where the oxygen demand outweighs the supply e.g. in hypoxia, the incidence of apneustic breathing can be greater and as such the increase in 5-HT release may serve to restore the normal respiratory pattern.

1.4.2 Noradrenaline and Dopamine

The neurotransmitter noradrenaline (NA) also plays a key role in modulation of the respiratory pattern and contributes to the maturation of respiratory control after birth. NA expressing neurons can be found in the pons (A5 and A6/LC) and medulla (A1/C1, A2/C2). A5 and A6/LC (Locus Coeruleus) neurons are thought to be important in both development and modulation of respiration, highlighted by studies of Phox2a mutant mice, which lack neurons of the A6. These mice die shortly after birth (Morin *et al.*, 1997) and *in vivo* studies of surgically delivered E18 animals show that mutants had a more variable respiratory cycle duration and also a slower respiratory rate compared to WT (Viemari *et al.*, 2004). The reduced respiratory rate in A6 mutants is also indicative of the fact that neurons of the LC have an excitatory effect on the respiratory rhythm. Neurons within the LC area also exhibit an increased firing rate when the level of CO₂ in the whole animal is raised (Coates *et al.*, 1993), data which indicate the importance of NA expressing neurons in mediating the chemosensitive response.

In contrast to the excitatory effects of the neurons of the LC, noradrenergic neurons of the A5 are thought to have an inhibitory effect on respiratory output, since removal of the pons from the neonatal rat brainstem spinal cord prep results in an increase in respiratory activity as measured from the cervical ventral roots (Hilaire *et al.*, 1989). The same study also revealed that electrical

lesioning of the area of A5 results in a significant increase in respiratory frequency.

The medullary regions of A1/C1 and A2/C2 are proposed to be involved in the frequency and stability of the respiratory rhythm respectively. Application of the α -2 noradrenergic receptor antagonist Yohimbine to medullary preparations revealed that the A1/C1 responds to signalling via the alpha-2 noradrenergic receptor, and application of an α -2 antagonist to mouse medullary “en bloc” preparations and brainstem slices results in a decrease in respiratory frequency (Zanella *et al.*, 2006). In contrast, electrolytic lesioning of the dorsal A2/C2 region in mouse brainstem slices does not suppress respiratory output but does result in an increased variability of the respiratory cycle period (Hilaire *et al.*, 1990; Zanella *et al.*, 2006) suggesting that A2/C2 has an involvement in maintaining the stability of the respiratory pattern.

Noradrenergic neurons also express dopamine, a neurotransmitter involved in neuromodulation of the respiratory rhythm and the chemosensitive response. The paraventricular nucleus (PVN) is an important source of the neurotransmitter dopamine, which causes a decrease in respiratory rhythm frequency (Fujii *et al.*, 2004). Application of dopamine onto carotid bodies causes a decrease in ventilatory response to hypoxia (Bee & Pallot, 1995) and blockade of dopamine autoreceptors results in increased chemoafferent activity and ventilation in anaesthetized cats (Iturriaga *et al.*, 1994).

1.4.3 Opiates

Early studies indicate that opiates may have a suppressive effect on respiration as the application of the opioid receptor blocker naloxone caused an increase in phrenic firing and respiratory frequency in anaesthetised cats (Lawson *et al.*, 1979). The preBötC has been shown to express the μ -opioid receptor (Gray *et al.*, 1999). It has been shown that injection of a μ -opioid receptor agonist DAMGO into the preBötC *in vitro* causes an inhibition of respiratory frequency (Gray *et al.*, 1999) while application of opioids to the parafacial nucleus has no effect on respiratory rhythm, suggesting that the pFRG is opioid insensitive (Janczewski *et al.*, 2002; Mellen *et al.*, 2003). This data indicates that the suppressant effects of opioids on the respiratory rhythm are due to suppression of the opiate-

sensitive preBötC. Opiates also act upon other neurons in the VRG which regulate tidal volume, upper airway resistance and pulmonary compliance (Lalley, 2008).

1.4.4 Substance P

Substance P (subP) is a neuropeptide found in many neurons including neurons of the nTS, nucleus ambiguus and raphe magnus (Kachidian *et al.*, 1991), all areas which project to or receive input from the respiratory rhythm generating pre-BötC region (Bianchi *et al.*, 1995). Activity at the 4th cervical nerve (C4) is often used as a measure of respiratory activity, since this is an area where the phrenic nerve (involved in innervation of the diaphragm) originates from. *In vitro* studies of the rat brainstem-spinal cord prep show that perfusion with subP can have varying effects on pre-inspiratory and C4 activity depending on the basal rate of respiration. C4 activity is enhanced by application of subP when basal rate is low, yet the activity seems depressed when subP is applied to preparations with a higher basal rate (Yamamoto *et al.*, 1992). Taking discharge from the hypoglossal nerve rootlets a measure of inspiratory activity, it was shown in rat neonatal medullary slice preparations that bath application of subP leads to an increase in inspiratory frequency (Johnson *et al.*, 1996). In rhythmically active adult rat brainstem slices the injection of subP into the preBötC enhances bursting of the inspiratory neurons via activation of the NK1 receptors (Gray *et al.*, 1999).

1.5 Rhythmic Breathing

Rhythmic movements such as walking, running and breathing are produced by central pattern generator (CPG) networks, specialised circuits capable of producing rhythmic activity and subsequent motor output without requiring input from other central circuits or sensory feedback signals (Marder & Calabrese, 1996). Individual CPG networks may become part of larger neural networks which can be influenced by central and peripheral sensory inputs to allow the pattern of motor output generated by the CPG to be modulated. This type of control is important in respiration as the frequency and amplitude of motor output must change to allow the appropriate response of respiratory muscles to metabolic demand e.g. increased respiration during exercise. It has

long been suggested that rhythmic breathing is generated by a single rhythm generator, the preBötC (Smith *et al.*, 1991). More recent data suggest that rhythmic breathing is controlled by two rhythm generators (Feldman *et al.*, 2003; Mellen *et al.*, 2003; Onimaru & Homma, 2008); the pre-bötzinger complex (Smith *et al.*, 1991) and the retrotrapezoid nucleus/parafacial respiratory group (RTN/pFRG; (Onimaru & Homma, 2003). These generators differ anatomically, yet are functionally connected. It has been proposed that the dominance of one generator over the other may be dependent on the level of excitation of various respiratory neurons (Onimaru & Homma, 2008). For example, the expiratory rhythm generator (RTN) could pace respiration if the inspiratory generator activity (the preBötC) is low (Janczewski & Feldman, 2006).

It has been suggested that the rhythmic activity produced by the preBötC could be based on excitatory and inhibitory interactions between neurons within the area of the preBötC, or rhythm may result from intrinsic cellular mechanisms that give the neurons pacemaker properties. The pacemaker theory suggests that one particular core of neurons with intrinsic bursting properties are responsible for the production of rhythmic activity which is then distributed to subsequent respiratory neurons (Del Negro *et al.*, 2005). Pacemaker neurons were found to exist within the preBötC (Smith *et al.*, 1991) and their properties may be dependant upon the persistent sodium current (Shao & Feldman, 1997; Gray *et al.*, 1999) or calcium mediated currents (Thoby-Brisson & Ramirez, 2001). The idea that pacemaker neurons are necessary for rhythm generation is negated by the fact that in mouse brain stem slices the application of riluzole (6-(trifluoromethoxy)benzothiazol-2-amine), a sodium channel blocker which acts to silence pacemaker neurons that rely upon sodium currents, has no effect on the frequency of the motor output of these slices. It has thus been proposed that calcium dependent pacemaker neurons may drive respiratory rhythm in the absence of the sodium current. Indeed, simultaneous blockage of the sodium and calcium current via application of riluzole and flufenamic acid (FFA) leads to abolished respiratory rhythm in the mouse (Del Negro *et al.*, 2005). However, the expression of sodium and calcium channels are not specific to pacemaker neurons alone and thus application of channel blockers decreases neuronal excitability in the network as a whole (Feldman & Del Negro, 2006) therefore

cessation of respiratory rhythm may not be due solely to the elimination of the pacemaker neurons.

Chloride ions (Cl^-) are important in the maintenance of the resting potential of a cell. In the neonatal rat brainstem spinal cord prep, reduction or removal of extracellular chloride (Cl^-), which effectively removes inhibition of the cell, does not cause cessation of the rhythm in the respiratory motor nerve output, rather a modification of the duration and amplitude of the respiratory bursts (Feldman & Smith, 1989). These results suggest that rhythm generation is not solely dependent on inhibition, yet inhibitory mediators such as Cl^- are needed to modulate the excitability of the rhythm generating neurons. Furthermore, the same group illustrated that antagonising inhibitory amino acid receptors such as GABA or glycine also fails to abolish respiratory rhythm, reiterating the idea that reciprocal inhibition between groups of respiratory neurons is not the underlying mechanism of respiratory rhythm generation. However, these results do not lie in agreement with the *in situ* arterially perfused brainstem spinal cord prep experiment in which reduction of Cl^- in the perfusate eventually led to cessation of respiratory activity as measured from the phrenic and hypoglossal nerve (Hayashi & Lipski, 1992).

In contrast to the idea of a single kernel of pacemaker neurons, the group pacemaker hypothesis suggests that neurons do not possess intrinsic bursting behaviour, instead two connected neurons may excite one another through recurrent synaptic connections (Del Negro *et al.*, 2005) and such stimulation of a group of interconnected neurons could produce self-sustaining burst firing.

1.6 Areas of Rhythm Generation

1.6.1 The Pre-Bötzinger Complex

As mentioned previously, Lumsden (1923) carried out *in vivo* experiments in the cat which suggest respiratory rhythm is generated in the lower brain stem. This concept was further developed in a study which involved removing thin slices from the rat brain stem preparation rostrally and caudally, while recording respiratory activity from spinal or cranial nerves. The result was that rhythmic activity continued until transection was made at the level of the caudal

retrofacial nucleus. Indeed, slicing above this area led to the cessation of rhythmic motor output and therefore a small, ventral medullary region was found to contain the essential rhythm generating circuitry. The area was termed the pre Bötzing Complex (Smith *et al.*, 1991) and forms small bilateral clusters of neurons (approx 600 neurons - 300 on each side) in the ventrolateral medulla. Altering neuronal excitability of the pre Bötzing Complex (preBötC) in neonatal rat brain slices via the application of CNQX (an AMPA receptor antagonist) caused a decrease and eventual elimination of the oscillatory output of the slices (Smith *et al.*, 1991). Since the oscillatory output was used as an indication of respiratory activity, the results implied that that excitatory neurotransmission within the preBötC (via glutamate acting at AMPA receptors) was important for respiratory rhythm generation (Smith *et al.*, 1991). Further *in vitro* experiments in neonatal rats illustrated that a preBötC containing “island” dissected from a brain slice, which eliminates a number of peripheral inputs and gives a truer representation of the intrinsic activity of the preBötC, still produces a respiratory output (Johnson *et al.*, 2001). Activity in the preBötC region precedes XII nerve (a nerve often associated with inspiratory activity) motor output which supports the argument that the preBötC is the site of origin of inspiratory drive (Johnson *et al.*, 2001). The preBötC has a high percentage of propriobulbar interneurons (those which arise and terminate within the brain stem) which may imply that the preBötC has its own individual neuronal organisation. Interneurons within the preBötC were also shown to have connections to other brain areas containing bulbospinal interneurons. This could be a possible pathway for the transmission of respiratory rhythm from the generator, to pre-motor neurons and to spinal motor neurons which control the movement of respiratory muscles (Smith *et al.*, 1991).

Application of substance P and opioids were found to change respiratory frequency (Gray *et al.*, 1999) suggesting that the receptors for these particular peptides were expressed by rhythm generating neurons. The results indicated that the receptor for substance P (neurokinin 1 receptor -NK1R) was expressed by the respiratory neurons in the ventrolateral respiratory column, in the same area in which the preBötC had been shown to reside. Thus NK1Rs were proposed to be markers for the preBötC (Gray *et al.*, 1999). These NK1 expressing neurons were found to be expressed at embryonic day E15 in the mouse, the point at

which spontaneous rhythmic activity occurs in neurons ventral to the nucleus ambiguus, an area analogous to the preBötC (Thoby-Brisson *et al.*, 2005). It was also illustrated that this embryonic preBötC can be modulated by the same neuromodulators which affect the activity of the neonatal preBötC e.g. 5-HT and BDNF (Thoby-Brisson *et al.*, 2005; Bouvier *et al.*, 2008).

An *in vivo* study in rats demonstrated that lesioning of the preBötC via injection of substance P conjugated to saporin (targets only NK1R expressing neurons and deactivates ribosomes) leads to ataxic breathing patterns (Gray *et al.*, 2001; McKay *et al.*, 2005). The preBötC NK1R neurons also express the vesicular glutamate transporter VGLUT2 (Guyenet *et al.*, 2002) and have been identified as immunoreactive for glutamate (Liu *et al.*, 2001), characteristics which suggest that the preBötC NK1R expressing neurons are excitatory. Although mice that lack the NK1R receptor have altered respiratory characteristics, they still continue to breathe (De Felipe *et al.*, 1998) indicating that the NK1R expressing neurons in the preBötC are not essential for breathing itself, but do play a key role in rhythm generation.

The preBötC is also thought to play a part in the response to hypoxia and hypercapnea. Following unilateral ablation of the preBötC there is no significant difference in the ventilatory response of rats exposed to hypoxia during wakefulness (McKay & Feldman, 2008) but a bilateral lesion of the area leads to impaired chemosensitivity (Gray *et al.*, 2001) implying that the preBötC may have a role in the integration of chemosensitive information.

1.6.2 Parafacial Respiratory Group/RTN

The retrotrapezoid nucleus (RTN) was identified as a cluster of interneurons found ventral to the facial nucleus (Smith *et al.*, 1989). These neurons express Phox2b and VGLUT2 mRNA suggesting that they may be glutamatergic (Mulkey *et al.*, 2004; Stornetta *et al.*, 2006). The parafacial respiratory group (pFRG, (Onimaru & Homma, 2003) was identified as an area ventrolateral to the facial nucleus, close to the ventral surface of the medulla which contains Phox2b, VGLUT2 and NK1R expressing neurons (Onimaru *et al.*, 2008). The RTN and pFRG may not be two wholly distinct populations as the regions are known to overlap anatomically (Smith *et al.*, 1989; Onimaru & Homma, 2003; Guyenet

et al., 2005a) and both areas display similar chemical markers e.g. Phox2b and VGLUT2.

There are various opinions as to the function of the RTN/pFRG, one being the maintenance of respiratory rhythm. Janczewski *et al.*, suggest that the preBötC generates inspiratory rhythm whilst the RTN/pFRG produces expiratory rhythm as the application of fentanyl, which is a u-opioid agonist results in absences of inspiration (Janczewski & Feldman, 2006). This may be due to the suppression of activity in the opioid-sensitive inspiratory rhythm generator (preBötC) which ultimately causes loss of activity in inspiratory motor neurons. The fact that expiratory rhythm continues whilst inspiratory rhythm fails suggests that the two phases of respiration are controlled by different rhythm generators. Further to this, partial ablation of the preBötC in awake goats seems to affect inspiration while rhythmic expiratory activity of the abdominal muscles continues (Wenninger *et al.*, 2004), indicating the presence of another respiratory oscillator.

Studies of the newborn rat brain stem-spinal cord preparation have shown bilateral lesioning of the RTN/pFRG results in a reduction in respiratory frequency but not a complete loss of respiratory rhythm (Onimaru & Homma, 2003), once again suggesting that the preBötC is not the sole mediator of rhythmic breathing. It has been shown in neonatal mice that there exists a DAMGO-insensitive rhythm generator functionally coupled to the preBötC (Mellen *et al.*, 2003) which has been suggested to be the RTN/pFRG.

Isolated brainstem preparations of mice embryos exhibit cells bordering the facial motor nucleus which produce spontaneous rhythmic activity at E14.5, preceding activity in the preBötC (E15). This area is termed the embryonic parafacial oscillator (e-pf). The e-pf is known to express NK1R but unlike the preBötC, application of DAMGO ([D-Ala², N-MePhe⁴, Gly-ol]-enkephalin), an opioid peptide, does not abolish rhythmic activity in the e-pf (Fortin & Thoby-Brisson, 2009). The e-pf expresses Phox2b, NK1R and is intrinsically rhythmic, characteristics similar to those of the RTN/pFRG which suggests that the e-pf may be a forerunner of the RTN/pFRG (Fortin & Thoby-Brisson, 2009).

Riluzole is a drug which acts to block TTX-sensitive sodium channels. Application of this drug to silence the e-pf in medullary slices (at a concentration that has no effect on the activity of the preBötC in transverse slices) reveals a reduction in preBötC frequency. This would indicate that although the preBötC can function independently of the e-pf, it may receive input from the e-pf which modifies the preBötC's rhythmic output (Fortin & Thoby-Brisson, 2009).

Since breathing in adult rats becomes disrupted by destroying neurons of the preBötC (Gray *et al.*, 2001) it seems that this area is likely to be the dominant respiratory generator in adulthood. The shift of dominance between the preBötC and RTN/pFRG may change during development, with evidence suggesting that the RTN/pFRG acts as the principal rhythm generator in neonates (Feldman & Del Negro, 2006). This view supported by experiments carried out on Krox-20 mice, animals which do not form the area of the brainstem which houses the RTN/pFRG (Schneider-Maunoury *et al.*, 1993). These animals suffer fatal apnoeas and die early after birth possibly due to the fact that respiration is depressed by the surge of endogenous opiates that occurs at birth acting on the opiate sensitive preBötC (Jacquin *et al.*, 1996). In the WT mouse it is assumed that the presence of the opiate-insensitive e-pf (proposed forerunner of the pFRG/RTN) can compensate for this depression of the preBötC. This proposal is further vindicated by the fact that treatment of the Krox-20 mutants with naloxone (competitive antagonist of opioids) within 48 hours after birth eliminates the fatal apnoeas and the animals survive (Jacquin *et al.*, 1996). Thus it seems that the e-pf/RTN/pFRG may play a vital role in controlling breathing in the neonate until the surge of opiates has subsided.

The RTN/pFRG may also be involved in central chemoreception due to the fact that; a) it lies above a portion of the ventral medullary surface believed to contribute to respiratory chemoreception (Loeschcke, 1982) b) it contains neurons that are sensitive to CO₂ levels and acidification (Mulkey *et al.*, 2004; Guyenet *et al.*, 2005a) and c) mutant mice with a severe depletion of Phox2b (expressed by the RTN/pFRG) lack responsiveness to CO₂ at birth (Dubreuil *et al.*, 2008).

1.7 Chemosensitivity

Respiratory activity serves to regulate blood gases and studies of chemoreception illustrate that in humans, even a 1 mmHg increase in PCO_2 increases ventilation by 20-30% (Feldman *et al.*, 2003). Early studies suggested oxygen levels as being the driving force behind breathing (Rosenthal, 1886) an idea challenged by studies that indicate changes in the pressure of CO_2 in the blood have a much greater bearing on the ventilatory response than the equivalent change in oxygen (Miescher-Rusch, 1885). Haldane and colleagues found that a rise of only 0.2% in alveolar CO_2 led to a doubling of ventilation (Haldane & Priestley, 1905) and it is accepted that PCO_2 is a greater respiratory stimulus than PO_2 . But where does this sensitivity to changes in blood gases arise from? It is debated as to whether the ventilatory response to changes in levels of CO_2 are dependent on specialised sites of central chemosensitivity, or whether they result from the combined effect of several different chemosensitive areas.

1.7.1 Central Chemoreception

To be considered as a central chemoreceptor, neurons must show intrinsic chemosensitivity to changes in PCO_2 that are physiologically relevant, have an appropriate effect on the respiratory output and lie within a region that responds to acidification via altering ventilation (Putnam *et al.*, 2004). Data suggests that it is changes in the pH of the blood which result from increased levels of CO_2 that are detected by neurons rather than direct detection of CO_2 itself. As such, the following areas have been proposed to be involved in central chemoreception.

1.7.1.1 The Locus Coeruleus (LC)

The Locus Coeruleus (LC) contains noradrenergic neurons which display chemosensitive properties *in vitro* (Putnam *et al.*, 2004). Disruption of neurons of the LC via bilateral lesioning using 6-Hydroxydopamine (6-OHDA) leads to a 64% reduction of the ventilatory response to CO_2 in rats (Biancardi *et al.*, 2008). However, 6-OHDA may cause destruction of other neurons rather than specific ablation of the LC NA neurons, thus the results observed may not be due to a depletion of LC NA neurons alone. Other studies indicate that neurons within the

LC exhibit an increase in firing rate when the level of CO₂ in the whole animal is raised (Coates *et al.*, 1993).

1.7.1.2 5-HT Neurons

5-HT neurons make up to 25% of the neuronal population found in the medullary raphe and have been proposed as chemosensors due to the fact that they display chemosensitivity *in vitro* (Wang *et al.*, 2001) and are found in close proximity to cerebral blood vessels (Bradley *et al.*, 2002). Dysfunction of the serotonergic neurons in the brain stem has been associated with disturbances in chemoreception and respiratory rhythm generation (Richerson, 2004). *In vitro* patch clamp recordings of raphe neurons in rat medullary slices show that some neurons respond to increasing CO₂ in a bath solution by increasing firing rate (Richerson, 1995b). Some neurons continued to exhibit a response to 8% CO₂ even after magnesium blockade which acts to stop synaptic transmission. This suggests that the medullary raphe neurons may have intrinsic chemosensitive properties and this may be a specialised site of chemoreception (Richerson, 1995b). The importance of 5-HT expressing neurons in the chemosensitive response is highlighted by the fact that Pet-1 *-/-* mice lack the pet-1 ETS transcription factor, the expression of which is key to the development of 5-HT neurons. These animals exhibit a 70% reduction in the number of central 5-HT neurons (Hendricks *et al.*, 2003) resulting in adult mice which exhibit normal respiration but a blunted ventilatory response when exposed to hypercapnia (Hodges 2005). Focal acidosis of the neurons of the raphe in rats by application of acetazolamide leads to an increase in ventilation, as indicated by an increase in phrenic amplitude (Bernard *et al.*, 1996), data which collectively suggest that the medullary raphe neurons may act as specialised chemosensors. There is evidence to suggest that serotonergic neurons in the rat are not activated by CO₂ when under anaesthesia (Mulkey *et al.*, 2004) suggesting that there may be some degree of state dependent activity with regards to 5-HT neuron activity.

1.7.1.4 The RTN/pFRG

It has been suggested that there exists a predominant site of central chemoreception, namely the RTN (Feldman *et al.*, 2003; Guyenet *et al.*, 2008).

RTN neurons in coronal brain slices of the adult rat brain exhibit increased firing rates with a decrease in pH (Guyenet *et al.*, 2005a). Studies in rats with denervated carotid chemoreceptors illustrate that the response of the RTN to hypercapnia is no different to animals whose chemoreceptors remained intact. This suggests that the CO₂ sensitivity of the RTN is not solely dependent on input from peripheral chemoreceptors and the chemosensitivity may well be an intrinsic property of these neurons (Mulkey *et al.*, 2004). RTN neurons express Phox2b, a transcription factor that is essential to the proper development of respiratory systems (Dauger *et al.*, 2003). Phox2b27Ala/+ mice possess a mutation which mimics the condition known as congenital central hypoventilation syndrome (CCHS) which results in the patients inability to respond to increases in CO₂. In the same way, Phox2b27Ala/+ mice do not respond to hypercapnia, dying soon after birth. The neurons of the RTN are found to be severely depleted in this model, indicating their importance in modulating chemosensitivity (Amiel *et al.*, 2009). RTN neurons still respond to changes in CO₂/pH in the presence of glutamate and GABA receptor blockers, which serve to block synaptic connections (Mulkey *et al.*, 2007), indicating that the neurons are intrinsically chemosensitive and do not rely on network activity. If the RTN is important in chemosensitivity then it can be assumed that the death of Krox20^{-/-} mutants, which lack the area containing the RTN (Jacquin *et al.*, 1996), may be due to a deficiency in the chemosensitivity response rather than a failure in the maintenance of respiratory rhythm.

1.7.2 The Specialised and Distributed Theories of Central Chemoreception

The specialised theory of central chemoreception suggests that the chemoreflex results from the reaction of a limited number of specialised neurons which function to detect changes in pH and feed this information to the respiratory network. As mentioned above, RTN neurons of the adult rat brain are found to exhibit increased firing rates in response to a decrease in pH (Guyenet *et al.*, 2005a) and studies in rats with denervated carotid chemoreceptors illustrate that RTN can mediate a respiratory response to hypercapnia in the absence of peripheral input, suggesting chemosensitivity may well be an intrinsic property of these neurons (Mulkey *et al.*, 2004). As such, the area of the RTN has been

implicated as a key area in the specialised theory of central chemoreception, however there also exist arguments which suggest the RTN could be a part of the distributed theory central chemoreception.

The distributed theory of chemoreception proposes that the central chemoreflex is due to the collective response of various groups of respiratory neurons to changes in pH. This theory is based on observations that *in vitro* and in cell culture a large number of neurons respond, at some level, to acidification (Putnam *et al.*, 2004). Also, bathing regions such as the nTS and RTN, which are known to be involved in the regulation of respiration, in CO₂ rich saline results in respiratory stimulation (Nattie, 2006). Krause *et al.*, show that although focal acidosis in the preBötC of the awake goat does increase ventilation, the increase that results from global brain acidosis is greater (Krause *et al.*, 2009) thus supporting the idea that central chemosensitivity results from collaborative activity of various chemosensitive sites rather than one or two specialised areas. For example, it has been suggested that the effects of the medullary raphe on the central chemoreflex is due to the fact that serotonergic neurons have an excitatory effect on cells of the RTN and the preBötC rather than actually being able to detect changes in PCO₂ *in vivo* (Mulkey *et al.*, 2007). Also, as discussed in previous sections, RTN neurons have a large response to hypercapnia *in vivo* (Mulkey *et al.*, 2004) but it is still unclear as to how much of this response is intrinsic to the RTN neurons themselves. Although there is much evidence to suggest that the RTN may act as a specialised site of chemoreception, it has also been suggested that the RTN may act as a site to integrate chemosensitive information from other regions (Guyenet *et al.*, 2008) such as the medullary raphe and the nTS.

1.7.3 Peripheral Chemoreception

The ventilatory response to changes in PCO₂ and PO₂ may not only be driven by central chemoreception. Changes in oxygen levels within the blood are detected by peripheral chemoreceptors, namely the carotid and aortic bodies, and exposure to hypoxia has been shown to increase the sensory discharge of both carotid and aortic bodies (Lahiri *et al.*, 1981). Located at the aortic arch, the aortic bodies play more of a secondary role in detection of oxygen levels within the blood compared to the carotid bodies, with suggestions that the aortic

chemoreceptors only become of more importance in the absence of the carotid chemoreceptors. For example, injection of sodium cyanide into the external carotid artery of the rat results in a greater stimulation of respiration than application of the drug at the ascending aorta (Sapru & Krieger, 1977).

Recent studies have suggested that central chemosensitivity may interact with and be modulated by input from peripheral chemoreceptors. For instance, studies in the rat have shown that neurons of the RTN, an area proposed to be involved in both respiratory control and chemosensitivity may receive input from the carotid bodies. Results show that output from neurons of the RTN in response to hypoxia or injection of sodium cyanide ceases in animals with denervated carotid bodies (Takakura *et al.*, 2006). Further studies in unanaesthetised dogs also reveal that inhibition of the carotid body chemoreceptor output results in a reduction in the ventilatory response of the central chemoreceptive mechanism whereas stimulation of the carotid body leads to an increase in ventilation in response to central hypercapnia (Blain *et al.*, 2010).

1.8 Rett Syndrome

Rett syndrome (RTT) is a neurodevelopmental disorder that was first described in 1966 in publications by the paediatrician Dr Andreas Rett, who noted that some of his female patients exhibited similar abnormal behaviours and also demonstrated similar clinical histories. The disease became more widely recognised when later published on by Dr Hagberg in 1983 (Hagberg *et al.*, 1983). Rett syndrome affects approximately 1 in 10,000 girls (Hagberg, 1985; Amir *et al.*, 1999b) with classic Rett patients reaching developmental milestones and progressing normally until 6-18 months of age, at which point symptoms start to become apparent. These symptoms include loss of speech, seizures, autism, stereotypic hand movements and breathing irregularities (Hagberg *et al.*, 1983) such as apnea, breath holding, and periods of hyperventilation. It has been proposed that these irregularities may be the cause of sudden death seen in some RTT patients (Kerr *et al.*, 1997).

1.8.1 Genes Involved in Development of the Rett Phenotype

Differing variants of the Rett phenotype exist and often each variant possesses overlapping symptoms. Studies of female Rett patients suggest that a congenital variant of Rett syndrome, first described in 1985 (Rolando, 1985), results from mutations in the FOXP1 gene and gives rise to symptoms such as hypotonia, impaired motor development and stereotypical hand movements (Ariani *et al.*, 2008; Mencarelli *et al.*, 2010) some of which are reflected in classic Rett syndrome. Unlike classic Rett syndrome, there is no period of normal development associated with the congenital variant. Another variant of Rett syndrome again involves symptoms similar to classic Rett syndrome, with patients presenting hand wringing movements and loss of speech skills, but also gives rise to seizures which begin in infancy. This early-onset seizure variant is thought to be caused by mutations in the CDKL5 gene (Weaving *et al.*, 2004; Evans *et al.*, 2005).

Exclusion mapping studies involving RTT families show the locus of classic Rett syndrome is mapped to Xq28 (Curtis *et al.*, 1993) and genetic analysis of this location identified mutations in the gene which encodes for methyl-CpG-binding protein 2 (MECP2) (Amir *et al.*, 1999a). It has been found that 70-90% of classic RTT patients show a loss of function mutation in MeCP2 gene (Shahbazian & Zoghbi, 2001). Familial recurrence accounts for approximately 1% of reported RTT cases while the majority result from sporadic mutations (Schanen *et al.*, 1997).

1.9 MECP2

MECP2 was originally believed to act as a DNA transcriptional repressor (Jones *et al.*, 1998; Nan *et al.*, 1998), attracted to methylated CpG sites of the genome (Nan *et al.*, 1996; Skene *et al.*, 2010). Methylated cytosine is often found at the beginning of a gene, the site at which regulation of expression occurs via binding of transcription factors. When a gene is expressed, the chromatin is unfolded and DNA is “open”, a state which is maintained by the acetylation of histones (Fig 1-2 image A). MeCP2 acting as a repressor binds to the CpG sites at the beginning of the gene via its methyl binding domain and recruits the co-repressor complex (Sin3A and HDAC1&2) which leads to subsequent

deacetylation of histones (Nan *et al.*, 1998) and compression of the chromatin. This causes folding of the DNA resulting in the inability of the transcriptional machinery to transcribe the gene (Amir & Zoghbi, 2000) thus rendering it silent. This model of MeCP2 action was challenged by investigation of hypothalamic RNA from *Mecp2* null mice which reveals that some genes are down regulated in the absence of *Mecp2*, suggesting its action as an activator (Chahrour *et al.*, 2008a). When acting as an activator of gene expression, MeCP2 binds to the CpG site and recruits a co-activator complex (creb-1) which results in release of histones and unfolding of chromatin. The unfolded DNA is then open to transcriptional machinery and the gene becomes active. More recent studies go on to suggest that MeCP2 may not be just a neuronal based transcriptional repressor but may infact act to reduce transcriptional noise in the whole genome (Skene *et al.*, 2010)

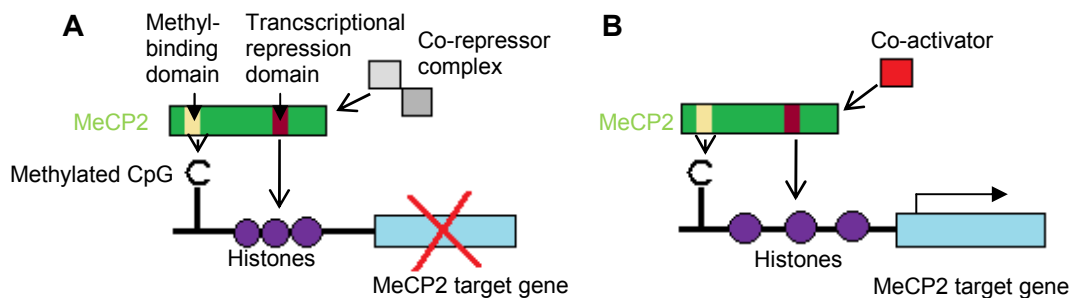


Fig 1-2 MeCP2 as a transcriptional activator and repressor. A – MeCP2 as a transcriptional repressor. MeCP2 binds to methylated CpG sites at the beginning of the target gene. MeCP2 subsequently recruits the co-repressor complex, leading to deacetylation of histones and compression of the chromatin. The resultant folding of DNA prevents transcriptional machinery from transcribing the target gene. **B** – MeCP2 as a transcriptional activator. MeCP2 binds to methylated CpG site at beginning of target gene and recruits the co-activator complex. This results in acetylation of histones and an unfolding of the chromatin. The DNA is then in an open state and accessible to transcriptional machinery. Image modified from (Samaco & Neul, 2011).

1.9.1 Expression of *Mecp2*

MeCP2 is present in the lungs, spleen and brain (Shahbazian *et al.*, 2002b) and as such has been proposed to act as a global transcriptional repressor/activator. However, deletion of the *Mecp2* gene from neurons alone in mice results in a phenotype similar to that of mice with a ubiquitous deletion of *Mecp2* which indicates that the gene may have a more prominent neurological role (Chen *et al.*, 2001). It was originally proposed that *Mecp2* was abundant in neurons but absent from glia (Shahbazian *et al.*, 2002b; Kishi & Macklis, 2004) but recent evidence now indicates that *Mecp2* is expressed in the glia of normal adult rat brains but is absent from the glia of *Mecp2* deficient brains (Ballas *et al.*, 2009).

Expression of *Mecp2* correlates with the maturation of the central nervous system in both humans and mice e.g. the spine and brain stem develop first, followed by cerebral hemispheres. Likewise, *Mecp2* is first expressed in the brainstem and spinal cord, followed by late expression in the cortex and hippocampus (Shahbazian *et al.*, 2002b). As such, *Mecp2* is proposed to play a key role in maturation of neurons and also neuronal maintenance (Minh *et al.*, 2012).

1.9.2 MeCP2 in Development

Girls that suffer from RTT develop normally until about 6-18 months of age at which stage they begin to experience neurological regression. Since there is no evidence of neuronal death (Armstrong *et al.*, 1995) the regression may be due to the fact that in the absence of MECP2, neurons are unable to reach the appropriate level of maturity. Indeed it has been shown that cortical neurons in RTT patients have reduced dendritic branching (Armstrong *et al.*, 1995) and reduced neuronal size (Bauman *et al.*, 1995) suggesting a certain degree of immaturity. RTT-like symptoms in a MeCP2 deficient mouse model can be reversed by reactivation of the *Mecp2* gene (Guy *et al.*, 2007). Activating *Mecp2* expression between 1-2 weeks of age in MeCP2 deficient mice leads to a significant rescue of the symptoms while activation at a later time point (2-4weeks) proves less efficient at rescuing the phenotype. However, the most efficient rescue occurs in the animals that undergo activation at a very early stage of development (E10) and also activation of *Mecp2* in post mitotic neurons

(Giacometti *et al.*, 2007). The phenotype of the mutant animals was never rescued to WT level, even after the earliest reactivation of *Mecp2*, perhaps due to a lack of activation of *Mecp2* expression in areas such as the cerebellum, important in sensory perception and motor output, resulting in reduced motor activity. Conversely, the failure to recover could also be due to an over expression of MeCP2 when the gene is reactivated, as studies have shown that over expression of the protein can have detrimental effects on CNS function in mice (Collins *et al.*, 2004).

1.9.3 Mutations of *Mecp2*

There are over 200 different mutations of *MECP2* associated with RTT (Ogier & Katz, 2008) most of which occur *de novo*. Some affect the residues of the MeCP2 protein which are involved in DNA binding, while other mutations may change the structure of the protein, alter its function, or modify the way in which it interacts with other proteins. There exist nonsense, frame shift and splicing mutations which result in the production of a truncated protein (Amir & Zoghbi, 2000) and it has been suggested that these shortened proteins retain the methyl binding domain. This means the MeCP2 protein can still interact with DNA, but lacks the transcriptional repression domain so cannot recruit the co-repressor complex which is required to repress transcription (Chandler *et al.*, 1999). A study was carried out to attempt to correlate the mutation type with clinical traits of the syndrome and the results indicate that there is a positive correlation between truncating mutations and breathing abnormalities (Amir *et al.*, 2000).

Another important factor in the severity of the RTT phenotype is the fact that the *MeCP2* gene is subject to random X chromosome inactivation (XCI). Female heterozygotes are somatic heterozygotes e.g. the cells which have a mutated allele on the inactivated X chromosome will have a normal phenotype, and cells with the mutant allele on the active X will display the affected phenotype. The overall severity of the phenotype is therefore thought to depend on the pattern of X inactivation (Ogier & Katz, 2008) and in fact, some carrier females are completely asymptomatic due to extreme skewing of XCI (Wan *et al.*, 1999)

1.9.4 Animal Models of Dysfunctional *Mecp2*

MeCP2 deficient mice exhibit a similar phenotype to that of the human condition including irregular breathing activity *in vivo* (Viemari *et al.*, 2005). As such, various mouse models have been developed to allow further investigation into the role of MeCP2 in RTT (table 1.1).

Mecp2^{308/y} mice exhibit a truncation of the MeCP2 protein at amino acid 308, which is a known human mutation in RTT. These mice develop a neurological disorder that resembles RTT and display symptoms such as loss of motor skill, stereotypical paw movements and disturbances in behaviour (Shahbazian *et al.*, 2002a).

Mecp2^{flox/y} mice express a hypomorphic *Mecp2* allele resulting in only 50% of the WT level of MeCP2 being expressed. These animals exhibit altered social behaviour, reduced learning and motor deficits as well as an increased incidence of apnea and increases in the variability of respiratory rhythm (Samaco *et al.*, 2008).

Mecp2^{TG1} mice over express the MeCP2 protein at levels two fold greater than the WT and whilst they show enhanced motor learning and increase synaptic plasticity in the hippocampus, they also go on to develop seizures and display hypoactivity (Collins *et al.*, 2004) which indicates the importance of maintaining appropriate MeCP2 levels *in vivo*.

The *Mecp2*^{tm2Bird} model involves the insertion of a LoxStop cassette into the DNA, which silences the *Mecp2* gene. A deficit in MeCP2 develops and the mice begin to display RTT-like symptoms. The gene can be reactivated by Tamoxifen driven cassette deletion (Guy *et al.*, 2007). The mice develop breathing abnormalities, such as apnea, which are similar to those seen in the human condition and re-activation of the gene leads to a significant reversal in the phenotype of severely affected mice, including a restoration of the abnormal breathing and other behavioural parameters (Guy *et al.*, 2007; Robinson *et al.*, 2012).

Mouse model	Genetic Manipulation	Phenotype	References
Mecp2Bird	Deletion of exon 3 and 4. Results in Mecp2 null mice	Neurological symptoms, behavioural symptoms and early onset of death	Guy <i>et al.</i> ,(2001)
Mecp2Tam	Deletion of methyl binding domain. Mecp2 null mouse	Similar to Mecp2Bird model	Pelka <i>et al.</i> ,(2006)
Mecp2Jae	Deletion of exon 3 and partial deletion of exon 4. Results in truncated Mecp2 protein.	Neurological symptoms at 4 weeks and death between 6-12 weeks.	Chen <i>et al.</i> , (2001)
Mecp2 308/y	Truncation of Mecp2 protein at amino acid 308, preservation of methyl binding domain and transcriptional repression domain.	Progressive neurological symptoms but survival is longer compared to other models, with mice surviving for up to 1 year	Shazabian <i>et al.</i> , (2002)
Mecp2Tg1	WT human Mecp2 gene overexpressed in transgenic mice. Mecp2 is then expressed 2 fold WT levels.	Phenotype appears at around 10 weeks. Enhanced motor skills and synaptic plasticity but at 20 weeks seizures develop and a third of mice die at one year old.	Collins <i>et al.</i> , (2004)
Mecp2 Flox/y	Conditional "floxed" Mecp2 allele which mimics loss of function mutation. Results in 50% reduction of Mecp2 RNA and protein expression	Mice have learning and motor deficits along with respiratory disturbances	Samaco <i>et al.</i> ,(2008)
Sim1-cKO	Mecp2 absent from neurons of the hypothalamus	Normal life span but increased aggression, heightened stress response and hyperphagia	Fyffe <i>et al.</i> , (2008)
Nestin-cKO	Mecp2 absent from neurons and glia (from embryonic stage)	Similar to mecp2 null mouse	Chen <i>et al.</i> ,(2001) Guy <i>et al.</i> ,(2001)
CamKII-cKO	Mecp2 absent from forebrain (from postnatal stage)	Normal life span, increased anxiety and abnormal social behaviour	Chen <i>et al.</i> ,(2001) (Gemelli <i>et al.</i> , 2006)
Th-cKO	Mecp2 absent in catecholaminergic and noradrenergic neurons	Normal life span, mild phenotype and reduced NA/DA content as measure by reduced TH expression	Samaco <i>et al.</i> , (2009)
Pet-cKO	Mecp2 absent from serotonergic neurons	Normal life span, increased aggression, reduced 5-HT expression	Samaco <i>et al.</i> , (2009)

Table 1.1 Mouse models of MeCP2 deficiency and overexpression. A few select examples of the mouse models used to study Rett Syndrome.

1.10 Respiratory Phenotype in RTT

In humans, the breathing phenotype associated with RTT usually includes an increased occurrence of apneas and highly unstable breathing patterns with periods of breath holding, hyperventilation and variable breath duration (Weese-Mayer *et al.*, 2006; Cirignotta *et al.*, 1986). It was originally thought that these breathing abnormalities occurred only in wakefulness and that RTT patients showed a more rhythmic pattern of breathing in sleep, an unusual theory as respiratory patterns are normally more disordered in sleep states. However, recent research illustrates that breathing disturbances are observed in sleep (Rohdin *et al.*, 2007) though the severity of said abnormalities are not as severe as those observed in wakeful states.

Studies in both humans and mice have proposed several hypotheses as to why respiration is disturbed in RTT syndrome. Some suggest that there exists some degree of cortical dysfunction which affects behaviourally associated respiratory dysfunction (Marcus *et al.*, 1994). Some anecdotal observations suggest that irregularities in breathing may be pleasurable to the patients, as the girl's involved in their studies often emerge from the apnoeic episodes laughing and not in a state of panic (Elian & Rudolf, 1991). However, support for this particular hypothesis is sparse. Other hypotheses propose that the respiratory defects are due to the immaturity of the brain stem given that functions controlled by the brain stem such as the cardiac sensitivity to baroreflex and cardiac vagal tone are reduced in Rett syndrome patients (Julu *et al.*, 2001). The *in situ* perfused brainstem preparation of *Mecp2* KO mice reveals that evoking fictive HBR reflex causes apnea suggesting that there is a dysfunction in the central and vagal control of post inspiratory control in the *Mecp2* KO mouse. Also, WT animals show sensitisation to this reflex but the mutant mice do not (Stettner *et al.*, 2007) indicating an alteration in the functioning of the respiratory network.

Mecp2 KO mice also exhibit fewer connections between neurons in the respiratory network and the rhythmic pattern is often interrupted by spontaneous and long lasting calcium increases (Mironov, 2009). Calcium transients are important in neuronal development (Spitzer *et al.*, 2002) and the length and duration of these signals can cause elongation or retraction of the neuronal processes. For example, exposing inspiratory neurons of neonatal mice

to hypoxia produces an increase in calcium transients which in turn promote a retraction of neuronal processes (Mironov & Langohr, 2005). One of the breathing irregularities that RTT patients often exhibit are periods of apnea which can worsen and become more frequent with the progression of the disease. The hypoxic conditions that result from apneic breathing may lead to an increase in calcium transients, a subsequent retraction of the neuronal processes and as such a malformed and unstable respiratory network. This would induce further breathing difficulties and the cycle continues until respiratory failure, and ultimately death, occurs.

1.11 Neuromodulation and Chemosensitivity in RTT

1.11.1 Noradrenaline

As mentioned previously, the neurotransmitter noradrenaline (NA) is important in modulation of the respiratory pattern. Various studies of the brains of RTT patients and MeCP2 deficient mice have described a reduction in NA content associated with RTT (Riederer *et al.*, 1985; Zoghbi *et al.*, 1985). *Mecp2^{-/y}* mice show no significant difference compared to WT in the level of bioamines at birth, but NA content tends to be reduced at P14 and at P28 both NA and 5-HT content are reduced (Ide *et al.*, 2005) implying that progression of the irregular breathing phenotype may correlate with a degeneration of the NA neuromodulatory system.

NA deficits in *Mecp2^{-/y}* mice may be due to the deficient expression of tyrosine hydroxylase (TH) and dopamine beta hydroxylase (DBH)(Zhang *et al.*, 2010b), enzymes which are important in the synthesis of noradrenaline. TH is an enzyme which is critical in the production of noradrenaline and acts as the rate-limiting step of catecholamine production. As such, TH is often used as a marker for noradrenergic neurons. Evidence shows that there is a reduction in the number of LC TH positive neurons of *Mecp2^{-/y}* mice (Roux *et al.*, 2010). NA producing cells of the locus coeruleus are important in early life as mice with *Phox2a* mutations, which cause targeted loss of these NA neurons, have unstable breathing and die soon after birth (Viemari *et al.*, 2004). Neurons of the LC are also implicated in the chemosensitive response (Biancardi *et al.*, 2008) and thus a reduction in neurons of the LC in MeCP2 deficient mice may account for some of the respiratory abnormalities observed in these animals.

As previously discussed, medullary A1/C1 and A2/C2 regions are thought to be involved in maintaining the frequency and stability of the respiratory rhythm (Hilaire *et al.*, 1990; Zanella *et al.*, 2006). TH expression in male *Mecp2*-null mice is normal at birth but reduced in the A2/C2 region at one month old and the A1/C1 at 2 months old (Viemari *et al.*, 2005), an age when the respiratory phenotype becomes apparent. This indicates that NA deficits play a role in the development of the breathing abnormalities of *Mecp2* deficient mice. *In vitro* studies of *Mecp2*^{-y} mice show that spontaneously generated bursts recorded from the VRG (network that generates respiratory rhythm) have an irregular cycle period compared to WT slices and that exogenously applied NA eliminates this irregularity (Viemari *et al.*, 2005). Furthermore, increasing the levels of NA *in vivo* via the administration of the NA reuptake inhibitor Desipramine improves respiratory function in *Mecp2*-null mice (Roux *et al.*, 2007).

NA may be directly affected by the absence of MeCP2 as an *Mecp2*-binding site is found in the tyrosine hydroxylase promoter (Yasui *et al.*, 2007) revealing the possible regulation of TH by the MeCP2 protein.

1.11.2 5-HT

Serotonin (5-HT) is important in the development of the respiratory network, the stability of breathing and maintenance of respiratory rhythm. As with noradrenaline, reductions in 5-HT levels are associated with the RTT phenotype (Riederer *et al.*, 1985). Evidence suggests that breathing disturbances become more severe in *Mecp2*^{-y} mice at approximately 2 months of age when the 5-HT content of *Mecp2*^{-y} mice becomes reduced (Viemari *et al.*, 2005). Differences in 5-HT levels between WT and *Mecp2* KO mice become greater with age (Ide *et al.*, 2005) and the developing 5-HT deficit seems to coincide with the progression of the respiratory abnormalities in *Mecp2*^{-y} mice.

A reduced 5-HT content in MeCP2 deficient mice and RTT patients may account for some of the instability of the breathing pattern, given that studies in 5-HT deficient mice have demonstrated an increased variability in respiratory output compared to WT (Hendricks *et al.*, 2003) and frequent apnea during postnatal development (Hodges *et al.*, 2009) as discussed in section 1.4.1. Since 5-HT plays a key role in the developmental process, reduced 5-HT levels which results from a deficiency in MeCP2 may affect the maturation of the respiratory

network resulting in an immature and unstable respiratory network and a disturbed respiratory pattern.

Lmx1b f/f/p mice also exhibit a decreased ventilatory response to hypercapnia (Hodges & Richerson, 2008) suggesting that 5-HT neurons could play a part in the chemosensitive response. A reduction in 5-HT levels of MeCP2 deficient mice may therefore account for certain chemosensitive deficits of MeCP2 deficient mice, such as a disruption in hypercapnic sensitivity (Zhang *et al.*, 2010b)

1.11.2 Brain Derived Neurotrophic Factor (BDNF)

Brain Derived Neurotrophic Factor (BDNF), a target gene of MeCP2, plays a critical role in survival, maturation and plasticity of neurons and is important in the development of certain neurons involved in respiratory control (Erickson *et al.*, 1996; Katz & Balkowiec, 1997; Katz, 2005). Studies of the brainstem spinal cord prep of BDNF null mice reveals a greater variability in respiratory cycle length compared to the WT and also central respiratory output is depressed (Balkowiec & Katz, 1998) suggesting that BDNF is important in development of the respiratory network.

MeCP2 is thought to be a transcriptional repressor of BDNF (Chen *et al.*, 2003) in the absence of neuronal activity. Membrane depolarisation, as a result of neuronal activity, results in the release of MeCP2 from BDNF and an activity-dependent upregulation of BDNF occurs (Chen *et al.*, 2003) hence the level of BDNF expression is activity dependent (Balkowiec & Katz, 2002). As BDNF is thought to be suppressed by MeCP2, it could be hypothesised that an absence of MeCP2 would result in increased levels of BDNF in MeCP2 deficient mice. However, there is evidence of reduced levels of BDNF in the brains of MeCP2 deficient mice (Chang *et al.*, 2006b; Sun & Wu, 2006). This incongruity may be accounted for by the fact that studies have highlighted a reduction in cortical activity in the *Mecp2* mutant brain (Dani *et al.*, 2005), and as BDNF is activity dependent, it follows that reduced cortical activity could result in reduced levels of BDNF. It has also been shown that MeCP2 deficient mice have an upregulation of transcriptional repressors Rest and Co-rest (Abuhatzira *et al.*, 2007), which may bind to BDNF to repress it again accounting for reduced levels of BDNF expression in the absence of MeCP2.

Evidence implies *Mecp2*-null mice also exhibit deficits in BDNF levels that deplete further with age, and that increasing the expression of BDNF in the mutant mouse can improve the RTT phenotype (Chang *et al.*, 2006b; Wang *et al.*, 2006). Endogenous expression of BDNF can be elevated via the application of ampakine drugs which facilitate the activation of glutaminergic AMPA receptors (Ogier *et al.*, 2007). This facilitation results in a lengthened duration of AMPA mediated inwards current, causing an increase in the activity of neurons that express these receptors (Nagarajan *et al.*, 2001) and consequently an increase in the activity-dependent expression of BDNF. This increase in BDNF was shown to restore the breathing frequency and minute volume of MeCP2 null mice to that of the wild type (Ogier *et al.*, 2007).

BDNF has also been implicated in the chemosensitive response, as BDNF null mice show no ventilatory response to hypoxia (Gaultier & Gallego, 2008) and do not show the typical decrease in ventilation when exposed to 100% O₂, although the animals still displayed an increase in ventilation in response to 5% CO₂ (Erickson *et al.*, 1996). BDNF null mice also exhibit a loss of dopaminergic neurons of the petrosal ganglion (Erickson *et al.*, 2001), neurons which are important in the chemoafferent pathway. As RTT patients are known to exhibit reduced levels of BDNF, it follows that the breathing irregularities observed may again be due to a deficit in chemosensitivity.

BDNF also modulates glutamatergic transmission at second order neurons in the nTS (Balkowiec & Katz, 2000), an area where peripheral afferent input is relayed to the brainstem respiratory rhythm generating network. Reduced BDNF levels found in RTT patients and MeCP2 deficient mice could result in inadequate relaying of information by the nTS BDNF can have affect on the function of the fetal mouse preBötC given that NK1 expressing neurons of the preBötC also express the TrkB receptor, for which BDNF is the primary ligand. BDNF increases the frequency of rhythmic activity in the fetal preBötC network and modulates the activity of endogenous bursting neurons in the fetal preBötC .However, in contrast to these findings that BDNF increases respiratory frequency, the newborn mouse brain stem reveals a decrease in respiratory frequency when exposed to BDNF (Thoby-Brisson *et al.*, 2003; Bouvier *et al.*, 2006). Since BDNF is

shown to be reduced in RTT patients it may follow that misregulation of the rhythm generating neurons of the preBötC by BDNF may contribute to the respiratory phenotype seen in RTT patients.

1.11.3 GABA and Glutamate

In normal postnatal development, there are alterations in the level of expression of NMDA, GABA and glycine receptors. It has been suggested that there exists an increase in the number of inhibitory receptors while the number of excitatory receptors decreases (Wong-Riley & Liu, 2005). In the hippocampus of *Mecp2*-null mice, the lack of MeCP2 expression seems to correspond with an altered expression of certain NMDA receptor sub units in the fore brain, leading to changes in synaptic plasticity that may ultimately result in the functional defects that are observed in RTT syndrome (Asaka *et al.*, 2006). MeCP2 may have a role in the developmental changes in levels or receptors (Young *et al.*, 2005) given that there is a down regulation of GABA subunit regulatory genes in the *Mecp2*^{-/y} KO mice compared to WT (Samaco *et al.*, 2005). A deficiency in MeCP2 may lead to changes in the ratio of excitatory to inhibitory transmission and change excitability of certain neurons in the brain, illustrated by reports that girls who suffer with RTT have increased excitatory activity (Johnston *et al.*, 2001). There is also evidence of changes in the excitability of neurons within the Kölliker-fuse nucleus and parabrachial nuclei, highlighted by the fact that there is an exaggerated respiratory response to microinjections of glutamate into the Kölliker-fuse nucleus of *Mecp2*^{-/y} mice at P40, an age at which the RTT phenotype is said to be fully expressed (Stettner, Huppke *et al.* 2007). The same study also reports a level of hyper excitability in post-inspiratory neurons of the *in situ* perfused brain stem preparation of *Mecp2*-null mice. Both the Kölliker-fuse and parabrachial nuclei densely express NMDA receptors therefore changes in levels of expression of these receptors may lead to hyperexcitability of the neurons. Treatment of RTT syndrome patients with drugs that have GABAergic effects (eg. Topiramate, anti epileptic drug) improves respiratory abnormalities perhaps enhancing inhibitory neurotransmission (Goyal *et al.*, 2004). *Mecp2*^{-/y} mice exhibit breathing abnormalities which can be transiently restored via application of the benzodiazepine Midazolam (Voituron & Hilaire, 2011) again highlighting that fact that the respiratory disorders observed in RTT may be a result of the imbalance between excitatory and inhibitory neurotransmission.

1.11.4 Substance P

As discussed earlier in the review, substance P is known to have a role in the modulation of respiration. Substance P is an agonist of the NK1 receptor which is expressed by cells of the preBötC (Gray *et al.*, 1999). Levels of subP are reduced in the cerebrospinal fluid of RTT patients (Matsuishi *et al.*, 1997; Deguchi *et al.*, 2000) with immunoreactivity of subP in the human brain reduced in various parts of the medulla, pons and locus coeruleus (Deguchi *et al.*, 2000). A reduction in substance P levels may have a knock on effect on the functioning of the preBötC and could be hypothesised as a contributing factor to the breathing abnormalities seen in RTT patients.

1.12 Mecp2 in the Periphery

The majority of research into MeCP2 and its role in the respiratory disorders of RTT has been neurological and there are few studies investigating the effects of MeCP2 in the periphery. The role of MeCP2 in the whole body is of interest because MeCP2 protein is also present in non-neuronal tissues such as the kidney, heart, spleen and lung tissue (Shahbazian *et al.*, 2002b). There is also evidence of reduced bone density in RTT patients (Leonard *et al.*, 1995; Haas *et al.*, 1997) and reductions in bone volume and bone formation in *Mecp2*^{-/-} mice, which precede any neurological symptoms and which also worsen with age (O'Connor *et al.*, 2009). These data highlight that MeCP2 may play a role in the development of peripheral tissues and indeed a recent study revealed that some degree of pulmonary disease may be associated with RTT. Imaging studies were carried out on girls with *MECP2* mutations and revealed that pulmonary lesions and respiratory bronchiolitis associated interstitial lung disease (RBILD)-like lesions were present in half of the patients studied (De Felice *et al.*, 2010). However, experimentation using mouse models of RTT syndrome have yet to approach studying the morphology of the lung in MeCP2 deficient animals.

1.13 Aims of the Thesis

The studies in this thesis were aimed at observing the development of respiratory abnormalities in male and female MeCP2 deficient and investigating the underlying mechanisms.

By utilising a male model of RTT syndrome in which the *Mecp2* gene can be silenced and subsequently reactivated, observations were made *in vivo* of a) the development of the RTT-like phenotype in absence of MeCP2, and b) the rescue of the RTT like phenotype when *Mecp2* has been reactivated. A further aim was to investigate any alterations in the chemosensitive response of male MeCP2 deficient mice by monitoring the respiratory response to hypercapnia.

Neuromodulators play a key role in shaping the respiratory pattern and thus investigation was aimed at elucidating a) whether or not there were changes in the cell count of various noradrenergic and serotonergic regions in MeCP2 deficient male mice, and b) how cell numbers were affected by the presence, absence and reactivation of *Mecp2*.

As RTT syndrome is a female based disorder it was of benefit to observe the development of respiratory abnormalities in the female model of RTT syndrome. Chemosensitivity of the female MeCP2 deficient mice was also tested by exposing the animals to varying intensities of hypercapnic stimuli and also to hypoxia, and observing the respiratory response.

The role of MeCP2 in the periphery is also of interest, with research indicating that RTT patients may present with lung pathology. Studies were carried out in male MeCP2deficient lung tissue to observe how the absence of MeCP2 may affect lung development and how changes in the morphology of the lungs may have an impact on the respiratory pattern of these animals.

Chapter 2: General Methods

2.1 Mouse models

2.1.1 Male Mouse Model

Mice were produced by crossing $Mecp2^{stop/+}$ mice in which the endogenous *MeCP2* allele is silenced by a targeted stop cassette ($Mecp2^{tm2Bird}$, Jackson Laboratories stock no. 006849) with hemizygous CreESR transgenic mice (CAG-Cre/ESR1*, Jackson Laboratories stock no. 004453) (Guy, 2007). These animals were bred with C57BL6/CBA F1 animals and the resulting F2 male offspring used in the study in chapter 3. The genotype of the mice was determined by PCR (Guy, 2007). Mice were housed in groups of 3 each containing a wild type, $Mecp2^{lox^{-}stop/+}cre-ER$ (*Stop/y,cre*: possibility of reversal) and $Mecp2^{lox^{-}stop/y}$ (*Stop/y*: reversal not possible), maintained on a 12 hour light/dark cycle and provided with food and water *ad libitum*.

2.1.2 Female Mouse Model

Heterozygous female $Mecp2^{stop}$ mice ($Mecp2^{stop/+}$ genotype) in which one endogenous *MeCP2* allele is silenced by a targeted STOP cassette (Guy et al., 2007) were obtained from the laboratory of Prof. Adrian Bird (University of Edinburgh, Edinburgh, UK). A local colony was established by breeding heterozygous $Mecp2^{stop/+}$ females with wild-type males. All mice used in experiments were heterozygous $Mecp2^{+/-}$ females and wild-type female littermates resulting from a breeding scheme involving at least six generations of backcross from a congenic C57BL/6 background onto a BALB/c background. Offspring genotype was determined by PCR as described in Guy et al (2007). Mice were housed in cages containing a mixture of WT (n=7) and female heterozygotes ($Mecp2^{+/-}$; n=11), maintained on a 12 hour light/dark cycle and provided with food and water *ad libitum*.

All experimental procedures were carried out under license from the UK Home Office and were subject to the Animals (Scientific Procedures) Act, 1986.

2.2 Behavioural Scoring

Progression of the RTT-like phenotype was monitored by scoring the animals on six behavioural parameters. Animals were primarily scored on a weekly basis using a 3 point scoring system created by Guy et al (2007). Scoring was carried out in the same lab on the same day each week and, where possible, at the same time of day. Mice were also weighed at each scoring session. The 3 point scoring system involved scoring the mice on mobility, tremor, breathing, hindlimb clasping, gait and general condition on a scale of 0 = symptom absent, 1 = mild symptom and 2 = symptom severe to give a semi-quantitative measurement of the RTT-like phenotype (table 2.1)

As will be discussed in chapter 3, the male model was more variable than expected. Some animals developed a severe phenotype quickly and at a much younger age than previously reported by Guy et al. To monitor the behavioural phenotype more closely, more descriptors were added to the 3 point scale to produce a new 5-point scoring method (table 2.2). The 5 point system involved scoring the mice on the same 6 parameters mentioned in the 3 point scale: mobility, tremor, breathing, hindlimb clasping, gait and general condition but with extra descriptors in the scale (0 = no symptom, 1 = symptom present but very mild, 2 = symptom present and mild, 3 = symptom moderate, 4 = symptom severe). Adding more descriptors into the behavioural scale enabled a more accurate differentiation between mice that may both display the same symptom but with differing levels of severity. For example, the development of a tremor was evident in most animals. When using the 3 point scale two animals could be scored as 1, symptom being present, when in fact one animal displayed a tremor that was more severe than the other. Using the 5 point scale would highlight the difference in the severity of the phenotype displayed by the two animals.

TEST	SCORE		
	0	1	2
Mobility - Mouse observed when placed on bench	Freely Moving	Reduced movement, extended freezing periods when first placed on bench and longer periods spent immobile.	No spontaneous movement, mouse can move in response to a gentle prod or a food pellet placed nearby.
Gait - Mouse observed when placed on bench	Walking as WT	Hind legs spread wider than WT when walking or running, reduced pelvic elevation, “waddling” gait	Tremor when feet are lifted, walks backwards or 'bunny hops' by lifting both rear feet at once.
Hindlimb Clasp - Mouse observed when suspended by holding base of the tail	Legs splayed outwards	hindlimbs drawn towards each other (without touching) or one leg is drawn in to the body.	Both legs are pulled in tightly, either touching each other or touching the body.
Tremor - Mouse observed while standing on the flat palm of the hand	No tremor	Intermittent mild tremor	continuous tremor or intermittent violent tremor
Breathing - Movement of flanks observed while animal is standing still	Normal breathing	periods of regular breathing interspersed with short periods of more rapid breathing or with pauses in breathing	very irregular breathing - gasping or panting.
General Condition - Mouse observed for indicators of general well-being	Clean shiny coat, clear eyes,	eyes dull, coat dull/ungroomed, somewhat hunched stance	eyes crusted or narrowed, piloerection, hunched posture.

Table 2-1 3 point behavioural scoring system used to monitor progression of the RTT-like phenotype. This behavioural score comprises 6 tests which are each given a score up to 2. The scores for each test are added to given an aggregate score. In the males, an aggregate score of 6 warranted initiation of TM treatment.

TEST	SCORE				
	0	1	2	3	4
Mobility	Freely Moving	Slower than WT	Reluctant to move, period of freezing	More time spent immobile than moving	No movement
Gait	As WT	Laying flat	Abdomen to floor/shuffling movements	Dragging abdomen along floor, splayed hindlimbs	Abdomen and face to floor, difficult in balance when rearing
Hindlimb Clasping	No Withdrawal	Hindlimbs point inwards	One limb often drawn towards body	One limb always drawn towards body	Both limbs always drawn in towards body
Tremor	No tremor	Slight intermittent tremor	Constant mild tremor	Intermittent sever tremor	Constant sever tremor
Breathing	Normal breathing	Periods of fast breathing	Fast breathing and irregular rhythm	As 3, but more prevalent hiccup-like movement	Very irregular patter, gasping of mouth
General Condition	Bright eyes, shiny coat	Slightly unkempt	Coat ruffled and dull	Coat ruffled, eyes narrowed and dull	Eyes crusted, piloerection, coat dull and unkempt

Table 2-2 5 point behavioural scoring system used to monitor progression of the RTT-like phenotype. This scoring system is based on the 3 point scale but involves the addition of more descriptors to allow more accurate tracking of the behavioural phenotype.

2.3 Tamoxifen Treatment of Male Mice

As will be discussed in chapter 3, Tamoxifen (TM; Sigma UK) was used to activate the cre-mediated deletion of a stop- cassette in the male mouse model. TM was dissolved in corn oil at a concentration of 20mg/ml, aliquoted and stored at -20°C until required. Previous work on the *Mecp2^{tm2Bird}* model reveals toxicity in the sudden reactivation of *MeCP2* while a more gradual reactivation yields increased survival rates (Guy *et al.*, 2007). Hence intraperitoneal injections of TM (100mg/kg) were given once a week for three weeks, followed by four daily injections on the fourth week. WT mice were treated with TM at the same time as the *Stop/y, cre* and *Stop/y* mice they were housed with. If, as in the case of *Stop/y* mice, the TM treatment showed no effect and the aggregate symptom score failed to decrease over the two observation sessions that followed the first injection, then the mice were culled for humane purposes. In the first cohort of mice, one *Stop/y, cre* animal was successfully rescued after TM treatment but died at 20 weeks of age. As a result, the remaining *Stop/y, cre* animals were also terminated at 20 wks of age for humane purposes and tissue was preserved for histological analysis.

2.4 Plethysmography

2.4.1 The Plethysmographic Chambers

Whole body plethysmography is a widely used, non-invasive technique for measuring ventilation. It was noted by Bert in 1868 that pressure variations within a closed chamber are a result of an animal breathing within the chamber (Bert, 1868). Chapin built upon this idea in 1954, noting that placement of a human subject in a closed chamber results in an increase in pressure upon inspiration, presumably to be due to the heating and humidifying of the inspired air (Chapin, 1954). The development of whole body plethysmography has improved the study of ventilation in small animals as the need for the use of masks and anaesthetic are unnecessary. One drawback of the technique noted by Chapin is respiratory traces become very unsteady when the subject or animal within the chamber is active and as such it is common practice to avoid analysis of periods of respiratory trace where the animal is known to have been moving. Another disadvantage discussed by Drorbaugh and O'fenn is that

recording sessions cannot take place for longer than about 30 min as the chamber has to be opened to prevent the oxygen concentration falling and subsequently changing the animal's respiratory behaviour (Drorbaug & Fenn, 1955).

Whole body plethysmography (apparatus illustrated in Fig 2-1) was used to monitor the respiratory phenotype of both the male and female mouse models. The plethysmographic chamber (700 ml, built in-house) in which the animals were housed was connected to a differential pressure transducer (model DP103-4, Validyne Engineering, Northridge, CA), which measures pressure fluctuations (related to respiratory activity of animal) within the closed animal chamber relative to a reference chamber of the same volume.

The heat produced by the animal in the chamber may cause a thermal shift of the pressure within the animal chamber (Malan, 1973); thus, two controlled leaks were introduced via the use of 26 gauge needles (Terumo, Exchange Supplies UK) to compensate for any slowly occurring changes in pressure within the chambers. A flow meter controlled the velocity of gases which were humidified prior to entering the chamber. When in the plethysmographic chamber, mice were housed within a small rectangular open ended cardboard box to allow some degree of movement and repositioning but preventing the animals turning around to chew the rectal temperature probe by which they were partially restrained (IT-18 18 gauge isolated temperature probe, Linton Instrumentation, Norfolk, UK). The rectal temperature probe allowed continuous monitoring of animal temperature throughout the experiment. Prior to the first set of recordings the mice were handled daily and habituated to the chamber for one week. During each recording session, the chamber was hermetically sealed and chamber temperature was continuously recorded and maintained between 27-28°C. The temperatures of the box and of the animal were maintained using a heat lamp. Each recording session was ~2 min; a calibration volume of 200 µl was injected into the plethysmographic chamber towards the end of each recording session.

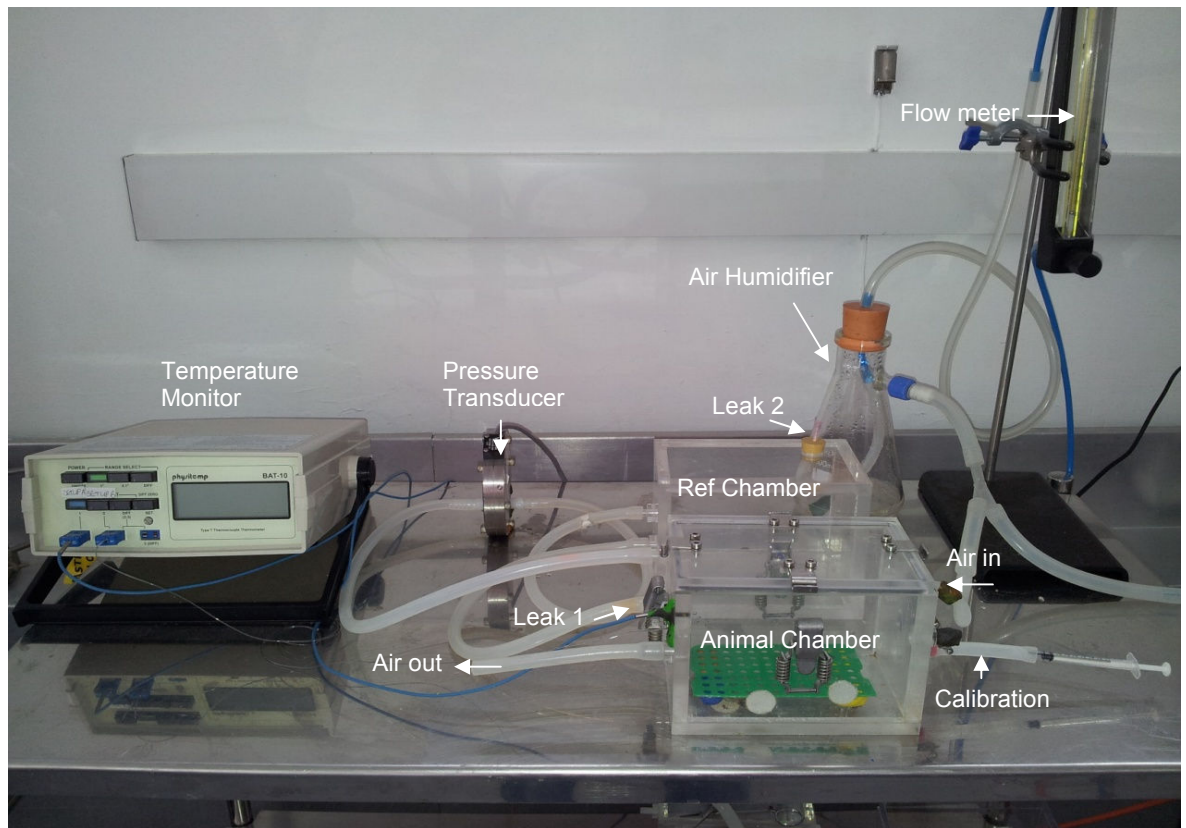


Fig 2-1 Illustration of the apparatus involved in respiratory plethysmography.

Mouse is placed within the animal chamber and gases fed in through the “air in” port via a flow meter. Pressure changes within the chamber are used as an index of respiration. Pressure changes are detected, relative to the reference chamber, by a pressure transducer. Temperature of the animal and of the chamber recorded using a temperature monitor.

Data were sampled at 1000Hz, filtered at 0.01HZ to remove DC components and analysed offline using Spike 2 (Spike2 software, Cambridge Instruments, UK). Movement distorted the signal and prevented reliable measurements thus only data during periods of quiet breathing when the animal was motionless were analysed.

2.4.2 Respiratory Analysis

Changes in respiratory frequency (Fr) were analysed on a breath by breath basis for each recording. An illustration of how these parameters are calculated is given in Fig 2-2.

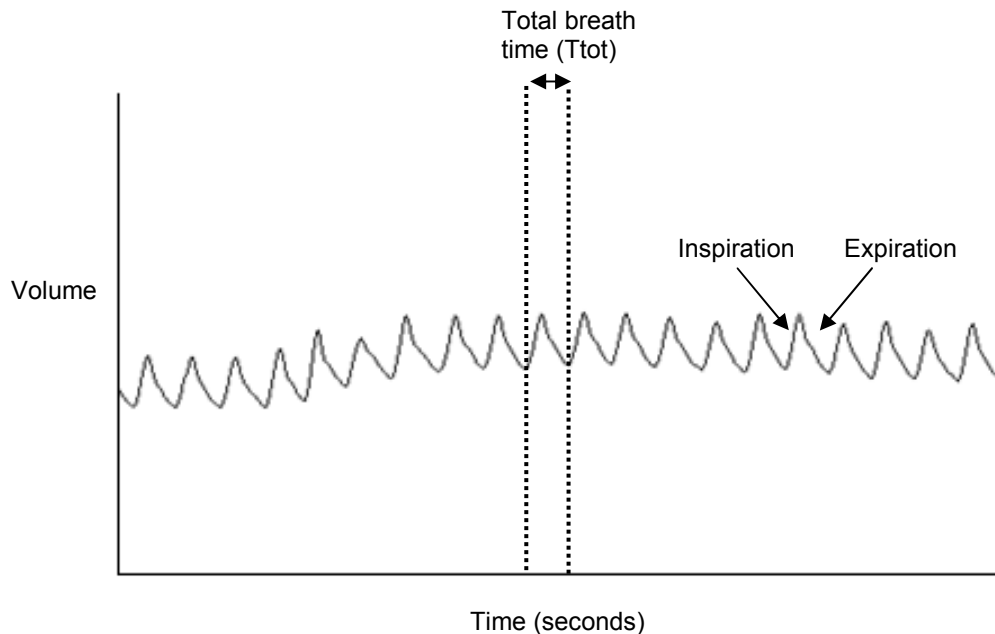


Fig 2-2 Respiratory trace(s) highlighting the respiratory parameters. Total breath time (T_{tot}) measured as the time from beginning of inspiration to end of expiration. Respiratory frequency calculated as $T_{tot}/60$ to give a value in breaths per min.

In addition to respiratory frequency, the number of apneas, sighs and double breaths which occurred per 2 min respiratory trace were quantified. Apnoeas are defined as a period of greater than 2 missed breaths (Zanella *et al.*, 2008; Voituron *et al.*, 2009), calculated as being equivalent to 0.6s in this model. Sighs are defined as breaths with double the amplitude of the previous three breaths followed by a post sigh apnea (Voituron *et al.*, 2009). Double breaths were defined as breaths with two inspiratory peaks separated by an incomplete expiration. A similar respiratory phenotype has been reported previously in both WT and *Mecp2^{-/-}* mice and termed as “complex sighing” (Voituron *et al.*, 2010). An example of each respiratory event is given in Fig 2-3.

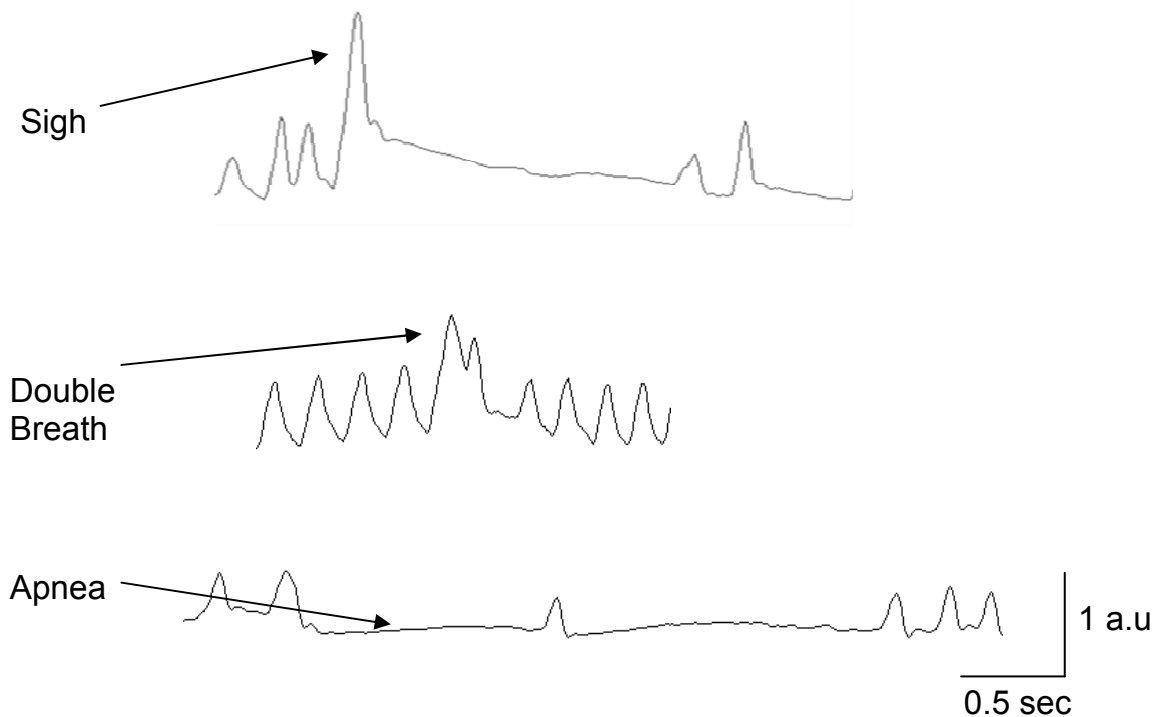


Fig 2-3 Respiratory traces to highlight various respiratory events. Sighs are classed as large amplitude breaths usually followed by a post-sigh apnea. Double breaths were defined as two inspiratory peaks separated by an incomplete expiration. Apneas are defined as two or more missed breaths which in the male and female models studied were calculated as being ≥ 0.6 sec.

As previously mentioned, symptom onset of MeCP2 deficient male mice was variable and it was apparent that age was not an adequate determinant of the onset of the RTT-like phenotype. Some animals reached the threshold for treatment at a much younger age than others resulting in mice receiving TM treatment at different ages. Results of the male mouse model are therefore presented with regards to stage of TM treatment as opposed to the age of the animal.

2.6 Tissue Fixation

2.6.1 Perfusion

Mice were injected with a lethal dose of pentobarbital (0.1 ml-0.2 ml depending on size of animal) and observed until the hind limb withdrawal reflex was

abolished. An incision was made just below the sternum to reveal the rib cage and abdominal muscles. The muscle layer was then cut to expose the diaphragm. The diaphragm was cut away from the rib cage, and the ribs themselves were cut through laterally to allow the ventral portion of the rib cage to be folded back, revealing the heart. A butterfly needle (Butterfly-23 INT, Venisystems) attached to the perfusion apparatus was inserted into the apex of the heart and fed into the left ventricle. Once the needle was secured in place, the right atrium was punctured and the animal was perfused at a constant pressure (~80mmHg) with Ringer's solution, a salt solution designed to be isotonic relative to the bodily fluid of the animal. Perfusion with Ringer's continued for approx 30 seconds or until the liver had cleared of blood and lightened in colour. This was followed by constant pressure perfusion with 250 ml 4% paraformaldehyde until the animal was rigid and tissues were drained of colour. The needle was then removed from the heart. The heart and liver were removed to allow better access to the lungs. The neck of the animal was cut open to expose the trachea, the collar bone removed and lungs carefully removed with trachea still attached and intact.

The fur and skin were then removed from the head of the animal and the skull carefully removed to expose the brain. The upper few vertebrae were cut open to expose a small amount of the spinal cord and cutting continued towards the head until the junction where the brain stem met the spinal cord was reached. An incision was made through the spinal cord and brains were harvested in such a way as to retain the brain stem and a small portion of cervical spinal cord. Brain tissue along with the lungs was left to post-fix for 4 hours in 4% paraformaldehyde. After this time the lungs were left in the paraformaldehyde for storage while brains were transferred into 30% sucrose. The purpose of the sucrose step was to allow removal of any excess water within the tissue and prevent ice crystals or artefacts forming when frozen sections were cut from the brainstem. Fixed tissue was stored short term in the fridge at 4°C or for longer term storage in a nitrogen freezer.

2.6.2 Paraffin Processing

Lungs were removed from the paraformaldehyde, placed in small embedding cassettes, labelled with the appropriate animal identity number and processed

using a Histokinette tissue-processing machine. The programme involves immersion in 70% alcohol for 2 hours, 90% alcohol for 2 hours, 3 immersions in absolute alcohol containing 2% Celloiden (nitrocellulose) for 2 hours each, 3 immersions in amyl acetate for 2 hours each and 2 rounds of immersion in molten wax for 4 hours each. The tissue was then embedded in paraffin wax on a chuck in preparation for microtome cutting.

2.7Cutting

2.7.1 Cryostat Sections

Cerebrum and excess spinal cord was removed from the brainstem before mounting on a chuck using Optimal Cutting Temperature (OCT; Tissue-Tek, UK) compound. Coronal sections of the brainstem were cut at 40 microns thick at -22°C using a Cryostat. Sections were collected into 24 well plates containing phosphate buffered saline (PBS) then split into 8 groups of free floating sections in small glass vials (see Fig 2-4).

2.7.2 Microtome

Excess paraffin was removed from the cassettes in which the tissue was mounted to ensure that the chuck was fitted securely into the microtome. Excess wax was also removed from around the lung tissue itself to prevent the thin wax sections folding when cut and causing creases in the tissue sections. Coronal sections were cut at 5µm thick. 2 sections were taken from the anterior surface of the lungs and 2 more from 450 µm into the tissue to give a fairer representation of the entire organ. Once cut, sections were placed in a water bath to heat and remove the remaining wax around the tissue. The sections were placed onto 3-aminopropyltriethoxysilane (APE) coated slides and placed in an oven at 52°C to dry out the excess water. Slides were stored in said oven until staining could begin (see Fig 2-7).

2.8 Brain ICC

The free floating sections were bathed for 30 min in 50% ethanol to aid penetration of the antibodies. The ethanol step was followed by three 10 min washes in PBS and incubation in a solution of 1% donkey blocking serum made up in PBS and 0.3% Triton X-100 (PBST) for 1 hour to block any non-specific binding sites. Primary antibodies were made up in a solution of 1% donkey serum +PBST, added to the sections and incubation was performed for 48 hours at 4°C. Sections were then given 3x10min washes in PBS before addition of secondary antibodies, also made up in a solution of 1% donkey serum +PBST. Secondary incubation was performed for 24 hrs at room temperature. A final round of washing took place (3 x 10 min in PBS) before sections were mounted in sequential rostrocaudal order on non-coated slides using Vectashield hard set anti-fade mounting medium (Jackson laboratories) and stored at -20°C.

Area of interest	Primary Antibodies	Secondary antibodies	N numbers
PreBötC Groups 1 and 5	Rabbit anti-NK1(1:500, Sigma, UK)	Alexa-488 anti-rabbit (1:500, Stratech-Jackson Immunoresearch)	WT = 8, cre TM=1, cre no TM = 1, stop/y =4
	Guinea pig anti-VGlu2 (1:5000, Millipore, UK)	Dylight-649 anti-guinea pig (1:100, Jackson Immunoresearch)	
	Mouse anti-mecp2 primary (1:200, Sigma,UK)	Rhodamine anti-mouse (1:100, Sigma, UK)	
RTN/pFRG Groups 2 and 6	Rabbit anti-phox2b (1:200, gift from C. Goridis, ENS, France)	Alexa-488 anti-rabbit secondary (1:500, Invitrogen, UK)	WT = 1, stop/y = 2
	Guinea pig anti-VGlu2 (1:5000, Millipore, UK)	Dylight-649 anti-guinea pig (1:100, Jackson Immunoresearch)	
	Mouse anti-mecp2 primary (1:200, Sigma,UK)	Rhodamine anti-mouse (1:100, Sigma, UK)	
Adrenergic neurons (A1/C1, A2/C2, LC) Groups 3 and 7	Sheep anti-TH primary (1:1000,Abcam,UK)	Alexa-488 anti-sheep secondary (1:500, Invitrogen,UK)	WT = 10, cre TM= 4, cre no TM = 4, Stop/y=7
	Mouse anti-mecp2 primary (1:200, Sigma,UK)	Rhodamine anti-mouse (1:100, Sigma, UK)	
Serotonergic neurons (rob, rpa/rmg, ventrolateral, DRI, Pnr/MnR) Groups 4 and 8	Rabbit anti-5-HT (1:200,Enzo life Sciences,UK)	Alexa-488 anti-rabbit secondary (1:500,Stratech-Jackson Immunoresearch)	WT = 5, cre TM = 2, cre no TM =3, stop/y= 7
	Mouse anti-mecp2 primary (1:200, Sigma,UK)	Rhodamine anti-mouse (1:100, Sigma, UK)	

Table 2-3 List of primary and secondary antibodies used to stain brainstem of male MeCP2 deficient and WT mice and highlight areas involved in control of respiration. As described in section 2.7.1, brainstem sections were split into 8 groups and each area of interest was studied in 2 groups. The preBötC complex was stained for in groups 1 and 5, the RTN/pFRG in groups 2 and 6, TH regions in groups 3 and 7 and 5-HT expressing regions stained for in groups 4 and 8. Sample sizes for each area of interest are highlighted in the final column of the table. N number for each genotype in each staining group is also highlighted.

2.8.1 Brain Imaging and Cell counting

Brainstem sections were imaged primarily using an epifluorescent microscope (Zeiss Axioskop microscope) to identify in which sections the areas of interest (namely the RTN/pFRG, preBötC, noradrenergic and serotonergic regions) were present. Once the sections of interest had been identified, confocal laser scanning microscopy (BioRad MRC 1024 confocal laser scanning microscope, AxioVision Vs40 V 4.8.2.0 software) was used to create bilateral Z-stacks of each region of interest. Z-stacks were compiled from 5 images, each separated by a depth of 2µm. Cells within each stack were counted manually using Image J. In all cases neurons were counted bilaterally in the areas of the preBötC, RTN/pFRG, Raphe nuclei and adrenergic areas. NK1, TH, Phox2b and 5-HT expressing cells were only counted as positive if 1) the cell boundary was complete and 2) there was a lack of staining in the centre of the cell to indicate a nucleus. MeCP2 expressing cells were counted as positive when staining was clearly exhibited within the nucleus, confirmed by DAPI staining. These methods and exact locations of imaging are described in further detail in chapter 4 (section 4.2).

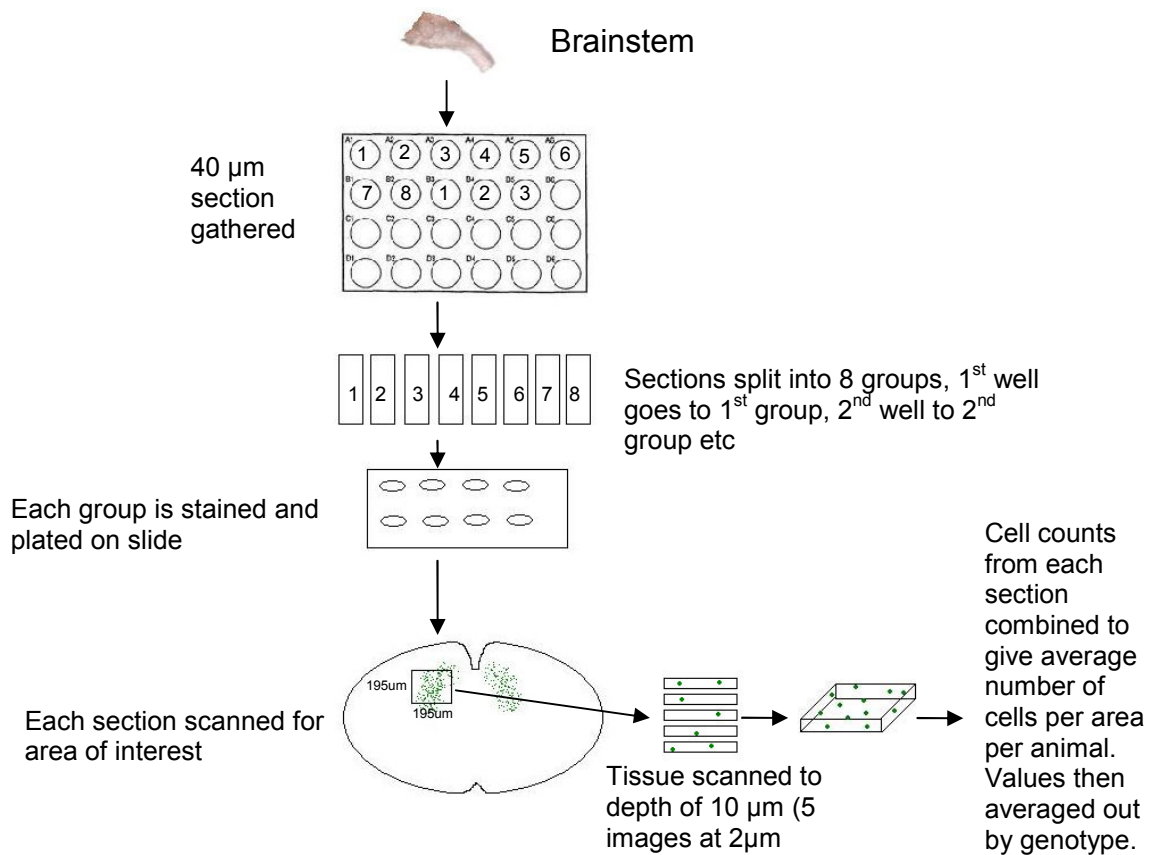


Fig 2-4 Illustration of how imaging and cell counting was performed within the brainstem. Brainstem sectioned into 24 well plate and sections subsequently split into 8 groups. Groups 1 and 5, 2 and 6, 3 and 7, 4 and 8 were coupled for staining (see Table 2-1). Once stained and mounted, sections were scanned using epifluorescent microscope to identify regions of interest. Confocal microscopy then used to take 10µm deep scan of area of interest. Cells in a 195x195µm window were counted bilaterally to a depth of 10µm in each section. Sections averaged to give average number of cells per area per animal. Values for each genotype then combined and averaged.

2.9 Lung Immunocytochemistry

Slides were placed in oven at 56°C for 2 hours to de-paraffinate the tissue. Slides were de-waxed in histoclear for 15 min prior to rehydrating by washing in 100%, 90% and 70% ethanol followed by washing in distilled water. Antigen retrieval is a necessary step used to break down cross links in the tissue that result from fixing the tissue with paraformaldehyde. Therefore slides were immersed in 2L

of 0.01M citrate buffer pH 6.0 in a domestic pressure cooker. These were cooked for 5 min at full pressure, pressure was then released by loosening of the lid and sections were left to stand for 20 min in the warm citrate buffer. After washing in distilled water, slides were washed in Tris buffered Saline (TBS) for 5 min on a rocker.

Sections were circled with a hydrophobic pen (DAKO, Cambridgeshire UK) to contain the histological solutions around each individual section and prevent the liquid draining off during incubation. Each section was blocked for 1 hour in 50 μ l of TBS, normal goat serum and bovine serum albumin (NGS/TBS/BSA) solution. Primary antibodies (rabbit anti-TrkB, 1:50, Insight Biotechnology, and mouse anti-MeCP2 M8618, 1:200, Sigma UK) were made up in NGS/TBS/BSA, added to the sections and left on overnight at 4 $^{\circ}$ C in a slide moisture chamber. Negative control sections were incubated in NGS/TBS/BSA only. Slides were washed in TBS Tween (TBST) for 5 min, a step which helps to decrease the background. Slides were washed in TBS for 5 min before secondaries (alexa-488 anti-rabbit, 1:500 and rhodamine red anti-mouse 1:100) made up in TBS were applied and tissue incubated for 30 min at room temperature in a slide moisture chamber. Slides were then washed 3 x 5 min in distilled water and coverslips added using Vectashield hard set anti fade mounting media +DAPI (Jackson laboratories) and stored at -20 $^{\circ}$ C. Details of the staining process are discussed further in chapter 5 (see section 5.2.2).

2.10 Lung IHC

Prior to application of the following histological stains, slides were placed in oven at 56 $^{\circ}$ C for 2 hours to de-paraffinate the tissue. Slides were de waxed in histoclear for 15 min prior to rehydrating by washing in 100%, 90% and 70% ethanol followed by washing in distilled water.

2.10.1 3, 3'-Diaminobenzidine (DAB) Reaction

The DAB method of staining involves targeting receptors of interest with a primary antibody which is subsequently targeted by a labelled secondary antibody, as in immunofluorescence. The difference lies in that the secondary antibody in the DAB reaction is conjugated with a peroxidase enzyme rather

than a fluorophore. The peroxidase enzyme binds DAB as a substrate and oxidizes it to produce an observable brown colour.

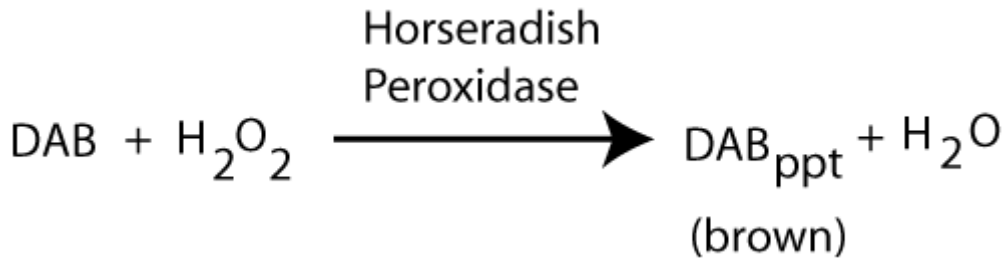


Fig 2-5 Schematic of the principle reaction in the DAB reaction.

Antigen retrieval was performed by immersing slides in 2L of 0.01M citrate buffer, pH 6.0 in a domestic pressure cooker. These were cooked for 5 min at full pressure, pressure was then released by loosening of the lid and sections were left to stand for 20 min. After washing in distilled water, slides were washed in TBS for 5 min on a rocker. Endogenous peroxidases in the tissue can react with the applied DAB to give a false positive thus it is imperative to quench endogenous peroxidase activity. This was achieved by blocking slides with 300mls 3% Hydrogen peroxide in methanol for 30 min at room temperature on a rocker. Slides were then rinsed in distilled water and washed for 5 min in TBS for 5 min on a rocker before blocking for 1 hour using NGS/TBS/BSA solution. The primary antibody rabbit anti-TrkB (1:50; Insight biotechnology), made up in NGS/TBS/BSA, was applied to the sections (negative control sections received NGS/TBS/BSA only) and left to incubate overnight at 4°C in a slide moisture chamber. Slides were washed in TBST for 5 min to help reduce background followed by 5min wash in TBS. Secondary antibody, Goat anti-rabbit biotinylated (Dako - E0432) was made up in NGS/TBS/BSA (1:500) and applied to sections for 30 min in the slide moisture chamber. Sections were washed twice in TBS for 5 min. The ABC/HRP solution was made up as per the suppliers instructions (Vectastain ABC kit) and added to slides for 30 min. Sections were then washed twice in TBS for 5 min. Staining was developed with DAB (Vectastain ABC kit,

Vector Labs) made up with 1 drop chromagen per ml buffered substrate. Test sections were used to identify the optimal length of developing time of 30 seconds. This pre-determined developing time had to be kept constant for each section so that comparisons could be drawn between sections from differing slides. Each section was developed individually, monitoring colour development microscopically for 30 seconds before immersing the slides in water to stop the reaction and prevent over development. After washing in distilled water, sections were dehydrated through a series of ethanol steps (70%, 90%, 100%, 100% ethanol for 20-30 sec each) before immersion in Histoclear for 5 min. Coverslips were added using pertex (Leica Microsystems, UK) a clear hard-set mounting agent.

2.10.2 Haematoxylin & Eosin

Haematoxylin & Eosin is one of the most commonly used permanent histological stains. The haematoxylin component stains nuclei blue while the counterstain eosin stains cytoplasm red/pink and red blood cells an intense red colour. De-paraffinated sections were placed in a solution of Mayer's Haematoxylin for 5-10 min, before placement in bluing agent in water for 3 min and 1% Eosin for 3 min. Slides were then washed in distilled water before dehydration via immersion in 70% Alcohol (for rapid eosin differentiation) and 90% Alcohol (for slow eosin differentiation) for 30 seconds each. Sections were immersed in 100% alcohol for 1 min, 100% alcohol for 2 min and then cleared using histoclear for 10-15 min, a second wash in histoclear for 5 min. Slides were then mounted in Histomount/DPX ready for imaging.

2.10.3 Miller's Elastin

Miller's Elastin stain is used to highlight elastin content and its localisation within tissue. Elastin fibres are rendered purple/black; collagen is a deep red, while cytoplasm, muscle, fibrin and red blood cells yellow stain a more yellow colour. The de-paraffinated sections were immersed in 0.5% Potassium permanganate for 5 min, washed in water and transferred to 1% Oxalic acid until clear. After washing in distilled water, sections were placed in Miller's Elastin stain for 2 hours. Sections were then rinsed in 90% alcohol to remove excess stain, washed in distilled water and counterstained with Van Gieson for 30 seconds and

washed in water once more. The sections were dehydrated by immersion in 70% then 90% alcohol for 30 seconds each, 100% alcohol for 1 minute then 100% alcohol again for 2 min. Slides were placed in histoclear for 15 min before mounting with histomount/DPX.

2.10.4 PAS/HA (*Periodic Acid, Schiff's/Haematoxylin & Aurantia*)

PAS is a stain used to identify polysaccharides and glycogen. Mucin, glycogen and occasionally some basement membranes will appear as a red/magenta stain. De-paraffinated sections were placed in a solution of Mordant and 2% Periodic acid for 5 min, washed in distilled water, placed in Schiff's (Feulgens) until brick red (20-30mins). Slides were washed in water until the water runs clear and sections counter stained using Mayers Haematoxylin for 5 min followed by immersion in bluing agent in water for 3 min. The sections were then dehydrated by immersion in 70% then 90% alcohol for 30 seconds each, 100% alcohol for 1 minute then 100% alcohol again for 2 min. Slides were placed in histoclear for 15 min before mounting with histomount/DPX.

2.10.5 Masson's Trichrome Stain

Masson's Trichrome stain is used to highlight collagen deposits and connective tissue. This stain renders collagen green/blue, the nuclei black, cytoplasm as pink and any red blood cells in bright red. De-paraffinated sections were placed in Mayer's Haematoxylin for 8 min followed by placement in bluing agent in water for 3 min. Slides were then submerged in 0.5% Ponceau Fuchsin/1% Acetic Acid for 2.5 min followed by a rapid rinse in distilled water. The sections were left in Mordant in 1% aqueous phosphomolybic acid for 15 min before draining the excess acid and staining in 2% Light green. Sections were washed in distilled water and dehydrated by immersion in 70% then 90% alcohol for 30 seconds each, 100% alcohol for 1 minute then 100% alcohol again for 2 min. Slides were placed in histoclear for 15 min before mounting with histomount/DPX.

2.10.6 Lung Imaging and Measurements

Lung sections were imaged using an epifluorescent microscope (Axioskop Zeiss microscope using AxioCam camera) and images collected using Axiovision

software (AxioVs40 V 4.8.2.0, Zeiss Microscopy). High magnification images (x40) were taken from six areas within each lung section; top right, top left, mid right, mid left, bottom right and bottom left of the lung (Fig 2-7). As each slide contained 2 lung sections, this yielded 12 images from the ventral surface of the lung and 12 images from 450 μ m deep into the tissue, totalling 24 images of the lung for each animal. Measurements of the bronchial epithelial lining, the interalveolar septum and elastin deposits surrounding the airways were made using these images, details of which are discussed further in chapter 5 (section 5.2.4).

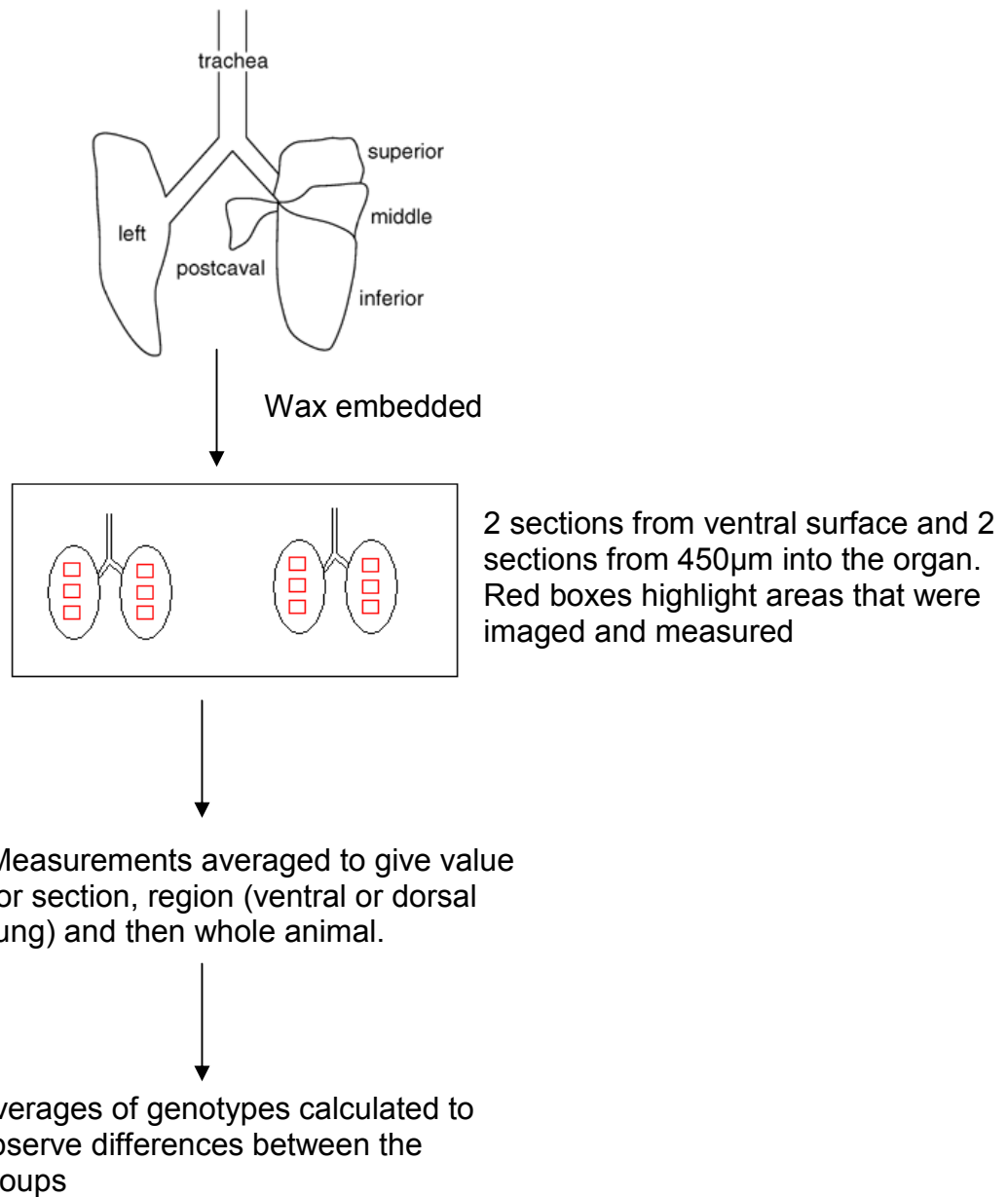


Fig 2-6 Illustration of lung tissue processing and imaging. After lungs were paraffin embedded, 5 μ m sections were cut from the ventral surface of the lung and also from 450 μ m into the organ. Images were taken bilaterally from top, middle and bottom of the lungs as highlighted by the red boxes. Images were used to measure of various aspects of the lung morphology, as will be discussed (chapter 5).

2.11 Pulmonary Arterial Hypertension (PAH) Analysis

2.11.1 Measurement of Right Ventricular Pressure and Systemic Pressure

PAH experiments were performed using 10-12 month old heterozygous *Mecp2*^{+/-} females (n=8) and wild-type (n=5) female littermates (see chapter 2 section 2.1.2). Animals were anaesthetized using a gas chamber filled with 3% isoflurane and depth of anaesthesia monitored using the hind withdrawal reflex. Once this reflex was abolished, the animal was removed from the chamber and anaesthesia maintained on a facemask at 1.75% isoflurane in O₂. The animal was placed on its back and its limbs secured to the table. The superficial tissue covering the sternum was removed to allow clearer access to the chest cavity. Care was taken not to puncture the chest cavity when removing the fur and skin as doing so would disrupt the pressure within the chest. Systolic right ventricular pressure (sRVP) was measured by advancing a 25 gauge needle, which was attached to a pressure transducer, trans-diaphragmatically into the right ventricle (MacLean *et al.*, 2004). The needle and tubing system was filled with saline and pressure at 150 mmHg. When the needle entered the heart, displacement of the saline by blood flow allowed pressure changes to be detected by the pressure transducer. The position of the catheter was confirmed by the morphology of the pressure trace. Entrance into the right ventricle was confirmed when systolic pressure was registered at ~ 20 mmHg. A 5 minute recording of the sRVP was taken before the carotid artery was cannulated to allow measurement of systemic pressure using the same liquid-displacement method as described for sRVP.

2.11.2 Assessing Right Ventricular Hypertrophy

Once sufficiently long traces of RVP and systemic pressure had been recorded, animals were euthanized using 5% isoflurane followed by cervical dislocation. The heart was then removed and any fatty tissue removed. An incision was made from the base of the heart to the apex to separate the right ventricular wall from the rest of the heart. Right ventricular hypertrophy (RVH) was assessed by weighing the wall of the right ventricle (RV) and the left ventricle together with the septum (LV+S), and calculating the ratio of RV/LV+S.

2.11.3 Measurement of Remodelling of Small Blood Vessels

Lungs were removed and paraffin processed (see section 2.6.2). 3 µm coronal sections were cut from the lung tissue using a microtome and stained with Miller's Elastin (see section 2.10.3) and counterstained with Van Giesson's. One lung section from each animal was assessed. Remodelled and non-remodelled pulmonary vessels were counted, criteria being that the external diameter must lie within a range of 25 to 100 µm. The percentage of remodelling within the lung was calculated by comparing the number of remodelled to non-remodelled vessels. A vessel was considered to be remodelled if the vessel appeared to be 50% muscularised compared to non-remodelled vessels.

2.11 Statistics

All statistical analysis was performed using GraphpadPrism4 software and differences were regarded as significant if $p < 0.05$.

2.11.1 Male Respiratory Data (chapter3)

Statistical analyses of the average respiratory frequency, the average number of sighs, the average number of apnea and the average number of double breaths of WT and MeCP2 deficient males were performed using two-way anovas assuming Gaussian distribution and Bonferroni post tests.

2.11.2 Female Respiratory Data (chapter 6)

Statistical analyses of the average respiratory frequency, the average number of sighs, the average number of apnea and the average number of double breaths of WT and *Mecp2*^{+/-} females under each respiratory stimulus were performed using two-way anovas assuming Gaussian distribution and Bonferroni post tests.

2.11.3 Brain ICC (chapter 4)

Two-way anovas were applied followed by the Bonferroni post test to analyse the difference in cell number of adrenergic and serotonergic areas between WT and MeCP2 deficient mice. N numbers were too low in NK1 and Phox2b groups to power any statistical analysis.

2.11.4 Lung ICC (chapter 5)

To make comparisons of the thickness of epithelial lining, alveolar septum and elastin deposits, between the genotypes one-way anovas were used. Sample sizes were too small to allow post analysis tests to be run.

2.11.5 PAH Anaylsis (chapter 6)

Unpaired t-tests were used to compare the values recorded in WT and *Mecp2*^{+/-} animals.

Chapter 3: Respiratory patterns of the male MeCP2 deficient mouse model

3.1 Introduction

Patients with RTT syndrome often experience respiratory abnormalities such as the increased occurrence of apneas, highly unstable breathing patterns with periods of breath holding, hyperventilation and variable breath duration (Weese-Mayer *et al.*, 2006). As discussed in chapter one, loss of function mutations of *MECP2* are responsible for the vast majority of cases of RTT (Shahbazian & Zoghbi, 2001) and various mouse models which mimic the human condition have been developed to allow further investigation into the role of *MECP2* in RTT. *MECP2* is an x-linked gene and is subject to X chromosome inactivation (XCI; see chapter one section 1.9.3). This results in a phenotype which is usually lethal to males but has varying degrees of severity in females due to the mosaic pattern of expression of the mutated *MECP2* in cells. A large proportion of RTT *in vivo* research makes use of male *MeCP2* deficient mice to study the disorder due to the fact that heterozygous *Mecp2*^{+/-} female populations have a more heterogeneous RTT-like phenotype which can take months to develop. The use of males circumvents this problem by providing a more homogeneous population of animals that should develop the RTT-like phenotype in a matter of weeks.

The *Mecp2*^{tm2Bird} model used in this study allows control over the production of MeCP2 in the whole animal. This involves the insertion of a LoxStop cassette into the DNA, which acts to silence the *Mecp2* gene. Consequently, a deficit in MeCP2 develops and the mice begin to display RTT-like symptoms such as the claspings of hind limbs and development of breathing abnormalities which are similar to symptoms observed in the human condition. The *Mecp2* gene can then be reactivated in Cre⁺ animals by Tamoxifen driven cassette deletion (Guy *et al.*, 2007). The Cre⁺ male mice (referred to in this thesis as *Stop/y,cre*) possess a cre-recombinase enzyme which is fused to oestrogen receptors (Fig 3-1). The oestrogen receptors remain in the cytoplasm until bound by Tamoxifen, at which point the complex translocates into the nucleus. This allows the removal of the stop cassette and subsequent reactivation of the *Mecp2* gene. Reactivation of *Mecp2* has been shown to result in a significant improvement in the phenotype of severely affected mice including improvements in breathing patterns and other behavioural parameters (Guy *et al.*, 2007; Robinson *et al.*, 2012). *Stop/y* mice act as *Mecp2* KO animals as they do not possess the cre recombinase

enzyme required for cassette deletion and thus *Mecp2* reactivation is not possible.

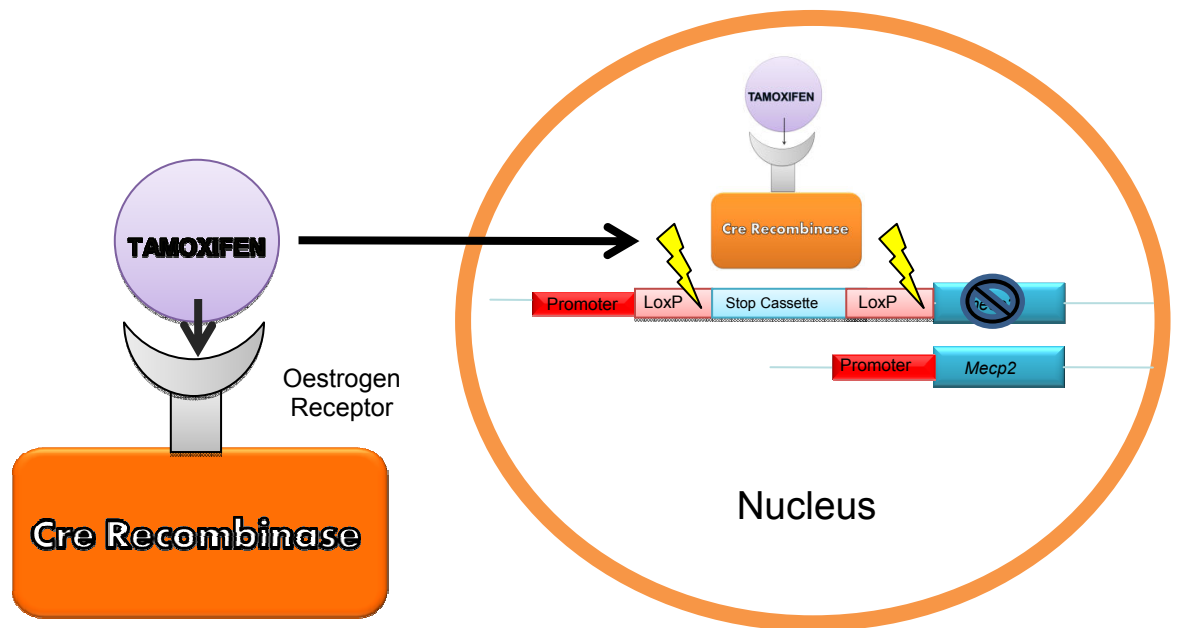


Fig 3-1 The *Mecp2^{tm2Bird}* model of RTT syndrome. Insertion of a LoxStop cassette prevents transcription of *Mecp2* and a resulting MeCP2 deficit develops. The application of tamoxifen causes activation of the cre recombinase enzyme which translocates to the nucleus where it functions to remove the stop cassette and allow transcription of *Mecp2*.

Studies in male *Mecp2^{-/-}* mice reveal an abnormal response to hypoxia and hypercapnia (Voituron *et al.*, 2009) indicating that the respiratory abnormalities presented in RTT syndrome may be due to problems with chemosensitivity. *Mecp2*-null mice also exhibit a variable basal respiratory rate with periods of fast and slow breathing (Ward *et al.*; Viemari *et al.*, 2005; Ward *et al.*, 2011) which may indicate that the mechanisms underlying respiratory rhythm generation or modulation are defective.

In this chapter, the aim was to study the development of respiratory abnormalities in the absence of MeCP2 in the *Mecp2^{tm2Bird}* model and to observe whether these abnormalities could be reversed by *Mecp2* reactivation. Mice were also subjected to varying levels of hypercapnic stimuli (mild, moderate and

severe) to investigate whether MeCP2 deficiency could affect the chemosensitive response and also to monitor how the chemosensitive response may change once *Mecp2* is reactivated.

3.2 METHODS

3.2.1 Male Mouse Model

See section 2.1.1 for more information regarding breeding. Mice were housed in groups of 3: wild type (WT), *Stop/y,cre* (possibility of reversal) and *Stop/y* (reversal not possible), maintained on a 12 hour light/dark cycle and provided with food and water *ad libitum*. All experimental procedures were carried out under license from the UK Home Office and were subject to the Animals (Scientific Procedures) Act, 1986.

3.2.2 N numbers

As will be discussed later in this chapter, the male model was more variable than expected and the resulting sample size was small. Originally the study began with 14 *Stop/y,cre* mice. 3 animals died before the study began due to sudden and severe onset of the RTT like phenotype. 2 *Stop/y,cre* mice did not respond to Tamoxifen treatment and had to be euthanised. One *Stop/y,cre* animal died when subjected to hypoxia while another was removed from the study due to receiving treatment for a tail injury. A final animal was removed from the study because Tamoxifen treatment had to be administered upon the arrival of the animal due to a severe behavioural phenotype. This meant that no pre treatment data could be collected and a pre and post *Mecp2* reactivation comparison could not be made. These factors resulted in the final *Stop/y,cre* group having an n of 6.

The *Stop/y* group originally consisted of 13 *Stop/y* mice, 3 of which died before the study began. One animal was euthanized due to a very early and severe onset of symptoms. This resulted in an n of 9.

The WT group began with an n of 21. Six of these animals were removed from the study as they exhibited very nervous and aggressive behaviour. The aggressive nature of the animals prevented behavioural scoring and no data

could be collected from plethysmography as the animals did not settle for an adequate amount of time for quiet breathing to be recorded. 4 animals were perfused as their *MeCP2* deficient cage mates had been removed from the study, thus in total WT n=11.

3.2.3 Behavioural Scoring

As discussed in chapter 2 (section 2.2), animals were observed and scored behaviourally on a weekly basis using a 3 point scoring system (see chapter 2 table 2 -1) created by Guy et al (2007). Behavioural scoring was implemented as a means of tracking the development of the overall RTT phenotype and gauging the stage at which Tamoxifen (TM) should be applied. This is important as application of TM before appropriate symptom onset has been proven fatal (Guy *et al.*, 2007). Scores from each parameter were compiled to give an aggregate and TM treatment was initiated when the aggregate score reached a value of 6 or above.

Guy et al (2007) reports that *Stop/y* animals show a low steady aggregate score up until about 8-10 weeks followed by a quick progression of the RTT-like phenotype approximately 4 weeks prior to death. Observation of the first cohort of male animals (4-5 weeks old) delivered from Harlan revealed that behavioural scores of the mutant mice did not maintain a steady, low score as reported by Guy et al (2007). When it became apparent that the progression of the RTT-like phenotype was highly variable a) from one animal to the next and b) within an animal from day to day, mice were scored 3 times per week using a new 5 point scoring system (table 2-1) along with the original 3 point scoring system (table 2-3) to more accurately track the development of the RTT-like phenotype.

3.2.4 Tamoxifen Treatment

Tamoxifen (TM; Sigma UK) was dissolved in corn oil at a concentration of 20mg/ml, aliquoted and stored at -20°C until required. Previous work on this model has shown that sudden reactivation of *Mecp2* can have toxic effects while a more gradual reactivation led to increased survival rates (Guy *et al.*, 2007). Hence intraperitoneal injections of TM (100mg/kg) were given once a week for three weeks, followed by four daily injections on the fourth week. WT mice

were treated with TM at the same time as the *Stop/y,cre* and *Stop/y* mice they were housed with. If, as in the case of *Stop/y* mice, the TM treatment had no effect and the aggregate symptom score failed to decrease over the two observation sessions that followed the first injection then the mice were culled on humane grounds. In the first cohort of mice studied, the phenotype of one *Stop/y,cre* mouse was successfully rescued after TM treatment but the animal died at 20 weeks of age. As a result, the remaining *Stop/y,cre* and WT animals were also terminated at 20 weeks of age on humane grounds and also in order that tissue could be preserved for histological analysis. As previously mentioned, symptom onset was seen to be variable between mice and it became apparent that age was not an adequate determinant of the onset of the RTT-like phenotype. Some animals reached the threshold for treatment at a much younger age than others resulting in mice receiving TM treatment at different ages. Results are therefore presented with regards to stage of TM treatment as opposed to the age of the animal.

3.2.5 Respiratory Measurements

The respiratory pattern of mice during normoxia (21% O₂) and hypercapnia (3%, 5% and 8% CO₂) was measured *in vivo* using whole body plethysmography (Fig 3-2; see chapter 2 section 2.4.1). Measurements were taken on a weekly basis starting from 4-5 weeks of age in WT (*n* = 2-5), *Stop/y,cre* (*n* = 2-4) and *Stop/y* (*n* = 2-4) mice.

In each experimental session, mice were given 45 min to habituate to the chamber in normoxia. During the 45 min period, control recordings were taken in normoxia at 15, 30 and 45 min time points. The chamber was then filled with 3% CO₂ (3% CO₂, 21% O₂, balanced with N₂) for 10 min and a recording made at the end of the 10 min period. This was repeated for 5% (5% CO₂, 21% O₂, balanced with N₂) and 8% CO₂ (8% CO₂, 21% O₂, balanced with N₂). After exposure to hypercapnia the chamber was flushed with air and recovery recordings made at 2, 15 and 30 min. Each recording session lasted 2 minutes and a calibration volume of 200 µl was injected into the animal chamber towards the end of each recording session.

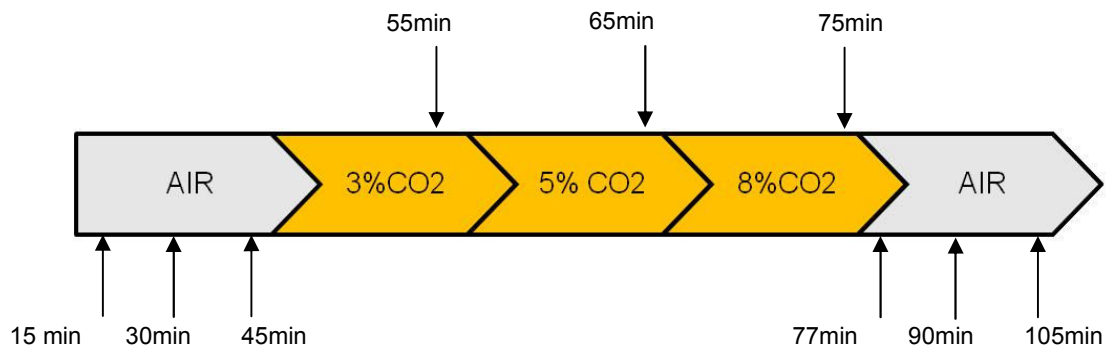


Fig 3-2 Protocol for measurement of respiratory parameters in *Stop/y,cre*, *Stop/y* and WT male mice. Mice habituated in normoxia for 45 min prior to experiment. Recordings taken at 15, 30 and 45 min in normoxia. Recordings also taken after 10 min exposure to each of 3%, 5%, 8% CO₂ and final recordings taken in normoxia at 2 min, 30 min, and 45 min recovery from the hypercapnic stimulus.

3.2.6 Analysis

Changes in respiratory frequency (Fr) were analysed on a breath by breath basis for each recording using Spike 2 (Spike2 software, Cambridge Instruments, UK). The plethysmographic signal can be disturbed by movement and so only data during periods of quiet breathing when the animal was motionless were analysed. In addition, the number of apneas, sighs and “double breaths” were quantified (see chapter 2 section 2.4.2 for definition of respiratory characteristics).

3.3 RESULTS

3.3.1 Behavioural Scoring

WT animals scored 0 throughout the study and the behavioural score was unaffected by TM. *Stop/y* animals displayed a steady increase in the severity of the RTT-like phenotype (Fig 3-3 plot A).

The phenotype of *Stop/y* mice was not rescued by the application of TM, as indicated by the increase in behavioural score in the three scoring sessions which followed TM in Fig 3-3 plot A, resulting in *Stop/y* mice being euthanized on humane grounds. *Stop/y,cre* mice exhibited a progression of the RTT-like phenotype (Fig 3-3 plot B) similar to that of the *Stop/y* mice, however the score was gradually reduced following treatment with TM and reactivation of *Mecp2* at 8-9 weeks. Although Fig 3-3 plot B illustrates a rise in score following TM, it should be noted that TM treatment took 4 weeks to complete and at 13 weeks the behavioural score begins to show a trend towards a reduction. At 18 weeks the behavioural score of the *Stop/y,cre* was not recovered to WT level but was comparable to the score recorded in the *Stop/y,cre* animal at the beginning of the study prior to severe symptom onset. Comparison of the 3 point and 5 point scoring system reveals that adding more descriptors to the behavioural scale enables more accurate tracking of the development of the phenotype. For example, in Fig 3-3 plot A the 3 point scoring system indicated a plateau in behavioural score at 9 weeks. However, the 5 point scale reveals that there was actually variability in the average behavioural score over the three testing sessions.

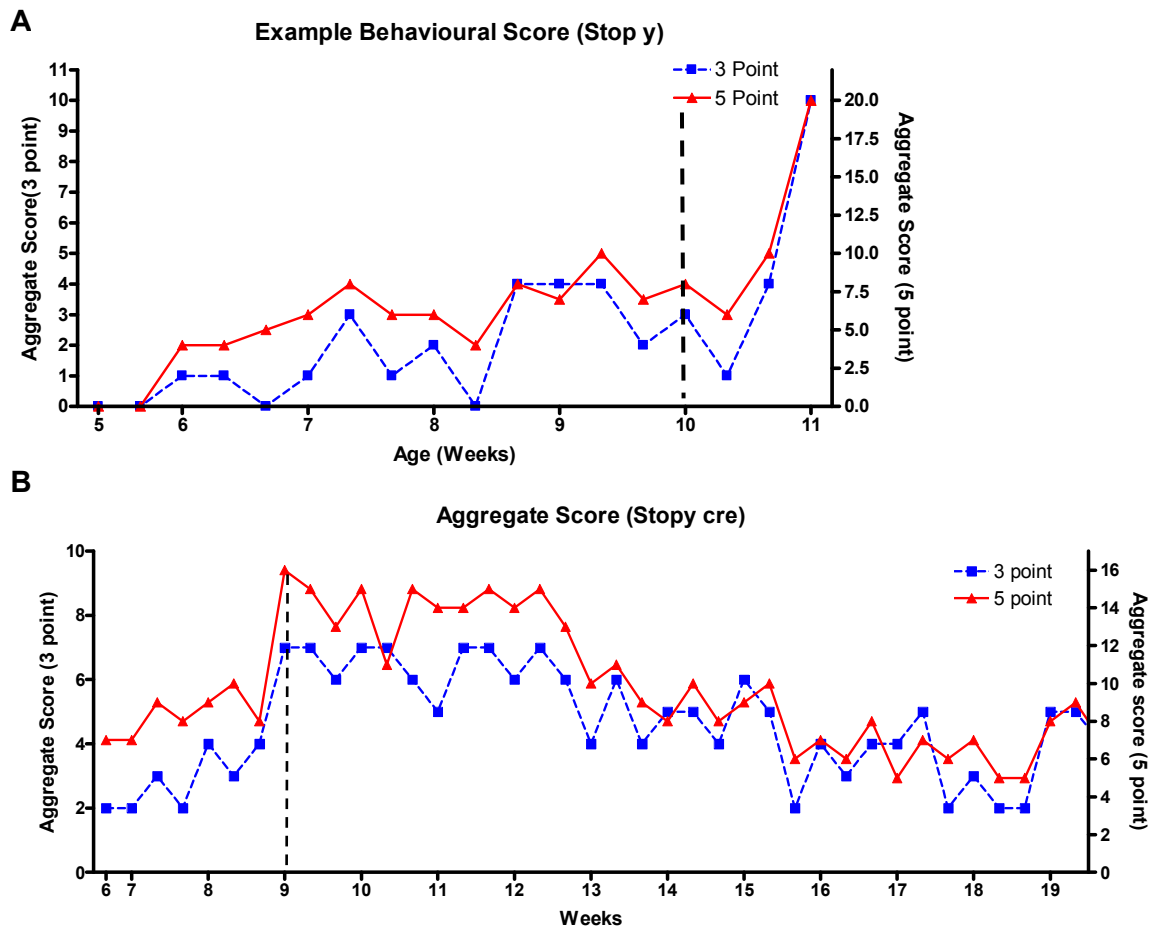


Fig 3-3 Average behavioural score of *Stop/y* (n=1) and *Stop/y,cre* (n=1) mice, comparing 3 point scale (left y axis) and 5 point scale (right y axis). Dotted line indicates point of TM treatment. *Stop/y* animal was treated at 10 wks of age when the *Stop/y,cre* cage mate scored aggregate of 6 points. *Stop/y* animal did not respond to TM, indicated by increased behavioural score, and had to be euthanised. *Stop/y,cre* was treated at 9 wks of age when aggregate score of 6 was reached. *Stop/y,cre* animal showed gradual decrease in behavioural score in response to TM. Initial increase in score can be accounted for by the fact that completion of TM treatment takes 4 weeks.

3.3.2 Raw Respiratory Traces

As mentioned previously, one of the key aims of this study was to monitor and characterise the development of abnormalities in the respiratory phenotype of MeCP2 deficient mice and observe whether these breathing abnormalities could be reversed by treatment with Tamoxifen.

Fig 3-4 plot A illustrates that the WT animal had a regular respiratory frequency in air. The respiratory frequency increased in response to hypercapnic exposure and was reduced when normoxic conditions were restored after hypercapnic exposure. After TM treatment (fig 3-4 plot B) the respiratory frequency of WT in air remained regular. Respiratory frequency also increased in response to hypercapnic exposure and reduced when normoxic conditions were restored.

Fig 3-5 plot A shows that the respiratory frequency of one *Stop/y* animal was regular in air and in hypercapnia with some variability arising in the 2 minute normoxic period following hypercapnic exposure. With regards to the mutant animals it should be noted that not all mice developed the same severity of breathing phenotype, as has been reported previously in studies using *Mecp2^{-/y}* mice (Guy *et al.*, 2001; Viemari *et al.*, 2005). Fig 3-5 plot B shows an example of a *Stop/y* animal which had a more severe respiratory phenotype. Breathing in air was irregular and interspersed with apnea in air, but became regular when exposed to hypercapnia. When normoxia was restored the respiratory frequency once again became variable and the breathing pattern was interspersed with apneas and sighs. There are no post TM traces for the *Stop/y* genotype as the animals did not respond to TM treatment and had to be euthanised for humane purposes.

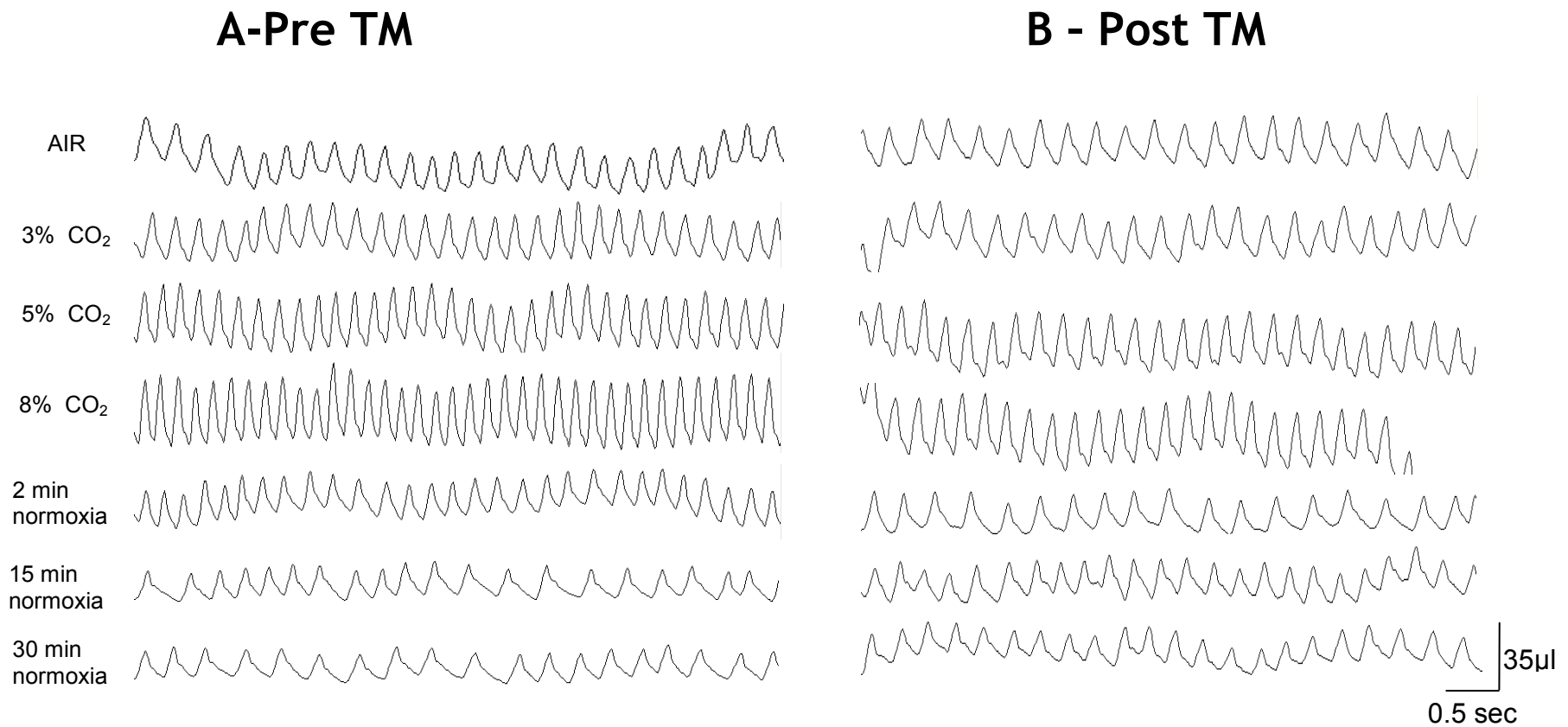


Fig 3-4 Respiratory traces to illustrate WT respiratory pattern pre and post TM treatment. The respiratory pattern of WT animals was comparable both pre (A) and post TM (B). Respiratory frequency was regular in both air and hypercapnia in the WT animal. Respiratory frequency increased in response to hypercapnic exposure.

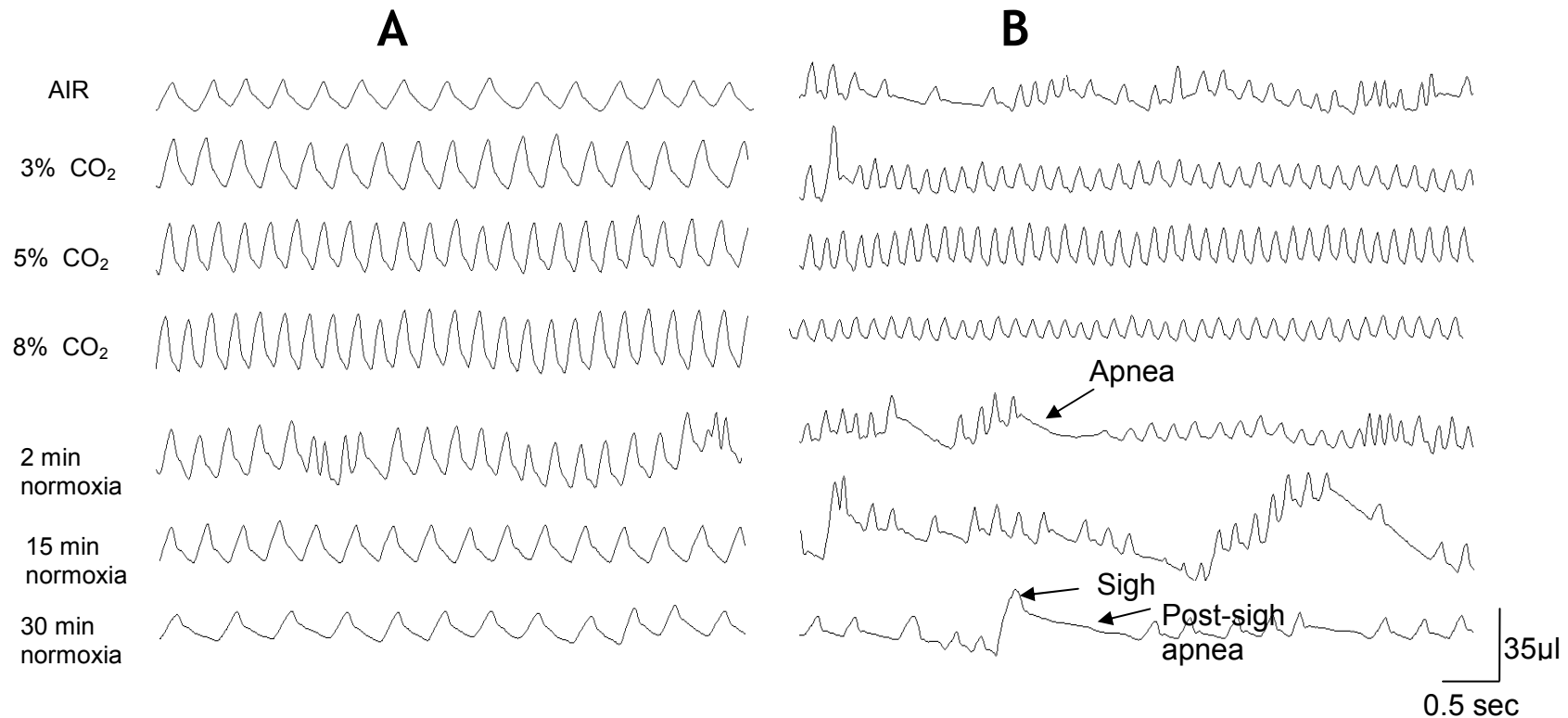


Fig 3-5 Respiratory traces to illustrate respiratory pattern of two *Stop/y* mice pre TM. No post TM data shown as animals did not respond to TM and had to be euthanised. **A** – Respiratory trace of *Stop/y* animal that presented a mild respiratory phenotype. Respiratory rhythm was regular in air and hypercapnia, with irregularity in respiratory frequency becoming apparent at 2 min normoxia. **B** – Respiratory trace of *Stop/y* animal with more severe respiratory phenotype. Respiratory rhythm was irregular in air and frequency in hypercapnia appeared increased compared to the milder respiratory pattern of the previous *Stop/y* mouse. Sighing and apnea were prevalent in the post hypercapnic periods, at 2, 15 and 30 min normoxia.

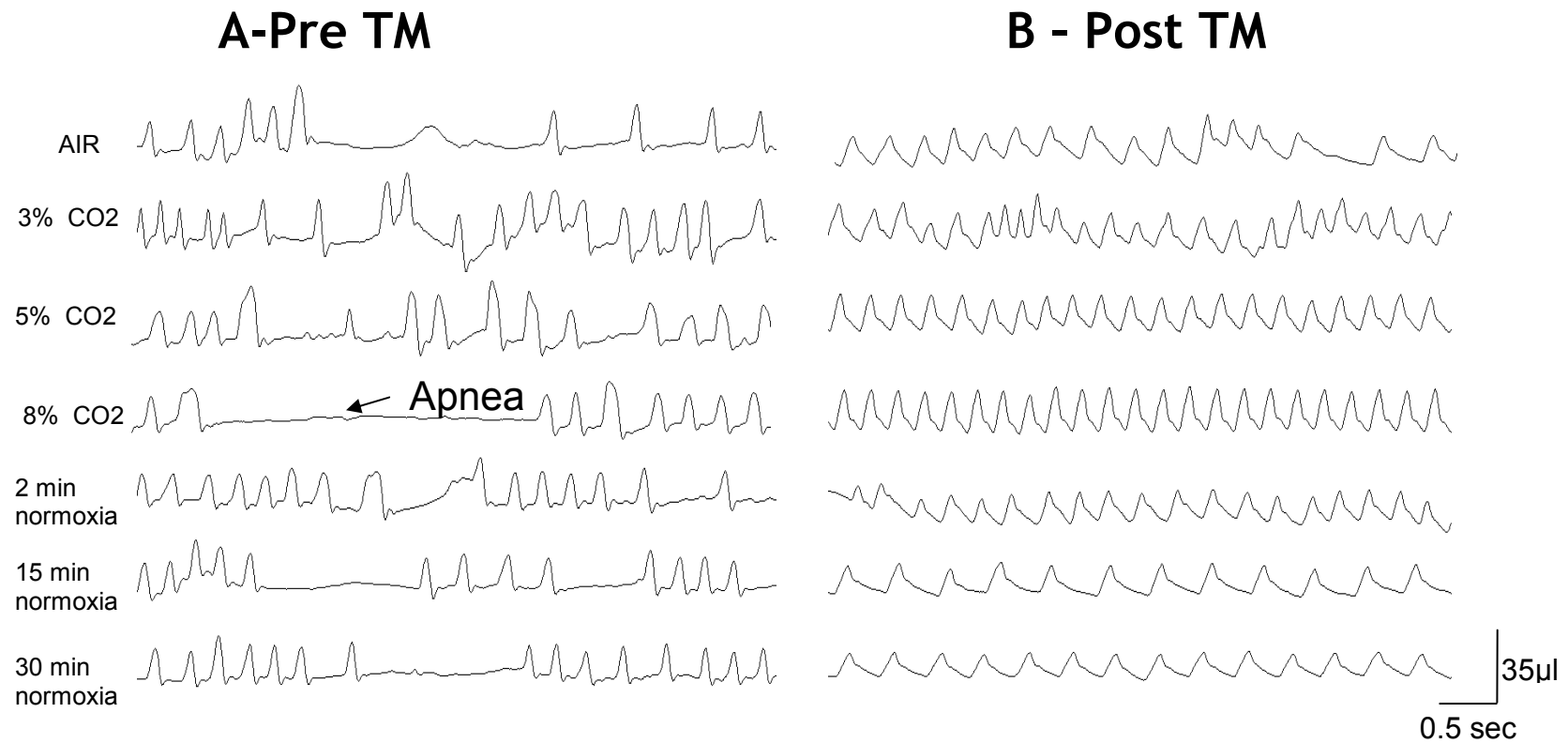


Fig 3-6 Respiratory traces to illustrate respiratory pattern of *Stop/y,cre* animal with severe respiratory phenotype. A - Pre TM, respiratory frequency was irregular in all conditions. Respiratory pattern was interspersed with numerous apnea and respiratory frequency did not appear to increase in response to hypercapnic exposure. B - Post TM, respiratory frequency was more regular in all conditions and apneas were eliminated.

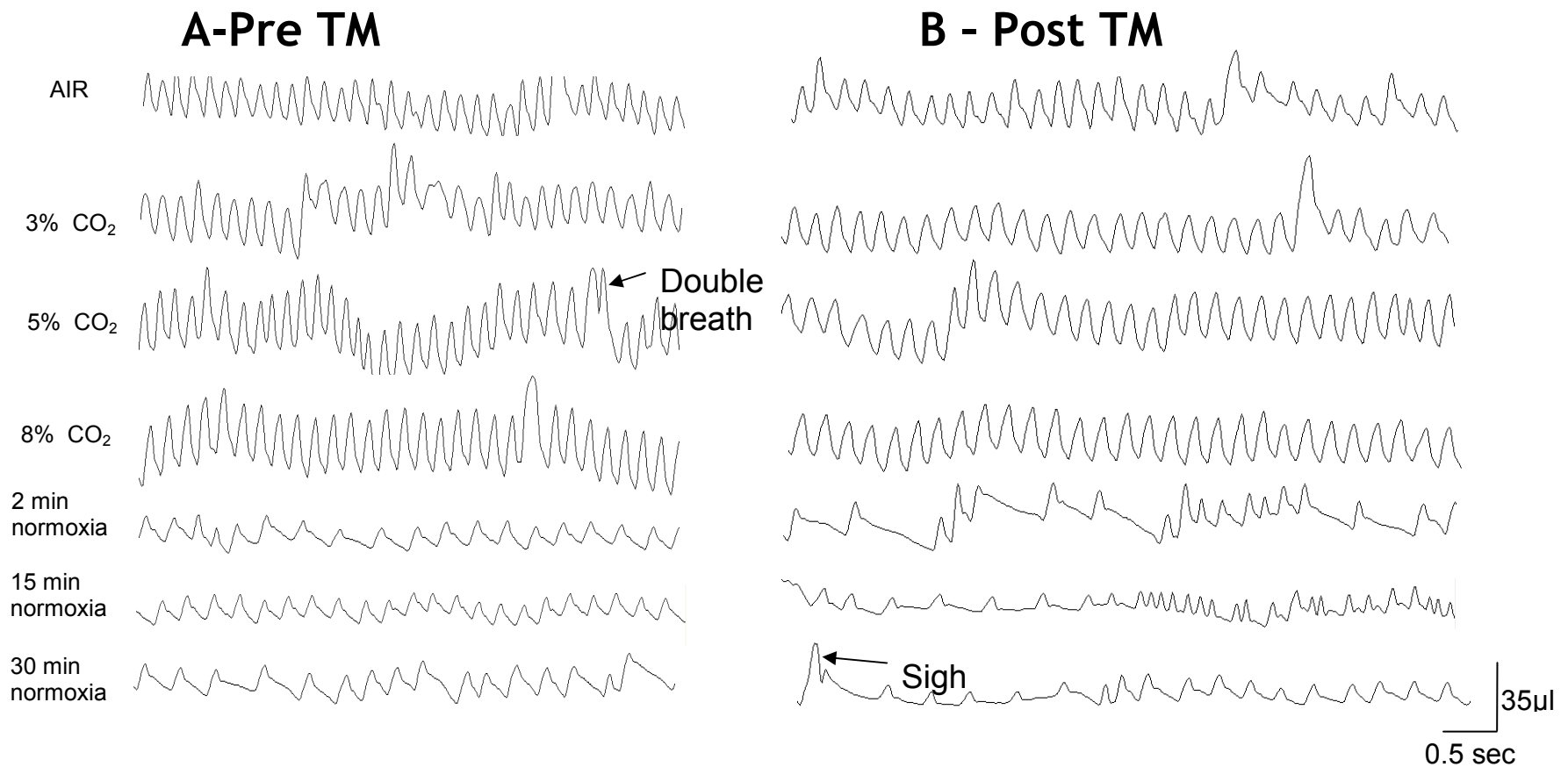


Fig 3-7 Respiratory traces to illustrate the respiratory pattern of a *Stop/y,cre* mouse with mild respiratory phenotype. A - Pre TM, respiratory frequency was high but rhythm was regular. Respiratory pattern became disturbed during hypercapnic exposure with large amplitude breaths and double breaths. Respiratory frequency decreased in the normoxic recovery periods but rhythm remained irregular. B - Post TM. Respiratory rhythm was regular in air and during hypercapnic exposure with fewer respiratory abnormalities than was seen pre TM. Sighing and apnea persist in normoxic periods following hypercapnic exposure. Respiratory rhythm is also irregular.

As was seen with *Stop/y* mice, not all of the *Stop/y,cre* mice developed the same severity of respiratory phenotype. Examples of severe respiratory traces of one *Stop/y,cre* animal are given in Fig 3-6. Before TM treatment (plot A) the breathing pattern was characterised by periods of faster and slower frequency and the occurrence of apnea. During hypercapnic exposure, the breathing pattern was still irregular and apneas persisted. During the normoxic period following hypercapnia, the breathing traces were still interspersed with apnea and periods of irregular respiratory frequency. The breathing of *Stop/y,cre* mice became more regular post-TM treatment (plot B) with a reduced respiratory frequency and abolishment of the majority, if not all, apneas. Fig 3-7 gives an examples of pre and post TM respiratory traces taken from a *Stop/y,cre* mouse with a milder respiratory phenotype than was observed in the traces of the animal shown in Fig 3-6. Before TM treatment (fig 3-7 plot A) the respiratory pattern was more regular than the pattern seen in fig 3-6 plot A, yet the respiratory pattern is still interspersed with sighs. Also, the breathing frequency observed in the 15 min and 30 min post hypercapnic period was irregular in the traces shown in fig 3-7 plot A. Fig 3-7 plot B shows that after TM treatment, the respiratory frequency of the *Stop/y,cre* animal was regular in air and in hypercapnia, with few sighs. However, the respiratory frequency remained irregular in the post hypercapnic periods with traces being interspersed with apnea and periods of faster and slower breathing.

3.3.3 Respiratory Frequency

Comparison of the average respiratory frequency of *Stop/y*, *Stop/y,cre* and WT mice when exposed to normoxia (Fig 3-8) revealed that WT animals had a similar respiratory frequency from week to week and that the frequency did not change in response to application of TM (TM-3 to 4: 284 ± 15 bpm. TM+11 to 13: 294 ± 30 bpm, $p > 0.05$). *Stop/y* animals exhibited a respiratory frequency which was not significantly different from WT at TM-3 to 4 (WT: 284 ± 15 , *Stop/y*: 274 ± 36 bpm, $P > 0.05$) yet frequency became significantly greater than WT at TM-1 to 2, TM and TM+1 to 2 (TM-1 to 2, WT: 295 ± 29 , *Stop/y*: 368 ± 8 bpm, $p < 0.05$. TM, WT: 277 ± 16 , *Stop/y*: 393 ± 26 bpm, $P < 0.05$. TM+1 to 2, WT: 265 ± 31 , *Stop/y*: 430 ± 54 bpm, $p < 0.05$). *Stop/y,cre* mice showed a respiratory frequency similar to that of WT at TM-4 to 3 (*Stop/y,cre*: 293 ± 30 bpm, WT: 284 ± 15 bpm, $p > 0.05$) but frequency increased at TM-1 to 2 to become significantly greater than the WT

(*Stop/y,cre*: 396±7 bpm, WT: 295±29 bpm, $p<0.05$). After TM treatment there was a decrease in the average respiratory frequency of *Stop/y,cre* mice (TM: 384±25 bpm, TM+7 to 8: 236±65 bpm) to a level that was not significantly different from the WT (TM+ 7 to 8, *Stop/y,cre*: 236±65 bpm, WT: 242±42 bpm, $P>0.05$). Towards the end of the study, the respiratory frequency of *Stop/y,cre* mice showed a trend towards an increase (TM+ 9 to 10: 290±69 bpm , TM+11 to 13: 314±17 bpm) which indicates that the rescue of respiratory frequency may not be permanent and that reactivation of *Mecp2* has a more transient effect on the rescue of breathing frequency.

The coefficient of variation for the average respiratory frequency was calculated to determine variability of the breathing traces. Figure 3-9 illustrates that WT animals maintained a similar coefficient of variation of respiratory frequency throughout the experiment. *Stop/y* animals exhibited a significantly greater amount of variability in the breathing pattern compared to WT at T-4 to 3 (WT: 18±2, *Stop/y*: 24±4 % co var of freq, $p<0.05$). There was trend towards a decrease in the variability of breathing of *Stop/y* mice from TM-4 to 3 to TM-1 to 2 (TM-4 to 3:24±4, TM-1 to 2:15±1 % co var freq). This decrease in variability coincided with an increase in respiratory frequency in *Stop/y* animals (Fig 3-8) suggesting that the respiratory pattern in the *Stop/y* mice is generally rhythmic and regular but high frequency. *Stop/y, cre* mice exhibited a significantly greater amount of variability in breathing pattern compared to WT at TM+3 to 4 (WT: 15±2, *Stop/y, cre*: 24±2 %co var freq, $p<0.05$). After completion of TM treatment, TM+5 to 6 and onwards, the variability in the breathing pattern of *Stop/y, cre* animals was not significantly different from WT. However, at TM+11 to 13 the variability in frequency of *Stop/y, cre* mice became significantly greater than the WT (WT: 20±1, *Stop/y, cre*: 29±4 % co var freq, $p<0.05$) which again indicates that the rescue of the respiratory phenotype may be more of a transient than permanent change.

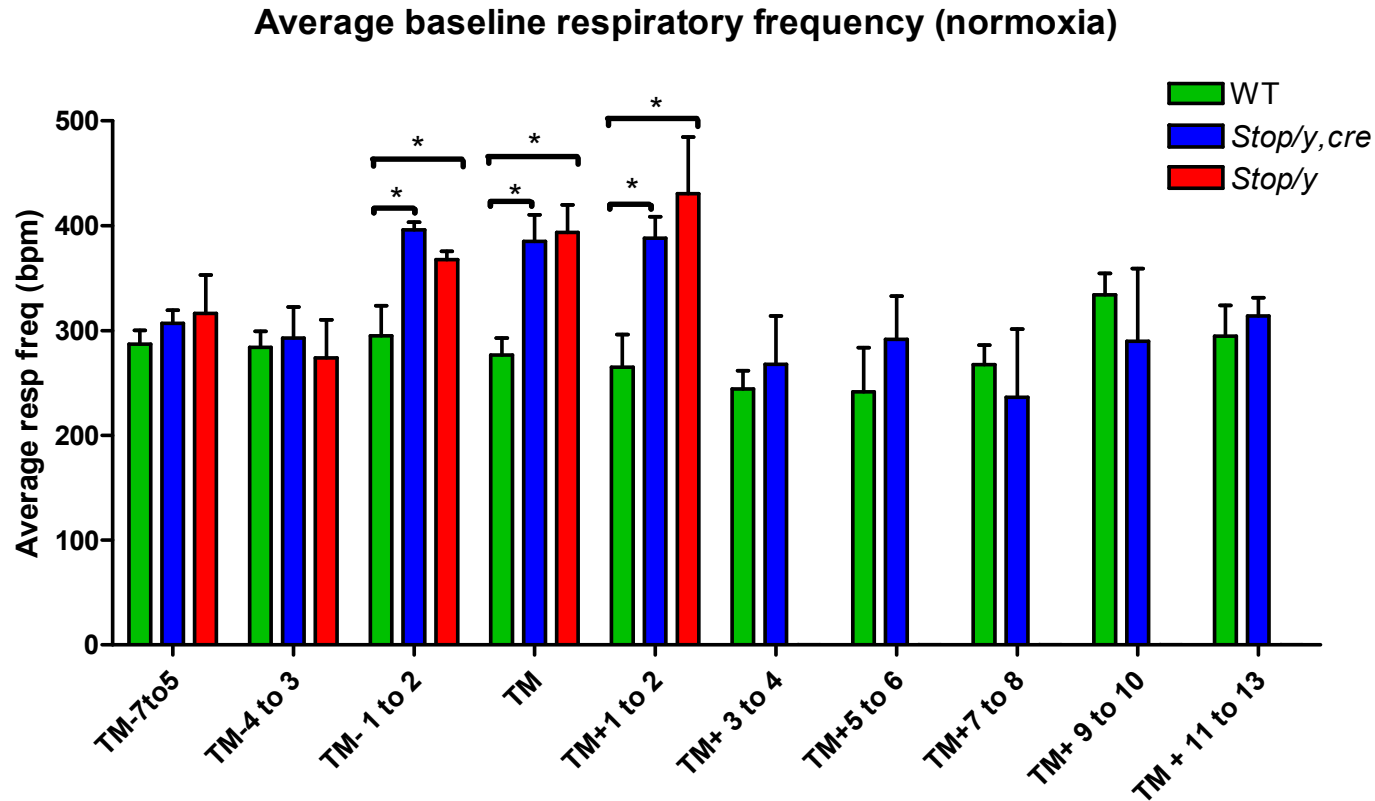


Fig 3- 8 Plot of the average respiratory frequency of *Stop/y*, *Stop/y, cre* and WT mice in normoxia (mean±SD). Data plotted in reference to TM treatment, with TM-7to5 representing 7 to 5 weeks before TM treatment. WT showed a similar respiratory frequency throughout the experiment. *Stop/y* and *Stop/y, cre* mice showed significantly greater frequency compared to WT at TM-1 to 2, TM and TM+1 to 2. *Stop/y, cre* mice displayed reduction in respiratory frequency following TM treatment and frequency was not significantly different from WT. 2 way anova with bonferroni post test; *p<0.05.

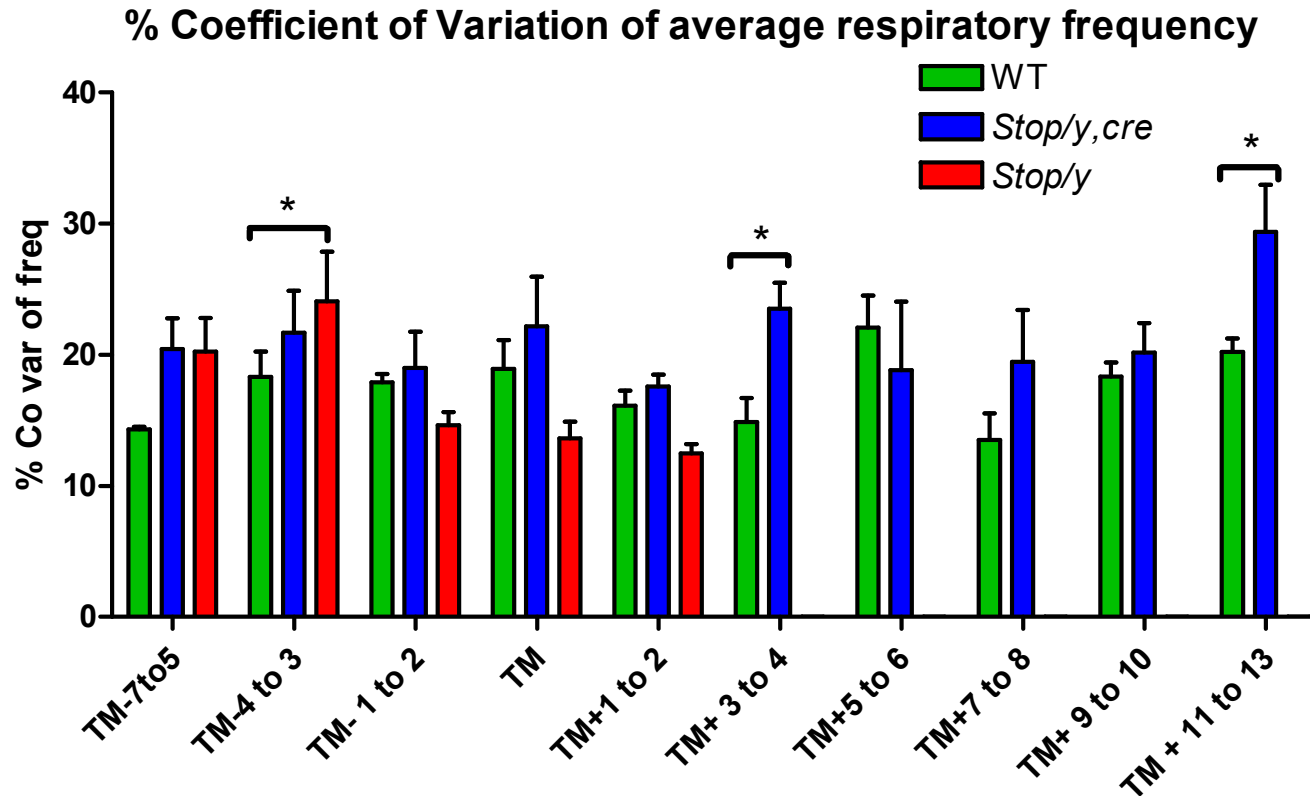


Fig 3-9 Plot of % co var of the average respiratory frequency of *Stop/y*, *Stop/y, cre* and WT mice in normoxia (mean±SD). WT showed a similar level of variability across all weeks. *Stop/y* mice showed significantly greater variability in breathing pattern compared to WT at T-4 to 3. *Stop/y, cre* mice showed significantly greater respiratory variability compared to WT at TM+ 3 to 4 and again at TM+11 to 13. 2 way anova with bonferroni post test;* p<0.05.

3.3.4 Response to Hypercapnia

As mentioned, it remains unknown whether respiratory deficits observed in the MeCP2 deficient mice such as apnea, sighing and variable respiratory frequency are due to a fault in rhythm generating centres of the brain stem or whether the abnormalities that arise are the result of a fault in chemosensitivity. Thus, the average respiratory frequency during exposure to varying levels of hypercapnia was plotted and also the 30 min recovery period when animals were returned to normoxia.

Four weeks prior to TM all three genotypes exhibited a similar baseline respiratory frequency (WT: 275 ± 28 , *Stop/y, cre*: 293 ± 30 and *Stop/y*: 274 ± 36 bpm; Fig 3-10). All genotypes displayed an increase in respiratory frequency upon exposure to 3% (WT: 343 ± 30 , *Stop/y, cre*: 320 ± 48 , *Stop/y*: 298 ± 62 bpm), 5% (WT: 360 ± 24 , *Stop/y, cre*: 329 ± 30 , *Stop/y*: 323 ± 55 bpm) and 8% CO₂ (WT: 388 ± 19 , *Stop/y, cre*: 369 ± 17 , *Stop/y*: 354 ± 34 bpm). The respiratory frequency during post hypercapnic recovery was comparable across the genotypes with a reduction in respiratory frequency from 2 min to 15 min post hypercapnic period (WT, 2min: 384 ± 72 , 15 min: 235 ± 61 , *Stop/y*, 2min: 352 ± 74 , 15 min: 248 ± 48 , *Stop/y, cre*, 2min: 375 ± 79 , 15 min: 225 ± 28 bpm). The *Stop/y* mice showed a decrease in respiratory frequency at 30 min post hypercapnic stimuli (202 ± 49 bpm) while the *Stop/y, cre* animals maintained a frequency similar to that observed at 15 min recovery (224 ± 35 bpm). The WT animals illustrated an increase in respiratory rate from 15 min to 30 min post hypercapnic recovery (15 min: 234 ± 61 bpm, 30mins: 285 ± 14 bpm).

At the point of TM treatment, WT animals displayed an increase in average respiratory frequency when exposed to increasing severity of hypercapnic stimulus (Fig 3-11; Air: 277 ± 16 bpm, 3%CO₂: 331 ± 63 bpm, 5%CO₂: 345 ± 44 , 8% CO₂: 392 ± 34 bpm). WT animals exhibited a subsequent decrease in respiratory frequency when the gas in the chamber was returned to normoxia (2min post hypercapnia: 355 ± 51 , 15 min post hypercapnia: 293 ± 86 , 30 min post hypercapnia: 240 ± 64 bpm). In normoxia, *Stop/y* animals had a significantly greater respiratory frequency than WT (*Stop/y*: 393 ± 26 bpm, WT: 277 ± 16 bpm, $p < 0.05$) and this higher frequency was maintained during hypercapnic exposure. Any increase in ventilation in response to hypercapnia appeared to be masked by

an already increased respiratory frequency. Like the *Stop/y* animals, *Stop/y,cre* mice displayed a higher average respiratory frequency than WT in normoxia (*Stop/y,cre*: 385 ± 25 bpm, WT:277 ±16 bpm, p<0.01). However, *Stop/y,cre* mice presented an abnormal response to hypercapnia, with a decreased respiratory frequency upon exposure to hypercapnia (Air: 385±25, 3%CO₂: 370 ±69, 5%CO₂: 325 ±91, 8%CO₂: 318± 51 bpm) which continued into 2 min recovery in air (269 ± 11 bpm), followed by an increase in respiratory frequency at 15 min recovery (307 ± 45 bpm).

The average respiratory frequency of the WT animals was unaffected by TM treatment and it can be seen in Fig 3-12 that WT animals continued to display an increase in respiratory frequency from air (231±27 bpm) to 3% (249±13 bpm), 5% (272±19 bpm) and 8% CO₂ (323±27 bpm). WT showed a subsequent decrease in frequency to upon return to normoxia (2 min: 251±68, 15 min: 202±33, 30 min: 199±39 bpm). In air, *Stop/y,cre* mice had a lower respiratory frequency than was seen at the point of TM treatment (Air, TM+5: 292±41, TM: 384.8±25.4 bpm, Fig3-10) but this remained greater than the respiratory frequency of WT (WT: 230.5±27.5 bpm, *Stop/y,cre*: 291.7±41.1bpm). The *Stop/y,cre* mice still exhibited an abnormal response to hypercapnia with a decrease in frequency when exposed to 3% (275.3±64.3bpm) and 5% CO₂ (268.2±49.9bpm). After TM treatment, the post-hypercapnic recovery of the *Stop/y,cre* animals was not significantly different to that of WT animals (2min, WT: 251±68, *Stop/y,cre*: 243±38 bpm. 15 min, WT: 202±33 bpm, *Stop/y,cre*: 190±35 bpm. 30 min, WT: 199±39 , *Stop/y,cre*: 170±2 bpm,p>0.05).

Nine weeks post-TM (Fig 3-13) WT animals continued to exhibit an increase in respiratory frequency when exposed to hypercapnic stimuli (Air: 313±15bpm,3% CO₂: 326±50, 5% CO₂: 335±30, 8% CO₂: 370±17 bpm) and a decrease in frequency upon return to normoxic conditions (2 min post hypercapnia: 303±20, 15 min post hypercapnia: 281±33, 30 min post hypercapnia: 288±49 bpm). *Stop/y,cre* mice displayed a respiratory frequency that was similar to WT in air (WT: 313±15, *Stop/y,cre*: 290±69 bpm) but showed a decrease in respiratory frequency when in 3% CO₂ (223±20 bpm). An increase in frequency compared to 3% CO₂ exposure was observed upon exposure to 5% (262±76 bpm) and 8% CO₂ (298±50 bpm) but these values were not greater than baseline breathing (Air: 290±69 bpm). The *Stop/y,cre* also displayed a decrease in respiratory frequency

upon return to normoxic conditions (2 min post hypercapnia: 272 ± 137 , 15 min post hypercapnia: 211 ± 93 , 30 min post hypercapnia: 182 ± 77 bpm).

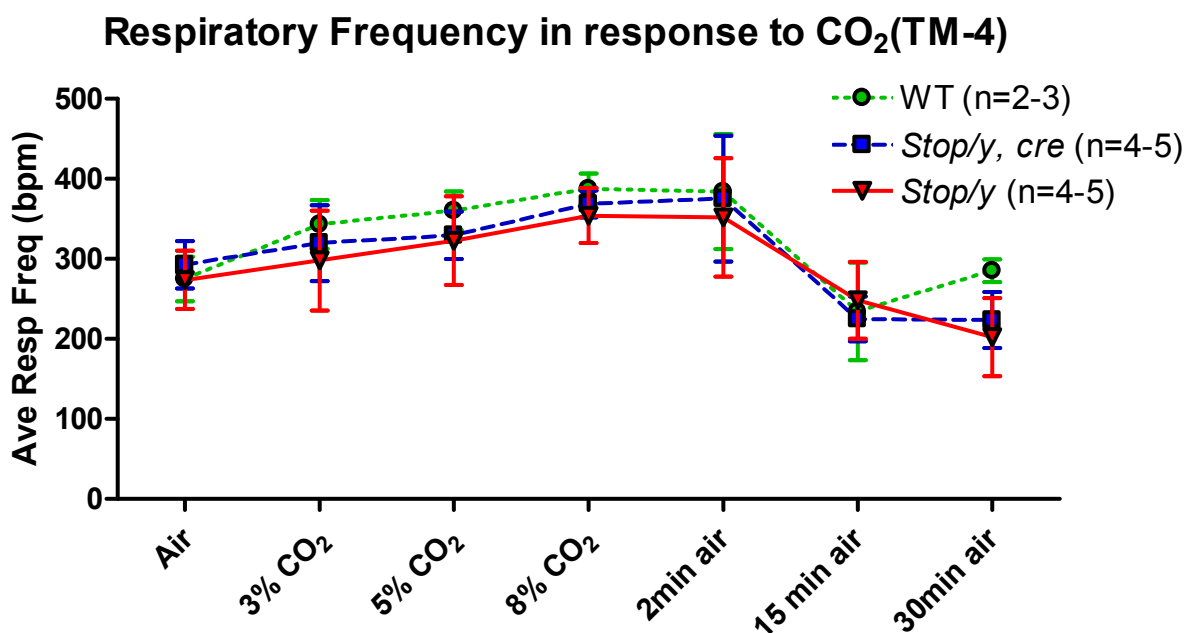


Fig 3-10 Plot of the average respiratory frequency of *Stop/y*, *Stop/y,cre* and WT mice 4 weeks before TM treatment (mean \pm SD). All genotypes exhibited similar respiratory frequency in air and an increase in respiratory frequency in response to hypercapnia (3%, 5% and 8%). Genotypes exhibited similar post-hypercapnic decrease in respiratory frequency on return to air at 2min and 15min. WT exhibited increase in respiratory frequency at 30 min post hypercapnic recovery while *Stop/y,cre* TM maintained the same frequency observed at 15 min recovery. *Stop/y* mice exhibited a decrease in respiratory rate from 15 min to 30 min post hypercapnia recovery. 2 way anova with Bonferroni post test showed no significant differences between the genotypes.

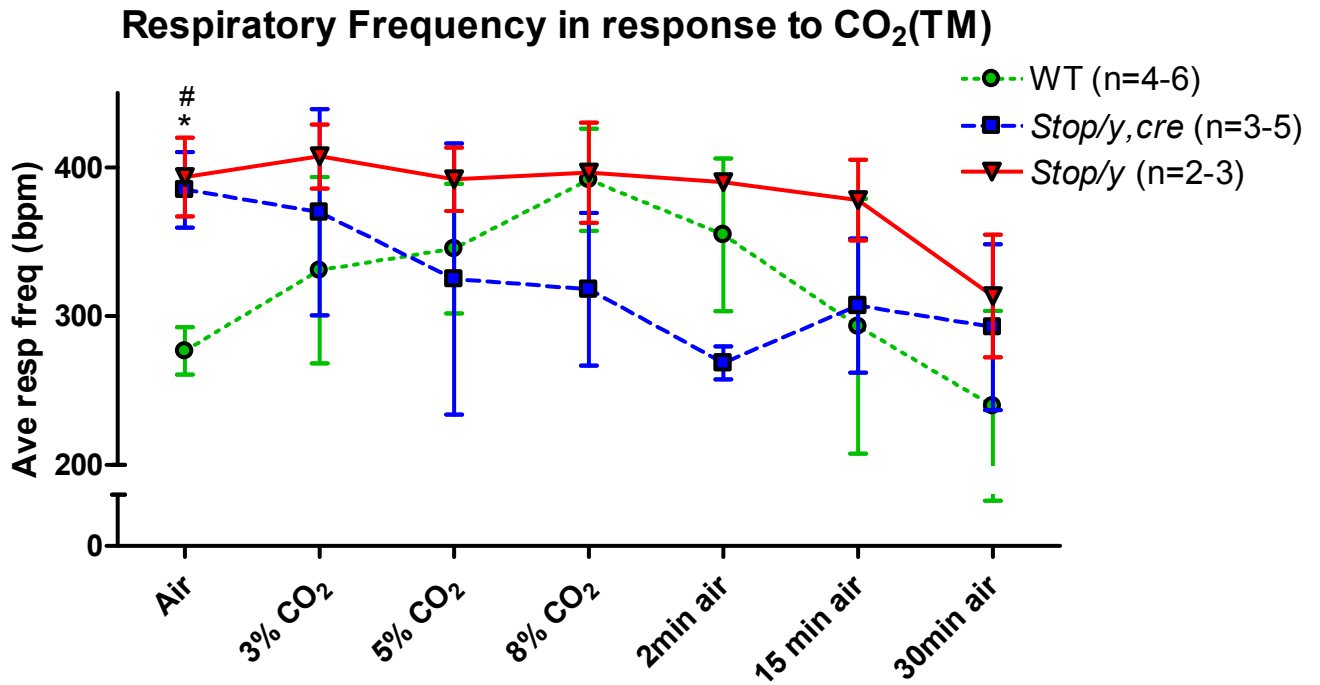


Fig 3-11 Plot of the average respiratory frequency of *Stop/y*, *Stop/y,cre* and WT mice before TM treatment (mean±SD). In air, *Stop/y* had a significantly greater average respiratory frequency compared to WT (#; p<0.05) as did *Stop/y,cre* animals (*; p<0.05). WT displayed typical increase in respiratory frequency in response to increasing intensity of hypercapnic stimulus, with subsequent reduction in frequency upon return to normoxic conditions. *Stop/y* mice maintained a high respiratory frequency throughout the protocol and *Stop/y,cre* animals exhibited a very abnormal response to hypercapnia (reduction in average respiratory frequency) compared to WT. 2-way ANOVA bonferroni post test.

Respiratory Frequency in response to CO₂(TM+5)

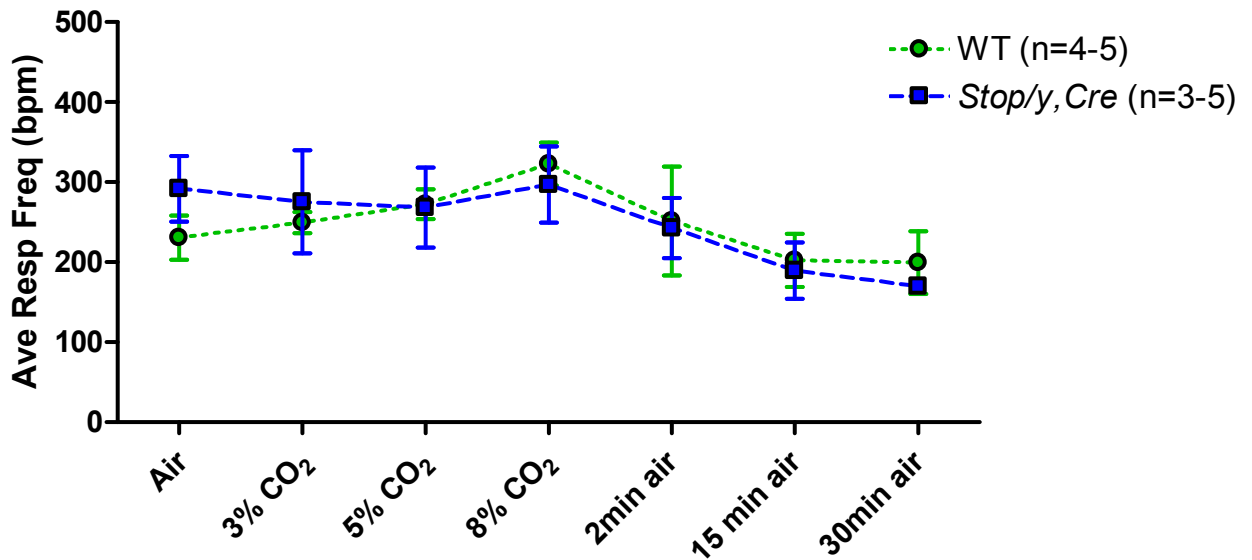


Fig 3-12 Plot of the average respiratory frequency of *Stop/y,cre* and WT mice 5 weeks after TM treatment (mean±SD). In air, *Stop/y,cre* had a higher respiratory frequency than WT (291.73±41.07bpm and 230.55±27.47bpm respectively). WT mice exhibited the typical response to hypercapnia, displaying an increase in respiratory frequency upon exposure to the hypercapnic stimuli, and a reduction in frequency upon return to normoxia. *Stop/y,cre* mice still displayed a somewhat abnormal chemosensitive response, with a decrease in respiratory frequency in 3% and 5% CO₂. There appeared to be a trend towards an increase in frequency upon exposure to 8% CO₂ but this increase did not take respiratory frequency to a greater value than was observed during baseline breathing. *Stop/y,cre* mice showed reduction in respiratory frequency upon exposure to normoxia. 2 way anova with Bonferroni post test showed no significant differences between the genotypes.

Respiratory Frequency in response to CO₂(T+9)

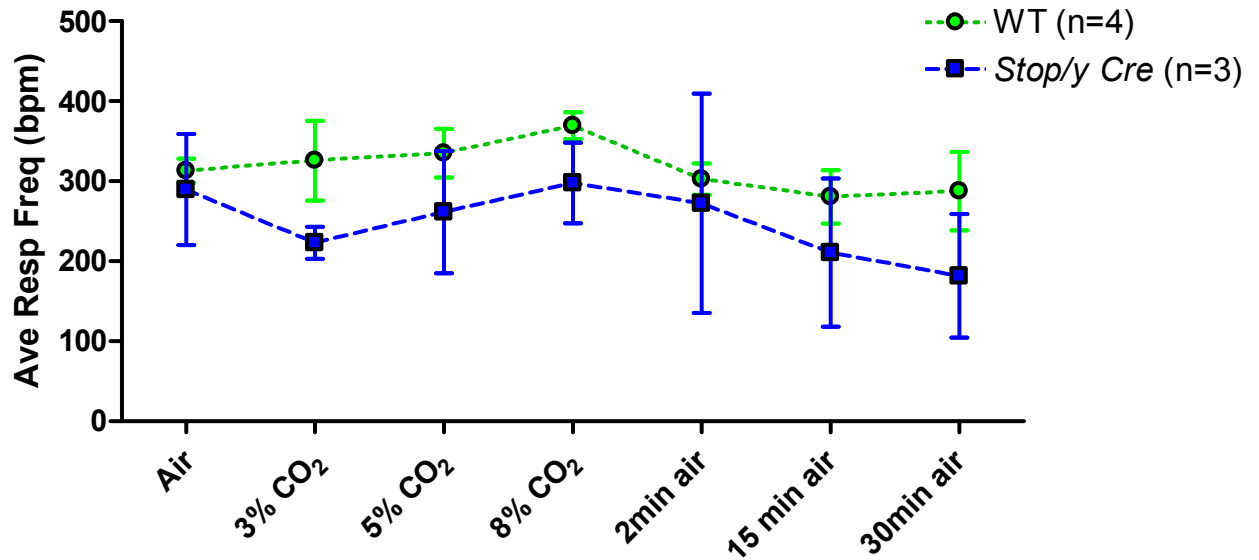


Fig 3-13 Plot of the average respiratory frequency of *Stop/y,cre* and WT mice 9 weeks after TM treatment (mean±SD). WT exhibited increased respiratory frequency when exposed to hypercapnia and reduced respiratory frequency when returned to normoxia. *Stop/y,cre* demonstrated a reduction in frequency when exposed to 3% CO₂ and a return to baseline frequency at 5% and 8% CO₂. *Stop/y,cre* animals showed a reduction in respiratory frequency when returned to normoxia. 2 way anova with Bonferroni post test showed no significant differences between the genotypes.

3.3.5 Sighing



Fig 3-14 Example of sigh taken from respiratory trace of *Stop/y,cre* mouse. Sighs are defined as large amplitude breaths followed by a post sigh apnea.

Observing the number of sighs which occur in normoxia (Fig 3-15), it can be noted that WT animals exhibited 1-2 sighs per 2 min trace, which is considered to be normal respiratory behaviour (Bartlett Jr 1971). The frequency of sighing in WT animals is unaffected by the application of TM. *Stop/y,cre* mice showed an increase in the number of sighs from TM-1 to 2 (8.5 ± 6.4 sighs per 2 min) to TM+3 (9.7 ± 9.1 sighs per 2 min). *Stop/y,cre* mice also exhibited significantly more sighs than WT at T-4to3 ($p < 0.05$), T-2to1 ($p < 0.05$), TM ($p < 0.05$) and T+3to4 ($p < 0.05$). After the completion of TM treatment the frequency of sighing was reduced in *Stop/y,cre* animals (TM: 6 ± 6.4 sighs, T+5 to 6: 2 ± 2.3 sighs) and there was no significant difference between the number of sighs in WT and *Stop/y,cre* mice. *Stop/y* mice demonstrated an increase in the number of sighs from TM-7to5 (1.3 ± 0.6 sighs) to TM+1to2 (3.3 ± 4.9 sighs).

Two weeks prior to TM treatment, WT animals displayed no sighs in air and very few sighs under hypercapnic conditions (Fig 3-16). In air, *Stop/y,cre+TM* mice had significantly more sighs compared to WT ($p < 0.05$). *Stop/y cre+TM* mice showed a trend towards a decrease in the frequency of sighs from air to 3% CO₂ (Air: 8.5 ± 6.4 sighs, 3% CO₂: 2 sighs). This frequency then remained similar throughout 5% (3 sighs) and 8% CO₂ (2 sighs) and during the post hypercapnia recovery period (2 min: 2 sighs, 15 min: 1 sigh, 30 min: 2 sighs). The frequency of sighing in *Stop/y,cre-TM* mice did not differ significantly from one respiratory stimulus to another but displayed a trend towards a decrease from air to 3%CO₂

(Air: 2.6 ± 1.1 sighs, 3% CO₂: 1.7 ± 2.1). *Stop/y* mice displayed a similar sigh frequency in air and hypercapnic stimulus (Air: 1.5 ± 1.4 , 3%CO₂: 2 ± 1.9 , 5%CO₂: 1.8 ± 1.1 , 8%CO₂: 1.8 ± 1.6 sighs) with a trend towards a reduced sigh frequency in the post hypercapnic period (2 min: 0, 15 min: 0.4 ± 0.5 , 30 min: 0.4 ± 0.5 sighs).

At 5 weeks post-TM treatment (Fig 3-17, TM+5), one week after the completion of TM treatment, sighs remained infrequent in WT, with sighs occurring approximately once per minute. *Stop/y,cre+TM* mice still exhibited a greater number of sighs than WT in air (*Stop/y,cre+TM*: 2 ± 2.3 , WT: 0.5 ± 1.1 sighs). However, in air, the number of sighs which occurred in the *Stop/y,cre+TM* mice was reduced compared to values recorded in *Stop/y,cre+TM* mice pre-TM (preTM: 8.5 ± 6.4 sighs, post TM: 2 ± 2.3 sighs) indicating that reactivation of *Mecp2* may have reduced the frequency of sighing in the *Stop/y,cre+TM* mice.

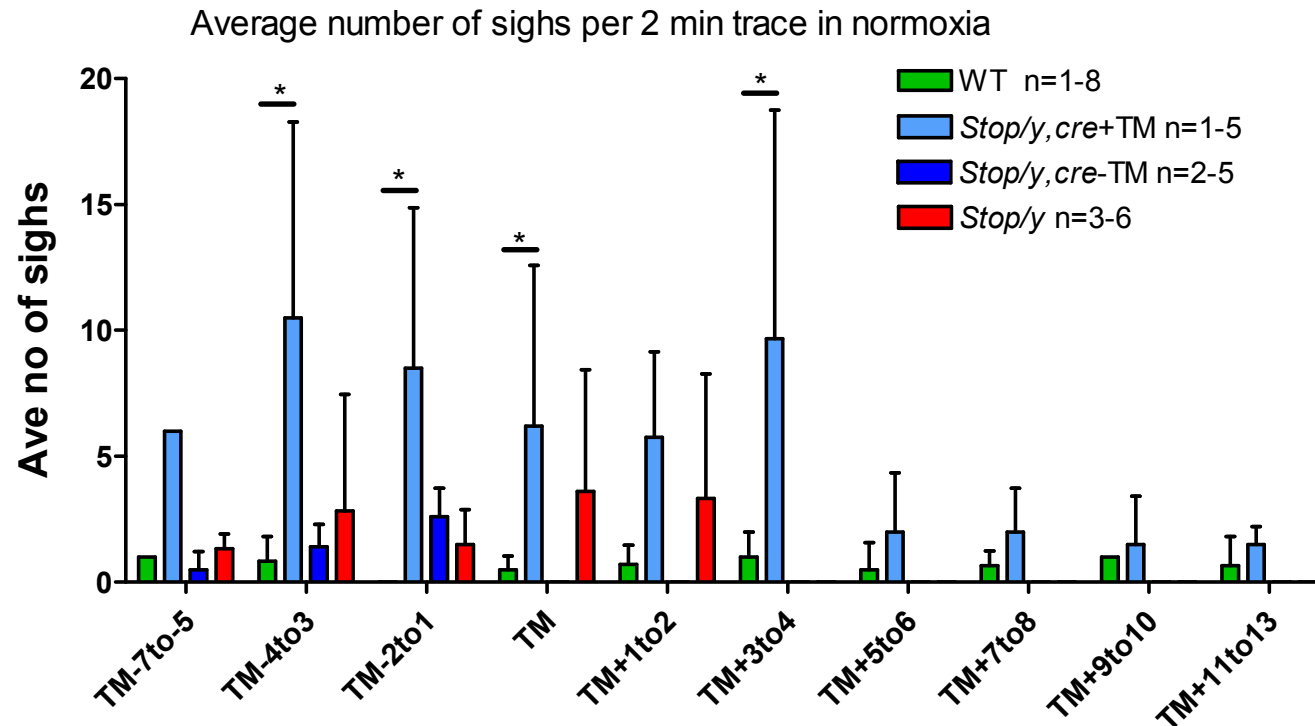


Fig 3-15 Average number of sighs which occur in normoxic conditions in WT, *Stop/y* and *Stop/y, cre* mice (mean ±SD). WT animals showed 1 sigh per 2 min trace at T-7 to 5. Frequency of sighing in WT animals was unaffected by the application of TM. *Stop/y* animals showed an increase in the number of sighs from T-7 to 5 (1.3±0.5 sighs) to T+1 and 2 (3.3±4.9 sighs). *Stop/y, cre-TM* animals also showed an increase in the occurrence of sighing from T-7 to 5 (0.5±0.7 sighs) to T-2to1 (2.6±1.14 sighs). *Stop/y, cre+TM* mice showed increase from 6 sighs at T-7 to 5, to 10.5±7.7 at T-3to4. Sighing was reduced at T+5to6 following the completion of TM treatment (2±2.3 sighs). *Stop/y, cre+TM* mice exhibited significantly more sighs than WT pre TM but no significant difference was observed between the two genotypes following completion of TM (T+5to6 onwards). 2 way anova with bonferroni post test; * p<0.05.

Average number of sighs in response to hypercapnia (TM-2)

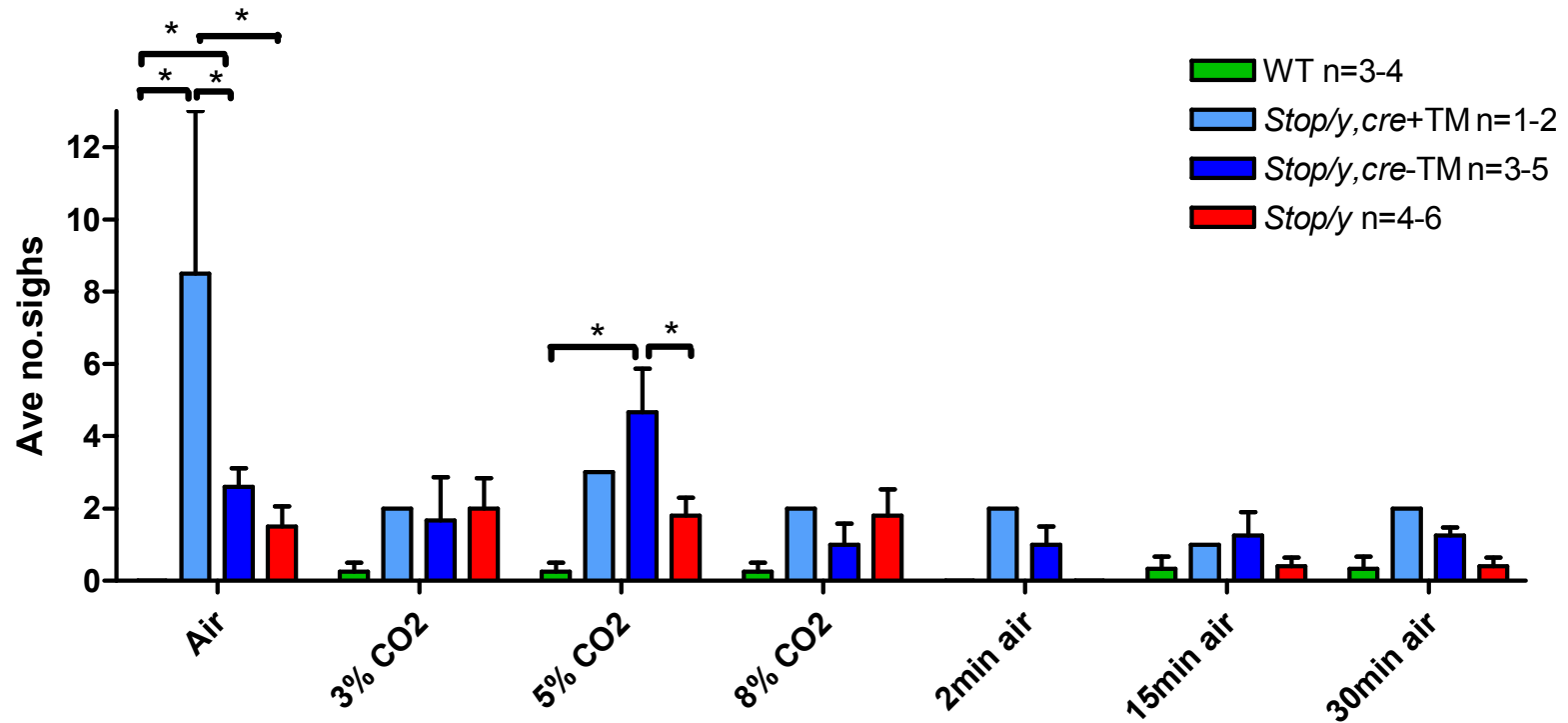


Fig 3-16 Average number of sighs in WT, *Stop/y,cre* and *Stop/y* mice 2 weeks prior to TM (mean \pm SD). Sighs were more prevalent in the MeCP2 deficient mice compared to WT and the frequency of sighs did not seem to be influenced by hypercapnic exposure or recovery from the stimulus. In air, *Stop/y,cre+TM* and *Stop/y* animals had significantly more sighs compared to WT. 2 way anova with bonferroni post test; * $p < 0.05$.

Average number of sighs in response to hypercapnia (TM+5)

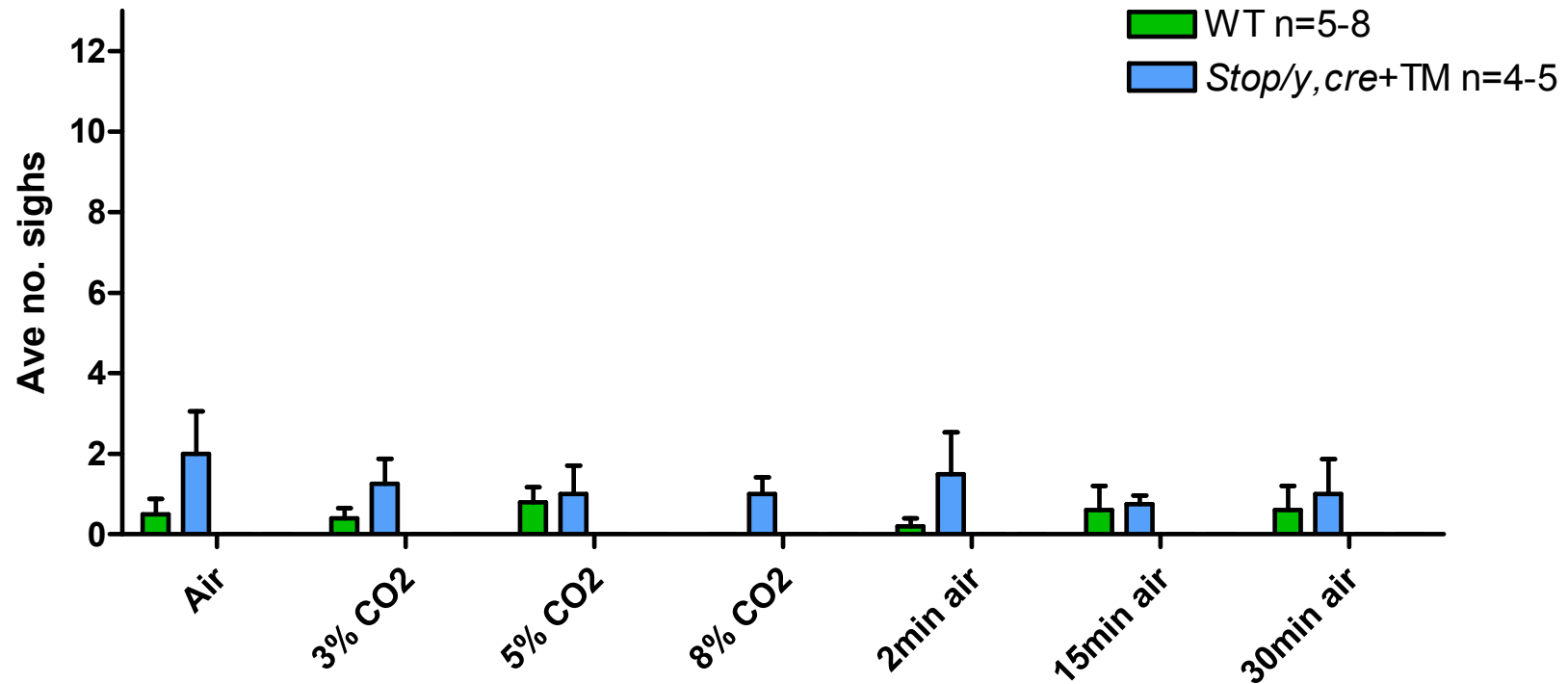


Fig 3-17 Plot to illustrate the average number of sighs which occur per 2 min trace in WT and *Stop/y, cre+TM* mice at 5 wks post TM treatment (TM+5; mean \pm SD). 2 way anova with bonferroni post test showed no significant difference between the frequency of sighs in WT compared to *Stop/y, cre+TM* mice.

3.3.6 Double Breaths



Fig 3-18 Example of respiratory trace containing double breath from *Stop/y,cre* animal. These breaths are as two inspiratory peaks which are separated by an incomplete expiratory phase. There may also follow a very short period of post double breath apnea.

Another of the respiratory phenotypes frequently observed in the MeCP2 deficient mice were those termed “double breaths”. These were defined as two inspiratory peaks separated by an incomplete expiration (Fig 3-18). A similar respiratory phenotype has been reported previously in both WT and *Mecp2*^{-/y} mice and termed as “complex sighing” (Voituron *et al.*, 2010). As with sighs, the average number of double breaths per 2 min trace was quantified to investigate whether this characteristic was more frequent in the MeCP2 deficient animals than WT.

In normoxia, double breaths were found to be infrequent in WT animals (Fig 3-19) and occurred at the same frequency as sighing (e.g. 1-2 per 2 min trace). The number of double breaths increased in the *Stop/y* mice from TM-7 to 5 to TM+1to2 (TM-7to5: 1 double breath, TM+1 to 2:6:±5.3 double breaths). *Stop/y, cre+TM* mice illustrated a trend towards an increase in the number of double breaths from TM-7to-5 to TM-4to3 (TM-7 to 5: 0.5±0.71 double breaths, TM-4 to 3:2.6±1.6 double breaths). However, there was a trend towards a decrease in the number of double breaths in *Stop/y, cre+TM* mice following TM treatment (TM-1 to 2: 4±5.7, TM+5 to 6: 1.4±1.7 double breaths). The occurrence of double breaths in *Stop/y, cre+TM* mice appeared to increase over time even though *Mecp2* had been reactivated (TM+7 to 8:1.7±2.1, TM+9 to 10:3±2.6, TM+11 to 13: 4.5±2.1 double breaths). This suggests that the lack of MeCP2 may have caused changes in the respiratory system that cannot be fully rescued by reactivation of *Mecp2*.

Average number of double breaths in normoxia

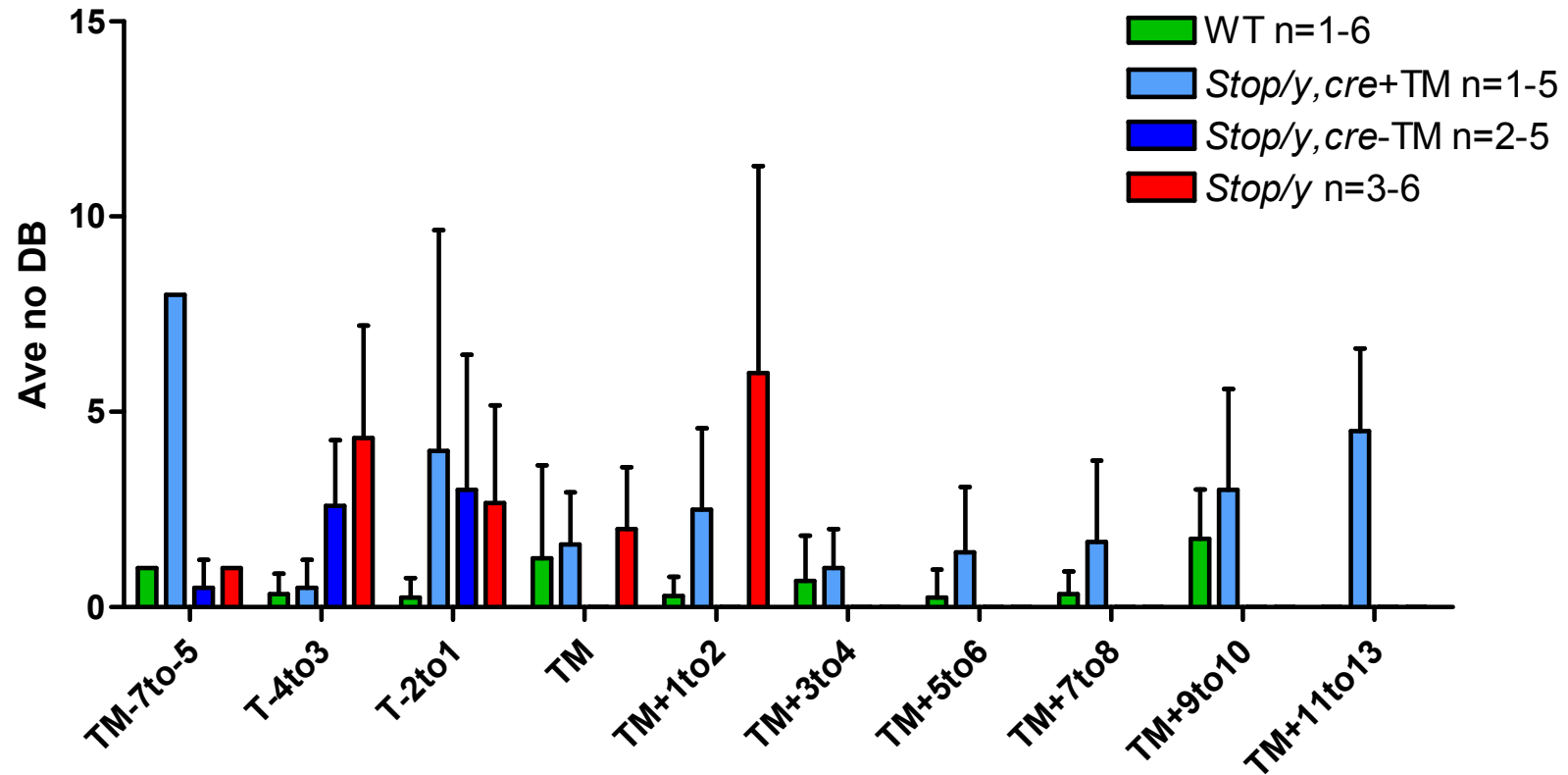
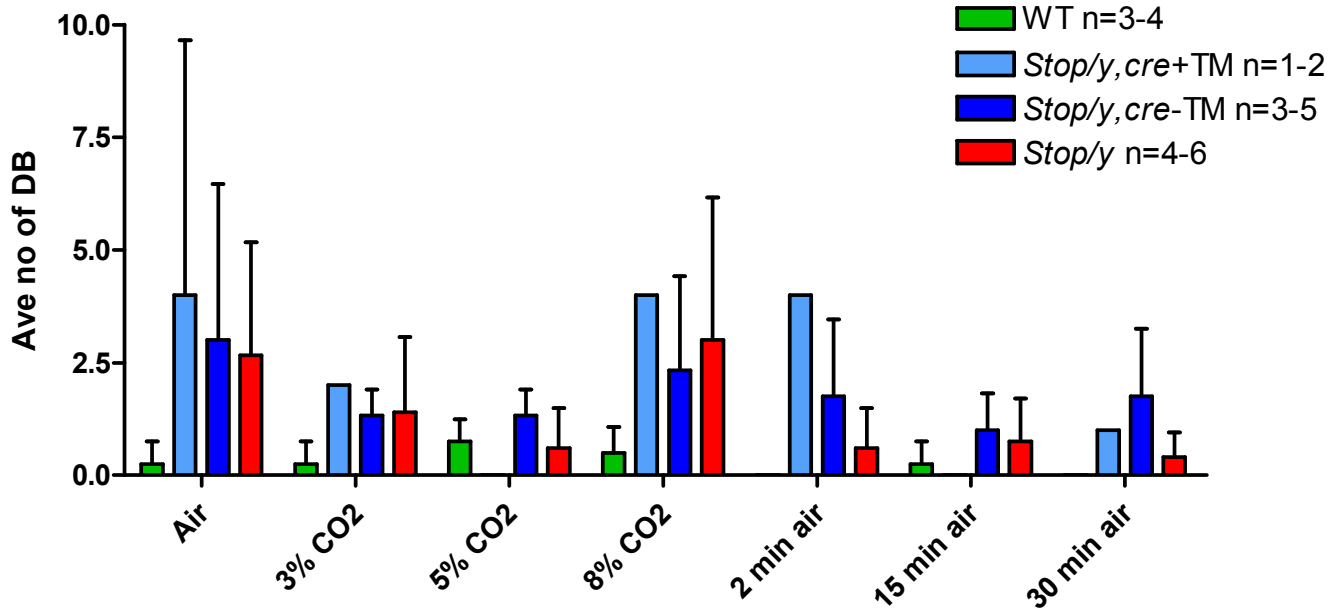


Fig 3-19 Plot to show the average number of double breaths that occur per 2 min trace in WT, *Stop/y, cre* and *Stop/y* animals, (mean \pm SD). Double breaths were more prevalent in MeCP2 deficient mice compared to WT. *Stop/y, cre* animals showed a trend towards a reduced number of double breaths following TM treatment, until TM+9 to 10 where double breath frequency showed a trend towards an increase. 2 way anova with bonferroni post test showed no significant difference between the genotypes.

A

Average number of double breaths in response to hypercapnia (TM-2)



B

Average number of double breaths in response to hypercapnia (TM+5)

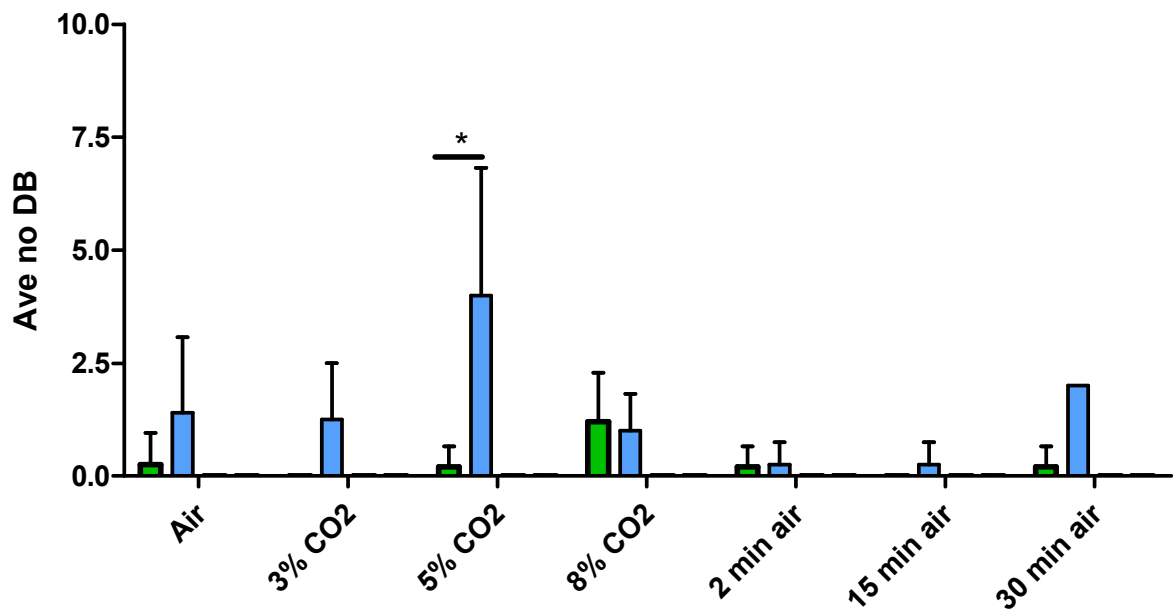


Fig 3-20 Plot to show the average number of double breaths that occur per 2 min trace in WT, *Stop/y,cre* and *Stop/y* animals (mean \pm SD). **A** - 2 weeks prior to TM, double breaths were more prevalent in *MeCP2* deficient mice compared to WT. **B** - 5 weeks post TM, *Stop/y,cre+TM* mice continued to exhibit double breaths even following *Mecp2* reactivation. *Stop/y,cre+TM* mice had significantly more double breaths than WT in 5% CO₂ (*p<0.05).

Two weeks prior to TM, the average number of double breaths in the WT was low (Fig 3-20 plot A) as previously mentioned. Double breath frequency was not altered upon exposure to hypercapnia or recovery in air. 5 weeks post TM, sigh frequency remained unchanged in the WT. *Stop/y,cre+TM* mice had the greatest number of double breaths in air, 8% CO₂ and in 2 min post hypercapnia (*Stop/y,cre+TM* Air: 4±5.7, 8%CO₂: 4 double breaths, 2 min post hypercapnia: 4 double breaths) and therefore did not appear to be induced by any particular stimulus. *Stop/y* animals also showed more double breaths than WT in all stimuli but the frequency of double breaths in the *Stop/y* animal did not seem to be induced by one particular stimuli. The greatest number of double breaths in *Stop/y* animals was seen in air and 8% CO₂ (*Stop/y*, Air: 2.7±2.5, 8% CO₂: 3±3.2 double breaths). Five weeks after TM treatment (fig 3-20 plot B) was initiated, the number of double breaths in the WT remained low. In air, *Stop/y,cre+TM* animals exhibited a reduced number of double breaths 5 weeks post-TM when compared to 2 weeks pre-TM (TM+5: 1.4±1.7, TM-2: 4±5.7 double breaths).

3.3.7 Apneas



Fig 3-21 Example of respiratory trace from *Stop/y,cre* animal containing apnea. Apnea was defined as three missed breaths or longer, calculated to be 0.6 sec.

Apneas are a frequent feature in the respiratory phenotype of RTT patients (Cirignotta *et al.*, 1986). The number of apneas that occurred per 2 min trace in WT, *Stop/y* and *Stop/y,cre* animals were quantified pre and post TM to investigate whether an MeCP2 deficit results in a change in the frequency of occurrence. Apneas were also quantified during hypercapnic exposure and following hypercapnic exposure.

2 weeks prior to TM, apneas in WT adults were infrequent in air (0.5 ± 1 apnea) and did not occur in hypercapnia or during post hypercapnia recovery in air (fig 3-22 plot A). Pre TM, *Stop/y* mice exhibited few apneas in air (0.7 ± 0.96 apneas) and 3% CO₂ (0.6 ± 0.0 apneas), yet none in 5% and 8% CO₂. *Stop/y,cre+TM* mice showed no apneas in air or hypercapnia but apneas became apparent in the 15 min post-hypercapnic recovery period (2 ± 2 apneas). Post TM treatment, WT animals showed no apneas. *Stop/y,cre+TM* mice showed few apneas in air (0.6 ± 0.8 apneas) but none during hypercapnic exposure. Apneas became apparent in the post hypercapnic recovery period (0.2 ± 0.0 apneas 2 min, 2.3 ± 0.0 apneas at 15 min, 3.8 ± 2.0 apneas at 30 min).

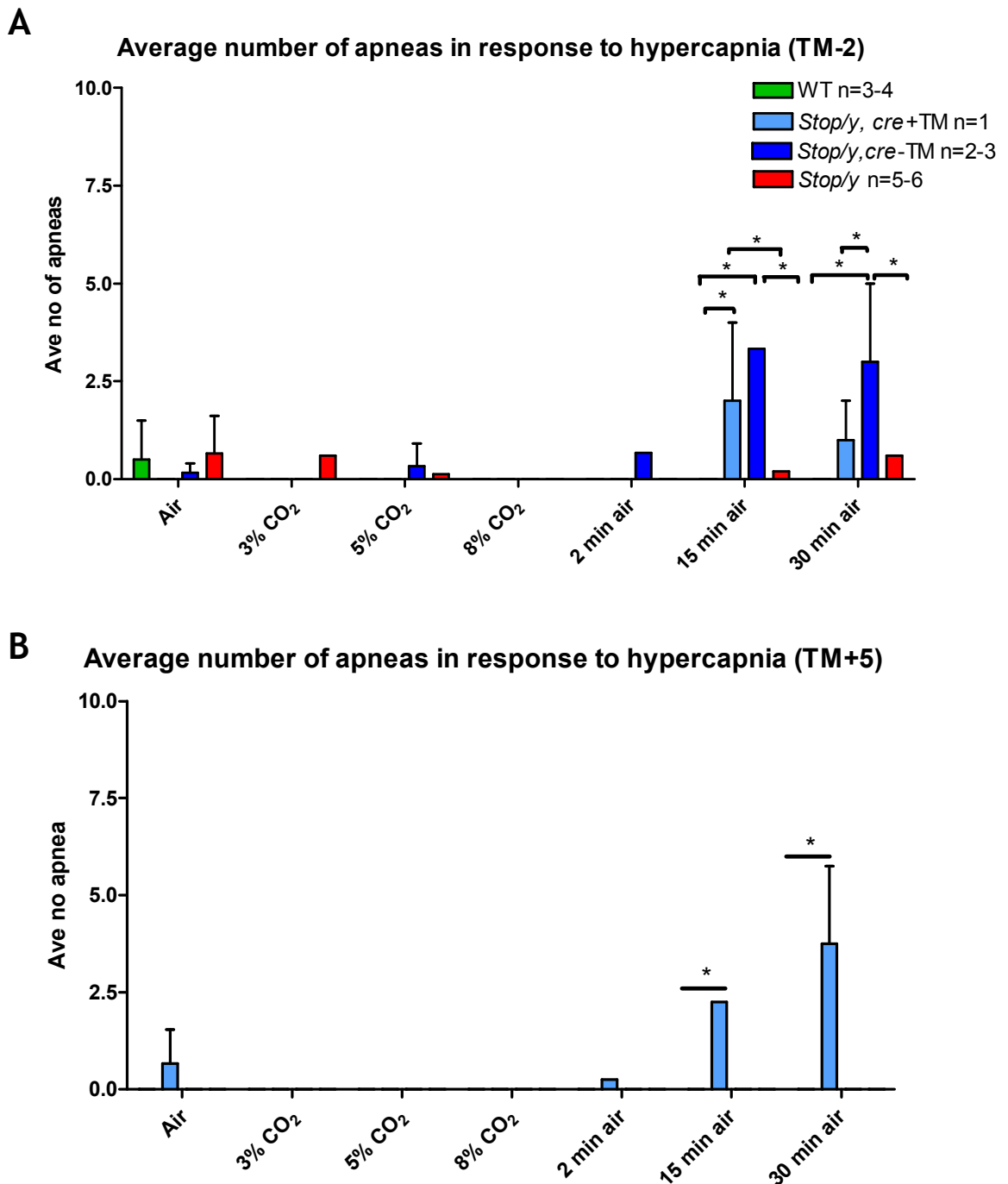


Fig 3.22 Plot to show the average number of apneas that occur per 2 min trace in WT, *Stop/y,cre* and *Stop/y* animals. **A** - 2 weeks prior to TM, apneas were more prevalent in MeCP2 deficient mice compared to WT. Apneas were also more prevalent during the post hypercapnia normoxic periods (2 way anova with bonferroni post test, $*p < 0.05$). **B** - 5 weeks post TM, apneas persist in the *Stop/y,cre+TM* mice during normoxic post hypercapnia recovery periods. Apneas were significantly more numerous in the *Stop/y,cre+TM* mice compared to WT (2 way anova with bonferroni post test, $*p < 0.05$).

3.4 Discussion

3.4.1 Experimental Issues

3.4.1.1 *The Male Mouse Model and Variability*

As discussed in section 3.2.2, the mouse model used in this study proved to be more variable than anticipated. It was originally proposed that animals would be scored on a weekly basis and comparisons of the respiratory phenotype would be made on an age-matched basis. However, age did not prove a reliable determinant of the onset of the RTT-like phenotype. Guy et al (2007) reports that *Stop/y* animals show a steady aggregate score up until about 8-10 weeks followed by a quick progression of the RTT-like phenotype approximately 4 weeks prior to death. However, observation of the first cohort of male animals, 4-5 weeks old, delivered from Harlan Labs revealed that not only could animals develop the RTT-like phenotype much earlier than expected, but also that the behavioural scores of the mutant mice were not as stable as reported by Guy et al (2007). This variability in phenotype resulted in TM treatment being administered to animals at different ages. For the purpose of comparing the respiratory phenotype before, during and after TM treatment, collected data has therefore been represented using time of TM treatment rather than age of the animal.

The fact that the animals used in this study and the animals utilised by Guy et al differed so greatly could be due to a number of factors. Firstly, the animals used in this study were bred on a C57BL6/CBA background whereas those used by Guy et al backcrossed to C57BL6 for several generations (4 or more) from 129/Ola mice (personal communication with Jacky Guy). Background is known to affect various aspects of murine physiology including the respiratory pattern (Stettner *et al.*, 2008) and therefore the incongruity observed in the development of RTT-like symptoms of the *MeCP2* deficient mice of this chapter could be influenced by the background onto which the model was bred. Secondly, the mice utilised by Guy et al were bred in house whereas the mice in this study were transported from Harlan UK limited (England) to the research centre (Scotland). It may be possible that the stress of transportation resulted in a quicker onset of RTT-like symptoms and subsequent death in some *MeCP2* deficient mice. Further

evidence that the animals were somewhat stressed is that some WT animals had to be discounted from the study on account of their aggression and extremely nervous disposition as previously discussed. Some *Stop/y,cre* animals were symptomatic on arrival and had to be treated with TM immediately. This resulted in no pre-TM data being collected and these animals had to be discounted from the study. Some *Stop/y* mice had to be euthanised before the study began due to the severity of the behavioural phenotype. As a result of so many animals being removed from the study, the n numbers for the respiratory measures were greatly reduced. Due to the variable nature of the model and its incompatibility with this particular experimental design it was decided that it was not viable to continue studying the model in an attempt to increase n numbers.

3.4.1 Respiratory Frequency and Rhythm

Early on in the study (TM-4 to 3, Fig 3-8) the mean respiratory frequency in the mutant groups did not differ significantly from WT, which suggests a period of normal development and respiratory activity in MeCP2 deficient mice. This finding is in agreement with previous studies that indicate that at 6 weeks of age *Mecp2^{-/y}* mice have a similar mean respiratory frequency to WT (Viemari *et al.*, 2005). The same group noted that although the average respiratory rate is similar between the young *Mecp2^{-/y}* and WT animals, mutant mice exhibit an increase in the variability of the respiratory pattern interspersed with respiratory disturbances. The data presented in this chapter (Fig 3-9) somewhat contradicts this finding by illustrating that *Stop/y* mice actually exhibited a decrease in the variability of average respiratory frequency as measured by the coefficient of variation of the respiratory frequency. However, from Fig 3-15 it is clear that *Stop/y,cre* mice, of a similar age to the *Mecp2^{-/y}* mice used by Viemari *et al* (TM-4; approx 6 weeks old), showed an increase in the frequency of sighs compared to WT, indicative of respiratory variability. Also, 6 week old *Stop/y* mice in this study illustrated an increased number of double breaths compared to WT (Fig 3-19) again highlighting a degree of variability within the respiratory pattern. It must be noted that our mice were bred on a slightly different background compared to those used by Viemari *et al*. The male mice used by Viemari *et al* are effectively MeCP2 KO animals that do not present the possibility of reactivating *Mecp2* and are also bred on a C57BL6 background

whereas the mice in this chapter were maintained on a C57BL6/CBA background and reactivation of *Mecp2* was possible. As mentioned previously, background is known to influence respiratory profile. For example C57BL/6J mice exhibit spontaneous central apneas and particular post-sigh breathing behaviours (Stettner *et al.*, 2008; Yamauchi *et al.*, 2008).

The fact that respiratory abnormalities become more apparent as MeCP2 deficient mice age recapitulates the idea that neurons that lack MeCP2 may not reach full maturity (Shahbazian *et al.*, 2002b). As a result, as the animal matures the systems which are “underdeveloped” become more evident. When the *Stop/y,cre* animals were treated with TM and *Mecp2* was reactivated, there was a reduction in baseline respiratory frequency (Fig 3-8), the frequency of sighs (Fig 3-15) and the frequency of double breaths (Fig 3-19). A reversal of the respiratory abnormalities by reactivation of *Mecp2* suggests that 1) any changes that occurred due to a lack of MeCP2 were not irreversible and 2) it may be possible to rescue the neurons that did not reach full maturity by reintroducing MeCP2 into these cells. Indeed there are studies to show that introducing MeCP2 into postmitotic neurons of MeCP2 deficient mice actually rescues a number of aspects of the RTT like phenotype (Luikenhuis *et al.*, 2004).

Ward et al (2011) demonstrated that *Mecp2*-null mice exhibit a baseline respiratory frequency that was higher than WT, a phenotype that was also observed in animals lacking MeCP2 only in cells of HoxB1 lineage. It is suggested that the respiratory controllers RTN and preBötC are derived from HoxB1 expressing tissues and as such removal of MeCP2 from this lineage could have an impact on respiratory controllers. The increased baseline respiratory frequency in *Mecp2*-null mice reported by Ward et al agrees with the data in this chapter which illustrates that *Stop/y* mice, with a ubiquitous removal of *Mecp2*, have an increased respiratory frequency compared to WT (Fig 3-8). It can be hypothesised that removal of MeCP2 from the areas of the preBötC and RTN may lead to an increase in baseline respiratory frequency compared to WT. Ward et al illustrated that reactivating MeCP2 in cells of the HoxB1 lineage did not rescue the increased respiratory frequency of the mice, implying that faults in the respiratory rhythm generators contained within the HoxB1 region may not be solely responsible for the changes in baseline respiratory frequency.

It should be noted that while the variability of the respiratory frequency of *Stop/y,cre* animals was reduced for a period after *Mecp2* reactivation (Fig 3-9), towards the end of the study the variability in frequency began to increase again. This suggests that while reactivation of *Mecp2* initially rescues the phenotype of *Stop/y,cre* mice, some abnormality in the respiratory network persists.

3.4.2 Chemoreception

Central CO₂ chemoreception is key for providing brain stem networks with information regarding CO₂ levels in the bloodstream. Any disturbance in this mechanism can result in abnormal respiratory activity. Previous reports indicate that the respiratory pattern of *Mecp2* mutant mice is disturbed and that they have an altered chemosensitive response (Zhang *et al.*, 2011); Viemari, Roux *et al.* 2005; Voituron, Zanella *et al.* 2009; Voituron, Zanella *et al.* 2010). The data in this chapter (Fig 3-10) illustrates that *Stop/y,cre* mice had an abnormal ventilatory response to hypercapnic stimuli at 4 weeks prior to TM treatment. The fact that the respiratory frequency of *Stop/y* or *Stop/y,cre* mice did not increase in response to hypercapnic exposure suggests a possible problem with the chemosensitive response.

It was suggested by Andreas Rett and colleagues that the RTT disease state could be the result of deficits in certain monoaminergic systems due to the discovery that NA and 5-HT levels were low in some brains of Rett patients (Riederer *et al.*, 1985). Noradrenaline is an important respiratory modulator and the majority of this monoamine is produced by the NA cells of the locus coeruleus (LC). These cells of the LC are located in close proximity to blood vessels (Felten & Crutcher, 1979), have been shown to be CO₂/pH sensitive (Putnam, Filosa *et al.* 2004; Johnson, Haxhiu *et al.* 2008) and thus have been proposed to be chemosensitive (Zhang *et al.*, 2011). LC neurons in brain stem slices from *Mecp2*^{-/-} animals showed a smaller increase in basal firing rate when exposed to mild hypercapnic stimuli (3% and 6% CO₂) compared to WT, which suggests there may be a deficit in these chemosensitive cells. The results prior to TM treatment (Fig 3-10) in this study agree with this finding, demonstrating that *Stop/y* mice failed to exhibit an increase in respiratory frequency when exposed to mild hypercapnia (3% and 5% CO₂). However, Zhang *et al* reports a larger increase in

respiratory frequency of *Mecp2*^{-/y} mice in response to exposure to severe hypercapnia (8% CO₂), a result which was not reflected by our *Stop/y* animals. This contradiction in result may be due again to intrinsic differences in the animals studied, bearing in mind that the two studies use differing animal models and backgrounds as previously discussed. Another factor could be that *Stop/y* mice in this study already had a much higher respiratory frequency than WT animals to begin with which may have resulted in the masking of the response of the mice to CO₂.

A deficit in chemosensitivity is further illustrated in the MeCP2 deficient male mice of this chapter as *Stop/y,cre* mice prior to *Mecp2* reactivation exhibited a decrease in respiratory frequency when exposed to hypercapnia, rather than the expected increase (Fig 3-11). After TM treatment and *Mecp2* reactivation, it was noted that the *Stop/y,cre* mice still had an abnormal response to hypercapnic stimuli (Fig 3-12 and 3-13). This indicates again that changes in chemosensitivity which may have occurred due to the lack of MeCP2 may actually have led to some permanent changes in the chemosensitive response. Whether or not these changes in chemoreception are due to changes in neuromodulatory monoamines cannot be ascertained by observation of the respiratory data alone. Hence studies involving immunocytochemical analysis of important noradrenergic and serotonergic areas will be discussed later in the thesis.

The methods applied in this chapter prevented blood gas sampling which may have provided a greater insight to the chemosensitivity of mutant animals. Since hypercapnia is defined as a blood gas level of 45mmHg CO₂, it would be of benefit to perform blood gas analysis of the animals during the experiments to check that the bloodstream of each animal develops the same level of hypercapnia. If the RTT mice are subject to periods of apnea and hyperventilation then these respiratory characteristics could affect blood gas levels and thus the blood of each animal may not develop a uniform level of hypercapnia even when exposed to the same hypercapnic stimulus. Also, to gain a better insight into the chemosensitive response of the mouse model studied in this chapter it would be beneficial to expose the mice to hypoxia to observe the respiratory response. Animals in this cohort were too fragile to cope with this stimulus.

3.4.3 Sighing

Sighs are generally defined as high amplitude breaths which are followed by a post-sigh apnea (Fig 3-14; Voituron *et al.*, 2009). Although the function of sighing is still not well understood, sighing is considered to be a normal facet of respiratory activity. It has been proposed that sighing may have a number of functions including the increase of lung compliance and thus prevention of aelectasis (Glogowska *et al.*, 1972), resetting of respiratory controllers (Baldwin *et al.*, 2004) and triggering arousal from sleep, failure of which may be a factor in sudden infant death syndrome (SIDS; Franco *et al.*, 2003). Previous work on *MeCP2* KO mice has indicated that sighing may be characteristic of the breathing phenotype of RTT (Voituron *et al.*, 2010). Since sighs are common in the neonate and young infant (Cross *et al.*, 1960) who both present not yet fully developed respiratory patterns, sighing could be said to be an indication of respiratory immaturity. Data in this chapter demonstrated that sighing was more common among the mice that lacked *MeCP2* compared to WT (Fig 3-15) which suggests a lack of maturity in the respiratory network. In both human RTT patients and some *MeCP2* deficient mice there is a period of normal development which predates the onset of RTT and there is no evidence of neuronal death associated with the onset of RTT symptoms (Armstrong *et al.*, 1995). This implies that there may be a failure of neurons to reach maturity, an idea that is reinforced by the observation that dendritic branching is reduced in some cortical layers of RTT patients (Armstrong *et al.*, 1995) as is the size of neurons (Bauman *et al.*, 1995). *Stop/y,cre* mice exhibited a reduced occurrence of sighing post-TM treatment (Fig 3-15) which implies once again that reactivation of *Mecp2* may lead to a rescue of the immature neurons and a stabilisation of the respiratory pattern.

It has been demonstrated that in the cat, local application of cyanide to excite the carotid bodies induces sighing activity (Glogowska *et al.*, 1972) and rats which have had the nerves arising from the carotid chemoreceptors severed no longer exhibit sighing activity. These data taken together suggest that sighs could potentially be driven by the chemosensitive response. Fig 3-16 shows that exposure to CO₂ had little to no effect on the frequency of sighing in *Stop/y* and *Stop/y,cre* animals prior to TM treatment, and it was also shown that *Stop/y,cre* animals had an abnormal ventilatory response to CO₂ prior to TM treatment (Fig

3-11). It could therefore be hypothesised that mice lacking MeCP2 have abnormal chemoresponses, reinforced by the fact that *Stop/y,cre* mice do not exhibit the typical increase in respiratory frequency in response to hypercapnic exposure when the MeCP2 is absent (Fig 3-11).

Sighing behaviour has been proposed to act as a preventative measure against lung collapse (Reynolds, 1962) and also serves to inflate the neonatal lung (Cross *et al.*, 1960). The increased occurrence of sighing in MeCP2 deficient mice could indicate that the animals are attempting to improve aeration within the lung or trying to combat some form of lung pathology. It was noted that some of the MeCP2 deficient mice who presented a severe RTT-like behavioural phenotype also began to exhibit foaming at the mouth, which may have indicated over-production of surfactant in the lungs. Since surfactant serves to increase compliance in the lung, it follows that increased sighing behaviour and increased surfactant production could be mechanisms employed by the animal to combat lung pathology. It has recently been shown that some RTT patients do indeed exhibit lung pathology (De Felice, Guazzi *et al.* 2010). This subject matter will be discussed further in chapter 5 which deals with the histological approaches used to study the lungs of the MeCP2 deficient male mice.

Since the preBötC has been proposed to act as a site of inspiratory control (Smith *et al.*, 1991) and sighs are breaths with a large inspiratory amplitude, it can be suggested that the excessive sighing in *Stop/y* and *Stop/y,cre* mice may be driven by changes in the preBötC. This area is key in respiratory rhythmogenesis and ablation of NK1R expressing neurons of the preBötC leads to an ataxic breathing pattern in rats (McKay *et al.*, 2005). Therefore a morphological change in the preBötC as a result of MeCP2 deficit may also explain the variability in respiratory pattern and frequency that we see in mice lacking MeCP2. However, targeted ablation of NK1R expressing cells described by McKay *et al* in the rat also had the effect of reducing the number of sighs, which is in contradiction to the data shown in this chapter. Furthermore, reactivation of *Mecp2* in only cells of the HoxB1 lineage, from which the preBötC is proposed to be derived, does not rescue the increased respiratory frequency seen in the mice in which MeCP2 was absent (Ward *et al*, 2011) suggesting that the preBötC may not be solely responsible for this baseline respiratory abnormality.

3.4.4 Double Breaths

The term “double breath” was coined to define a respiratory behaviour which looked similar to two sighs separated by incomplete expiration. Another group report a similar breathing phenotype but refer to it as “complex sighing” (Voituron *et al.*, 2010) and report that as mice grow older, complex sighs become more apparent in the *Mecp2*^{-y} compared to WT. These are data which agree with the observation in this chapter that double breaths are more apparent in mice lacking MeCP2 than the WT (Fig 3-14). The frequency of double breaths also increased as the RTT-like behavioural phenotype progressed and it is interesting to note that prior to the onset of changes in respiratory frequency (T-1 to 2, Fig 3-8), double breaths were already more apparent in mice lacking MeCP2 than in the WT (Fig 3-19). This implies that the presence of double breaths may act as an indicator of a more severe breathing phenotype to follow and, as suggested by Voituron *et al* (2010), non-invasive assessment of breathing patterns early on in RTT patients, using methods such as plethysmography, could prove useful in predicting the onset of more severe respiratory abnormalities later in life.

The mechanisms underlying double breaths (or complex sighs) are poorly understood, and it is unknown as to whether double breaths could be driven by systems similar to those responsible for sighing. The occurrence of double breaths in *Stop/y,cre* mice was reduced post-TM treatment (Fig 3-19) for a number of weeks but began to increase again towards the end of the study, a pattern which was not reflected in sighing. Therefore, since *MeCP2* reactivation reduced the numbers of sighs which occurred in the *Stop/y,cre* mice permanently and yet failed to do so with regards to double breaths then we may infer that different pathways are mediating each of these respiratory characteristics.

Voituron *et al* (2010) reports that the sighing pattern is dependant on age. At P15, the majority of sighs in WT and *Mecp2*^{-y} are complex, yet at P60 simple sighs are the most prominent in WT and complex sighs dominate in *Mecp2*^{-y} mice. The transition from complex sighs to simple sighing in the WT suggests a change in the respiratory system, perhaps due to a maturation step. Data in this chapter show double breaths were reduced in *Stop/y,cre* mice post TM which, as

before mentioned, may imply the rescue of immature neurons. However, maturation is usually presumed to have occurred in the murine respiratory system between P1-P4 (Mortola, 2001) and thus changes in sighing behaviour between p15 and p60 may not be related to a post-natal maturation of the respiratory network. The fact that abolition of double breaths is not maintained and they start to reappear at TM+11 to 13 could be a due to the fact that application of TM only removes the stop cassette in approx 80% of neurons (Guy *et al.*, 2007). *Mecp2* is not reactivated in every cell and a small MeCP2 deficiency remains, perhaps explaining why some respiratory abnormalities also remain.

The data in this chapter have not established precisely in which cells *Mecp2* is reactivated, and previous studies have shown that restoring *Mecp2* in one specific location within the brain i.e. the forebrain, is not able to rescue the RTT-like phenotype of *Mecp2* deficient mice (Alvarez-Saavedra *et al.*, 2007). Thus, the fact that double breaths began to reoccur in *Stop/y,cre* mice may indicate that *Mecp2* has not been restored to an area of the brain which is key in controlling this part of the respiratory phenotype. There is also the possibility that lung pathology exists that could not be reversed by the reactivation of *Mecp2*. Again this will be discussed further in chapter 5.

3.4.5 Apnea

It was noted that apneas were most prevalent in the mutant mice pre-TM (Fig 3-22 plot A) in the 15 minute and 30 minute recovery period following hypercapnic stimulation. A similar respiratory response was reported in *Mecp2^{-y}* mice (Voituron *et al.*, 2009) but the majority of apneas were reported in the 2 min recovery stage. The group reported that *Mecp2^{-y}* animals recovered normal breathing parameters 10-15 min after being restored to normoxic conditions yet our results suggest that *Stop/y,cre* mice have a longer recovery time of up to 30 min. Voituron et al (2009) reported that tidal volume remained high in the recovery period and they suggest that the high Vt may lead to activation of pulmonary stretch receptors and consequently the Herring-Breuer reflex. The inhibition of the respiratory rhythm generators involved in this reflex would then result in prolonged expiration and assist the occurrence of apnea. However, if this was the case then one would expect to see a reduced respiratory frequency

in the recovery periods due to the inhibition of the respiratory rhythm generator. This is not reflected in our data (Fig 3-11) which actually illustrates an increase in respiratory frequency of *Stop/y,cre* mice at 15 min recovery. Again, the background on which the animal is bred must be taken into account as this can influence certain aspects of the respiratory profile. Apnea still occurs in the recovery periods following hypercapnia in *Stop/y,cre* mice after TM (Fig 3-22) indicating that reactivation of *Mecp2* is not restoring all of the post-stimulus respiratory abnormalities.

In conclusion, this present study confirms *Mecp2* reactivation leads to the reversal of the behavioural score and some respiratory parameters, as had been previously shown (Guy *et al.*, 2007). The fact that respiratory frequency, sighing and double breaths were reduced following *Mecp2* reactivation indicates that there may be aspects of the respiratory network that do not reach full maturity due to a lack of MeCP2, and that reactivation of the gene can rescue this immaturity. However, there may be aspects of the network which remain permanently changed by the absence of MeCP2, indicated by factors such as the persistence of apnea and the reoccurrence of double breaths in MeCP2 deficient mice. The data have also indicated that the chemosensitive response of MeCP2 deficient mice is altered, more specifically the response to and recovery from hypercapnic exposure. This suggests that MeCP2 may have an involvement in the development and maturation of the chemosensitive network. Taken as a whole the data suggests that the respiratory abnormalities seen in RTT patients and MeCP2 deficient mice may not stem from problems solely in the respiratory rhythm generators or only in the chemosensitive regions, rather they may result from a culmination of deficits in both networks.

Chapter 4: Immunocytochemistry (ICC) of respiratory rhythm generators and sites of neuromodulation in male mouse brain

4.1 Introduction

As discussed in chapter one, RTT patients exhibit highly unstable breathing patterns with periods of breath holding, hyperventilation, variable breath duration, and increased occurrence of apneas (Cirignotta *et al.*, 1986; Weese-Mayer *et al.*, 2006). These respiratory abnormalities are observed during both awake and sleep states (Rohdin *et al.*, 2007), but are more prevalent during wakefulness. The cause of disordered breathing in RTT patients remains unknown but there are suggestions that cortical dysfunction may underlie respiratory abnormalities of RTT patients during wakefulness, since breathing appears more normal in sleep, a state where cortical influence is absent (Marcus *et al.*, 1994). In addition, cardiac sensitivity to baroreflex and cardiac vagal tone, functions which are controlled by the brain stem, are also reduced in RTT patients (Julu *et al.*, 2001). The data in chapter 3 highlighted that the respiratory pattern of MeCP2 deficient male mice was characterised by an increased occurrence of sighs and apneas compared to WT and also an increased average respiratory frequency. The increased baseline respiratory frequency of mutant mice compared to the WT may suggest a problem within rhythm generating areas. MeCP2 deficient animals also showed no increase in respiratory frequency in response to hypercapnic exposure which may indicate a problem within the chemoreceptive response.

4.1.1 Rhythm Generation, Chemosensitivity and Neuromodulation

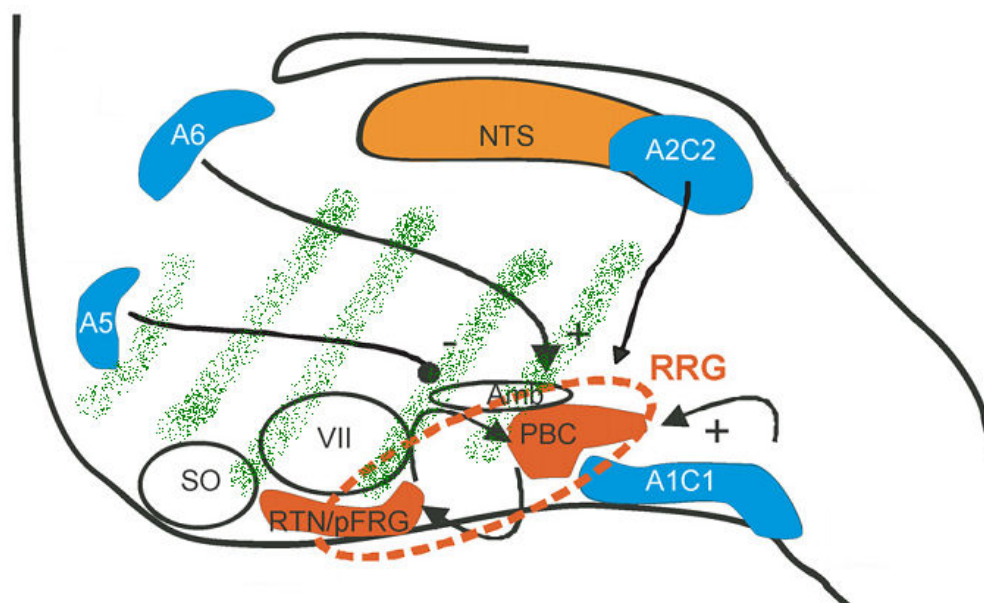


Fig 4-1 Diagram of midsagittal brain section to illustrate respiratory rhythm generators and sites of neuromodulation. Areas of respiratory rhythm generation highlighted in orange. Noradrenergic regions illustrated in blue and regions of green indicate location of 5-HT expressing neurons of the raphe nuclei. RRG, respiratory rhythm generator; PBC, preBötzing Complex; RTN/pFRG, retrotrapezoid nucleus/parafacial respiratory group; VII, facial nucleus Amb, nucleus ambiguus; SO, superior olive; NTS, nucleus tractus solitarius. (*Adapted from (Blanchi & Sieweke, 2005): Mutations of brainstem transcription factors and central respiratory disorders*).

Respiratory rhythm is thought to be generated by two key areas. One of these is the preBötzing complex (preBötC) in the ventrolateral medulla which is a bilateral cluster of interneurons, expressing high levels of Neurokinin-1 receptor (NK1R) and Vesicular Glutamate Transporter 2 (VGLUT2) (Gray *et al.*, 1999). The preBötC has been shown to be essential in the generation of respiratory rhythm in the neonatal rodent brainstem prep and *in vivo* (Smith *et al.*, 1991); (Johnson *et al.*, 2001). Furthermore, destruction of the NK1R expressing neurons in the preBötC of the rat leads to disordered breathing during sleep and eventually disturbances in breathing during wakefulness (McKay *et al.*, 2005), illustrating the importance of the preBötC in pacing respiratory rhythm. The preBötC is also

implicated in the chemoreceptive response, demonstrated by the fact that bilateral lesion of the area leads to impaired chemosensitivity in rats (Gray *et al.*, 2001). The preBötC in mouse brainstem slices expresses TrkB, the receptor for BDNF (Thoby-Brisson *et al.*, 2003), a neurotrophic factor which is important in the development of the respiratory network. Exogenous application of BDNF to mouse brainstem slices results in an increase in the respiratory output of the cells in the preBötC (Thoby-Brisson *et al.*, 2003) indicating the ability of BDNF to modulate the output of this respiratory oscillator. MeCP2, the protein of the *Mecp2* gene which is found to be at fault in the majority of cases of RTT syndrome, was thought to bind to regulatory elements of the BDNF promoter and acts as a transcriptional repressor (Chen *et al.*, 2003; Wade, 2004) with BDNF levels being reduced in *Mecp2*-null mice (Chang *et al.*, 2006b; Wang *et al.*, 2006). The fact that BDNF levels were reduced in the absence of *Mecp2*, thought to be a transcriptional repressor, seems contradictory. It was proposed that the reduced BDNF levels in *Mecp2* null mice were as a result of overall reduced brain activity the mutant animals (Dani *et al.*, 2005), since BDNF expression is activity dependent. However, another hypothesis has come to light given that there is evidence that BDNF levels are upregulated in mouse models which over express *Mecp2*, suggesting that *Mecp2* actually acts as an activator of BDNF as opposed to a repressor (Chahrour *et al.*, 2008b). Reductions in BDNF may account for some of the respiratory abnormalities observed in MeCP2 deficient mice as it has been shown that increasing BDNF expression in the mutant mouse can improve the RTT-like phenotype (Chang *et al.*, 2006b; Wang *et al.*, 2006; Ogier *et al.*, 2007). The preBötC is also modulated by Substance P (SubP), an agonist of the NK1 expressing neurons of the preBötC (Gray *et al.*, 1999). Levels of SubP are reduced in the cerebrospinal fluid of RTT patients (Matsuishi *et al.*, 1997; Deguchi *et al.*, 2000) with immunoreactivity of SubP in the human RTT brain reduced in various parts of the medulla, in the pons and locus coeruleus (Deguchi *et al.*, 2000).

Another key region of the respiratory network is the retrotrapezoid nucleus/parafacial respiratory group (RTN/pFRG). This region consists of a cluster of interneurons found ventral to the facial nucleus which express Phox2b, VGLUT2 and NK1R (Smith *et al.*, 1989; Onimaru & Homma, 2003, 2008). Studies of the newborn rat brain stem-spinal cord preparation reveal that bilateral

lesioning of the RTN/pFRG results in a reduction in respiratory frequency but not complete loss of respiratory rhythm (Onimaru & Homma, 2003), indicating that the preBötC may not be the sole mediator of rhythmic breathing and that the RTN/pFRG may contribute to respiratory rhythmogenesis. The RTN/pFRG is further implicated in respiratory control in that application of fentanyl, a μ -opioid agonist, suppresses the opioid-sensitive inspiratory rhythm generating preBötC (Gray *et al.*, 1999) yet the expiratory rhythm continues suggesting that the two phases of respiration are controlled by different rhythm generators (Janczewski & Feldman, 2006). The RTN/pFRG is proposed to act mainly as a rhythm generator in the neonate (Janczewski & Feldman, 2006) yet in adulthood, this area appears to have a greater role in chemosensitivity. Its role in chemoreception is indicated by the fact that the RTN/pFRG lies above a portion of the ventral medullary surface believed to contribute to respiratory chemoreception (Loeschcke, 1982), it contains neurons that are sensitive to CO₂ levels (Mulkey *et al.*, 2004) and *in vivo*, focal acidification of the RTN/pFRG region in the rat increases ventilation in the wakeful state (Li *et al.*, 1999). Also, mutant mice with a severe depletion of Phox2b expressing cells (cells which are found in the RTN/pFRG region) lack responsiveness to CO₂ at birth (Dubreuil *et al.*, 2008).

There are other areas in the brainstem which also contribute to respiratory control, such as serotonergic and noradrenergic nuclei. While these sites do not generate the respiratory rhythm itself, the neurotransmitters they release have an important role in development, maturation and maintenance of a stable respiratory pattern.

4.1.2 The Role of Noradrenaline (NA)

Andreas Rett and colleagues describe a reduction in NA content in the brains of Rett patients (Riederer *et al.*, 1985) and it has been suggested that the respiratory abnormalities of *Mecp2*^{-y} mice may stem from problems with neuromodulation of the respiratory network. NA is a neurotransmitter which plays a key role in modulation of the respiratory pattern and also contributes to the maturation of respiratory control after birth. Noradrenergic neurons can be found in the pons (A5 and A6/Locus Coeruleus) and medulla (A1/C1, A2/C2) and have varying effects on the respiratory pattern. A6/LC neurons have an

excitatory effect on respiratory rhythm and are shown to be important in early development, given that *Phox2a* mutant mice, which lack A6/LC neurons, die shortly after birth (Morin *et al.*, 1997). Study of animals surgically delivered at E18 show a more variable cycle duration and slower respiratory activity compared to WT (Viemari *et al.*, 2004). The A6/LC also contains noradrenergic neurons which display chemosensitive properties *in vitro* (Putnam *et al.*, 2004), with bilateral lesions of LC neurons using 6-Hydroxydopamine (6-OHDA) leading to a 64% reduction of the ventilatory response to CO₂ in rats (Biancardi *et al.*, 2008). Neurons within the LC area also exhibit an increased firing rate when the level of CO₂ in the whole animal is raised (Coates *et al.*, 1993), data which indicate the importance of NA expressing neurons in mediating the chemosensitive response.

Studies involving the application of the α -2 noradrenergic receptor antagonist Yohimbine to medullary preparations revealed that the A1/C1 responds to signalling via the alpha-2 noradrenergic receptor, and application of an α -2 antagonist to mouse medullary “en bloc” preparations and brainstem slices results in a decrease in respiratory frequency (Zanella *et al.*, 2006). This suggests that the medullary A1/C1 region may be involved in modulation of respiratory frequency. In contrast, electrolytic lesioning of the dorsal A2/C2 region in mouse brainstem slices does not suppress the output of the ventral respiratory group, but does result in an increased variability of the respiratory cycle period (Hilaire *et al.*, 1990; Zanella *et al.*, 2006) suggesting that A2/C2 has an involvement in maintaining the stability of the respiratory pattern. Tyrosine hydroxylase (TH) is an enzyme required for the conversion of tyrosine into L-DOPA, a key stage in the production pathway of NA. As such, TH is used as a marker for NA expressing neurons. TH expression in male *Mecp2*-null mice is normal at birth but reduced in the A2/C2 region at one month old and the A1/C1 at 2 months old (Viemari *et al.*, 2005), when the respiratory phenotype becomes apparent. Previous studies also illustrate that increasing the levels of NA *in vivo* via the administration of the NA reuptake inhibitor Desipramine improves respiratory function in *Mecp2*-null mice (Roux *et al.*, 2007). NA may be directly affected by the absence of MeCP2 as an *Mecp2*-binding site is found in the tyrosine hydroxylase promoter (Yasui *et al.*, 2007) revealing the possible regulation of TH by the MeCP2 protein.

4.1.3 The Role of Serotonin (5-HT)

As with noradrenaline, Andreas Rett and colleagues also describe a reduction in 5-HT content in the brains of Rett patients (Riederer *et al.*, 1985). Evidence suggests that breathing disturbances become more severe in *Mecp2*^{-/-} mice at approximately 2 months of age when the 5-HT content of *Mecp2*^{-/-} mice becomes reduced (Viemari *et al.*, 2005). Differences in 5-HT levels between WT and *Mecp2* KO mice become greater with age (Ide *et al.*, 2005) and the developing 5-HT deficit seems to coincide with the progression of the respiratory abnormalities in *Mecp2*^{-/-} mice.

Serotonin (5-HT) is important in the development of the respiratory network, the stability of breathing and maintenance of respiratory rhythm. Injection of the retrograde tracer cholera toxin b subunit (CTb) into the rostroventrolateral medulla (RVLM) combined with 5-HT immunolabelling illustrates that there are many serotonergic projections from raphe nuclei to respiratory areas within the medulla (Bago *et al.*, 2002). This reveals that 5-HT may influence respiratory control, an idea highlighted further in Pet-1 KO mice. As discussed in section 1.4.1, Pet-1 KO mice have a 70-80% loss of 5-HT neurons in the CNS (Hendricks *et al.*, 2003) neonates exhibit an increased variability in respiratory output compared to WT animals. Pet-1 KO mice also fail to achieve the maturation step seen at post natal day 4.5 in the WT mice, where the breathing patterns becomes stabilised (Erickson *et al.*, 2007) which highlights the importance of 5-HT in development. *Lmx1b* *f/f/p* mouse model has no central 5-HT neurons and *Lmx1b* *f/f/p* mice present severe and frequent apnea during postnatal development (Hodges *et al.*, 2009) indicating the importance of 5-HT in the developmental process.

5-HT neurons have been proposed as chemosensors as they are often located close to cerebral blood vessels (Bradley *et al.*, 2002) which allows detection of changes in pH levels of the blood. Further to this, *in vitro* patch-clamp recordings of rat medullary brain slices illustrate that the midline raphe, an area with high levels of 5-HT expression, contains neurons which are intrinsically sensitive to increases in carbon dioxide (Richerson, 1995a).

Despite much research, it remains unknown as to whether the respiratory disturbances presented in RTT patients and MeCP2 deficient mice are due to impaired chemosensitivity or a disruption in respiratory rhythmogenesis. The main aim of this chapter was to use immunocytochemical staining to determine if there are differences in markers within several areas involved in respiratory control including the preBötC, the RTN/pFRG, serotonergic and noradrenergic nuclei in MeCP2 deficient mice compared to WT. Since the model studied results in a ubiquitous silencing of *Mecp2*, reactivation of *Mecp2* in the afore mentioned respiratory areas was also quantified in the *Stop/y,cre+TM* mice to assess the location(s) of MeCP2 expression.

4.2 Methods

4.2.1 Fixation

Mice were injected with a lethal dose of pentobarbital and observed until the hind limb withdrawal reflex was abolished. Animals were then transcardially perfused with 4% paraformaldehyde (see chapter 2 section 2.6.1 for further details) and the brain stem removed. The brainstem was coated in OCT compound and frozen before 40µm thick coronal sections were cut using a cryostat. It was noted when processing that some of the mutant brainstem tissue was quite fragile compared to WT and could not be used for staining, resulting in a reduced n number in the *Stop/y,cre* and *Stop/y* groups. This issue is addressed in more detail in section 4.5.1. Sections were collected sequentially in 24 well plates containing PBS before being split into 8 groups for staining (see chapter 2 Fig 2-5 for more detail). All staining followed the protocol described in chapter 2 (section 2.8).

4.2.2 Imaging and Quantification of TH Expressing Neurons

Noradrenergic cells of A1/C1, A2/C2 and Locus Coeruleus (LC) were quantified using immunoreactivity to tyrosine hydroxylase (TH), a marker for noradrenergic cells. TH expression was detected using a sheep anti-TH primary (1:1000, Abcam, UK) and an alexa-488 donkey anti-sheep secondary (1:500, Invitrogen, UK). MeCP2 expression was originally detected using rabbit anti-mecp2 (1:100, Millipore, UK) and Alexa-488 anti-rabbit secondary (1:500, Stratech-Jackson Immunoresearch) but staining was weak. Staining with mouse anti-MeCP2 (1:200, cat no. M6818, Sigma, UK) proved clearer and more reliable for the purposes of quantification. Mouse anti-MeCP2 (1:200, Sigma, UK) was targeted using rhodamine donkey anti-mouse secondary (1:100, Invitrogen, UK).

Imaging of A1/C1 (figs 4-2 and 4-3) began in sections containing the rostral end of the nucleus ambiguus, level -8.00mm from bregma, until sections where the central canal opened into the 4th ventricle at level -7.32mm from bregma (Paxinos & Franklin, 2001). Every fifth section was analysed to prevent double counting, resulting in a 200 μ m interval between each imaged section. Confocal laser scanning microscopy (BioRad MRC 1024 confocal laser scanning microscope) was used to create a Z-stack of 5 images, each separated by 2 μ m, of the A1/C1.

A2/C2 was imaged (figs 4-4 and 4-5) beginning in sections where the nucleus tractus solitarius (nTS) became apparent, approximately -6.84 from bregma, and ceased at -7.2mm from bregma. The LC was imaged (figs 4-6 and 4-7) in sections caudal to level at which the fourth ventricle became narrowed (-5.52 mm from bregma) and ceased at approximately -5.34 mm from bregma where the fourth ventricle closes.

For each noradrenergic region, TH expressing cells in a 195x195 μ m window were counted bilaterally to a depth of 10 μ m in each section. A TH cell was only counted as positive when the whole cell boundary was present and the lack of staining within the centre of the cell indicated the presence of the nucleus. MeCP2 positive cells within the window were also counted and were considered positive when staining was clearly exhibited within the nucleus, confirmed by DAPI staining. Cells double labelled for TH and MeCP2 were also quantified.

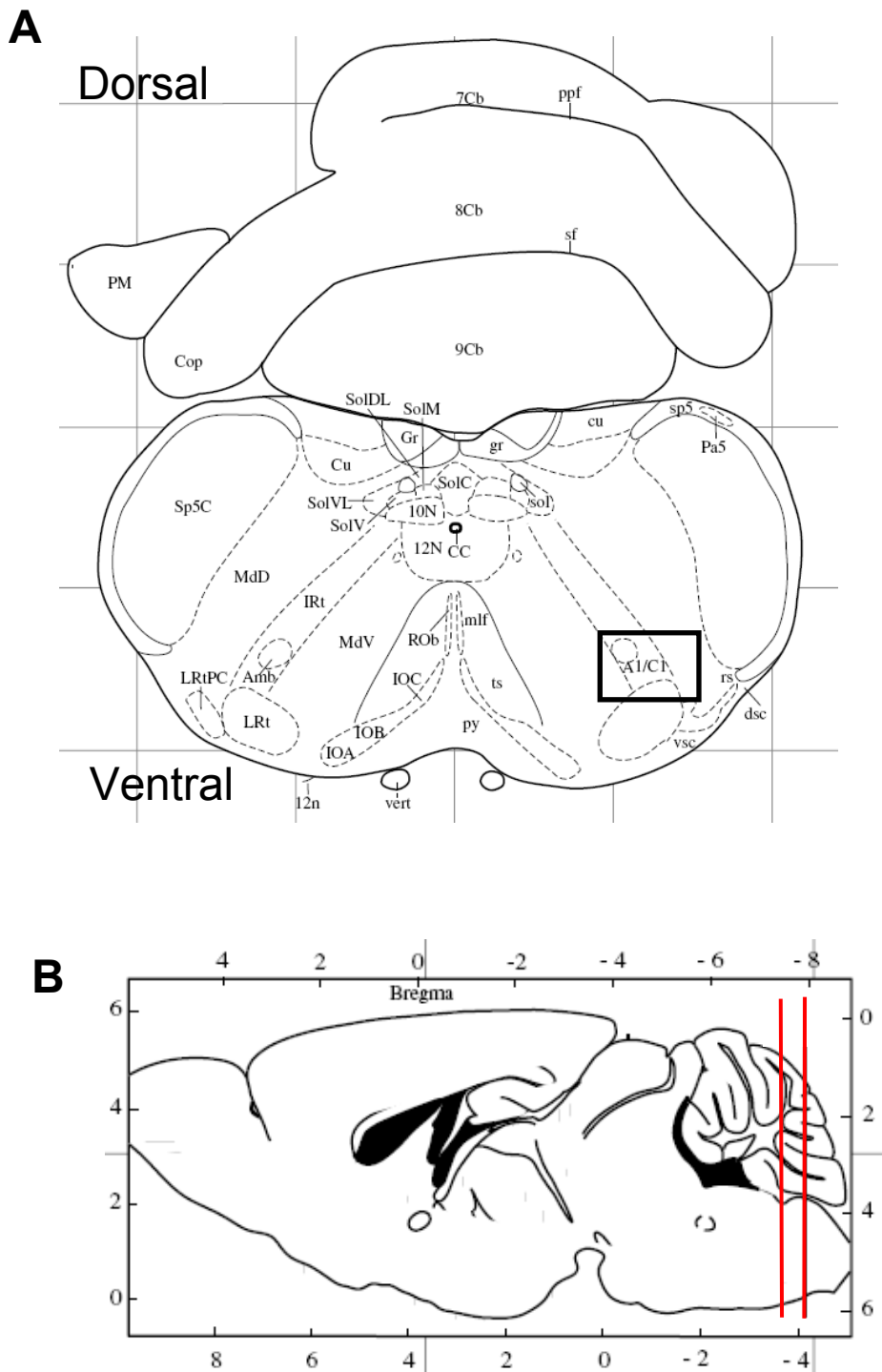


Fig 4-2 Illustration of the position of A1/C1 region. **A-** Coronal section of brainstem illustrating location of A1/C1 region. Black box indicates position of counting window (195 μ m \times 195 μ m). **B -** Saggital section of brainstem with red bars indicating span of cell count relative to bregma.

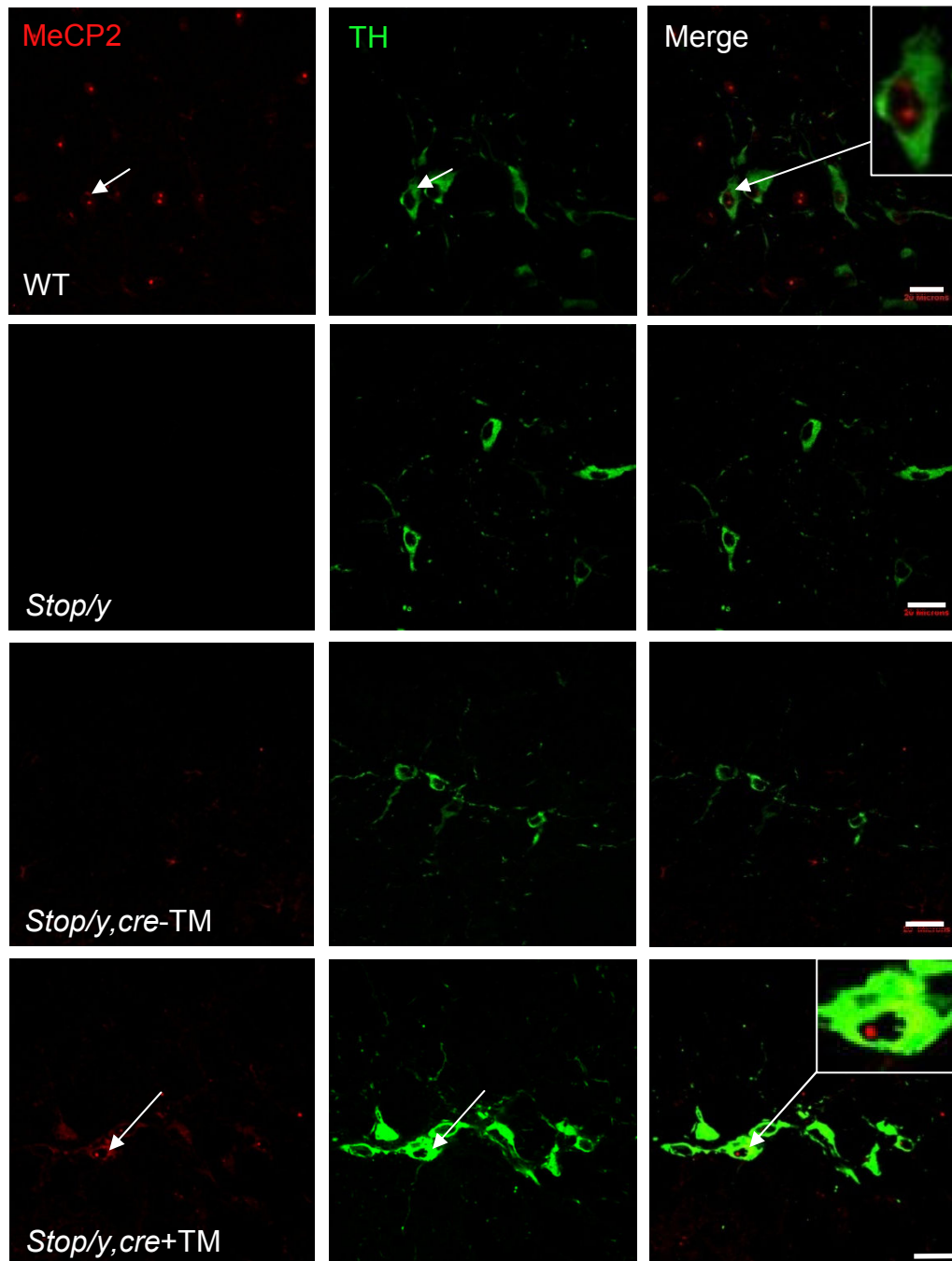


Fig 4-3 Single plane confocal image of Tyrosine hydroxylase and MeCP2 expression in A1/C1 of WT, *Stop/y*, *Stop/y,cre-TM*, and *Stop/y,cre+TM* animals. Red staining illustrates MeCP2 positive cells, green staining shows TH expressing cells. Merge panel illustrates that MeCP2 and TH were often co-expressed. White arrows indicate cell double labelled for MeCP2 and TH as shown in insert. Insert in top and bottom panel = higher magnification image of TH and MeCP2 co-localisation. Scale bar = 20 μm .

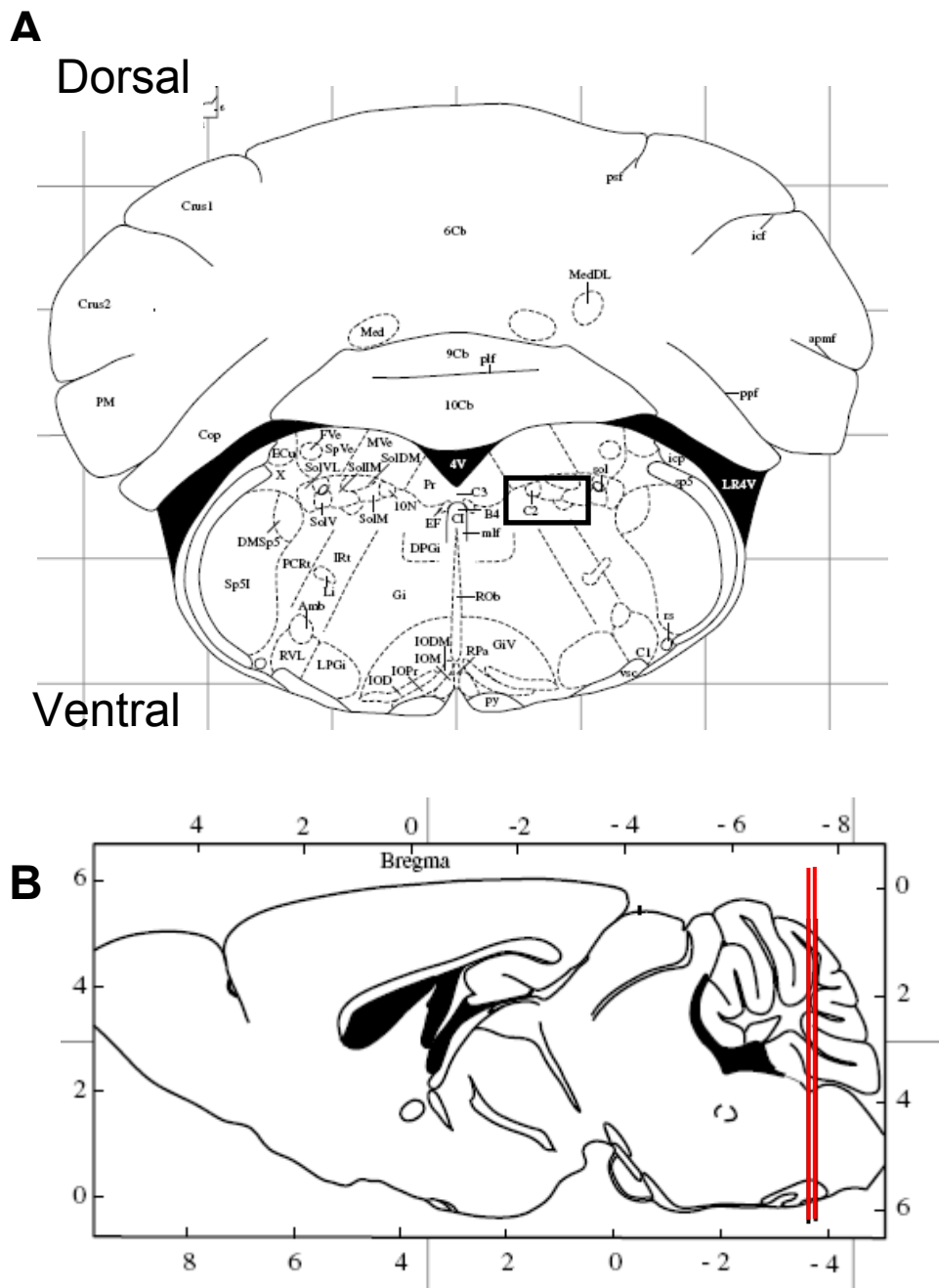


Fig 4-4 Illustration of the position of A2/C2 region. A - Coronal section of brainstem illustrating location of A2/C2 region. Black box indicates position of counting window (195 μ m \times 195 μ m). **B**- Saggital section of brainstem with red bars indicating span of cell count relative to bregma.

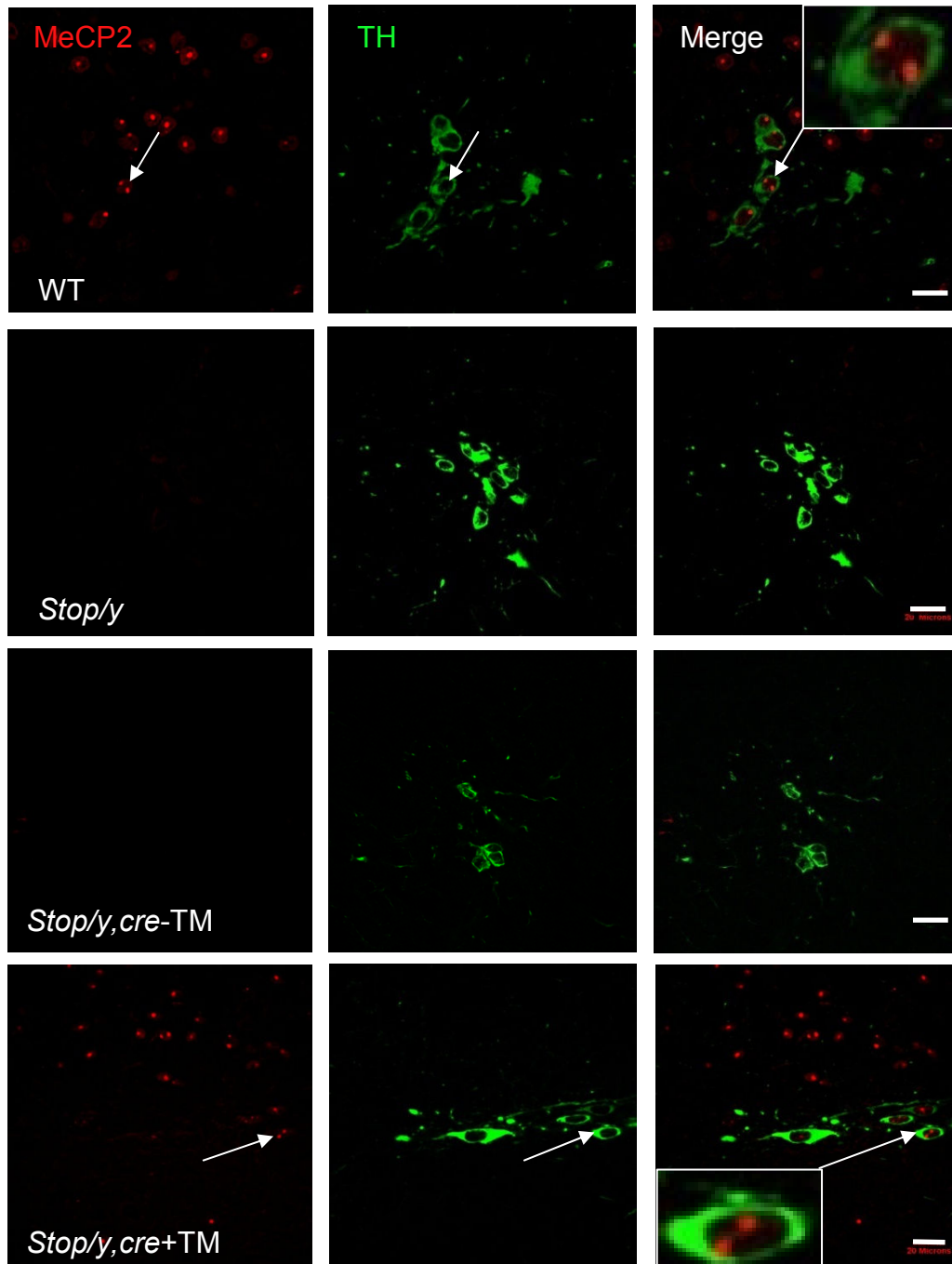


Fig 4-5 Single plane confocal image of Tyrosine hydroxylase and MeCP2 expression in A2/C2 of WT, *Stop/y*, *Stop/y,cre-TM*, *Stop/y,cre+TM* and animals. Red staining illustrates MeCP2 positive cells, green staining shows TH expressing cells. Merge panel illustrates that MeCP2 and TH were often co-expressed. White arrows indicate cell double labelled for MeCP2 and TH as shown in insert. Inserts in top and bottom panel = higher magnification images of TH and MeCP2 co-localisation. Scale bar = 20 μ m.

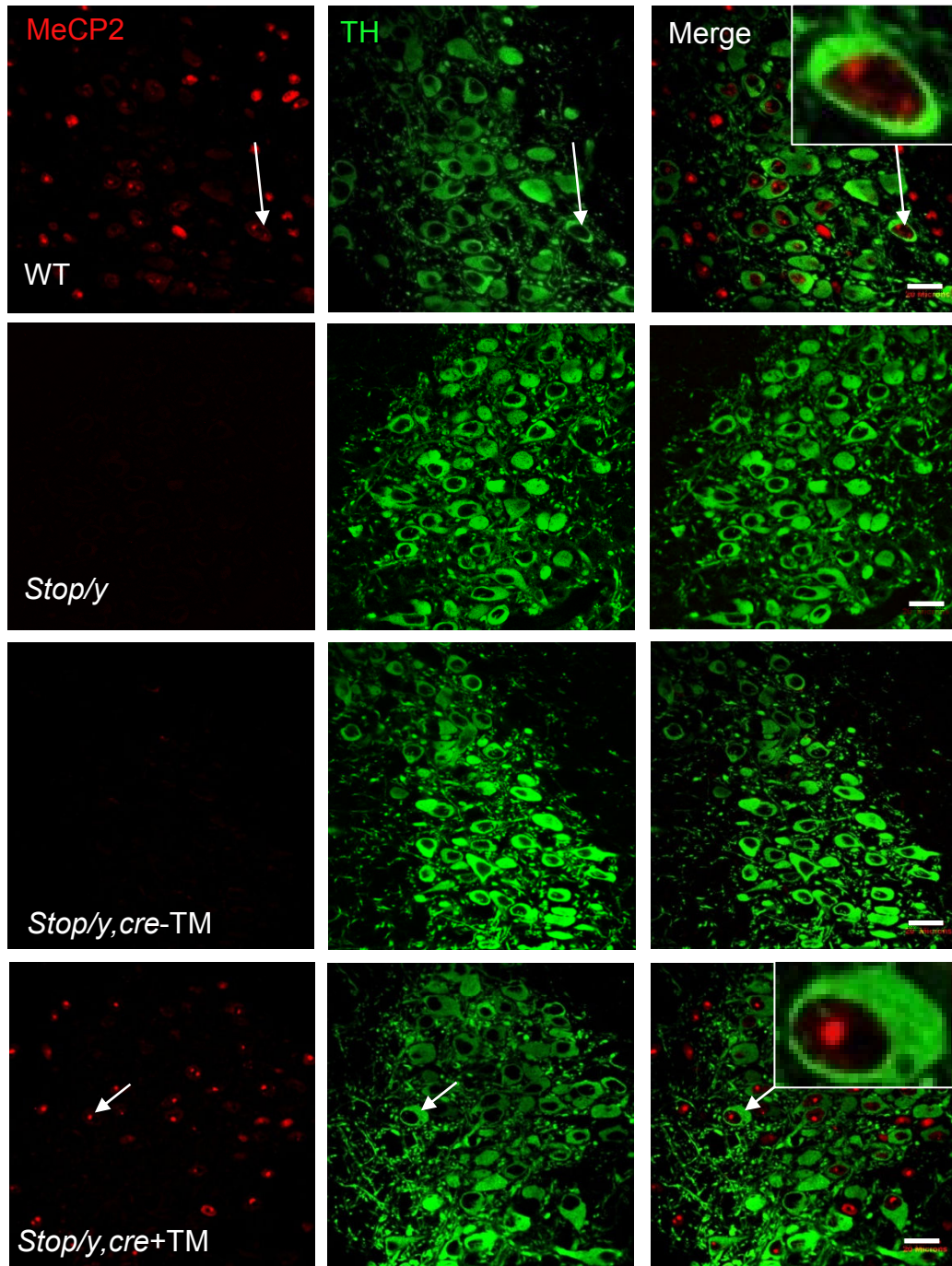


Fig 4-7 Single plane confocal image of Tyrosine hydroxylase and MeCP2 expression in A6/LC of WT, *Stop/y*, *Stop/y,cre-TM*, *stop/y,cre+TM* animals. Red staining illustrates MeCP2 positive cells, green staining shows TH expressing cells. Merge panel illustrates that *Mecp2* and TH were often co-expressed. White arrows indicate cell double labeled for MeCP2 and TH as shown in insert. Inserts = higher magnification images of TH and MeCP2 co-localisation. Scale bar = 20 μ m.

4.2.3 Imaging and Quantification of 5-HT Expressing Neurons

5-HT cells within the nucleus raphe obscurus (ROb), raphe magnus (RMg), raphe pallidus (RPa) and the more rostral raphe pontis (PnR) and raphe dorsalis (DRI) of the midbrain were quantified. 5-HT neurons were targeted with rabbit anti-5HT (1:200) and alexa-488 donkey anti-rabbit secondary (1:500, Stratech-Jackson Immunoresearch, UK). MeCP2 staining was detected using a mouse anti-MeCP2 (1:200, Sigma, UK) and rhodamine donkey anti-mouse secondary (1:100, Invitrogen, UK).

Imaging of the ROb and RPa (figs 4-8, 4-9 and 4-10) began in sections where obex was present and the ROb formed a single column, approximately level -7.64mm caudal to bregma. Imaging continued until the section in which the solitary tract disappears (level -6.12mm from bregma).

The RMg was imaged (figs 4-10 and 4-11) in sections where the facial nucleus became apparent (-6.48mm from bregma) and ceased in section where the DRI became apparent (-5.34mm from bregma).

5-HT neurons of the ventrolateral medulla were imaged (fig 4-12) in sections where the ROb and RPa were present and ceased in sections where the RMg became apparent.

Imaging of the DRI (fig 4-13 and 4-14) started in sections in which the fourth ventricle was narrowed (-5.34mm from bregma) and stopped when the aqueduct became narrowed (-4.60mm from bregma). The PnR was imaged (fig 4-13 and 4-15) in sections immediately rostral to the DRI and also ceased at approximately -4.60mm from bregma where the aqueduct became narrowed.

For each serotonergic region, 5-HT expressing cells in a 195x195 μ m window were counted bilaterally to a depth of 10 μ m in each section. A 5-HT cell was only counted as positive when the whole cell boundary was present and the lack of 5-HT staining within the centre of the cell indicated the presence of the nucleus. MeCP2 positive cells within the window were also counted and were considered positive when staining was clearly exhibited within the nucleus, confirmed by DAPI staining. Cells double labelled for 5-HT and MeCP2 were also quantified.

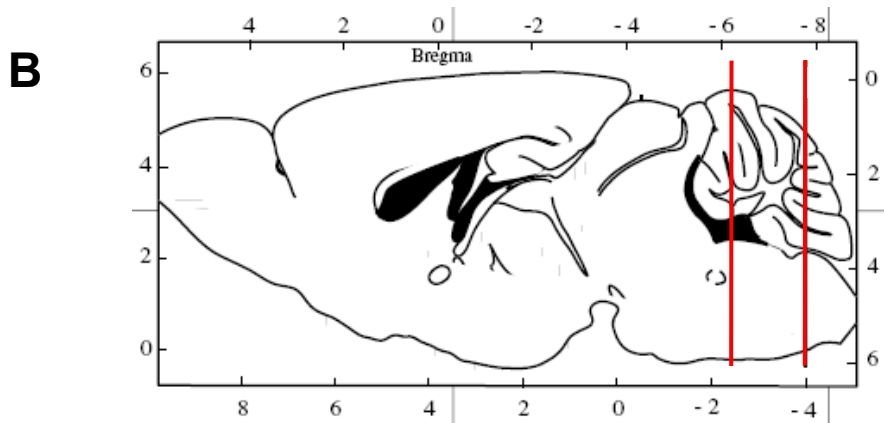
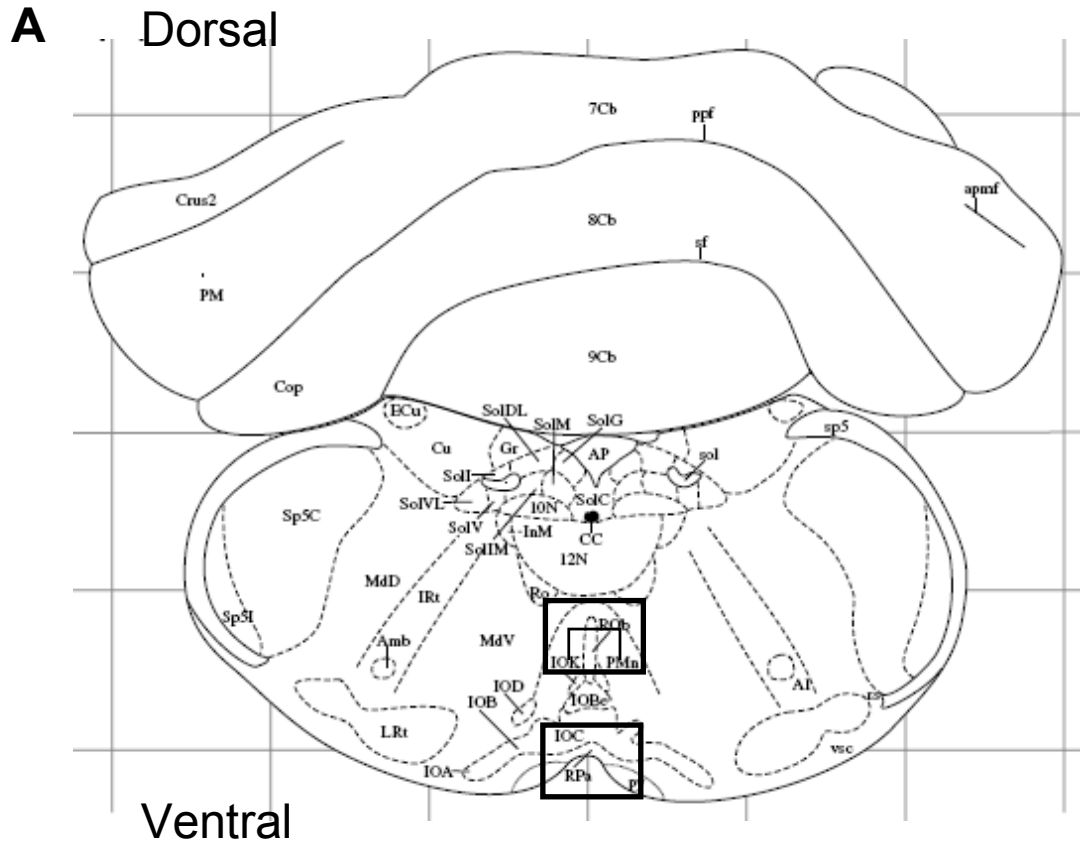


Fig 4-8 Illustration of the position of Raphe Obscure (ROb) and Raphe Pallidus (RPa) region. A - Coronal section of brainstem illustrating location of ROb/RPa region. Black box indicates position of counting windows (195 μ m \times 195 μ m). Upper box = ROb. Lower box = RPa. B - Sagittal section of brainstem with red bars indicating span of cell count relative to bregma.

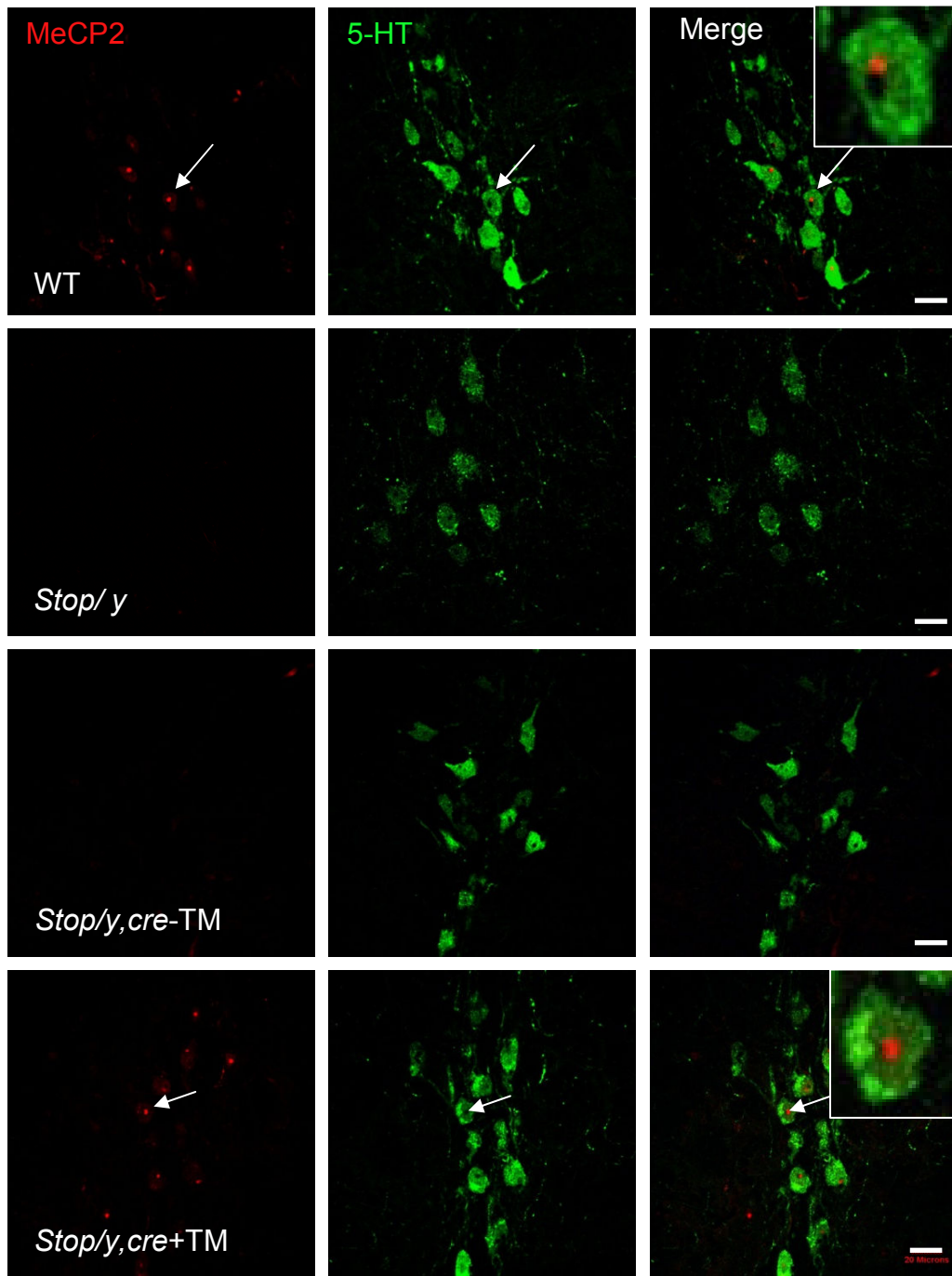


Fig 4-9 Single plane confocal image of 5-HT and MeCP2 expression in the Raphe Obscurus of WT, *Stop/y*, *Stop/y,cre-TM*, *stop/y,cre+TM* animals. Red staining illustrates MeCP2 positive cells, green staining shows 5-HT expressing cells. Merge panel illustrates that MeCP2 and 5-HT were often co-expressed. White arrows in top and bottom panels indicate cell double labelled for MeCP2 and 5-HT in WT and *Stop/y,cre+TM* mice respectively. Insert = higher magnification image of 5-HT and MeCP2 co-localisation. Scale bar = 20 μ m.

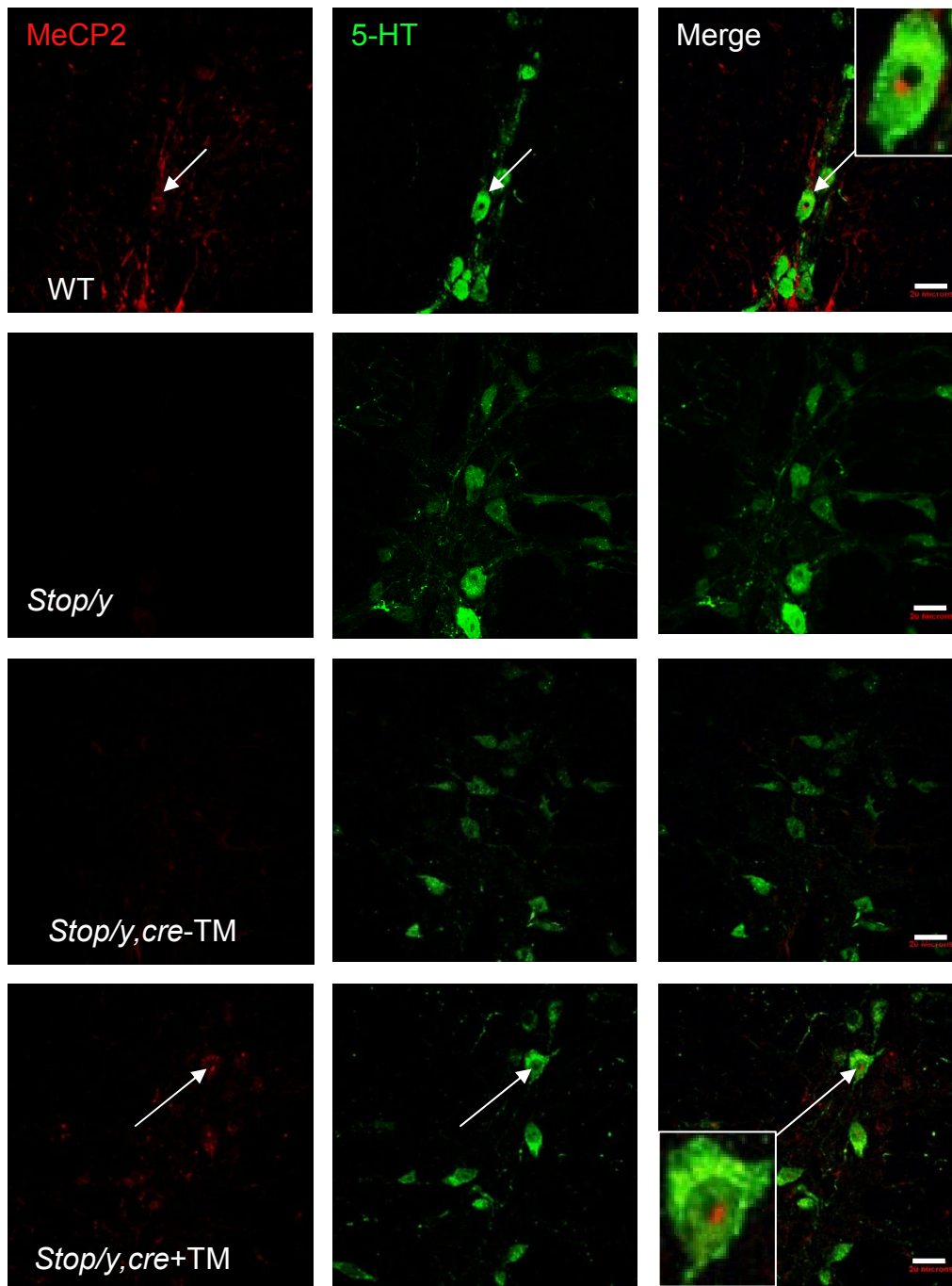


Fig 4-10 Single plane confocal image of 5-HT expressing neurons of the Raphe pallidus/magnus of WT, *Stop/y*, *Stop/y,cre-TM*, *Stop/y,cre+TM* animals. Red staining illustrates MeCP2 positive cells, green staining shows 5-HT expressing cells. Merge panel illustrates that MeCP2 and 5-HT were often co-expressed. White arrows in top and bottom panels indicate cell double labelled for MeCP2 and 5-HT in WT and *Stop/y,cre+TM* mice respectively. Insert = higher magnification image of 5-HT and MeCP2 colocalisation. Scale bar = 20 μ m.

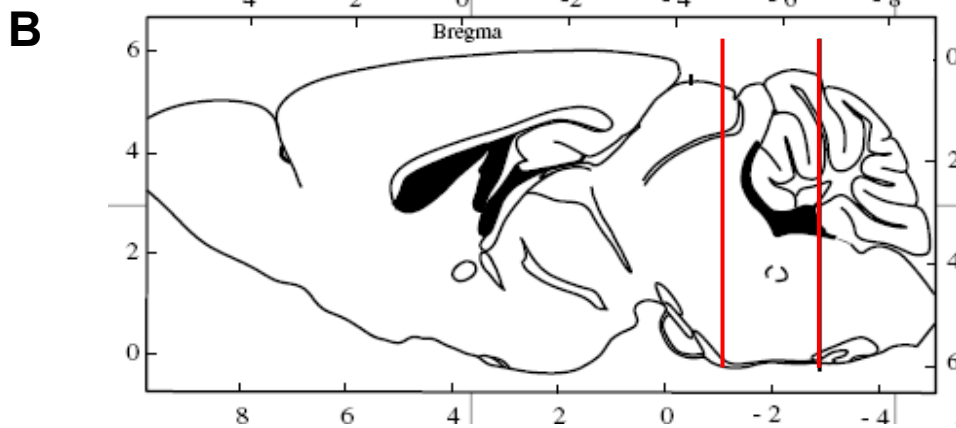
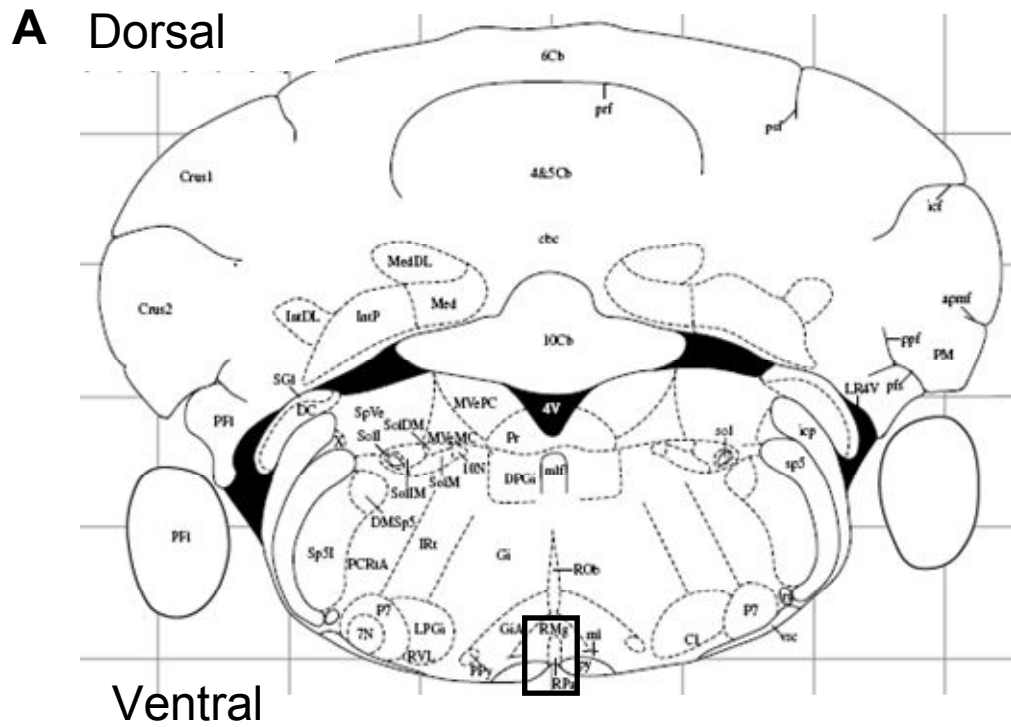


Fig 4-11 Illustration of the position of Raphe Magnus (RMg) region. A - Coronal section of brainstem illustrating location of RMg. Black box indicates position of counting window (195 μ m \times 195 μ m). **B -** Saggital section of brainstem with red bars indicating span of cell count relative to bregma.

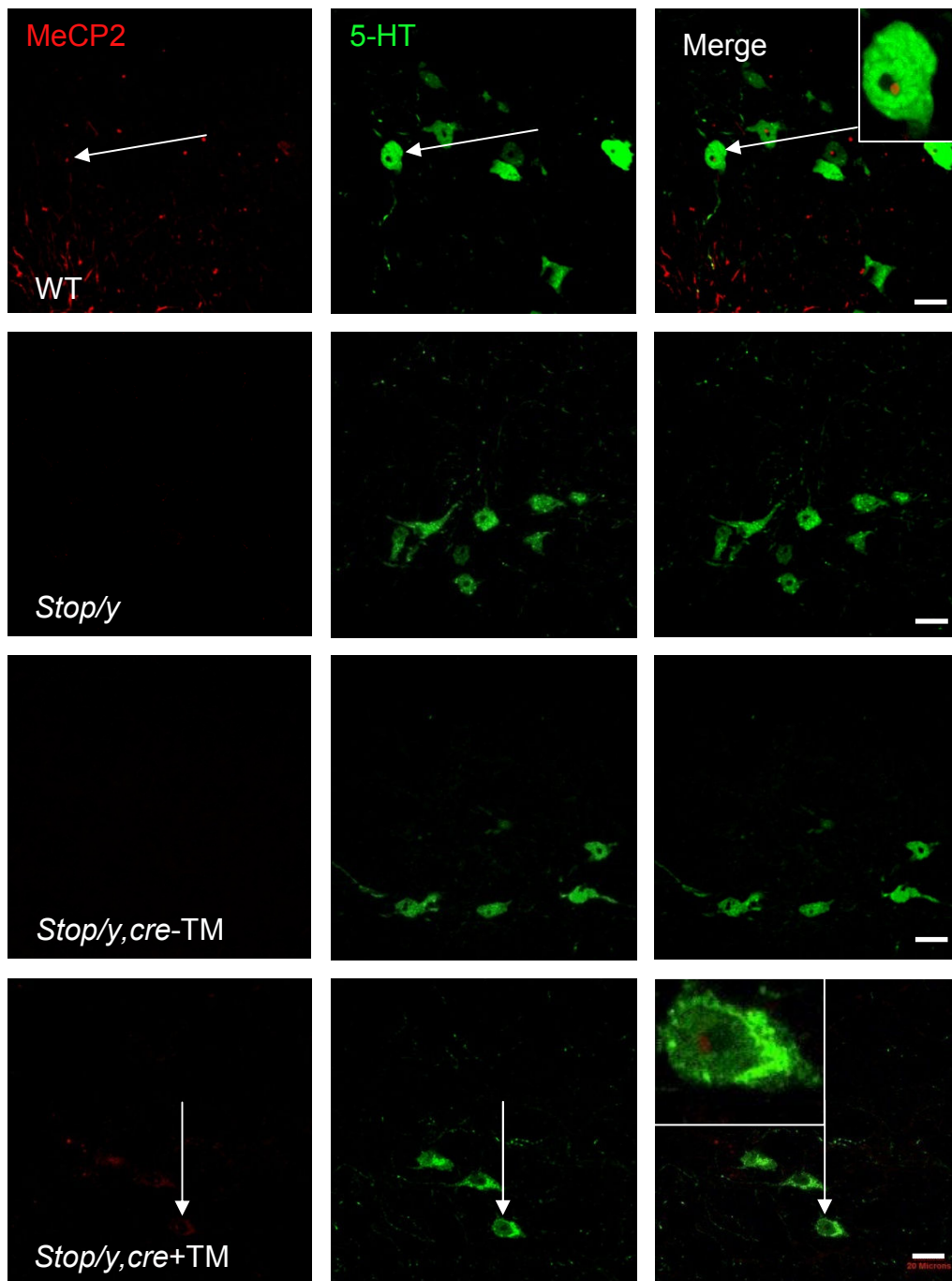


Fig 4-12 Single plane confocal image of 5-HT expressing neurons of the ventrolateral medulla of WT, *Stop/y*, *Stop/y,cre-TM*, *stop/y,cre+TM* animals. Red staining illustrates MeCP2 positive cells, green staining shows 5-HT expressing cells. Merge panel illustrates that MeCP2 and 5-HT were often co-expressed. White arrows in top and bottom panels indicate cell double labelled for MeCP2 and 5-HT in WT and *Stop/y,cre+TM* mice respectively. Insert = higher magnification image of 5-HT and MeCP2 colocalisation. Scale bar = 20 μ m.

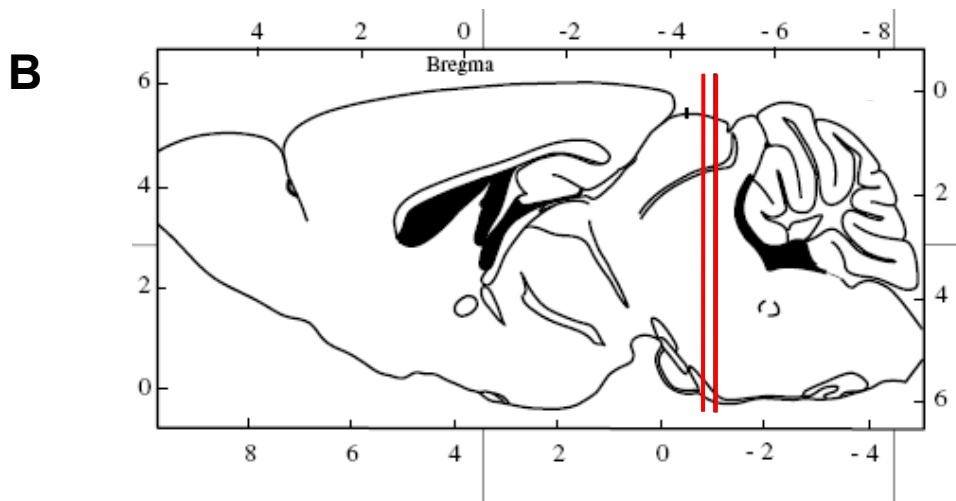
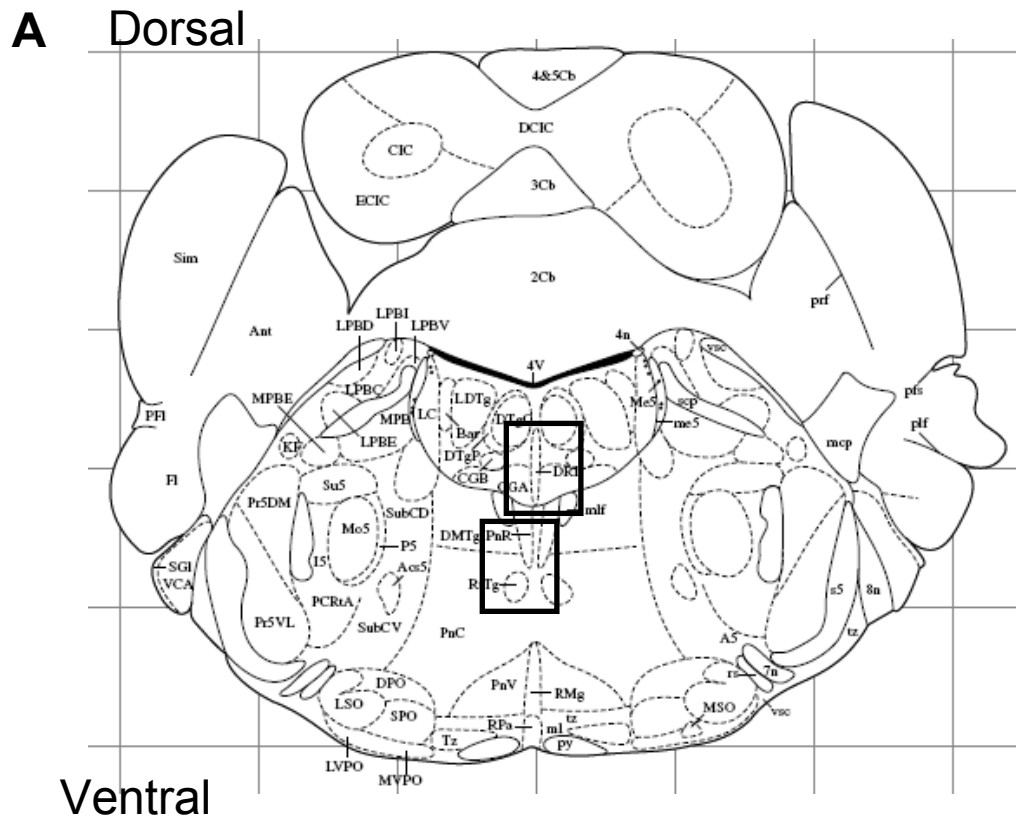


Fig 4-13 Illustration of the position of raphe dorsalis (DRI) and pontine raphe nuclei (PnR) region. A - Coronal section of brainstem illustrating location of DRI and PnR. Black boxes indicate position of counting windows (195 μ m \times 195 μ m). Upper box = DRI. Lower box = PnR. B - sagittal section of brainstem with red bars indicating span of cell count relative to bregma.

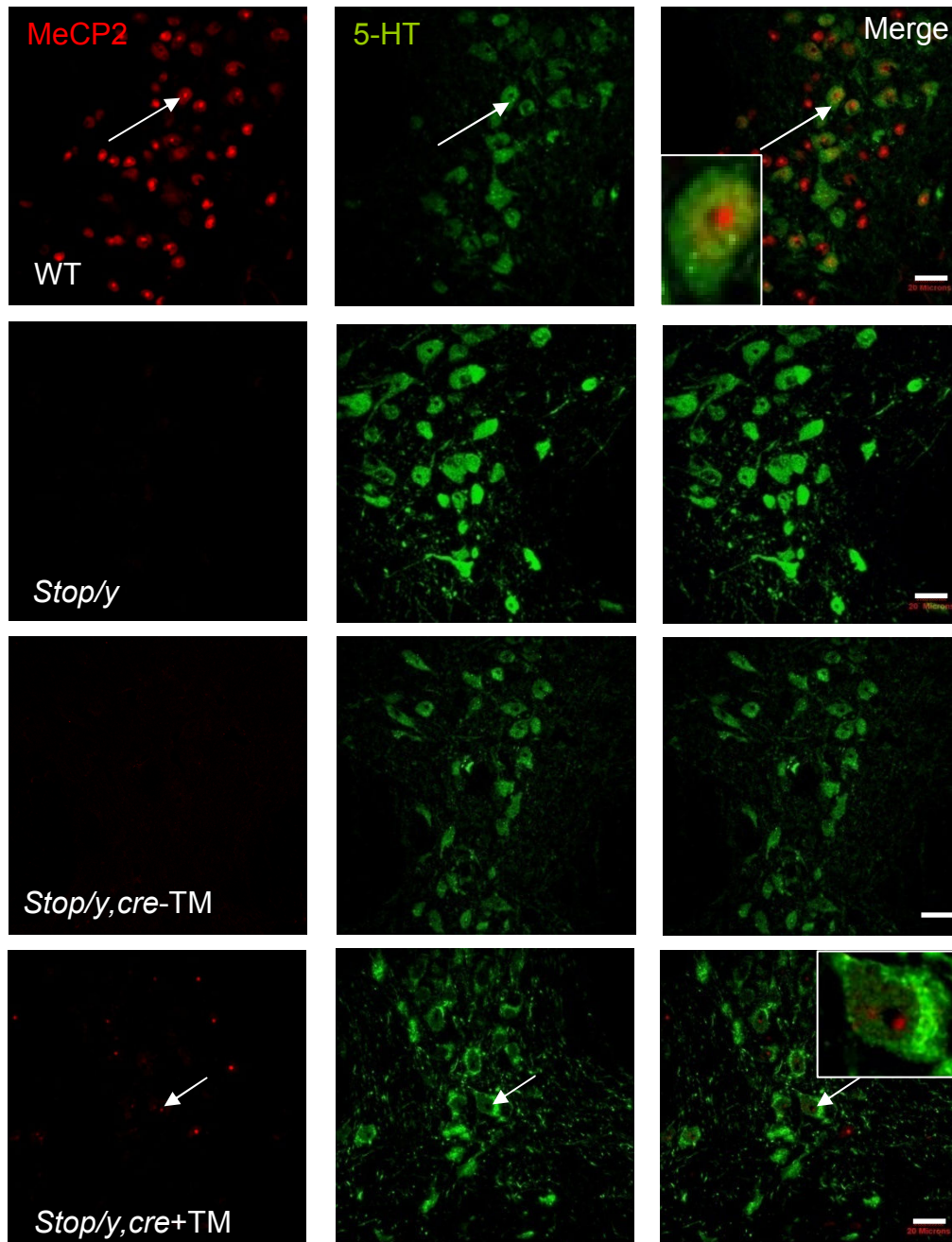


Fig 4-14 Single plane confocal image of 5-HT expressing neurons of the DRI of WT, *Stop/y*, *Stop/y,cre-TM*, *stop/y,cre+TM* animals. Red staining illustrates MeCP2 positive cells, green staining shows 5-HT expressing cells. Merge panel illustrates that MeCP2 and 5-HT were often co-expressed. White arrows in top and bottom panels indicate cell double labelled for MeCP2 and 5-HT in WT and *Stop/y,cre+TM* mice respectively. Insert = higher magnification image of 5-HT and MeCP2 colocalisation. Scale bar = 20 μ m.

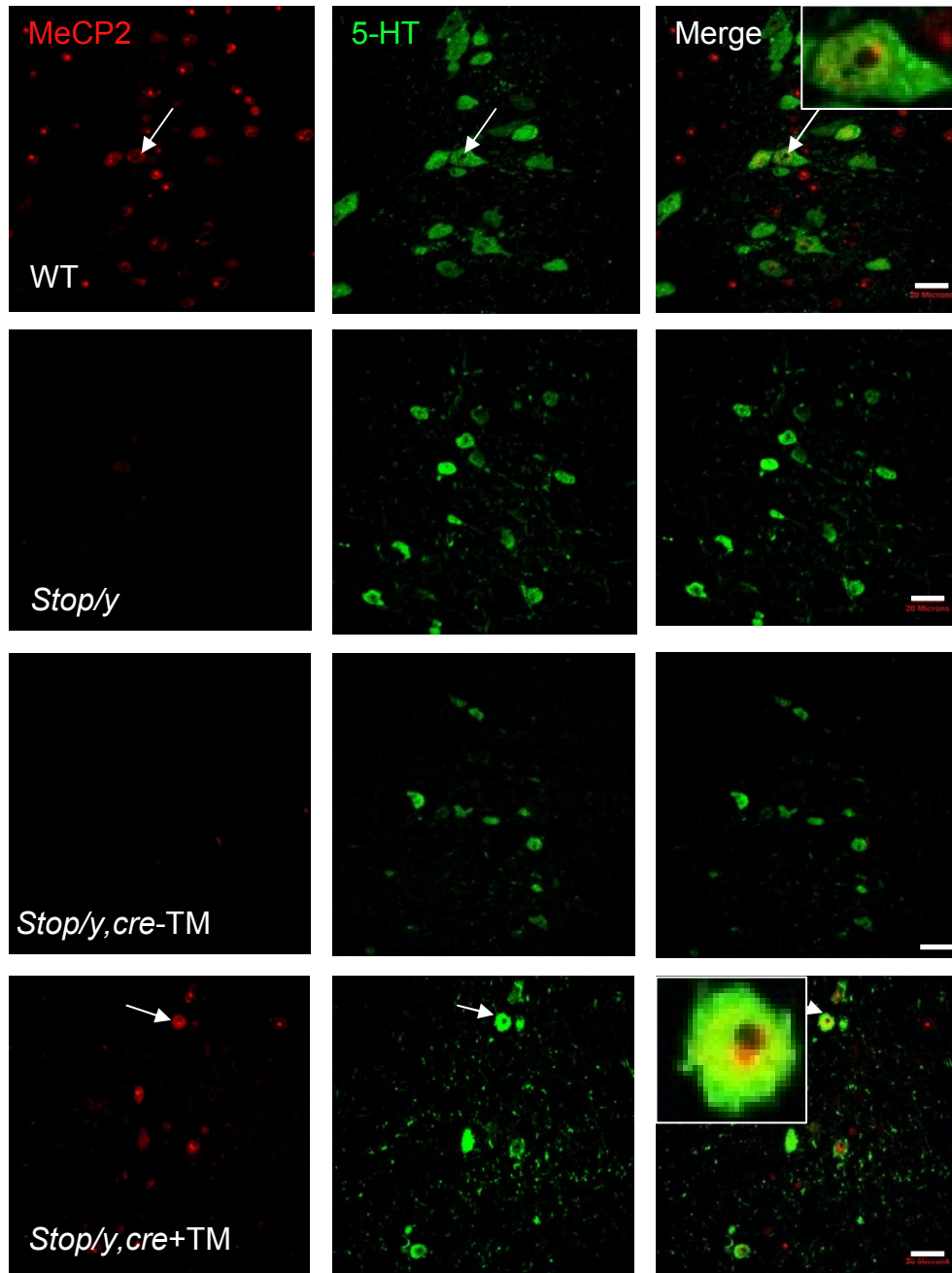


Fig 4-15 Single plane confocal image of 5-HT expressing neurons of the PnR/MnR of WT, *Stop/y*, *Stop/y,cre-TM*, *stop/y,cre+TM* animals. Red staining illustrates MeCP2 positive cells, green staining shows 5-HT expressing cells. Merge panel illustrates that MeCP2 and 5-HT were often co-expressed. White arrows in top and bottom panels indicate cell double labelled for MeCP2 and 5-HT in WT and *Stop/y,cre+TM* mice respectively. Insert = higher magnification image of 5-HT and MeCP2 colocalisation. Scale bar = 20 μ m.

4.2.4 Imaging and Quantification of NK1 Expressing Neurons

The area of the preBötC is found ventrolateral to the nucleus ambiguus and contains NK1 and VGLUT2 positive cells (Gray *et al.*, 2001; Guyenet *et al.*, 2002). Some sections were stained using guinea pig anti-NK1 (1:500, Millipore) and Rhodamine anti-rabbit secondary antibody (1:100, Jackson Immunoresearch) but it became apparent that the rabbit anti-NK1 primary antibody (1:500, Sigma, UK) gave clearer staining of the NK1 expressing neurons of the preBotC.

NK1 expressing cells were therefore targeted using rabbit anti-NK1 primary antibody (1:500, Sigma, UK) and Alexa-488 donkey anti-rabbit secondary (1:500, Stratech-Jackson Immunoresearch). VGLUT2 expression was detected using guinea pig anti- VGLUT2 (1:5000, Millipore, UK) and dylight-649 donkey anti-guinea pig secondary (1:100, Jackson Immunoresearch). VGLUT2 was used only as an aid to identify the region of the preBötC (fig 4-17) and was not used for quantification purposes. MeCP2 expression was detected using mouse anti-MeCP2 (1:100, Sigma, UK) and rhodamine donkey anti-mouse secondary (1:100, Sigma, UK).

The preBötC (figs 4-16, 4-17 and 4-18) lies ventrolateral to the subcompact formation of the nucleus ambiguus therefore imaging began in the section in which the subcompact formation of the nucleus ambiguus was present, level - 7.20mm caudal to bregma and ceased in the section in which the nucleus ambiguus was diffuse.

NK1 expressing neurons within the preBötC were counted bilaterally in a 195x195µm window to a depth of 10µm in each section. The counting window was positioned ventrolaterally to the nucleus ambiguus so that the upper corner touched the lower edge of the nucleus ambiguus and the box encompassed the area of the preBötC. NK1 expressing cells were counted as positive when the whole cell boundary was present. MeCP2 positive cells within the area were also quantified, with a cell being counted as MeCP2 positive when the staining was identified within the nucleus, confirmed by DAPI staining. Cells double labelled for NK1 and MeCP2 were also quantified.

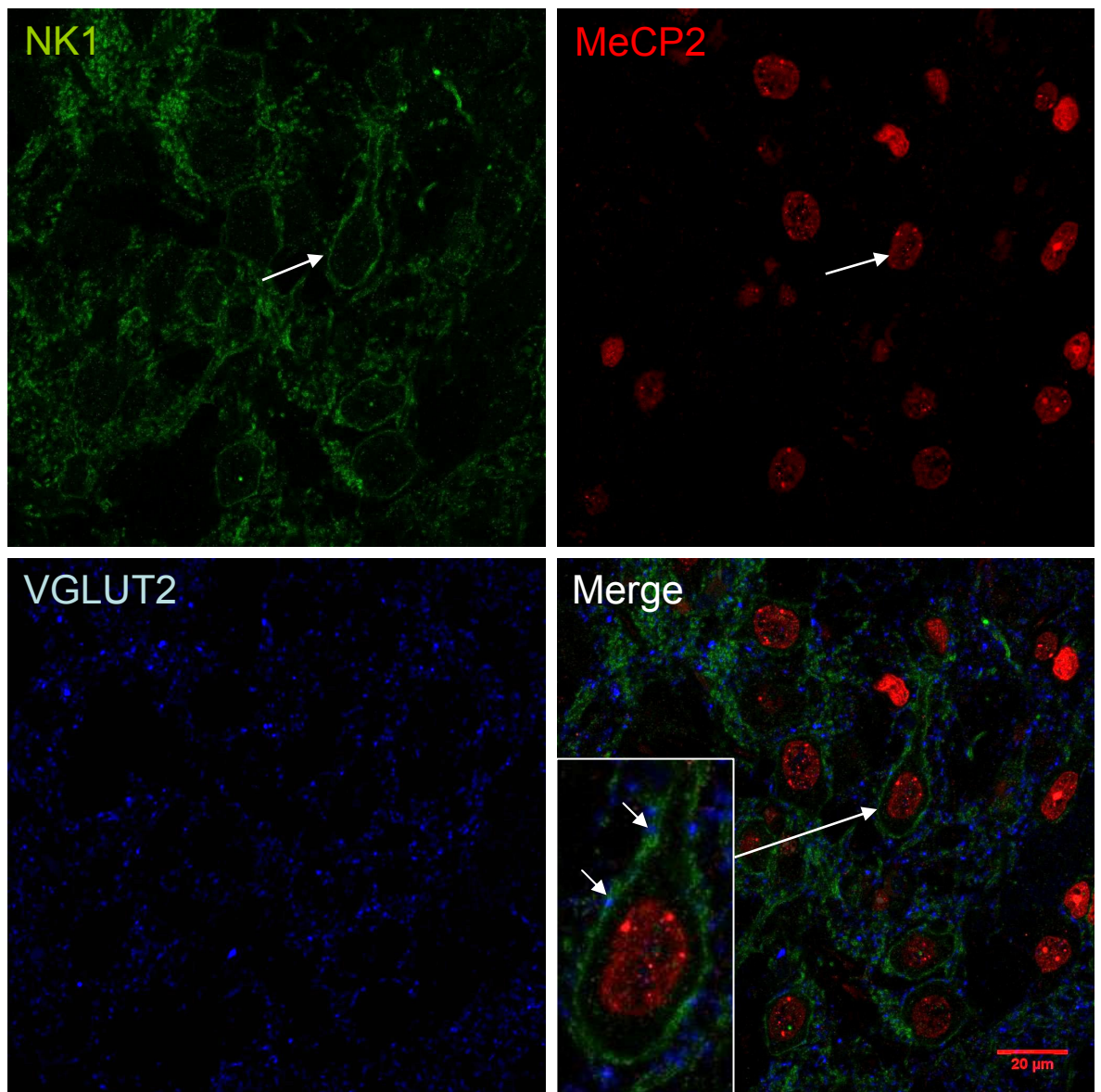


Fig 4-17 Single plane confocal image of NK1, MeCP2 and VGLUT2 expression within the PreBötC of WT animal. Green staining shows NK1 expressing cells, red staining illustrates MeCP2 positive cells and blue staining indicates VGLUT2 expression. White arrows indicate cell double labelled for MeCP2 and NK1. Insert = higher magnification image of cell of the preBötC showing VGLUT2, NK1 and MeCP2 expression. Scale bar = 20 μm.

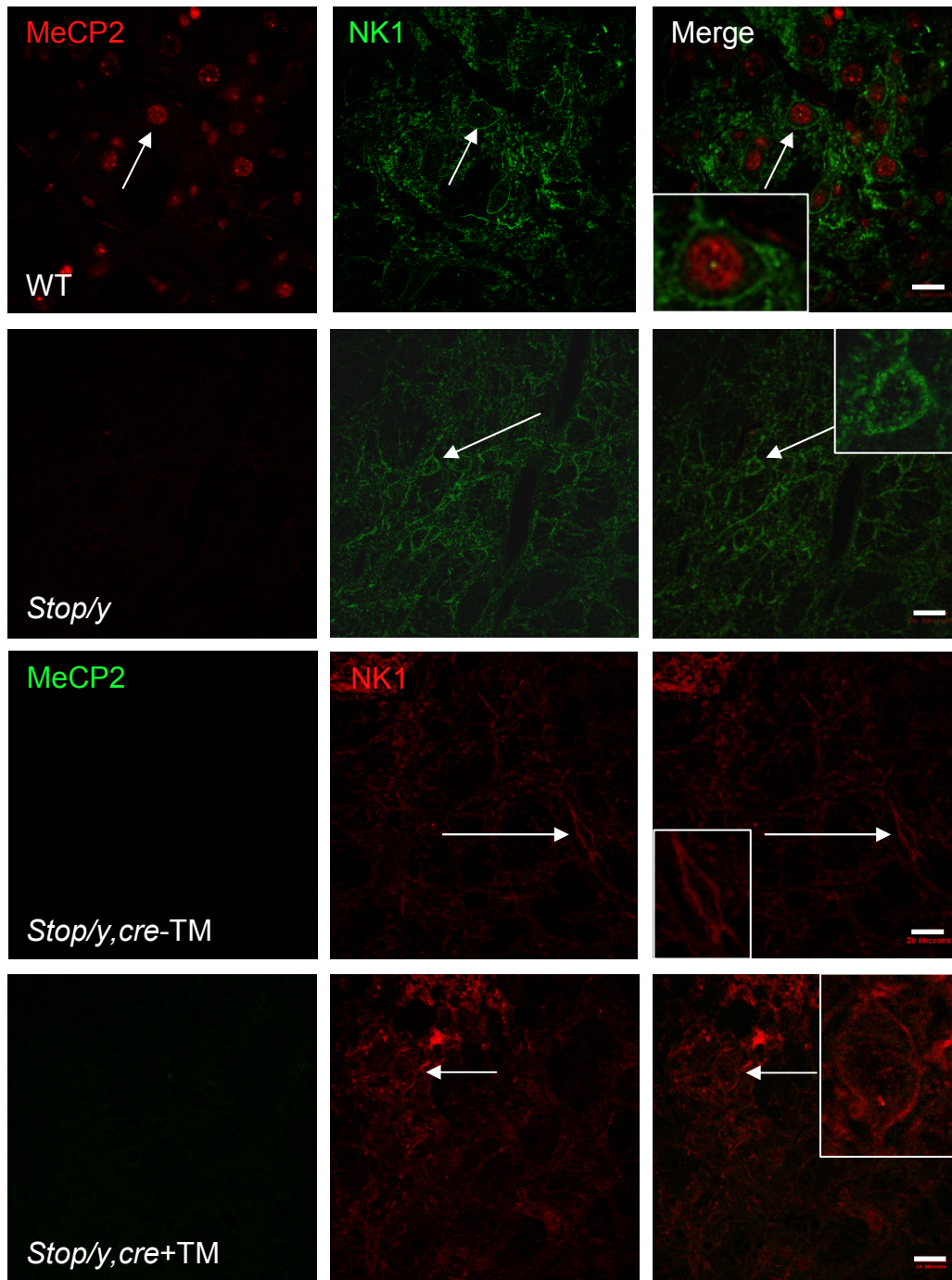


Fig 4-18 Single plane confocal image of NK1R and MeCP2 expression in the PreBötC of WT, *Stop/y*, *Stop/y, cre-TM*, *stop/y, cre+TM* animals. Red staining illustrates MeCP2 positive cells, green staining shows NK1 expressing cells. Merge panel illustrates that MeCP2 and NK1 were often co-expressed. Insert = higher magnification image of NK1 and MeCP2 co-localisation identified by arrow on lower magnification. Scale bar = 20 μ m.

4.2.5 Imaging and Quantification of Phox2b Expressing Neurons

The area of the RTN/pFRG is identified as an area ventral to the facial motor nucleus, extending rostro-caudally along the length of the facial motor nucleus (Onimaru & Homma, 2003; Guyenet *et al.*, 2005b). One particular rabbit anti-Phox2b primary (1:100, Abcam, UK) proved ineffective and as a result images were not quantifiable. Towards the end of the study a gift of another rabbit anti-Phox2b primary antibody (1: 500, C. Goridis, ENS, France) was received and staining was greatly improved. Attempts to reincubate sections which had previously failed to stain with Phox2b were attempted but still failed to show any positive Phox2b staining. This was presumably because the binding sites were already bound with the previous rabbit-anti Phox2b (Abcam, UK). Although an antigen retrieval step may have helped resolve this issue the tissue, as mentioned, in some cases was quite fragile and boiling of the tissue in citrate buffer may have resulted in severe damage to the sections. As a result, sample size of Phox2b stained sections was small (data not shown).

Cells of the RTN/pFRG were quantified using immunoreactivity to Phox2b and VGLUT2. Phox2b expression was detected using rabbit anti-Phox2b primary antibody (gift from C. Goridis, ENS, 1:500) with an alexa-488 donkey anti-rabbit secondary (1:500, Invitrogen, UK). VGLUT2 was detected using guinea pig anti-VGLUT2 (1:5000, Millipore, UK) and dylight-649 donkey anti-guinea pig secondary (1:100, Jackson Immunoresearch). VGLUT2 staining was used to identify the RTN/pFRG and was not used for quantification purposes. MeCP2 expression was detected using mouse anti-MeCP2 (1:100, Sigma, UK) and rhodamine anti-mouse secondary (1:100, Sigma, UK).

The RTN/pFRG lies ventral to the facial motor nucleus (fig 4-19 and 4-20) therefore Z-stack imaging began in the most caudal section which contained a cluster of facial motorneurons, level -6.48mm caudal to bregma, ceasing at level -5.8mm from bregma when the facial motor neurons were no longer apparent.

Phox2b expressing neurons of the RTN/pFRG were counted bilaterally in a 195x195µm window to a depth of 10µm. The counting window was positioned ventrally to the facial nucleus and the ventral edge of the section was visible within the window (fig 4-19).

A cell was counted as Phox2b positive if the whole cell boundary was present. MeCP2 positive cells were also quantified and a cell was counted as MeCP2 positive when the staining was clearly exhibited within the nucleus, confirmed by DAPI staining. Cells double labelled for Phox2b and MeCP2 were also quantified.

All cell counts are presented as mean \pm SD. Statistical analyses of cell counting involved application of two-way anova followed by Bonferroni post test. Values were considered significant if $p < 0.05$.

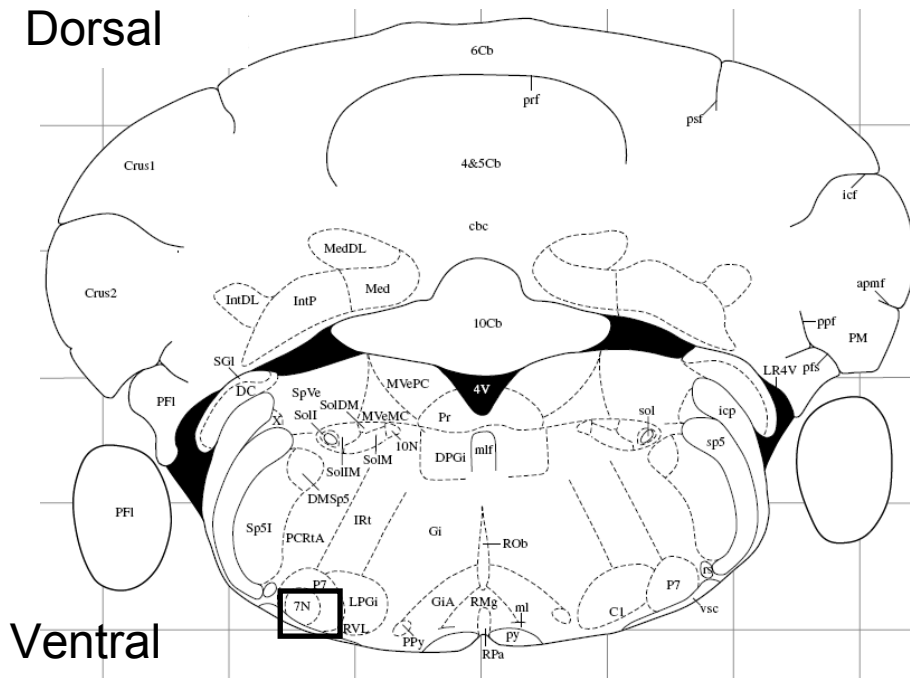
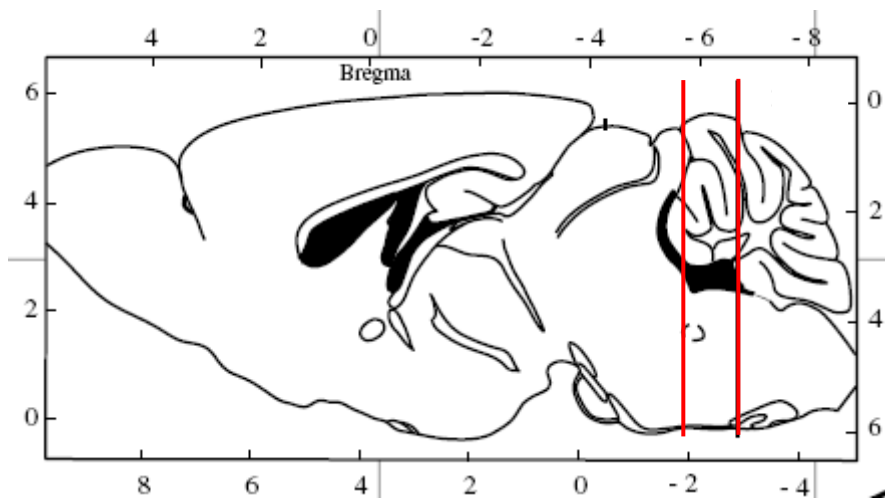
A**B**

Fig 4-19 Illustration of the position of RTN/pFRG region. A - Coronal section of brainstem illustrating location of RTN/pFRG. Black window indicates position of counting windows (195 μ m \times 195 μ m). **B** - Saggital section of brainstem with red lines indicating span of cell count relative to bregma.

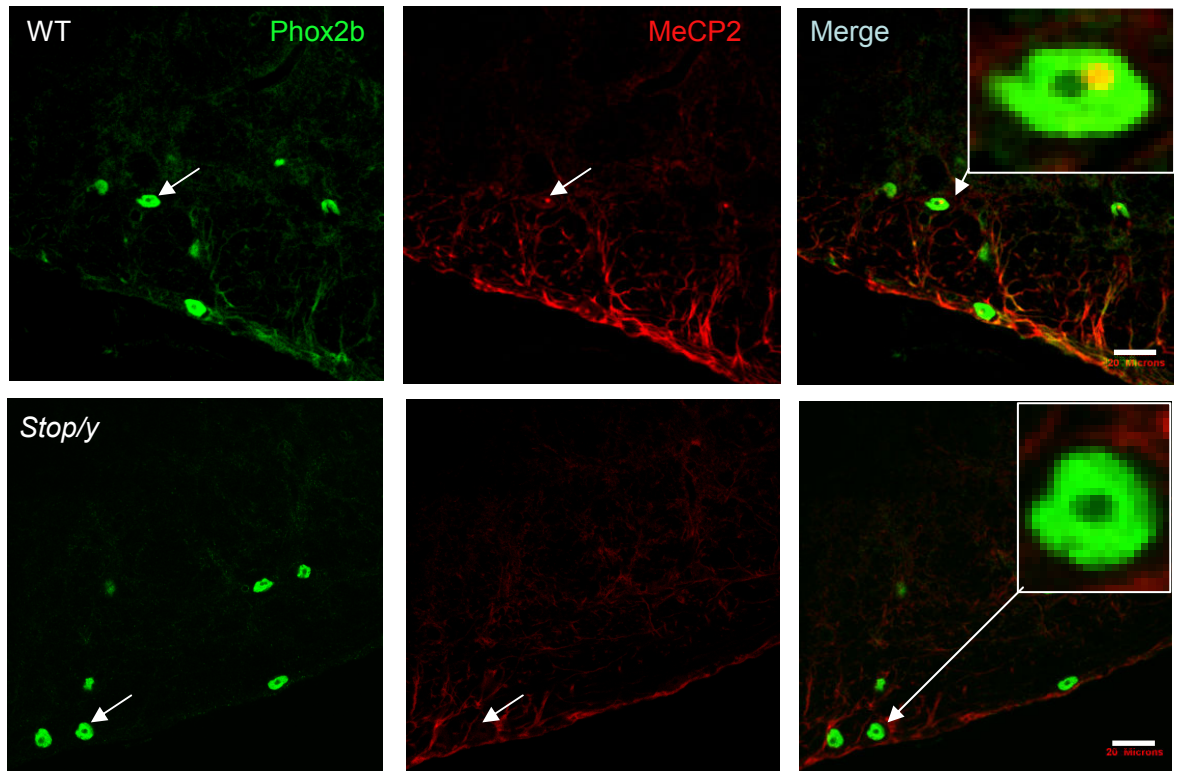


Fig 4-20 Single plane confocal images of Phox2b and MeCP2 expressing neurons of the RTN/pFRG of WT and *Stop/y* animal. Red staining illustrates MeCP2 positive cells, green staining shows Phox2b expressing cells. Merge panel illustrates that MeCP2 and Phox2b were often co-expressed. Top insert = higher magnification image of Phox2b and MeCP2 co-localisation in WT identified by arrow on lower magnification image. Lower insert = higher magnification image of Phox2b and no MeCP2 staining in *Stop/y* mouse. Scale bar = 20 μ m

4.3 Results

4.3.1 Tyrosine Hydroxylase (TH)

Fig 4-21 (plot A) shows that WT animals had the greatest number of TH expressing neurons in the LC and fewest TH cells in the A2/C2 (LC: 87.8 ± 36.1 , A2/C2: 25.4 ± 15.3 TH+ve cells). Compared to WT, *Stop/y, cre+TM* mice showed a trend towards fewer TH expressing cells in all adrenergic areas studied (A1/C1, WT: 51.9 ± 19.9 , *Stop/y, cre+TM*: 37.3 ± 25.5 TH cells; A2/C2, WT: 25.4 ± 15.3 , *Stop/y, cre +TM*: 14.7 ± 11.9 TH cells; LC, WT: 87.8 ± 36.2 , *Stop/y, cre +TM*: 60.8 ± 49.6 TH+ve cells). *Stop/y, cre -TM* mice also showed a trend towards fewer TH cells compared to the WT in A1/C1 (WT: 51.9 ± 19.9 , *Stop/y, cre -TM*: 44.9 ± 20.6 TH+ve cells) and A2/C2 (WT: 25.58 ± 15.3 , *Stop/y, cre -TM*: 23.4 ± 8.6 TH+ve cells), but an increase in the number of TH+ve cells in the LC (WT: 87.8 ± 36.1 , *Stop/y, cre -TM*: 99.2 ± 34.6 TH+ve cells). Compared to WT, the average number of TH expressing cells in the *Stop/y* animals were reduced in the A1/C1 (WT: 51.9 ± 19.9 , *stop/y*: 42.8 ± 38.6 TH cells) and the A2/C2 (WT: 25.4 ± 15.3 , *Stop/y*: 16.5 ± 12.9 TH+ve cells). *Stop/y* animals showed a trend towards an increased number of TH expressing neurons in the LC compared to WT (WT: 87.8 ± 36.2 , *Stop/y*: 112.4 ± 64.7 TH+ve cells).

WT mice showed 241.2 ± 111.5 MeCP2 +ve cells in the A1/C1, 222.6 ± 99.4 in the A2/C2 and 191.2 ± 89.6 in the LC (fig 4-21 plot C). *Stop/y, cre+TM* animals had significantly fewer MeCP2 +ve cells than the WT in the A1 (WT: 241.2 ± 111.5 , *Stop/y, cre +TM*: 102.9 ± 39.9 MeCP2 +ve cells. $P < 0.01$), and the A2/C2 (WT: 222.6 ± 99.4 , *Stop/y, cre +TM*: 93.2 ± 79.9 MeCP2 +ve cells. $P < 0.05$). The *Stop/y, cre +TM* mice also showed fewer MeCP2 cells in the LC compared to WT although this was not a significant difference (WT: 191.2 ± 89.6 , *Stop/y, cre +TM*: 116.4 ± 78.0 MeCP2 +ve cells, $p > 0.05$). No positive MeCP2 staining was found in the *Stop/y* or *Stop/y, cre - TM* mice.

In both WT and *Stop/y, cre +TM* mice the percentage of TH cells which also express MeCP2 was approximately 80-100% (fig 4-21 plot B). WT mice showed that 20-40% of the MeCP2 expressing cells in the adrenergic areas studied also expressed TH. In the *Stop/y, cre +TM* mice however, 40-60% of the MeCP2 expressing cells also expressed TH (fig 4-21 plot D).

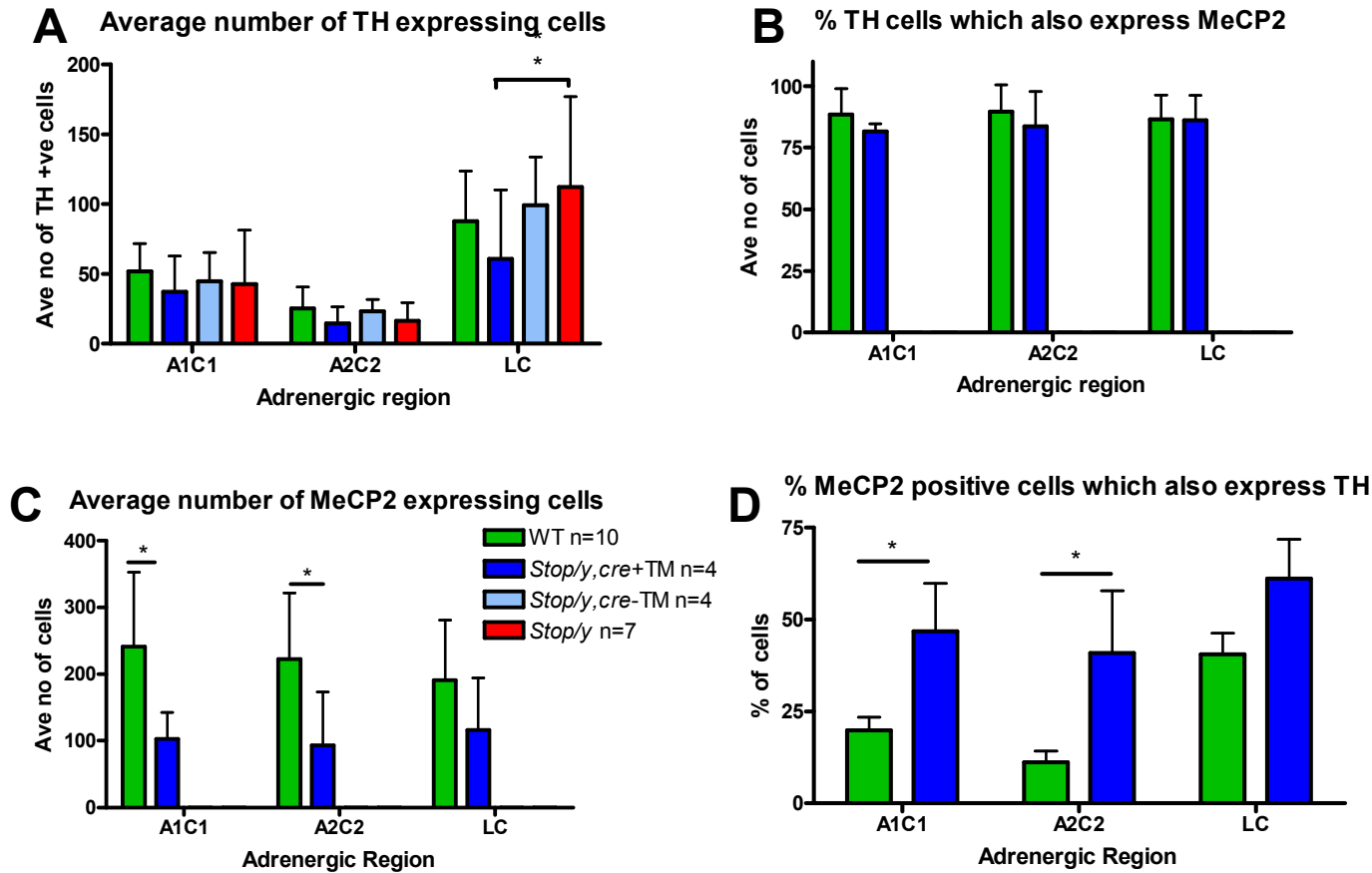


Fig 4-21 Plots to show average number of TH and MeCP2 expressing neurons in WT, *Stop/y,cre* +TM, *Stop/y,cre* -TM and *Stop/y* mice. **A** – Average number of TH expressing cells in each adrenergic region of each genotype. **B** – The percentage of TH+ve cells which also express MeCP2 in WT and *Stop/y,cre* +TM mice. **C** – The average number of MeCP2 expressing cells in each adrenergic region of all genotypes. **D** – The percentage of MeCP2 positive cells which also express TH in each adrenergic region of WT and *Stop/y,cre* +TM mice. Data presented as mean±S.D. 2-way anova with bonferroni post test;*p<0.05.

4.3.2 Serotonin (5-HT)

Fig 4-22 (plot A) illustrates that the number of 5-HT neurons in each serotonergic region was not significantly different, but with a trend towards a greater number of 5-HT expressing neurons in the Rpa and DRI (ROb: 29.3 ± 16.2 , RPa/RMg: 40.2 ± 21.5 , Ventrolateral: 29.2 ± 23.5 , DRI: 38.6 ± 17.6 and PnR: 23.7 ± 16.9 5-HT+ve cells).

Compared to WT, *Stop/y,cre* +TM animals had a trend towards fewer 5-HT positive cells in the RPa/RMg (WT: 40.2 ± 21.5 , *Stop/y,cre* +TM: 24.8 ± 10.2 5-HT cells, $p > 0.05$) and the Pnr/Mnr (WT : 23.7 ± 16.9 , *Stop/y,cre* +TM: 3.6 ± 0.9 5-HT cells) yet a trend towards a greater number in the DRI (WT: 38.6 ± 17.6 , *Stop/y,cre* +TM: 43.8 ± 3.1 5-HT cells, $p > 0.05$).

Stop/y,cre -TM mice exhibited a trend towards fewer 5-HT cells than the WT in all areas except ventrolateral areas where the *Stop/y,cre* -TM animals showed slightly more more 5-HT positive neurons than the WT (WT: 29.2 ± 23.5 , *Stop/y,cre* -TM : 33.2 ± 11.7 5-HT cells, $p > 0.05$).

Compared to WT, *Stop/y* mice had a trend towards fewer 5-HT expressing cells in all regions (ROb; WT: 29.3 ± 16.2 , *Stop/y*: 14.8 ± 11.1 5-HT cells. RPa/RMg; WT: 40.2 ± 21.5 , *stop/y*: 22.6 ± 13.3 5-HT cells. Ventrolateral; WT: 29.2 ± 23.5 , *Stop/y*: 22.5 ± 15.6 5-HT cells. Pnr/Mnr; WT: 23.7 ± 16.9 , *Stop/y*: 15.9 ± 16.7 5-HT cells, $p > 0.05$) bar the DRI where 5-HT expression was similar between the two genotypes (WT: 38.6 ± 17.6 , *Stop/y*: 39.7 ± 27.7 5-HT cells).

With regards to MeCP2 expression (Fig 4-22 plot C) no positive staining was found in *Stop/y,cre* -TM or *Stop/y,cre* mice. WT animals exhibited a greater number of MeCP2 positive cells than *Stop/y,cre*+TM mice in every serotonergic area studied with a significantly greater number of MeCP2 expressing cells in the Pnr/Mnr (WT: 120.0 ± 64.6 , *Stop/y,cre*+TM: 9.6 ± 0.5 MeCP2+ve cells, $p < 0.001$). In both WT and *Stop/y,cre* +TM, the greatest number of MeCP2 positive neurons were found in the DRI (Fig 4-22 plot C. WT: 140.4 ± 50.2 , *Stop/y,cre* +TM: 84.5 ± 16.2 Mecp2+ve cells).

In WT animals, 80-100% of cells which expressed 5-HT also expressed MeCP2 (Fig 4-22 plot B) yet in *Stop/y,cre* +TM mice only 60-80% of 5-HT cells also expressed MeCP2. *Stop/y,cre* +TM mice showed a significantly smaller percentage of double labelled neurons than the WT in the ventrolateral medulla (WT: $93.1 \pm 11.1\%$, *Stop/y,cre* +TM: $66.7 \pm 15.2\%$ % of 5-HT cells co-labelled for MeCP2, $p < 0.05$) and the Pnr/Mnr (WT: 88.5 ± 14.8 , *Stop/y,cre* +TM: $60.0 \pm 56.6\%$ % of 5-HT cells co-labelled for MeCP2, $p < 0.05$).

Both WT and *Stop/y,cre* +TM mice showed that 40-60% of the MeCP2+ve cells in the serotonergic areas also stained positive for 5-HT (fig 4-22 plot D). There was no significant difference between the WT and *Stop/y,cre* +TM with regards to the number of MeCP2+ve cells which also expressed 5-HT ($p > 0.05$).

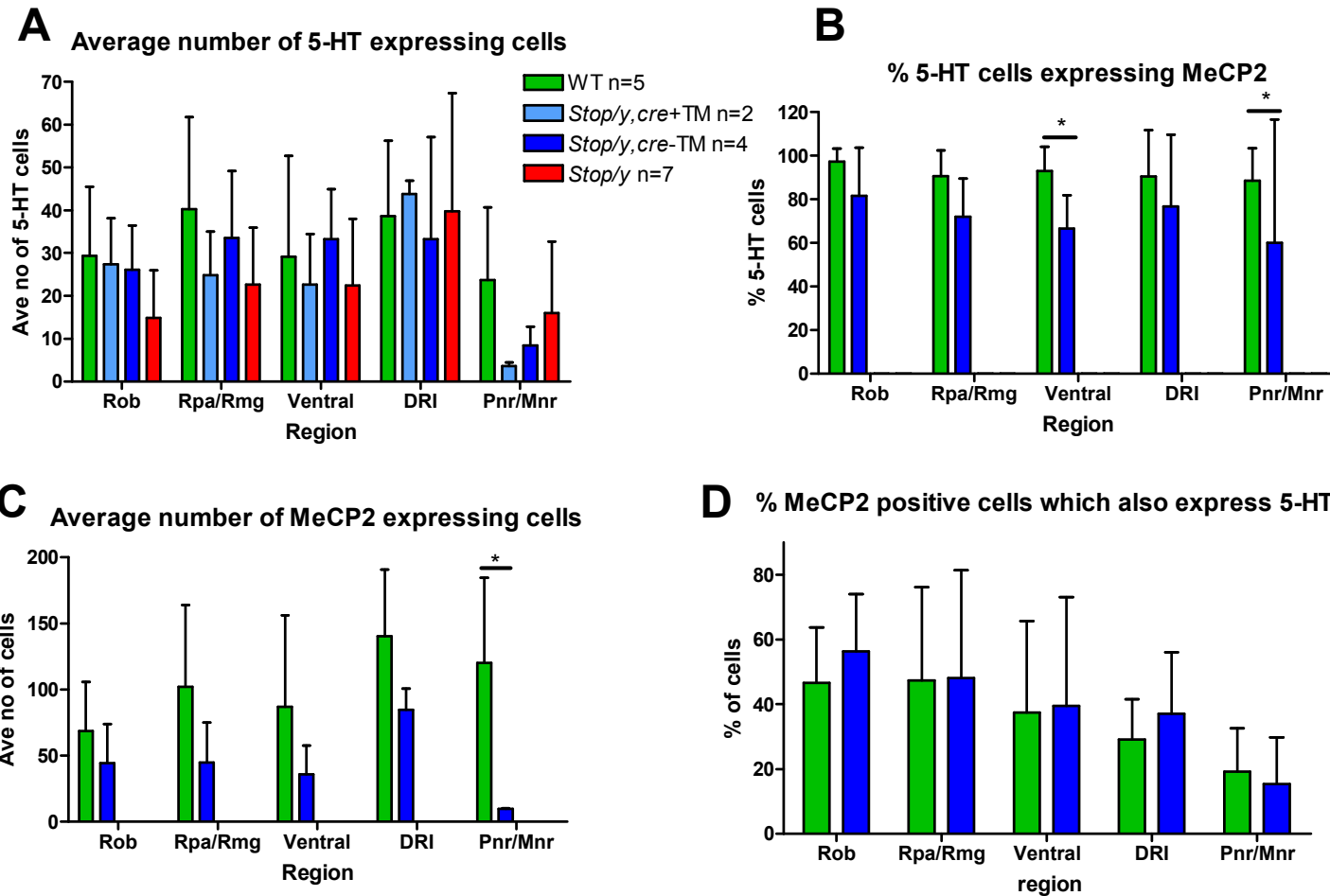


Fig 4-22 Plots to show average number of 5-HT and MeCP2 expressing neurons in WT, *Stop/y,cre +TM*, *Stop/y,cre -TM* and *Stop/y* mice. **A** – Average number of 5-HT expressing cells in each serotonergic region. **B** – Percentage of 5-HT+ve cells which also express MeCP2. **C** –Average number of MeCP2 +ve cells in each serotonergic region of all genotypes. **D** –Percentage of MeCP2+ve cells which also express 5-HT in WT and *Stop/y,cre +TM* mice. Data presented as mean±S.D. 2-way anova with bonferroni post test; * p<0.05.

4.3.3 Neurokinin-1 (NK1)

Fig 4-23 (plot A) illustrates that WT animals exhibited 10 ± 5.88 NK1 expressing cells, *Stop/y,cre*+TM exhibited 1 cell, *Stop/y,cre*-TM showed 7 NK1+ve cells and *Stop/y* expressed 7.87 ± 8.49 cells. All of the MeCP2 deficient mice showed a trend towards fewer NK1 expressing cells compared to the WT. With regards to MeCP2 expression (fig 4-23 plot C), WT animals exhibited 83.7 ± 31.0 MeCP2 expressing cells while *Stop/y,cre* +TM only expressed 3.3 ± 4.1 MeCP2 positive cells, however due to difficulties with staining (as will be discussed towards the end of the chapter) the *Stop/y,cre* +TM data was based on n=1. *Stop/y* and *Stop/y,cre* -TM animals did not show positive staining for MeCP2. In the WT, $76.9 \pm 26.4\%$ of NK1 cells also expressed MeCP2 (Fig 4.23 plot B) whereas in *Stop/y,cre* +TM mice only 16.7% of NK1 expressing cells also exhibited MeCP2 staining. In the WT, approximately 12-15% of the MeCP2 expressing cells also expressed NK1 and in the *Stop/y,cre* +TM less than 5% of the MeCP2+ve cells expressed NK1. Again it should be noted that the *Stop/y,cre* +TM data for the preBötC was based on n=1 and therefore makes the result difficult to interpret.

4.3.4 Phox2b

Due to these difficulties with staining, Phox2b staining did not produce enough data for quantification. It can be seen from the images in fig 4-20 that the WT animal exhibits positive Phox2b staining and MeCP2 staining, and that MeCP2 can be co-localised with Phox2b.

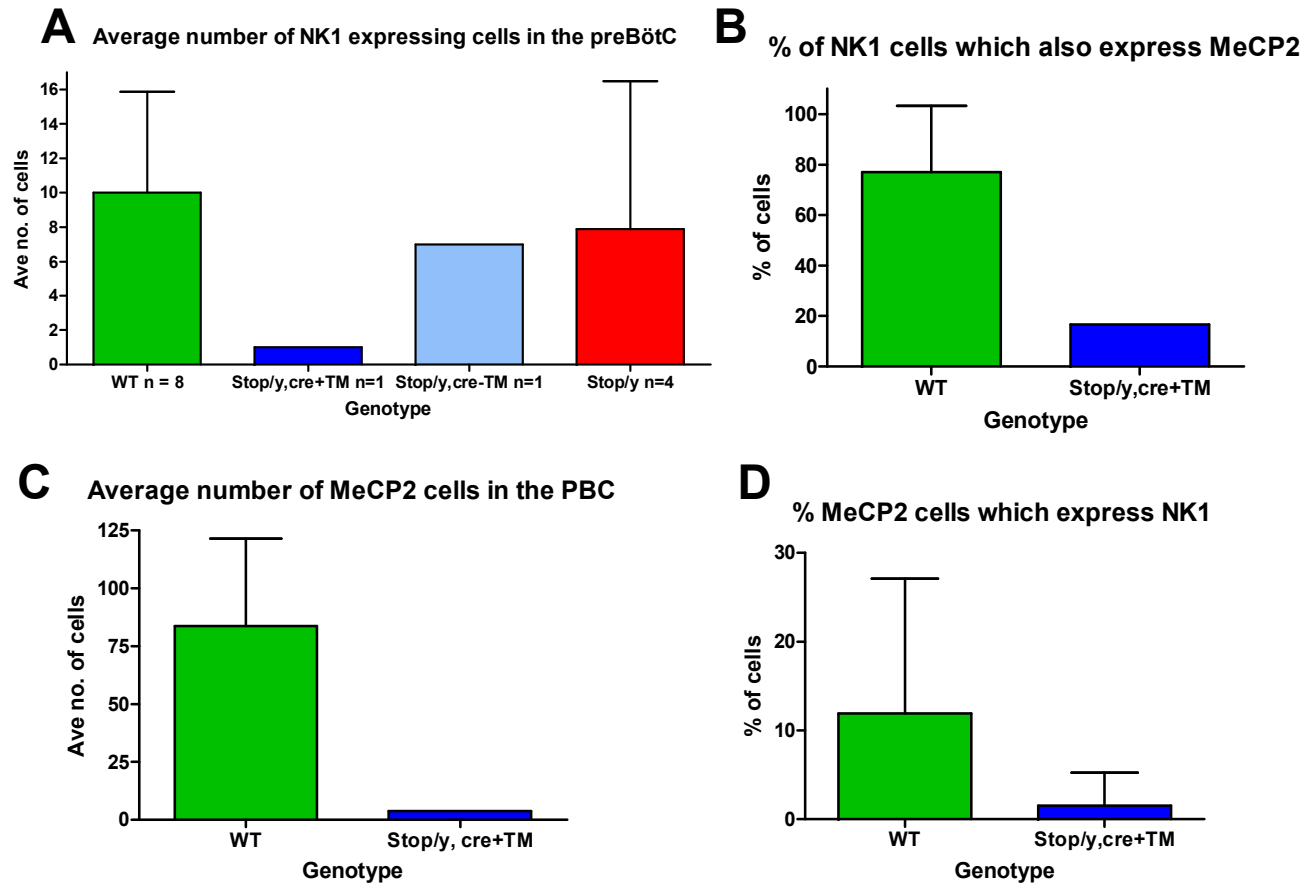


Fig 4-23 Plots to show average number of NK1 and MeCP2 expressing neurons in the preBötC of WT, *Stop/y, cre +TM*, *Stop/y, cre - TM* and *Stop/y* mice. **A** – Average number of NK1 expressing cells in the preBötC of each genotype. **B** – The percentage of NK1+ve cells which also express MeCP2 in WT and *Stop/y, cre +TM* mice. **C** – The average number of MeCP2 expressing cells in the preBötC of all genotypes. **D** – The percentage of MeCP2 positive cells which also express NK1 in the preBötC region of WT and *Stop/y, cre+TM* mice. Data presented as mean±S.D.

4.4 Discussion

The data in this chapter suggest that in MeCP2 deficient mice there is a trend towards fewer TH and 5-HT expressing cells compared to WT. However, this difference is not statistically significant and as such it is difficult to conclude whether or not these changes in neuromodulatory areas underlie the respiratory abnormalities which were recorded in the male mutant mice in chapter 3.

4.4.1 Noradrenergic Neuromodulation

It was shown in this study that all genotypes exhibited the largest number of TH expressing neurons within the LC (fig 4-21 plot A), known to be the largest noradrenergic nucleus in the brain (Swanson, 1976) and known to have an excitatory effect on respiratory activity (Hilaire *et al.*, 2004). The LC of *Stop/y* mice had a greater number of TH positive neurons compared to WT, *Stop/y,cre+TM* and *Stop/y,cre -TM* animals. Since neurons of the LC act to increase respiratory output, the greater respiratory frequency observed in *Stop/y* mice compared to WT in chapter 3 could be the result of greater NA output from the LC of *Stop/y* mice. However, these data contradict a previous study which reveals a reduction in LC TH positive neurons of *Mecp2^{-y}* mice (Roux *et al.*, 2010). The fact that *Stop/y* mice in this study had a greater number of TH positive neurons compared to WT in the LC could be age related. *Stop/y* mice were younger than WT and *Stop/y,cre +TM* mice by approximately 10 weeks at the time of perfusion. It has been reported that number of NA neurons in the LC decreases as mice age (Tatton 1991) and that the number of TH expressing neurons in the A1/C1 and A2/C2 regions is larger in neonates than in adult mice (Hilaire, 2006). Thus *Stop/y* mice may appear to have a greater number of TH positive neurons in the LC compared to WT, however it may be that the neurons of the *Stop/y* mice would have shown a progressive reduction in TH expression if they had survived to an older age.

MeCP2 is implicated in the maturation and maintenance of neurons. Since the NA system continues to mature postnatally, it could be hypothesised that the absence of MeCP2 affects the development and maintenance of the NA system. The MeCP2 deficient mice studied in this chapter exhibited a trend towards a reduction in the number of TH expressing neurons compared to the WT in the

region of the A1/C1, a result which is also reported by Viemari et al in the *Mecp2^{-/y}* mice (Viemari *et al.*, 2005). The A1/C1 region is proposed to be involved in modulating respiratory frequency (Hilaire, 2006; Zanella *et al.*, 2006) and therefore it could be hypothesised that a reduction in the number of TH neurons in the A1/C1 would yield a reduced respiratory frequency. However, this is not reflected in the data from chapter 3 which illustrated that MeCP2 deficient mice had an increased basal respiratory frequency compared to WT.

The MeCP2 deficient mice studied in this chapter also had a trend towards a reduced number of TH expressing neurons in the A2/C2 compared to WT. Neurons of the A2/C2 are thought to be involved in stabilising the respiratory rhythm (Hilaire *et al.*, 1990; Zanella *et al.*, 2006) and thus a reduction in the number of TH neurons in the A2/C2 may account for the variable breathing pattern that was reported in MeCP2 deficient mice in chapter 3. It is proposed that the apparent reduction in the number of TH positive cells is due to a change in the cells phenotype rather than as a result of cell death, as no evidence of apoptosis is found in the A1/C1 and A2/C2 regions of MeCP2 deficient mice (Roux *et al.*, 2007). NA deficits in *Mecp2^{-/y}* mice may be due to the deficient expression of TH and dopamine beta hydroxylase (Zhang *et al.*, 2010a), enzymes which are important in the synthesis of noradrenaline.

It has been shown that application of NA uptake inhibitor Desipramine for 2 weeks in MeCP2-deficient mice results in a reduction in the number of apneas suffered by MeCP2 deficient mice (Roux *et al.*, 2007) which indicates that the reduction in TH expression and presumably NA content which occurs in mice as a result of the absence of MeCP2 is not an irreversible change and may stem from a failure to maintain the cell phenotype.

MeCP2 reactivation did not raise MeCP2 expression levels in noradrenergic regions of *Stop/y,cre+TM* mice to WT level (fig 4-21 plot C), with levels of MeCP2 expression in *Stop/y,cre+TM* mice being only 40-60% of the WT level. A recent study by Lang et al involving reactivation of *Mecp2* in only catecholaminergic neurons of MeCP2 deficient male mice also shows that MeCP2 levels do not increase to that of the WT (Lang *et al.*, 2013). The data in this thesis show that in the WT, only 20-40% of the MeCP2 positive cells also expressed TH (fig 4-21 plot D) which suggests that there are a number of MeCP2 cells which may be colocalised with a neurotransmitter other than TH. *Stop/y,cre+TM* mice showed

that although on average there were fewer MeCP2 expressing cells compared to the WT (fig 4-21 plot C). The fact that a higher proportion of MeCP2+ve cells in the *Stop/y,cre+TM* mice also expressed TH (40-60% ;fig 4-20 plot D) than was seen in the WT (~15-40%) suggests that there is a predominant reactivation of MeCP2 in NA regions. The data given here was gathered from *Stop/y,cre+TM* animals of approximately 20-24 wks of age, which could be up to 13 wks after TM treatment. It may have been of interest to study levels of TH expression and MeCP2 in *Stop/y,cre+TM* animals at various timepoints after *Mecp2* reactivation to monitor the progression of reactivation. This may have provided more information regarding an interaction between levels of *Mecp2* expression and the expression of TH. Future work may also involve the use of luciferase or a reporter gene to monitor exactly which cells show reactivation of *Mecp2*.

There may be an association between reduced MeCP2 levels and TH expression as there exists an MeCP2-binding site in the tyrosine hydroxylase promoter (Yasui *et al.*, 2007). MeCP2 expression in the *Stop/y,cre+TM* mice was greatest in the LC where the greatest number of TH expressing cells were also found (Fig 4-21 plot A and C). The lowest amount of MeCP2 expression was found in the A1/C1 and A2/C2, areas where fewest TH cells were found again highlighting a possible link between MeCP2 expression and TH expression. However, one counter argument against MeCP2 mediating TH activity is that *Stop/y* mice that showed no MeCP2 expression at all still had a greater number of TH expressing neurons in the LC compared to WT.

4.4.2 Serotonergic Neuromodulation

In this chapter, there was a trend towards a reduction in the average number of 5-HT expressing cells in *Stop/y* compared to WT (fig 4-22 plot A), a result which agrees with the finding that RTT patients have reduced levels of 5-HT in the brain (Riederer *et al.*, 1985; Riederer *et al.*, 1986) as do *Mecp2*-null mice (Ide *et al.*, 2005).

Evidence suggests that there are projections from the preBötC to the raphe obscurus to modulate 5-HT activity (Richter *et al.*, 2003; Ptak *et al.*, 2009). If the absence of MeCP2 has an impact on this respiratory rhythm generator as may be suggested by an increased respiratory frequency in *stop/y* mice, it could be

hypothesised that there may be a deficit in the feedback from the preBötC to the raphe obscurus. As 5-HT is important in stabilisation of the respiratory rhythm, a subsequent reduction of 5-HT activity and could account for the variable respiratory pattern of the MeCP2 deficient mice observed in chapter 3. Pet-1 KO mice lack the Pet-1 transcription factor, crucial in the control of the 5-HT neuron phenotype (Hendricks *et al.*, 1999). As a result these mice exhibit 70-80% loss of 5-HT neurons in the CNS (Hendricks *et al.*, 2003) and at neonatal stages show an increased variability in respiratory output compared to WT animals. 5-HT endogenous activation is also thought to be required to stabilise the eupneic rhythm in brain slices (Pena & Ramirez, 2002) and activation of 5-HT_{1A} receptors reverses apneustic breathing (Lalley *et al.*, 1994). In light of these studies, the trend towards fewer 5-HT neurons in *Stop/y* and *Stop/y,cre* mice compared to WT may account for the instability of the respiratory traces of the MeCP2 deficient mice. After reactivation of MeCP2, although respiratory traces are much improved, the number of 5-HT neurons in *Stop/y,cre+TM* mice does not return to WT level. The persistence of a reduced number of 5-HT neurons in the mutant mice may account for the degree of variability that still remains within the breathing pattern of *Stop/y,cre+TM* mice even after *Mecp2* has been reactivated (Fig 3-7).

Care must be taken when drawing comparisons between the data in this study and previous investigations. This is due to the fact that some studies into the effects of 5-HT on the respiratory network are carried out *in vitro* in brain slices whereas this *in vivo* study makes use of the whole animal. This means input from the likes of peripheral chemoreceptors may result in a different respiratory output in response to changes in 5-HT content compared to those which are observed in brain slices. Also, studies such as those carried out by Lalley *et al.*, make use of anaesthetised cats to illustrate the reversal of apneustic breathing which may introduce bias since anaesthesia is a suppressor of respiratory activity (Lalley *et al.*, 1994).

In vitro patch-clamp recordings of brain slices proved that the medullary raphe contains neurons which are intrinsically sensitive to increases in carbon dioxide (Richerson, 1995b), suggesting that 5-HT neurons may be involved in the chemosensitive response. Thus, the trend towards a reduced number of 5-HT

expressing neurons in the MeCP2 deficient mice of this chapter may account for the abnormal respiratory response of the mice to hypercapnia which was observed in chapter 3.

With regards to MeCP2 expression, WT animals exhibited a trend towards a greater number of MeCP2 positive cells than *Stop/y,cre+TM* mice in every serotonergic area studied with a significantly greater number observed in the Pnr/Mnr (Fig 4-22 plot C, $P < 0.05$). Mutants expressed approximately 40-60% of the WT level of MeCP2. This reduced level of MeCP2 expression following reactivation of the gene may be accounted for by Guy et al.(2007), who previously reported that Tamoxifen mediated deletion of the stop cassette was only approximately 80% effective thus the *Stop/y,cre* mice would not be expected to exhibit the same number of MeCP2 expressing neurons as the WT. Interestingly, the greatest number of MeCP2 expressing neurons in the *Stop/y,cre+TM* animal were found in the DRI where the greatest number of 5-HT expressing cells are also found. The least amount of MeCP2 expressing cells were seen in the Pnr/Mnr where fewest 5-HT expressing cells were observed. As with TH, this may suggest a relationship between MeCP2 and 5-HT expression. However *Stop/y* mice had no MeCP2 positive cells yet exhibited the largest number of 5-HT neurons in the DRI, a pattern of expression which is similar to WT, which suggests 5-HT expression may not be mediated directly by MeCP2.

In WT animals, 90-100% of 5-HT expressing neurons also expressed MeCP2 (Fig 4-22 plot B) while only 20-50% of the MeCP2 positive cells also expressed 5-HT (Fig 4-22 plot D). As was seen with TH, this suggests that there are many MeCP2 positive cells within serotonergic areas which may be co-expressed with a neurotransmitter other than 5-HT. In *Stop/y,cre+TM* animals, 60-80% of 5-HT positive cells also expressed MeCP2 (Fig 4-22 plot B) and 20-50% of MeCP2 positive cells also expressed 5-HT (Fig 4-22 plot D). Although *Stop/y,cre+TM* mice showed a fewer number of MeCP2 positive cells compared to the WT (Fig 4-22 Plot C), the percentage of MeCP2 positive cells which also express 5-HT is comparable between the two genotypes, which suggests that reactivation of MeCP2 is not predominantly occurring in 5-HT neurons.

The respiratory abnormalities of the MeCP2 deficient mice are unlikely to be the result of a problem in one neuromodulatory area alone, rather a combination of both serotonergic and noradrenergic system failures. This hypothesis is supported by the fact that neither Pet-1 conditional knock out mice (which only have MeCP2 removed from serotonergic cells) nor TH-conditional knock out mice (which have MeCP2 removed from adrenergic cells) show the particular breathing phenotype as seen in *Mecp2*^{-/y} mice (Samaco *et al.*, 2009) which are reported to have a deficit in both NA and 5-HT systems.

4.4.3 NK1 Expression in the PreBötzinger Complex

The preBötC, as discussed previously, acts as a key rhythm generator but also is proposed to have some involvement in chemosensitivity. Fig 4-23 illustrates that the number of NK1 expressing neurons within the preBötC showed a trend towards a reduction in *Stop/y* and *Stop/y,cre*-TM mice although this was not a significant difference ($p > 0.05$). A reduction in the number of NK1 expressing cells within the preBötC may account for the irregular breathing pattern that the mutant animals presented (chapter 3) as bilateral lesioning of the preBötC using targeted ablation of NK1 expressing neurons leads to an ataxic breathing pattern (Gray *et al.*, 2001; McKay *et al.*, 2005).

Homeobox protein Hox-B1 (*Hoxb1*) gene encodes a transcription factor that is important in the morphogenesis of several areas within the brain, including the preBötC. Mice with no MeCP2 in *Hoxb1* tissues, which include the area of the preBötC, have altered respiratory response to hypoxia and also have an increased basal respiratory rate (Ward *et al.*). Data presented in chapter 3 highlighted that *Stop/y* mice, with a ubiquitous lack of MeCP2, also displayed an increased basal respiratory rate perhaps due to the same lack of MeCP2 in the *Hoxb1* tissues reported by Ward *et al* 2011. Also, Ward *et al* report that rescuing MeCP2 expression within the *Hoxb1* tissue rescues the hypoxic response of mice but does not alter the increased resting respiratory rate. Data in chapter 3 highlights that after reactivation of *Mecp2*, the respiratory rate of *Stop/y,cre*+TM animals was somewhat reduced compared to the pre-TM rate yet still remained greater than WT respiratory rate. Since reactivation of *Mecp2* within the preBötC area did not rescue MeCP2 expression to WT level (Fig 4-23 plot D) then it could be hypothesised that any changes within the preBötC are

not fully recovered by the amount of *Mecp2* which is reactivated. However, as noted previously, with such low *Stop/y,cre+TM* numbers it is difficult to draw a solid conclusion about the relationship between *Mecp2* reactivation and its effect on the NK1 expressing neurons of the preBötC. It was noted when processing some of the mutant brainstem tissue that it was quite fragile compared to WT tissue. This could be accounted for by the fact that some mutant animals were very weak at the time of perfusion and appeared to respond very quickly to the application of pentobarbital. Often the heart had ceased to beat by the time the chest cavity was opened up and perfusion was difficult. Poor perfusion may account for the fact that some of the mutant tissue was more fragile and failed to withstand the freezing and cutting process, and also may account for the decreased quality of staining which was observed in some mutant tissue compared to WT.

In the preBötC ~80% of WT cells which expressed NK1 also expressed MeCP2 whereas only 20% of NK1 cells in the *Stop/y,cre+TM* mice expressed MeCP2. As mentioned previously, the model studied in this chapter involves a ubiquitous blockade of the MeCP2 gene by insertion of a stop cassette and Guy et al.,(2007), previously reported that Tamoxifen mediated deletion of the stop cassette was only approximately 80% effective. The exact locations of *Mecp2* reactivation are unknown and with regards to TH, almost all of the TH expressing cells in the *Stop/y,cre+TM* mice also expressed MeCP2 which suggests a greater level of reactivation in adrenergic areas compared to the preBötC.

4.4.4 *Phox2b* Expression in the RTN/pFRG

The preBötC may not be the sole mediator of respiratory rhythm generation given that bilateral lesioning of the RTN/pFRG in the newborn rat brain stem-spinal cord preparation also results in a reduction in respiratory frequency (Onimaru & Homma, 2003). As discussed previously, the RTN/pFRG is composed of a cluster of interneurons found ventral to the facial nucleus which express *Phox2b*, VGLUT2 and NK1R (Smith *et al.*, 1989; Onimaru & Homma, 2003, 2008). This area is also implicated in the chemosensitive response since RTN neurons in coronal brain slices of the adult rat brain exhibit increased firing rates with a decrease in pH (Guyenet *et al.*, 2005a). *Phox2b* mutants that have a severe depletion of *Phox2b* expressing neurons lack responsiveness to CO₂ at birth

(Dubreuil *et al.*, 2008). In chapter 3 it was shown that MeCP2 deficient mice have an altered response to hypercapnia thus it could be hypothesised that the MeCP2 deficient males in this chapter would possess a reduced number of Phox2b neurons. However due to problems with tissue staining, little data regarding Phox2b expression was gathered in this chapter and quantification was not possible thus a solid conclusion cannot be drawn regarding the effects of the absence of MeCP2 on the Phox2b expressing neurons of the RTN/pFRG.

Chapter 5: Investigation of possible lung pathology in male mouse model of RTT syndrome.

5.1 Introduction

A neuronal based deficiency in MeCP2 leads to development of the same RTT-like symptoms, such as hindlimb clasping, tremor and respiratory abnormalities, which result from a ubiquitous MeCP2 deficiency (Chen *et al.*, 2001; Guy *et al.*, 2001; Guy *et al.*, 2007), data which suggest that RTT syndrome may be a neurological based disorder. The role of MeCP2 in the whole body, however, has become of interest with MeCP2 protein being found in non-neuronal tissues such as the kidney, heart, spleen and lung tissue (Shahbazian *et al.*, 2002b). There is also evidence of reduced bone density in RTT patients (Leonard *et al.*, 1995; Haas *et al.*, 1997) and reductions in bone volume and bone formation in *Mecp2*^{-/-} mice which precede any neurological symptoms and which also worsen with age (O'Connor *et al.*, 2009). These anatomical changes highlight the role of *Mecp2* in development and maturation in tissues other than the brain.

5.1.1 Lung Pathology in RTT patients and *Mecp2* Deficient Mice

As mentioned in section 1.9.4, modulation of an appropriate level of *Mecp2* expression is important with regards to neuronal mechanisms. Both under (Samaco *et al.*, 2008) and overexpression (Collins *et al.*, 2004) of *Mecp2* has a detrimental effect on the brains of the mice studied. It seems that the same principal may apply to *Mecp2* in the periphery. Clinical studies of male human Rett patients reported that close to 75% of the patients were experienced recurrent respiratory infections such as pneumonia, otitis media, and sinusitis with 40% of males with *MECP2* duplication dying under the age of 25 as a result of the severe respiratory infections (Ramocki *et al.*, 2010). A recent study of female RTT patients found suggestions of an underlying lung pathology, with over half the patients studied presenting abnormalities in the lung such as thickening of bronchial walls and bronchiectasis, characterised by dilated, thick-walled bronchi often with increased mucus production (De Felice *et al.*, 2010). These morphological changes within the lung may contribute to the respiratory problems faced by these patients, with a thickening of bronchial tissue restricting airflow in and out of the lungs and increased mucus production interfering with the perfusion of gases in and out of alveoli.

It was noted that in the male MeCP2 deficient mice studied in chapter 3, some animals began to develop a phenotype which included rale-like breathing (rattling sounds within the chest when breathing (Foltz & Ullman-Cullere, 1999) and foaming at the mouth.

5.1.2 Difference in Murine and Human Lung Anatomy

The basic human respiratory system is composed of the trachea, bronchi and lungs (Fig 5-1). While some aspects of the respiratory system of the mouse are much like that of the human, there exist some differences in the anatomy of the lungs. For instance, humans and mice both share the 5 lobe lung structure; however humans possess 3 right lobes and 2 left whereas mice possess 4 right lobes and a single left lung. Air is transported from the external environment to the lungs via the trachea which branches into bronchi, then smaller bronchioles and eventually terminates in air sacs called alveoli within the lung. In humans, the branching of airways occurs 17-21 times between the trachea and alveoli, whereas in mice this only occurs 13-17 times (Irvin & Bates, 2003). Branching within the human lung also follows a dichotomous pattern, in which one airway branches into two smaller airways, whereas mice undergo monopodial branching where smaller airways branch off from a larger airway (Fig 5-1). Mice have a much larger surface area to volume ratio than larger mammals and as such can lose body heat much more quickly than humans. To maintain body temperature, mice have a higher mass-specific metabolic rate than humans and the need to expel the resulting levels of CO₂ causes mice to have a higher respiratory rate. As a result of this increased respiratory rate, there are differences in the anatomy of the mouse lung compared to humans. Mice possess much smaller alveoli than humans and the blood-gas barrier, composed of thin epithelial cells across which gases diffuse in and out of the alveoli, is approximately half the thickness of that of the human. The thinner blood-gas barrier allows gases to diffuse rapidly in and out of the alveoli, an important factor in an animal with such a high respiratory rate. The airway lumen of mice is also found to be larger compared to human and this is thought to minimize the resistance to airflow (Bennett & Tenney, 1982).

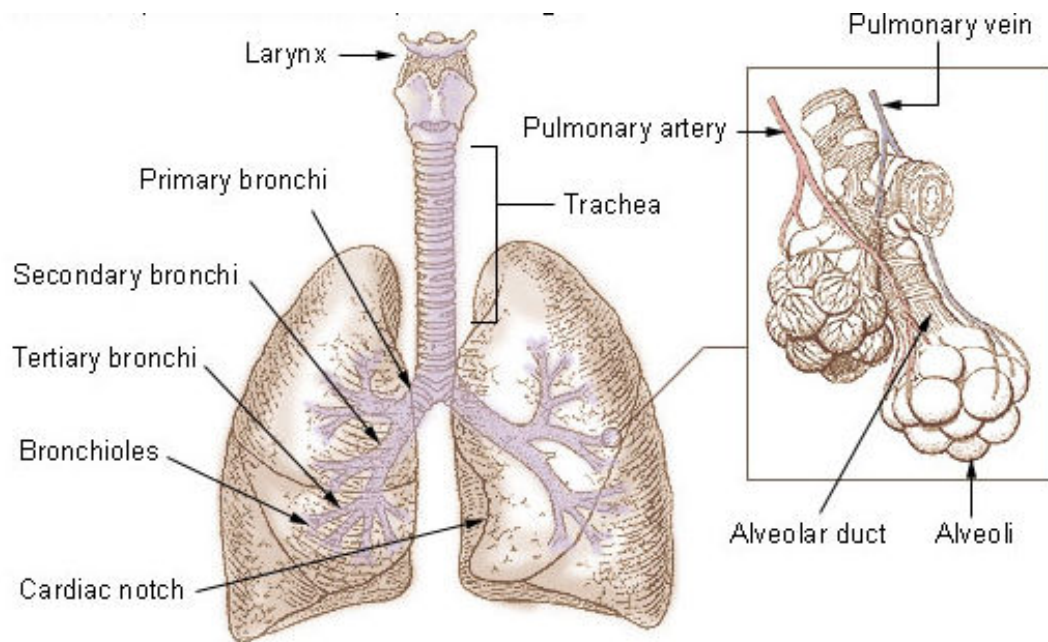
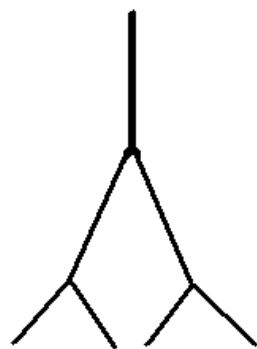


Fig 5-1 Anatomy of human trachea and lungs. Air is transported from trachea to primary bronchi, which split into smaller airways termed bronchioles. In the alveoli gases diffuse in and out of pulmonary blood vessels which surround the alveolar sacs.



Dichotomous branching



Monopodial branching

Fig 5-2 Comparison of airway branching in mouse and human lung. Branching of airways in the human lung follows a dichotomous pattern, where one airway branches into two smaller airways and so forth. In contrast, murine airways

exhibit monopodial branching where smaller airways branch off from one larger airway.

5.1.3 BDNF and the Role of Tyrosine Kinase Receptor (TrkB) in the Lung

Brain derived neurotrophic factor (BDNF) is one of the many genes targeted by MeCP2 (Chen *et al.*, 2003) and is important in neuronal survival, indicated by the fact that application of antibodies against BDNF, which serves to block BDNF intracellular signalling, reduced the survival of culture embryonic cortical neurons of rats (Ghosh *et al.*, 1994). Also, BDNF knock out mice show a reduced number of dopaminergic neurons in the nodose-pertrosal ganglion (Erickson *et al.*, 2001) indicating that this neurotrophin is key to their survival. *Bdnf* conditional KO animals, which have a deletion of BDNF in postmitotic neurons in the forebrain, part of the midbrain, and hindbrain, have some phenotypic similarities to MeCP2 deficient mice, including a smaller brain weight (Chang *et al.*, 2006b) which is also a feature of the human RTT condition (Hagberg & Hagberg, 1997). BDNF conditional KO mice also exhibit the hind limb clasping behavioural phenotype which is observed in *Mecp2* mutants (Guy *et al.*, 2001). These data indicate that a lack of MeCP2 may result in BDNF deficits which are key in the development of the RTT phenotype and indeed it has been shown that BDNF levels are reduced in the brains of MeCP2 deficient mice (Abuhatzira *et al.*, 2007). It is shown that overexpression of BDNF in the MeCP2 deficient mouse brain leads to an increased life span, and gain in locomotor function (Chang *et al.*, 2006b), again highlighting the role of BDNF in the progression of the RTT like phenotype in MeCP2 deficient mice.

MeCP2 is thought to be a transcriptional repressor of BDNF (Chen *et al.*, 2003) in the absence of neuronal activity. Membrane depolarisation, as a result of neuronal activity, results in the release of MeCP2 from BDNF and an activity-dependent upregulation of BDNF occurs. It is noted; however, that upregulation of BDNF in response to neuronal activity is not affected by *Mecp2* deletion. One may expect to see an increased level of BDNF expression in MeCP2 deficient mice, since the repressive action of MeCP2 upon BDNF has been removed. But the decrease in BDNF levels in the brains of RTT patients and mice may be due to the fact that cortical activity is reduced in the RTT brain (Dani *et al.*, 2005).

Indeed, treatment of *Mecp2*-null mice with an ampakine drug, which increases neuronal activity by facilitating AMPA receptor activation, leads to increased BDNF levels in nodose cranial sensory ganglia which are important in the control of cardiorespiratory systems (Ogier *et al.*, 2007). Treatment of *Mecp2*-null mice with ampakines, which mimics increased neuronal activity, also restores normal minute ventilation and respiratory frequency, indicating that BDNF deficits may a) develop as a result of reduced neuronal activity in RTT brains and b) play a key role in the development of the RTT respiratory phenotype in *Mecp2*-null mice.

BDNF is a signalling molecule for the tyrosine kinase B receptor (TrkB). TrkB mRNA is found in adult human lung tissue (Yamamoto *et al.*, 1996; Ricci *et al.*, 2004) and studies so far suggest that in the human lung, both the full length and truncated isoforms of the TrkB receptor are expressed (Ricci *et al.*, 2004) whereas only the truncated form is observed in the lungs of mice (Hikawa *et al.*, 2002). TrkB receptors are thought to play an important role in the developing mouse lung due to the finding that 15 day old *TrkB* *-/-* mice, which express a non functional form of TrkB, exhibit a thinner bronchial epithelium, larger air spaces and thinner blood vessel walls than WT (Garcia-Suarez *et al.*, 2009). The same study also found that TrkB is expressed by type 2 pneumocytes, cells which are important in the production of surfactant within the lung. TrkB may aid the maintenance of this particular cell type as there are some subtle differences in the morphology of the type 2 pneumocytes of the *TrkB* *-/-* animals compared with the WT.

Microarray analysis of MeCP2 in the brains of MeCP2 deficient mice and male and female RTT patients reveals an overexpression of *NTRK2*, the gene which encodes for the TrkB receptor (Abuhatzira *et al.*, 2007). The authors propose that over expression of the receptor may be a mechanism to compensate for the reduced levels of signalling molecule, BDNF. MeCP2 binds only to methylated CpG sites in order to repress or activate genes (Nan *et al.*, 1998; Abuhatzira *et al.*, 2007) and the promoter of *NTRK2* (gene coding for TrkB) is not methylated. Therefore, the increase in TrkB expression is unlikely to be a direct result of the absence of MeCP2. It is observed that the *NTRK2* promoter in MeCP2 deficient mice brains show changes in the methylation and acetylation of various histones

compare to WT which results in the chromatin being in a more open state in the MeCP2 deficient mice which may account for increased *NTRK2* gene expression (Abuhatzira *et al.*, 2007). The mechanism by which this over expression and upregulation of TrkB receptors occurs is yet unknown.

One aim of this chapter was to investigate whether MeCP2 deficient mice had developed lung pathology. This was achieved by processing the tissue of WT, *Stop/y,cre* and *Stop/y* tissue from chapter 3 with various histological stains and investigating whether there was a change in the thickness of the respiratory epithelium, thickness of the interalveolar septum and the thickness of elastin surrounding the airways. Since BDNF is a ligand of the TrkB receptor and BDNF levels are reduced in MeCP2 deficient mice (Chang *et al.*, 2006b) it was also hypothesised in this chapter that an up regulation of TrkB receptors may occur within the lung to compensate for the lack of BDNF. *TrkB* *-/-* mice exhibit a thinner bronchial epithelium and larger air spaces, whereas preliminary staining of lung tissue from MeCP2 deficient mice of chapter 3 showed signs of an increase in the thickness of the respiratory epithelium. Given that *NTRK2* expression, the gene which encodes the TrkB receptor, is found to be increased in the brains of MeCP2 deficient mice, then perhaps the MeCP2 deficient mice studied in chapter 3 may undergo over expression of TrkB in the lung to compensate for a lack of BDNF. There are other neurotrophic factors which can signal the TrkB receptor, such as NT-4, and thus it could be hypothesised that increased TrkB expression and signalling of this receptor by neurotrophins other than BDNF could lead to a thickening of the bronchial epithelium and consolidation of the lung tissue in the MeCP2 deficient mice studied in this chapter. Therefore another aim of the investigation was to use immunocytochemistry to observe whether or not there was an upregulation of TrkB expression in MeCP2 deficient lung tissue compared to WT.

5.2 Methods

5.2.1 Animals

All experimental procedures were carried out under license from the UK Home Office and were subject to the Animals (Scientific Procedures) Act, 1986. The lungs of one *Stop/y* animal, in which rale-like breathing and foaming at the

mouth was apparent, and one WT animal were removed and paraffin embedded as described in chapter 2 (section 2.6.2). This tissue was then used for preliminary staining to observe whether or not the mutant animal presented lung pathology. The tissue from these *Stop/y* and WT animals was not included in the more in depth analysis. Upon confirmation of lung pathology, the lungs of WT (n=5), *Stop/y,cre-TM* (n=3), *Stop/y,cre+TM* (n=2) and *Stop/y* (n=5) animals were also paraffin embedded and processed using various histological stains as discussed below.

5.2.2 Histology

Using a microtome, two 5µm coronal sections were cut from anterior surface of the lungs and a further two sections were cut from approximately 450µm deep into the tissue to give a representation of the entire organ. Protocols for all the following stains can be found in chapter 2 (section 2.10). Assistance in cutting and staining of male lung tissue given by Denise Padgett (University of Strathclyde, UK) and David Russell (University of Glasgow, UK).

5.2.2.1 Haematoxylin & Eosin (H&E)

Only the four lung sections that were cut from the *Stop/y* and WT animals for preliminary investigation were stained with haematoxylin and eosin (H&E; see section 2.10.2) to reveal the basic morphology of the lung tissue. The haematoxylin component stains nuclei blue while the counter-stain eosin stains cytoplasm red/pink and red blood cells an intense red colour.

5.2.2.2 Masson's Trichrome

The four lung sections that were cut from the *Stop/y* and WT for preliminary investigation were stained with Masson's trichrome (see section 2.10.5) to reveal connective tissues. This stain renders collagen blue, the nuclei black, cytoplasm as pink and any red blood cells in bright red. Following this preliminary staining, four 5µm lung sections were then cut from further *Stop/y*, *Stop/y,cre-TM*, *Stop/y,cre+TM* and WT animals and stained with Masson's for quantification purposes.

5.2.2.3 Periodic Acid, Schiff's/Haematoxylin & Aurantia (PAS)

Only the four 5µm lung sections from the *Stop/y* and WT animal, processed for initial assessment of lung pathology were stained with PAS (section 2.10.6). PAS is used to identify the presence of polysaccharides and glycogen. Mucin, glycogen and occasionally some basement membranes appear as a red/magenta stain.

5.2.2.4 Millers's Elastin

Miller's elastin stain was not included in the preliminary staining of the *Stop/y* and WT animal but was later considered to be important for quantifying the elastin deposits surrounding the airways in the lung tissue (see section 2.10.3). Four 5µm lung sections from WT, *Stop/y*, *Stop/y,cre-TM* and *Stop/y,cre+TM* lungs were stained with Miller's elastin to highlight the elastin fibres within the lung. Elastin fibres are rendered purple/black; collagen is a deep red, while cytoplasm, muscle, fibrin and red blood cells are stained yellow.

5.2.3 Immunocytochemistry

Immunocytochemistry was used to highlight MeCP2 and TrkB expression within the lung as described in chapter 2 (section 2.9).

5.2.3.1 MeCP2 and TrkB Staining.

Four 5µm lung sections from WT, *Stop/y*, *Stop/y,cre-TM* and *Stop/y,cre+TM* lungs were stained using mouse anti-MeCP2 (1:200, Sigma, UK) and rabbit-anti TrkB (1:50, Insight, UK) primary antibodies and rhodamine donkey anti-mouse (1:100; Invitrogen, UK) and alexa 488 donkey anti-rabbit (1:500, Stratech-Jackson Immunoresearch, UK). Sections were mounted using Vectashield hard set mounting medium.

5.2.3.2 TrkB DAB Staining

TrkB immunofluorescent staining was too weak to allow comparisons to be drawn between TrkB expression across the genotypes. Thus the DAB method was utilised to highlight TrkB expression within the lungs of the WT, *Stop/y*, *Stop/y,cre-TM* and *Stop/y,cre+TM* animals as described in chapter 2 (see section

2.10.1). As mentioned previously, there exist two forms of the TrkB receptor and the antibody applied in this chapter, rabbit anti-TrkB (1:50; Insight biotechnology), recognised both isoforms of the TrkB receptor. The DAB method of staining involves targeting receptors of interest with a primary antibody which is subsequently targeted by a labelled secondary antibody, as in immunofluorescence. The difference lies in that the secondary antibody in the DAB reaction is conjugated with a peroxidase enzyme rather than a fluorophore. The peroxidase enzyme binds DAB as a substrate and oxidizes it to produce an observable brown color.

5.2.4 Imaging

Lung sections were imaged using an epifluorescent microscope (Axioskop MRC Zeiss microscope using AxioCam camera) and images collected using Axiovision software (AxioVs40 V 4.8.2.0, Zeiss Microscopy) as described in chapter 2 (section 2.10.6).

5.2.4.1 Measurements of the Respiratory Epithelial Lining

All measurements of the images obtained from the epifluorescent microscope were performed using Axiovision software (AxioVs40 V 4.8.2.0, Zeiss Microscopy). The thickness of the respiratory epithelial lining was measured from the basal lamina to the apex of the cell as measured by a straight line (Fig 5-3). Two epithelial cells per image were chosen at random and the average thickness of the respiratory epithelium measured. The average thickness of the epithelium was then calculated for each area (e.g. top left, top right of the lung), for each section (section 1 on slide, section 2 on slide), for each region (ventral surface or anterior) and for the whole lung (explained in Fig 5-4). The data presented represents the average value for the whole lung.

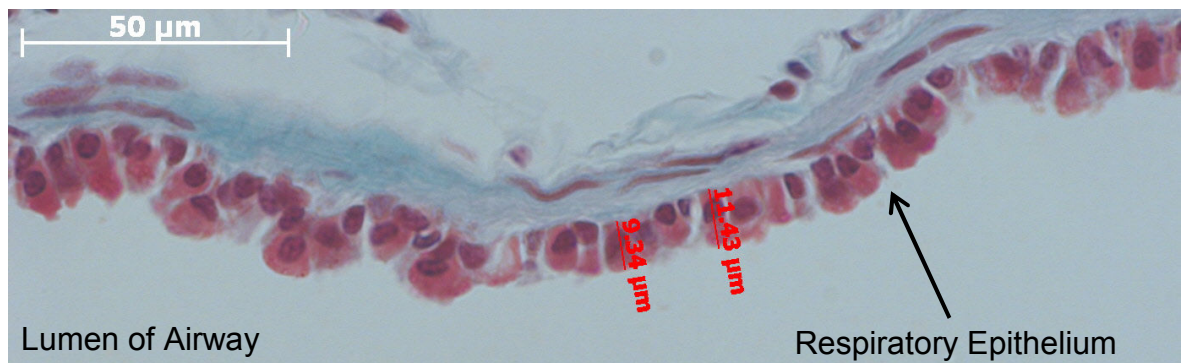
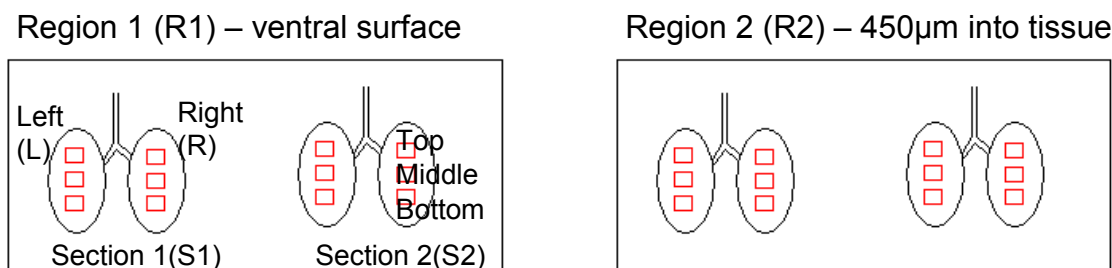


Fig 5-3 Illustration of the measurement of bronchial epithelium of WT mouse. Light microscopy image of respiratory epithelium stained with Masson's trichrome. Measurements were taken from the basal lamina to the apex of the cell as measured by a straight line. Two representative measures are indicated by the red lines. Scale bar = 50 μm.

5.2.4.2 Measuring the Alveolar Septum Thickness

Two measurements of the thickness of the tissue separating adjacent alveoli (the interalveolar septum) were made in each image, the criteria being that the septum measured must separate two whole and complete alveoli. Measurements were made at the thinnest point of the septum and measured by a straight line as illustrated in Fig 5-5. Data was collected as described in Fig 5-4.



Brain No.	Area	Top of lung	Top of lung	Mid Lung	Mid Lung	Bottom Lung	Bottom Lung	Average (side)	Average (Section)	Average (Region)	Whole Lung Average
577	R1S1 L	4.97	5.20	5.43	5.82	4.28	3.65	4.89			
	R1S1 R	4.98	3.21	4.23	3.27	5.08	3.90	4.11	4.50		
	R1S2 L	6.16	3.35	3.4	5.56	3.51	4.6	4.43			
	R1S2 R	3.62	4.63	4.28	4.76	2.63	6.98	4.48	4.46	4.48	
	R2S1 L	4.27	3.48	5.88	4.13	4.86	5.61	4.71			
	R2S1 R	2.58	3.62	4.83	4.61	7.59	5.40	4.77	4.74		
	R2S2 L	4.93	4.94	3.97	4.51	4.62	3.9	4.61			
	R2S2 R	5.26	6.67	5.97	7.00	5.32	5.90	6.02	5.32	5.03	4.75

Fig 5-4 Illustration of data collection from images taken within the lung tissue for measurement of alveolar septum thickness, respiratory epithelium thickness and thickness of elastic fibres surrounding the airways. Images at top of panel illustrate the locations of image capture. Images were taken from top, middle and bottom areas of both the left and right lobes of the lung. The table indicates how data was subsequently collected from the images. For example, area R1S1L indicates that measurements were made in region 1 (R1) in the first section on the slide (S1) in the left lobe (L). Heading in the table “Top of lung” indicates that the value presented was recorded from an image taken from top of the lung. Values were recorded in μm .

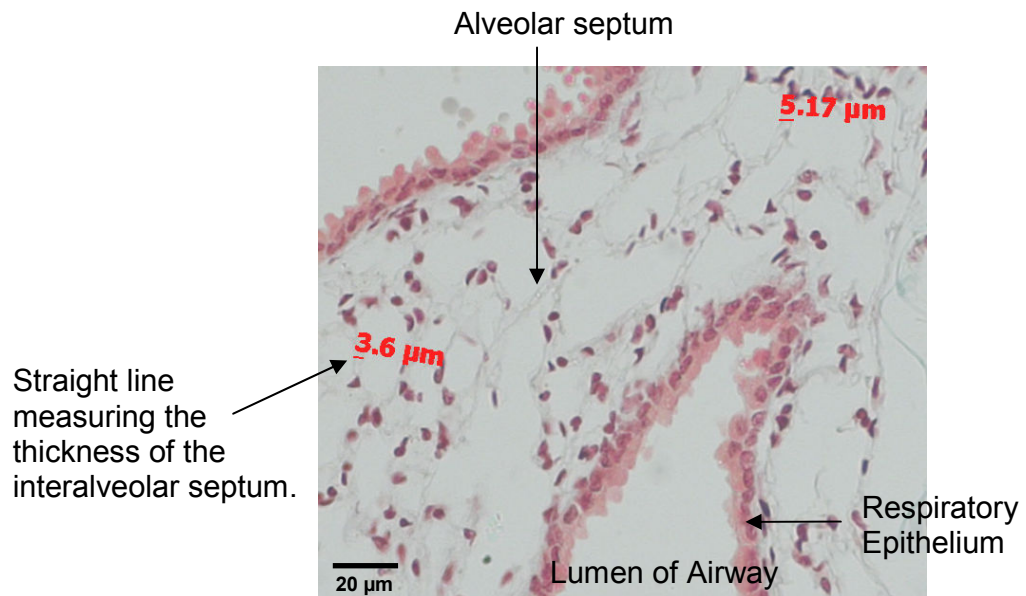


Fig 5-5 Illustration of the measurement of alveolar septum thickness. Light microscope image of lung tissue of WT animal stained with haematoxylin and eosin. Cytoplasm highlighted in pink, nuclei purple. Tissue separating two adjacent, whole alveoli was measured by a straight line at its thinnest point. Scale bar = 20μm.

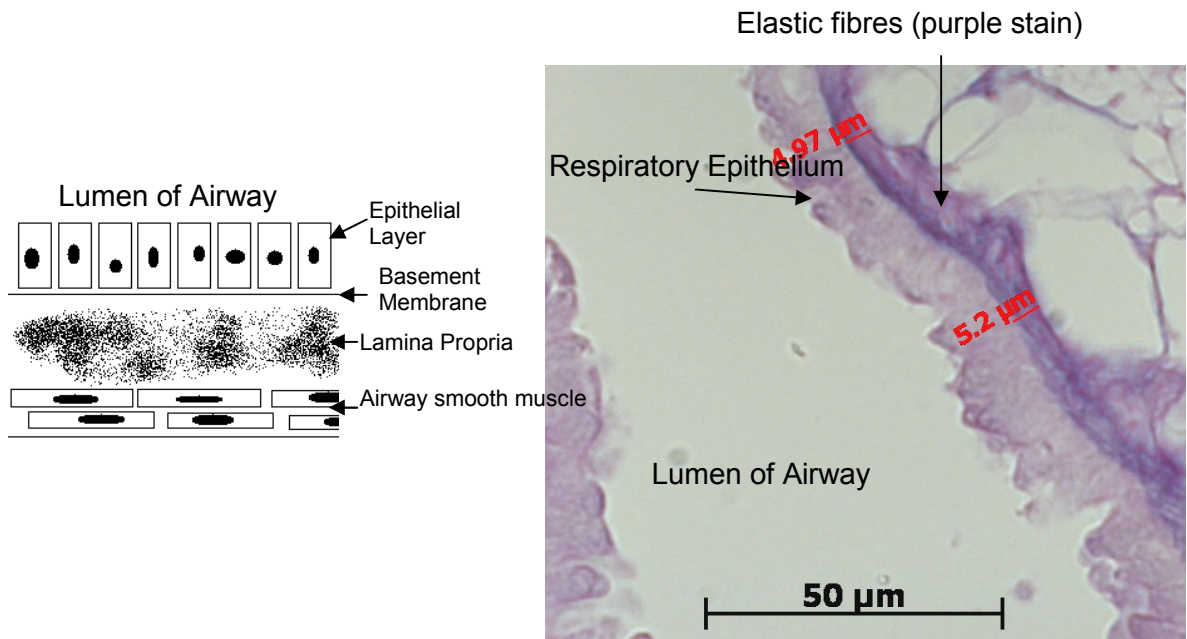


Fig 5-6 Illustration of the measurement of the elastic fibres surrounding airways. Light microscope image of WT tissue stained with Miller's elastin. Measurements of the thickness of the elastic fibres were made from the basement membrane of the epithelial layer of the airway to the outer edge of the airway smooth muscle as measured by a straight line. Scale bar = 50 µm.

5.2.4.3 Measuring Thickness of Elastic Fibres Surrounding Airways

Two measurements of the thickness of the elastic fibres surrounding the airways were made in each image. Measurements were made from the basement membrane of the epithelial layer of the airway to the outer edge of the airway smooth muscle as measured by a straight line (Fig 5-6)

5.2.5 Statistics

All statistics were performed using GraphPad Prism 4 software. Parametric statistics were performed using one way ANOVA with genotype as a factor. In cases where only 2 genotypes were to be compared an unpaired t-test was performed. Differences were regarded as significant if $p < 0.05$.

5.3 Results

5.3.1 Preliminary Histological Staining

As mentioned in the methods above, preliminary staining was carried out on a WT (n=1) and a *Stop/y* (n=1) animal, with the *Stop/y* animal noted as presenting rale-like breathing (rattling within the chest). Haemotoxylin and Eosin (H&E) was used to investigate the morphology of the lungs (Fig 5-7).

The WT presented evenly distributed alveoli and the lumen of the airways were clear. Compared to WT, the *Stop/y* animal presented abnormal lung morphology. There was an apparent thickening of the tissue in the parenchyma compared to WT, with a thickening of the interalveolar tissue resulting a less even spread of alveoli and a reduced number of air spaces. Also, the respiratory epithelium which lines the airways appeared to be thicker in the *Stop/y* lung than WT and some bronchioles of the mutant tissue were filled with an unidentified substance (Fig 5-7).

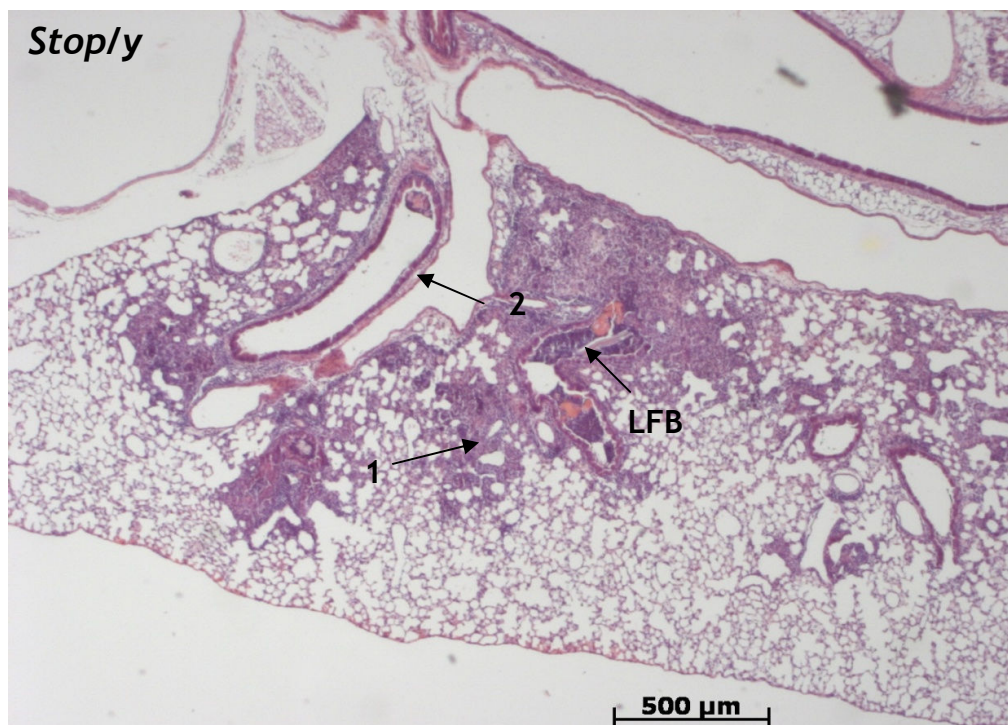
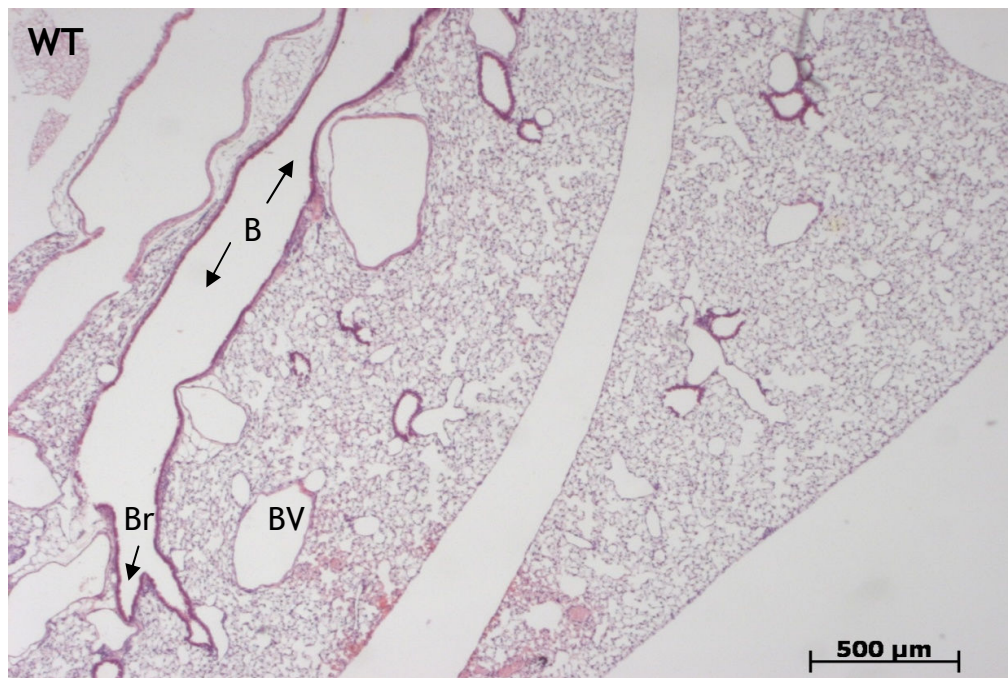


Fig 5-7 Light microscope image of H&E staining of WT and *Stop/y* lung tissue. B – Bronchus, BV- blood vessel, Br – Bronchiole, LFB – Liquid filled bronchiole. Nuclei and ER stain blue, cytoplasm and collagen stains pink and red blood cells are stained orange/red. There was an apparent change in alveolar structure in the *Stop/y* animal, with a thickening of the interalveolar septum (arrow 1) in parts of the lung (indicated by black arrow) and a thickening of bronchial epithelium (Arrow 2). One bronchiole also appeared to be filled with an unknown substance.

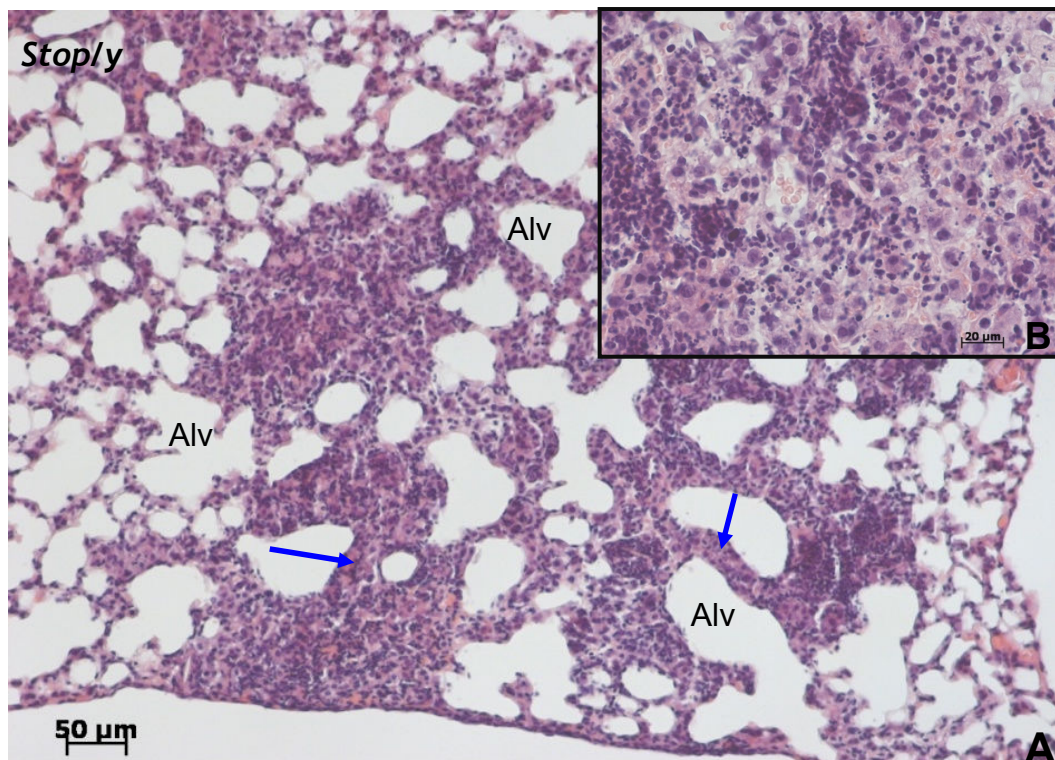


Fig 5-8 High power magnification light microscopy images of H&E stained *Stop/y* tissue. **A-** Blue arrows indicate areas of thickening of the interalveolar septum. Alv = alveolar spaces. **B** – high powered magnification of same lung section illustrating fibrosis-like areas of the lung. These areas appeared to be characterised by infiltration of, as yet, unidentified cells. Sale bar; main panel = 50µm, insert = 20 µm.

Higher magnification images of H&E stained *Stop/y* lung tissue (Fig 5-8) revealed an area of fibrosis-like tissue in the lung of the *Stop/y* animal, with a clear thickening of the interalveolar septum compared to the WT. These areas of fibrosis-like tissue appeared to be characterised by a large number of unidentified cell types. These images indicated that a fibrosis-like pathology may be present and as such staining with Masson’s Trichrome stain was utilised to highlight connective tissues and collagen. As can be seen in Fig 5-9, tissue from the WT lung revealed evenly distributed alveoli and collagen surrounding the airways and blood vessels. Tissue from the *Stop/y* animal revealed increased amounts of collagen compared to the WT in the lung parenchyma, with green staining prevalent in the areas of fibrosis-like tissue growth. Green staining was also more prevalent surrounding the airways and blood vessels of the *Stop/y* compared to WT which indicates an increased production of collagen and connective tissue.

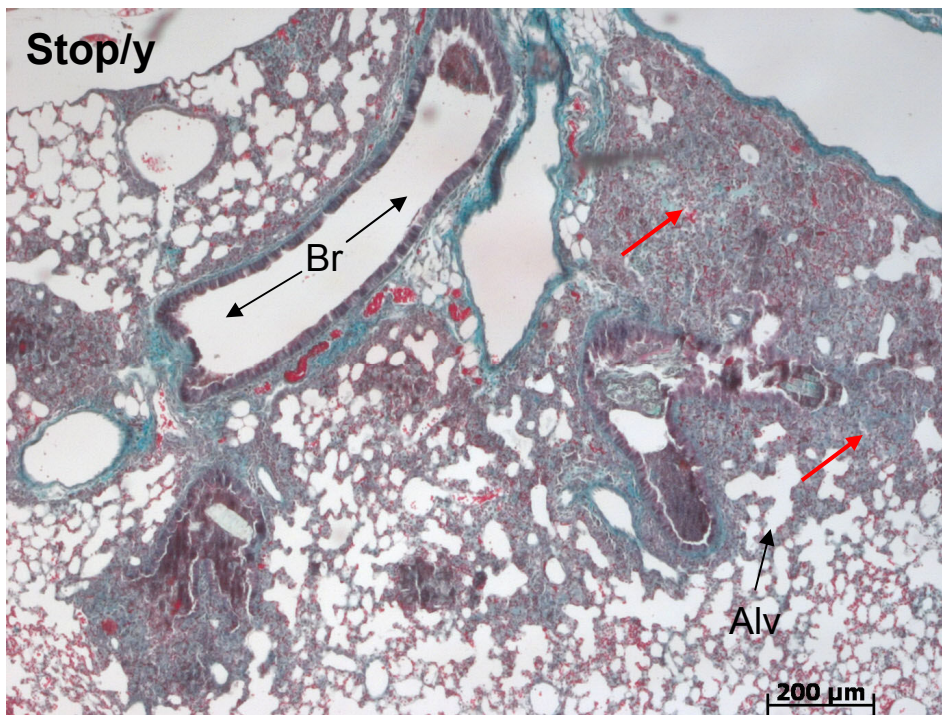
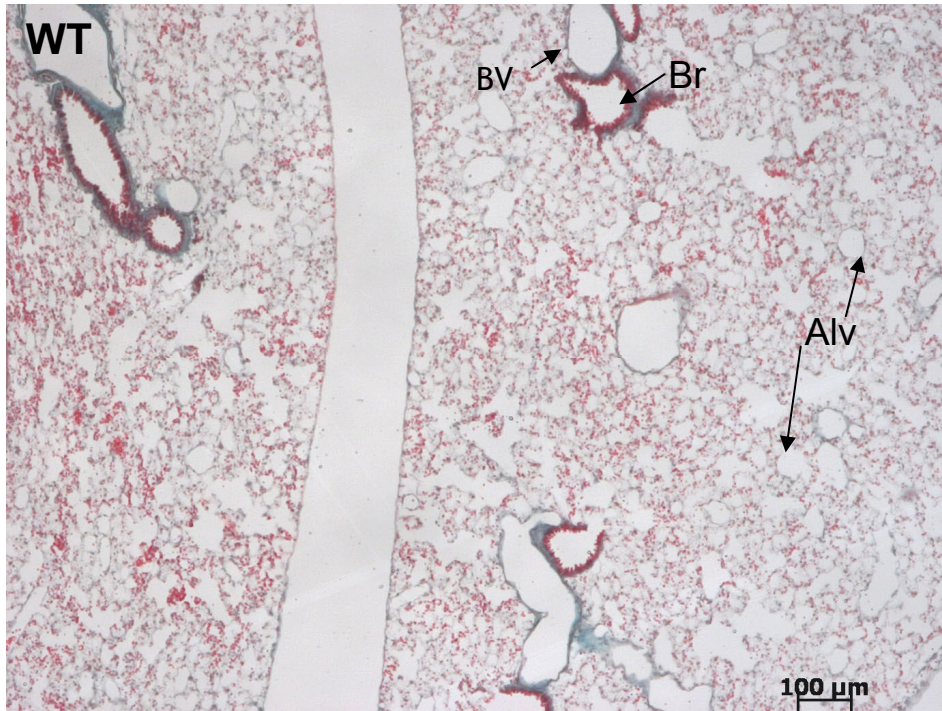


Fig 5-9 Masson's trichrome staining of WT and *Stop/y* lung tissue. Alv – alveoli, BR – bronchiole, BV – blood vessel. Nucleus stains black, cytoplasm stains red/pink, red blood cells stain bright red and collagen stains blue/green. There were increased collagen deposits (cyan) in the *Stop/y* lung compared with WT. The change in alveolar structure and thickening of the alveolar wall is also clearly illustrated (red arrows). Scale bar top panel = 100 μ m, lower panel = 200 μ m.

As mentioned, some animals exhibited difficulty in breathing characterised by a rattling within the chest and foaming at the mouth, suggesting that over production of surfactant may be occurring. PAS was therefore applied to observe whether there was evidence of excess surfactant or mucin within the alveoli.

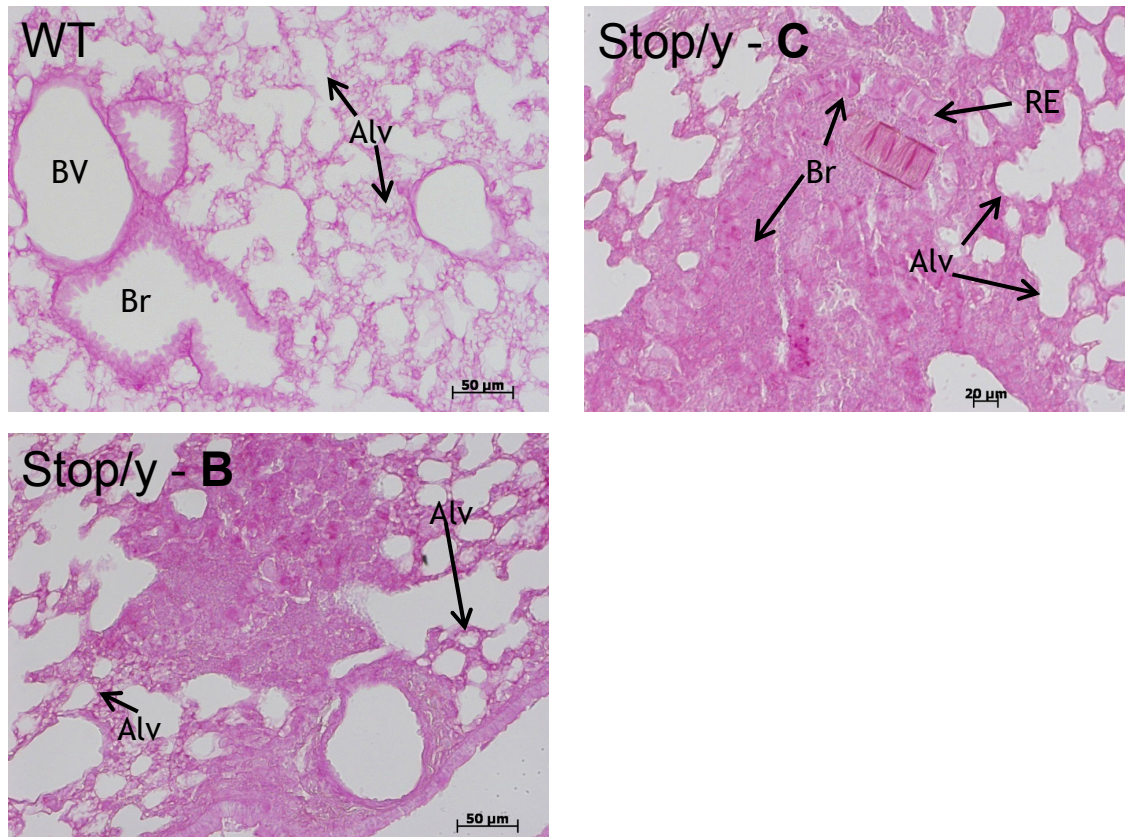


Fig 5-10 Light microscope image of Periodic acid-schiff stain (PAS) staining of WT and *Stop/y* lung tissue. Alv – alveoli, BV – blood vessel, Br – bronchiole, RE – respiratory epithelium. **B** - Large areas of positive pink staining within alveoli of *stop/y* animal indicated presence of glycoproteins and mucin. **C** - pink staining filled lumen of bronchiole. Scale bar; WT = 50 μ m, *Stop/y* **B** = 50 μ m, *Stop/y* **C** = 20 μ m.

PAS staining (Fig 5-10) of WT tissue showed positive pink staining within the epithelial layer of the airways and within the alveoli indicating the presence of glycoproteins and surfactant within the lung. In *Stop/y* tissue there were large areas of positive pink staining within alveoli and the airways of the *Stop/y* animal compared to the WT, indicative of the presence of excess amounts of mucin or glycoproteins. This may suggest an over production of surfactant which may account for the foaming at the mouth that was observed in this *Stop/y*

animal. Since preliminary stains revealed definite morphological changes in the lung of the *Stop/y* mouse compared to WT, further staining was performed to quantify various aspects of the morphology of the lung of WT (n=5), *Stop/y,cre+TM* (n=2), *Stop/y,cre-TM* (n=3) and *Stop/y* (n=5).

5.3.2 Measuring Various Morphological Aspects of the Lung

By comparing images from mutant and WT tissue, it was apparent that some *Stop/y,cre-TM* mice illustrated a thickening of the bronchial epithelium (Fig 5-10). There was also a thickening of the interalveolar septum and increased amount of collagen as highlighted by the greater proportions of Masson's trichrome green staining in the *Stop/y,cre-TM* animals compared to WT. *Stop/y,cre+TM* mice illustrated increased deposits of collagen and, in some animals, a thickening of the bronchial epithelium compared to WT. *Stop/y* mice also exhibited a thicker epithelial lining in the bronchi compared to WT and some thicker collagen deposits surrounding the airways. It should be noted that not all of the MeCP2 deficient mice studied presented the same severity of lung pathology, reflected in the data shown in Fig 5-11.

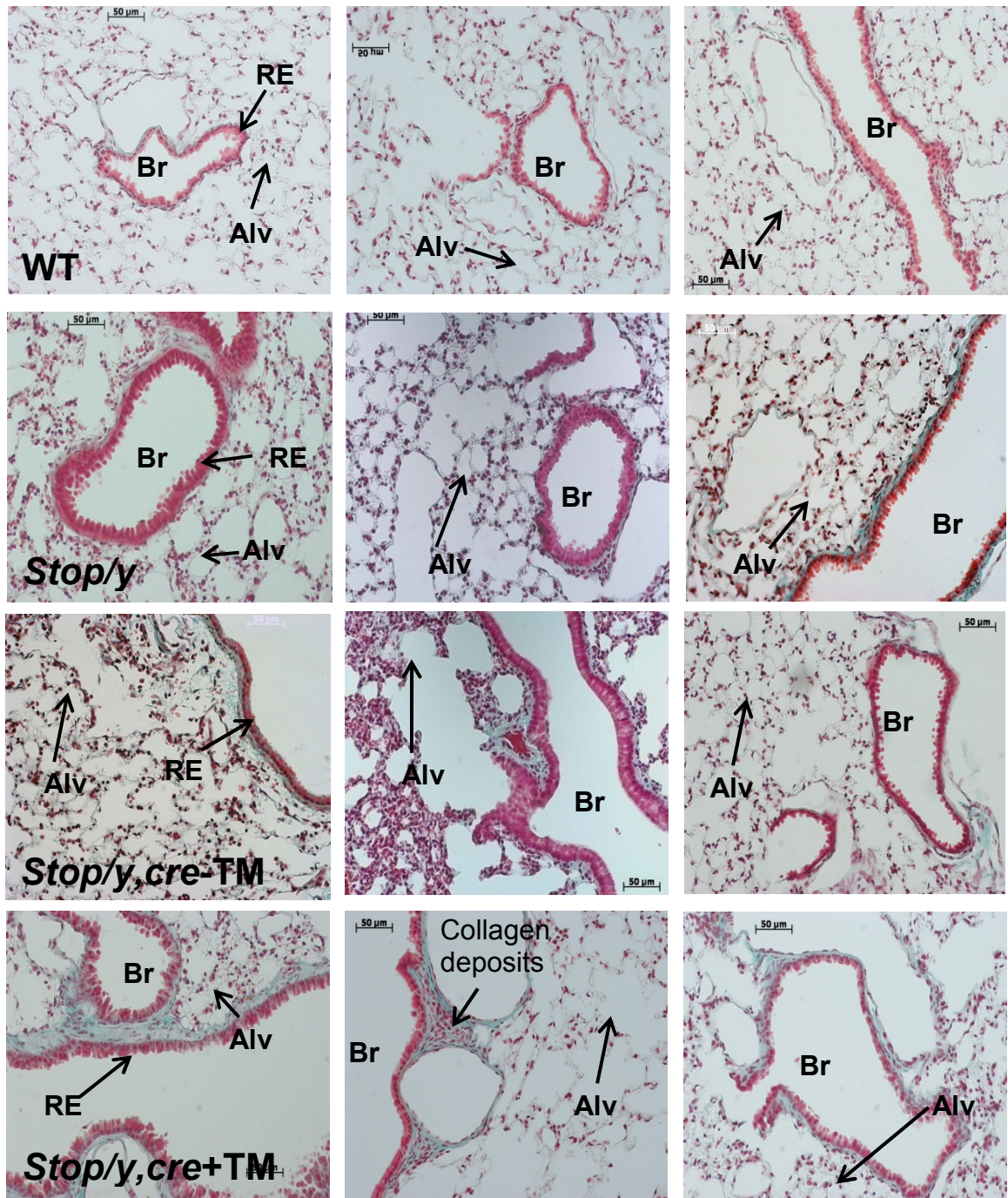


Fig 5-11 Light microscopy images of Masson's trichrome staining in WT, *Stop/y*, *Stop/y,cre-TM*, *Stop/y,cre+TM* and animals. Br – bronchioles, Alv – alveoli, RE – respiratory epithelium. Each image is representative of a different animal. Not all mutants presented the same severity of lung pathology. Some MeCP2 deficient mice exhibited thickening of the respiratory epithelium compared to WT and also an increase in the thickness of the interalveolar septum. Scale bar = 50μm.

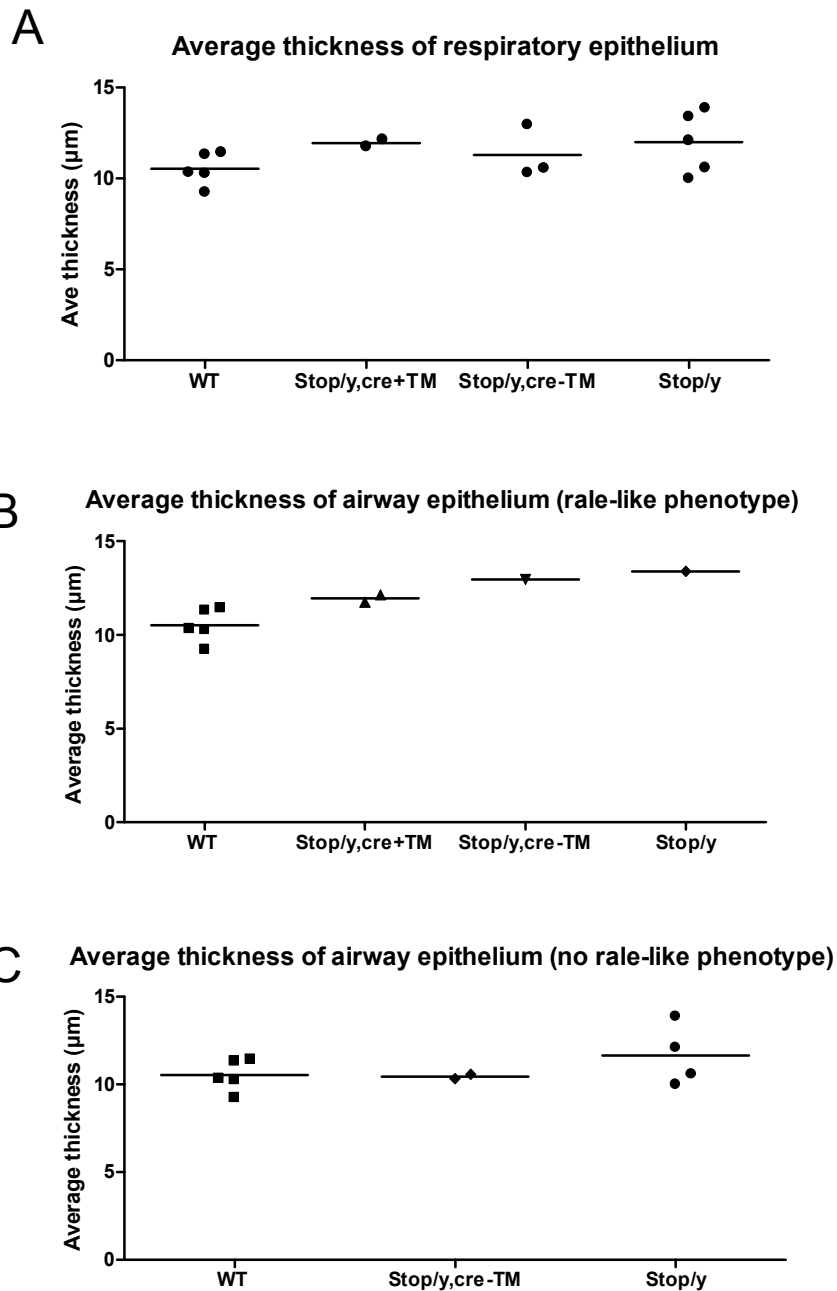


Fig 5-12 Plots to show the average thickness of the epithelial lining of the airways in WT, *Stop/y,cre+TM*, *Stop/y,cre-TM* and *Stop/y* animals. **A** – Plot comparing the thickness of the respiratory epithelium of all animals. There was no significant difference between the genotypes. **B** - Plot comparing only the MeCP2 deficient mice which presented rale-like symptoms with the WT. There was a trend towards an increase in the thickness of the respiratory epithelium of MeCP2 deficient mice. **C** - Plot to compare the thickness of respiratory epithelium of only the MeCP2 deficient mice that did not present the observable respiratory phenotype. The thickness of the epithelium was comparable between WT and the MeCP2 deficient mice.

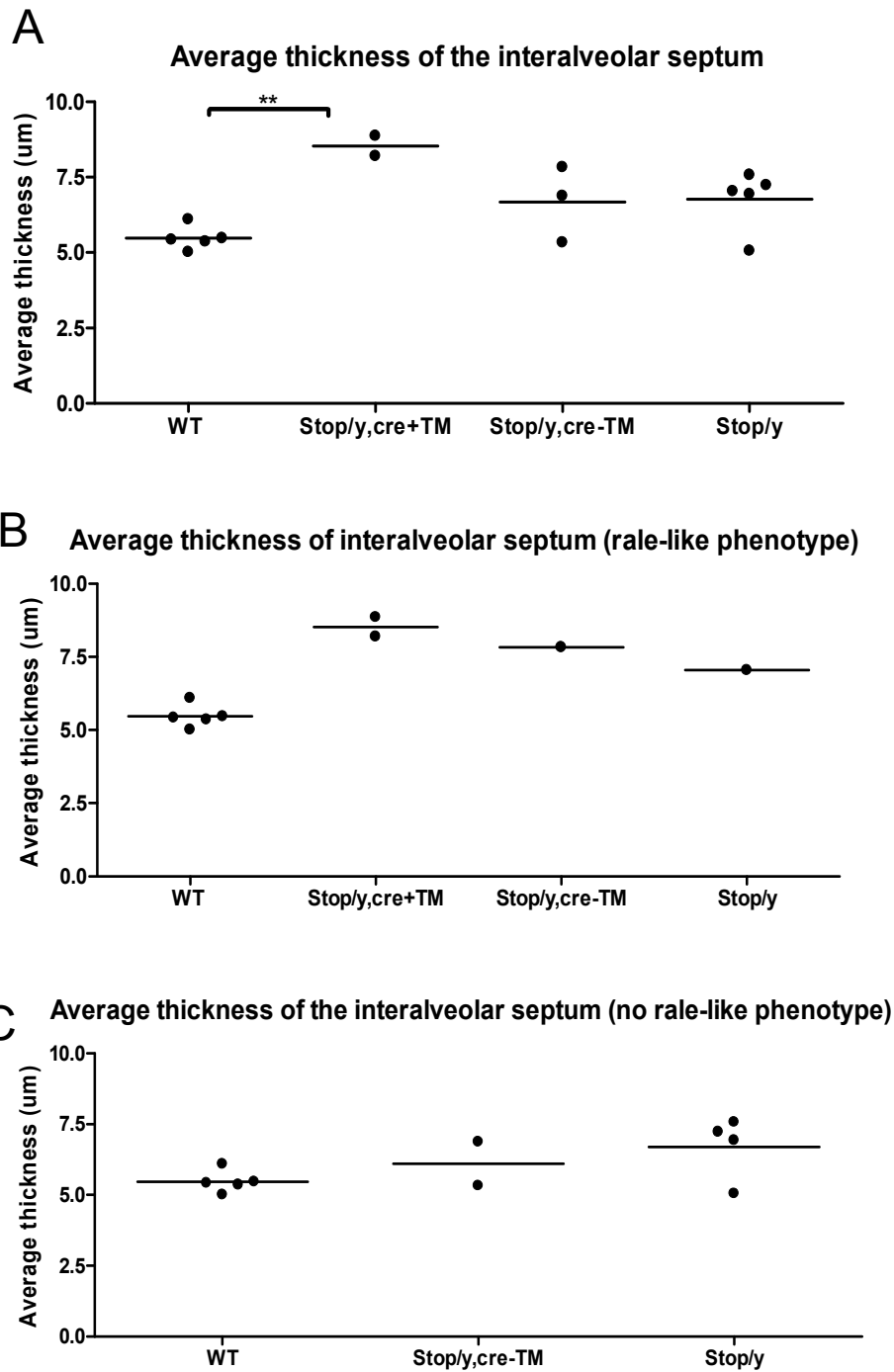


Fig 5-13 Plot to illustrate the average thickness of the interalveolar septum in WT, *Stop/y,cre+TM*, *Stop/y,cre-TM* and *Stop/y* animals. **A** – Plot comparing thickness of the interalveolar septum. *Stop/y,cre+TM* mice had significantly thicker interalveolar septum compared to WT (one way anova; ** $p < 0.05$). **B** – Plot comparing thickness of the interalveolar septum of WT vs mutant mice with rale-like breathing. Mutants showed a trend towards an increased septum thickness compared to WT. **C** – Plot comparing WT vs mutants that did not present rale-like breathing. Mutants had a tendency towards an increase in interalveolar septum thickness.

Measurement and quantification of the epithelial thickness revealed no significant difference between the WT and mutant animals (Fig 5-12 plot A). However, as previously mentioned a few mutant mice (*Stop/y,cre+TM* n=2, *Stop/y,cre-TM* n=1 and *Stop/y* n=1) presented a more severe respiratory phenotype than others. Thus data were plotted to compare the epithelial thickness of mutants who presented rale-like breathing and foaming at the mouth with WT animals (Fig 5-12 plot B). While this reduced n numbers to a level where statistical analysis could not be performed, it can be noted that all MeCP2 deficient mice that exhibited rattling within the chest and foaming at the mouth tended to have a thicker bronchial epithelium compared to the WT (WT: 10.53 ± 0.9 μm , *Stop/y,cre +TM*: 11.95 μm , *Stop/y,cre-TM*: 12.97 μm , *stop/y*: 13.40 μm). *Stop/y,cre+TM* animals showed a trend towards a thinner epithelial layer than *Stop/y* and *Stop/y,cre-TM* mice (Fig 5-12 plot B). Comparing data from *Stop/y* and *Stop/y,cre-TM* animals that did not present the rale-like phenotype with the WT revealed no significant difference in the average thickness of the epithelial lining, with only the *stop/y* animals showing a trend towards an increased thickness (Fig 5-12 plot C).

The images in Fig 5-11 illustrate that some mutant mice had a thickened interalveolar septum compared to WT and analysis of these images revealed that *Stop/y,cre+TM* animals had a significantly thicker inter alveolar septum compared to WT (Fig 5-13; *Stop/y,cre+TM*: 8.53 ± 0.47 μm , WT: 5.47 ± 0.39 μm , $p < 0.05$). There was no significant difference in the thickness of the interalveolar septum of WT, *Stop/y,cre-TM* and *Stop/y* mice (Fig 5-13 plot A; WT: 5.472 ± 0.35301 , *Stop/y,cre+TM*: 8.53 ± 0.33 , *Stop/y,cre-TM*: 6.68 ± 1.03 , *Stop/y*: 6.76 ± 0.88 μm). When comparing only the mutant animals which presented the most severe breathing phenotype (rale-like breathing and foaming at the mouth) with the WT it was observed that mutants showed a trend towards a thicker interalveolar septum compared to WT (WT: 5.5 ± 0.39 μm , *Stop/y,cre+TM*: 8.53 ± 0.46 μm , *Stop/y,cre-TM*: 7.83 μm , *Stop/y*: 7.04 μm). There was no significant difference in the thickness of the alveolar septum of WT and *Stop/y* animals that did not exhibit rale-like symptoms (Fig 5-13 plot C).

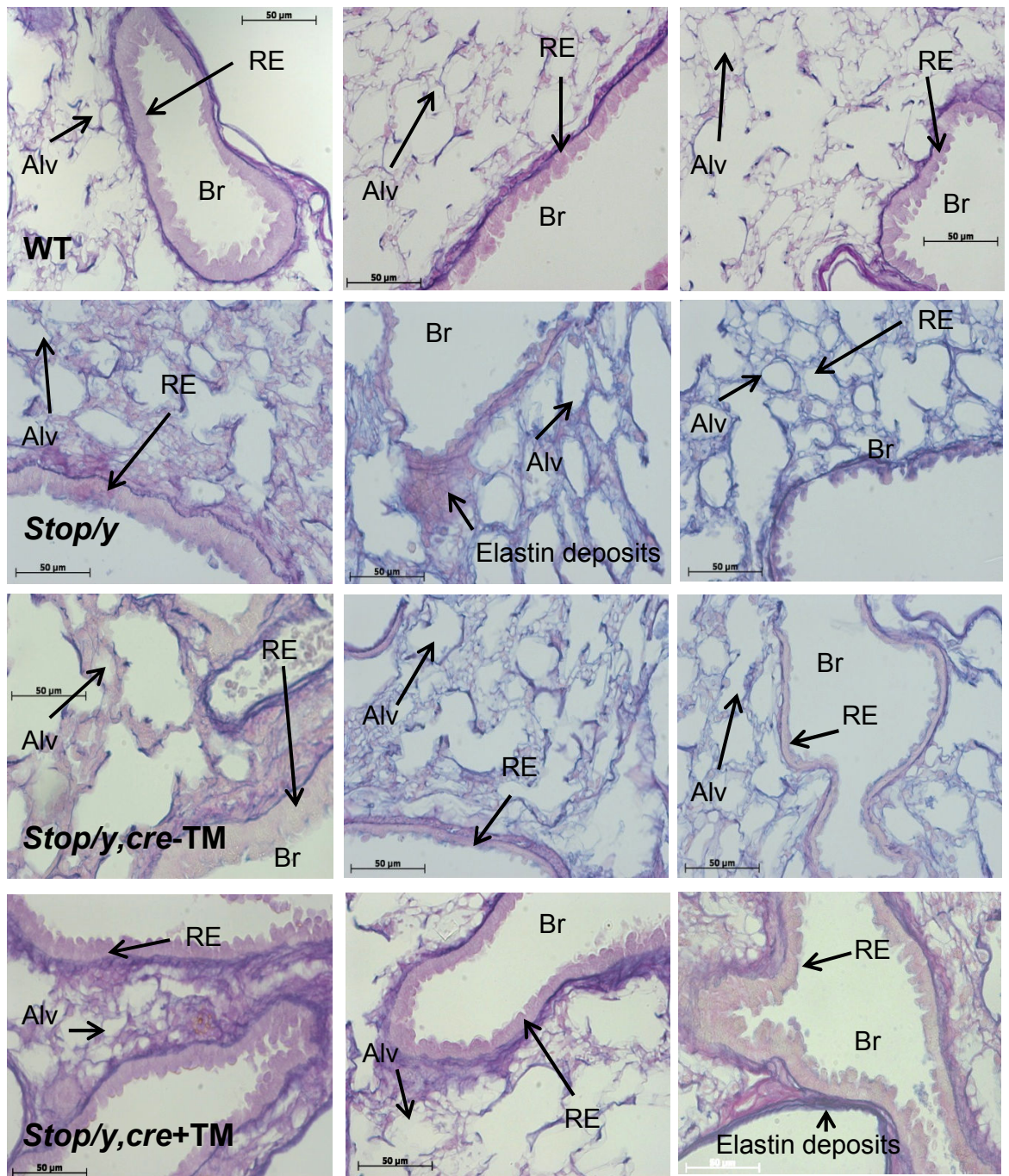


Fig 5-14 Plot to show the average thickness of the elastin surrounding airways in WT, *Stop/y*, *Stop/y,cre-TM* and *Stop/y,cre+TM*, and animals . Br – bronchioles, Alv –alveolar, RE – respiratory epithelium. Each image is representative of a different animal. Not all of the mutants developed the same severity of lung pathology. Some showed thickening of the elastic fibres surrounding the airways and also increased elastin within the interalveolar septum. Scale bar = 50 μm.

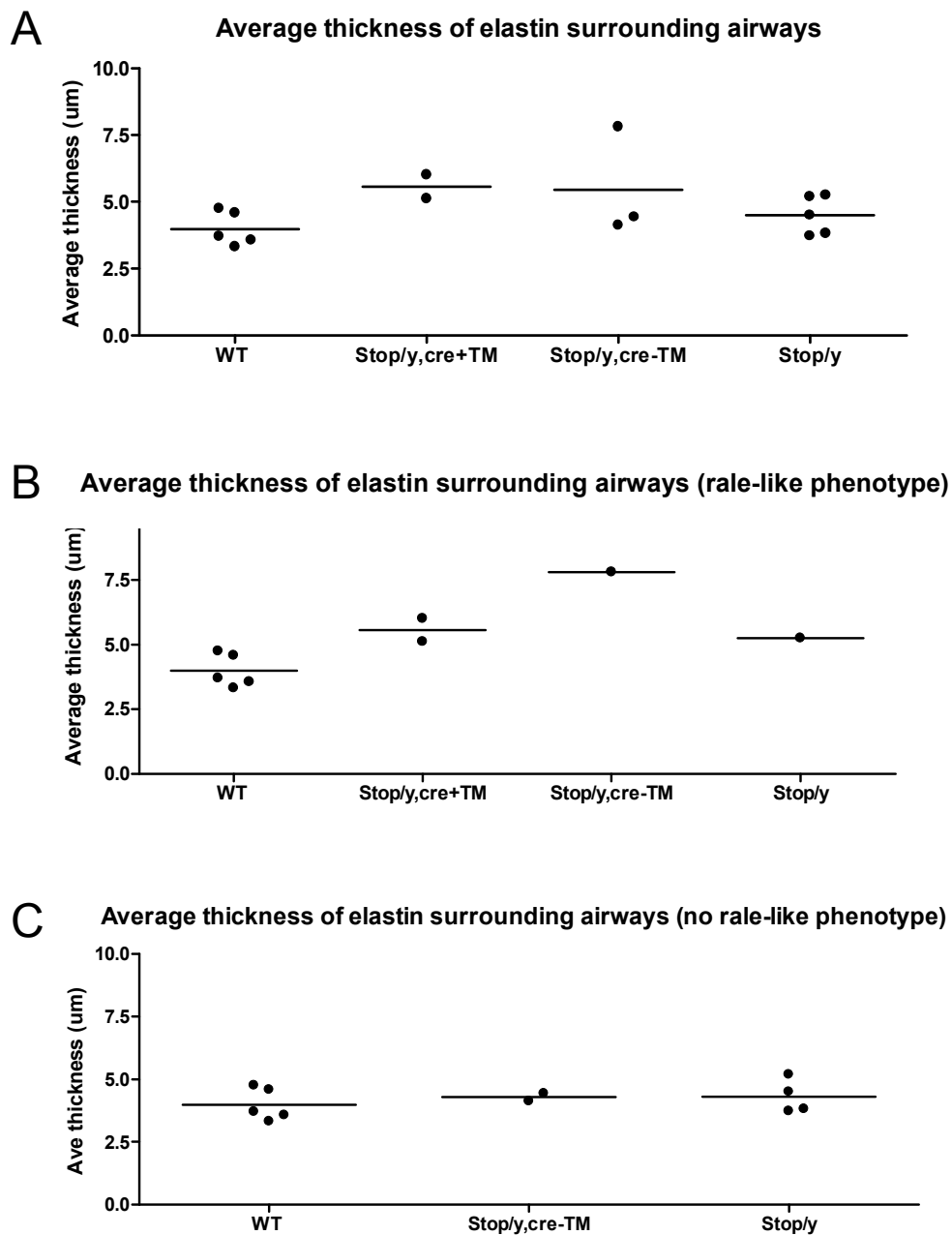


Fig 5-15 Plot to show the average thickness of the elastic fibres surrounding airways in WT, *Stop/y*, *Stop/y,cre-TM* and *Stop/ycre+TM* animals. A – Plot comparing thickness of elastic fibres surrounding airways. There was no significant difference in the average thickness of the elastic fibres between WT and MeCP2 deficient animals. B – Plot comparing thickness of elastin surrounding airways of WT vs mutants that presented rale-like phenotype. Mutants showed a trend towards increased thickness of elastic fibres surrounding the airways compared to WT. C – Plot comparing the thickness of the elastin surrounding the airways of WT vs mutants that did not present the rale-like phenotype. There was no significant difference between the genotypes and no trend towards an increase in the thickness of the elastic fibres surrounding the airways.

Some *Stop/y,cre-TM* mice exhibited an increased amount of elastin within the lung parenchyma compared to the WT as illustrated by the increased amount of Miller's elastin purple staining (Fig 5-14). *Stop/y,cre+TM* mice also displayed an increased amount of elastin compared to WT, particularly surrounding the airways. *Stop/y* animals had an increased amount of elastin in the parenchyma of the lung which may account for the increase in the thickness of the interalveolar septum.

The thickness of the elastic fibres surrounding the airways was quantified and results illustrated that there was no significant difference between the WT and mutant animals (Fig 5-15 plot A; WT: 3.9 ± 0.6 , *Stop/y,cre+TM*: 5.6 ± 0.6 , *Stop/y,cre-TM*: 5.5 ± 2.0 , *Stop/y*: $4.5 \pm 0.7 \mu\text{m}$ median values). Observing only the animals which displayed rales reduced the n number to a degree where stats could not be performed however all mutant genotypes had a trend towards an increased amount of elastic fibres surrounding the airways compared to the WT (Fig 5-15 plot B; WT: 3.9 ± 0.6 , *Stop/y,cre+TM*: 5.6 ± 0.6 , *Stop/y,cre-TM*: 7.81 , *Stop/y*: $5.25 \mu\text{m}$). There was no significant difference in the thickness of the elastin surrounding the airways of WT and *Stop/y* animals who did not present the rale like phenotype (Fig 5-15 plot C; WT: 3.9 ± 0.6 , *Stop/y,cre-TM*: 4.3 ± 0.2 , *Stop/y*: $4.3 \pm 0.7 \mu\text{m}$).

To investigate whether the severity of the respiratory phenotype was reflected in the behavioural score of the animals, comparisons were made between the behavioural scores of animals that did and did not present the rale-like breathing (RLB) phenotype (Fig 5-16). With regards to the *Stop/y* animals, mice that did not present the severe respiratory phenotype had a greater behavioural score than animals that did present rale-like breathing (Fig 5-16 plot A). In *Stop/y,cre-TM* mice however (Fig 5-16 plot B), animals which presented rale-like breathing had a greater behavioural score than those which did not show the severe respiratory phenotype. This suggests that the severity of lung pathology is not necessarily predicted by the onset of a more severe behavioural score.

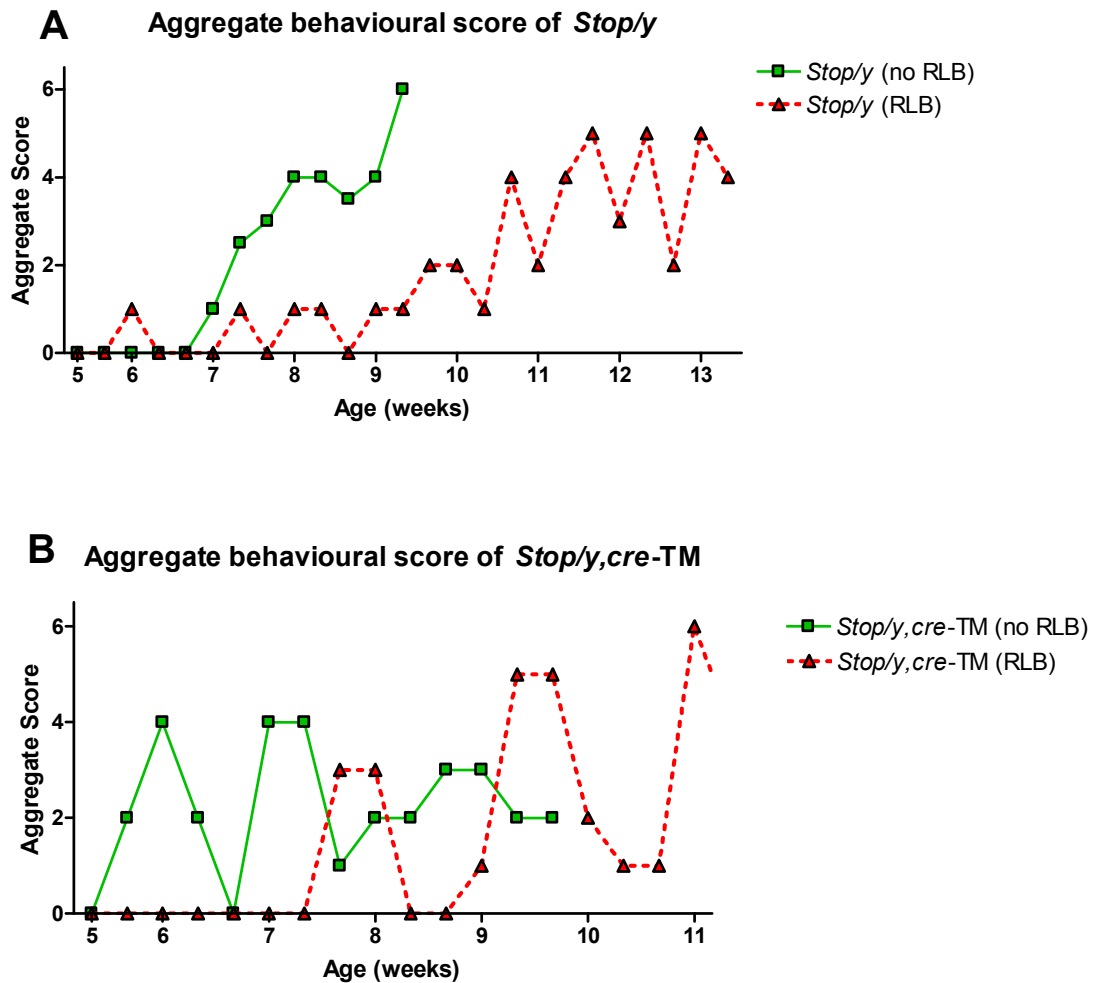


Fig 5-16 Plots comparing the aggregate behavioural score of *Stop/y* and *Stop/y,cre-TM* mice which did or did not present the rale-like breathing (RLB) phenotype. **A** – Plot comparing the behavioural scores of *Stop/y* mice. Animal that did not present rale-like breathing (green line) scored higher than animal that did present severe respiratory phenotype (red line). **B** – Plot comparing the behavioural scores of *Stop/y,cre-TM* animals. Animals which presented rale-like phenotype (red line) had greater behavioural score than those which did not present rale-like breathing (green line)

5.3.3 *TrkB* and *MeCP2* Expression

Immunofluorescent imaging of both *TrkB* and *MeCP2* was difficult to visualise in lung tissue due to the autofluorescent nature of the elastin and connective fibres within the tissue. Therefore the images presented below act are solely descriptive and no quantification was carried out using the images.

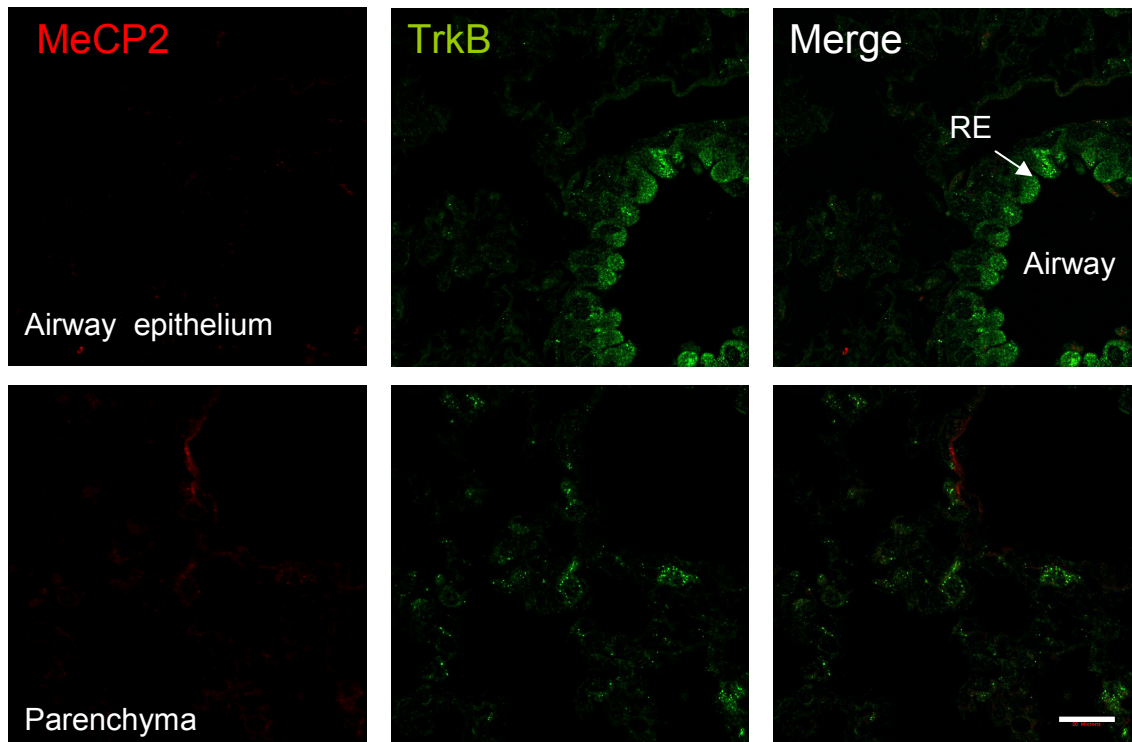


Fig 5-17 Single plane confocal images of *TrkB* and *MeCP2* expression in lung of WT animals. RE – respiratory epithelium. *TrkB* positive staining was observed in the epithelial cells of the respiratory airways but also within the interstitial cells of the lung parenchyma. *MeCP2* positive staining was not apparent. Scale bar = 20 μm .

In WT lung tissue, *TrkB* positive staining was observed in the parenchyma and the respiratory epithelium (Fig 5-17). *TrkB* staining was most intense at the apex of the cells of the respiratory epithelium. *MeCP2* staining was not detectable in the WT tissue.

In *Stop/y* lung tissue *MeCP2* positive staining was not detectable but *TrkB* positive staining was seen in both the cells of the respiratory epithelium and

interstitial cells in the lung parenchyma (Fig 5-18). Unlike WT, TrkB staining did not seem more intense in any particular area of the cell.

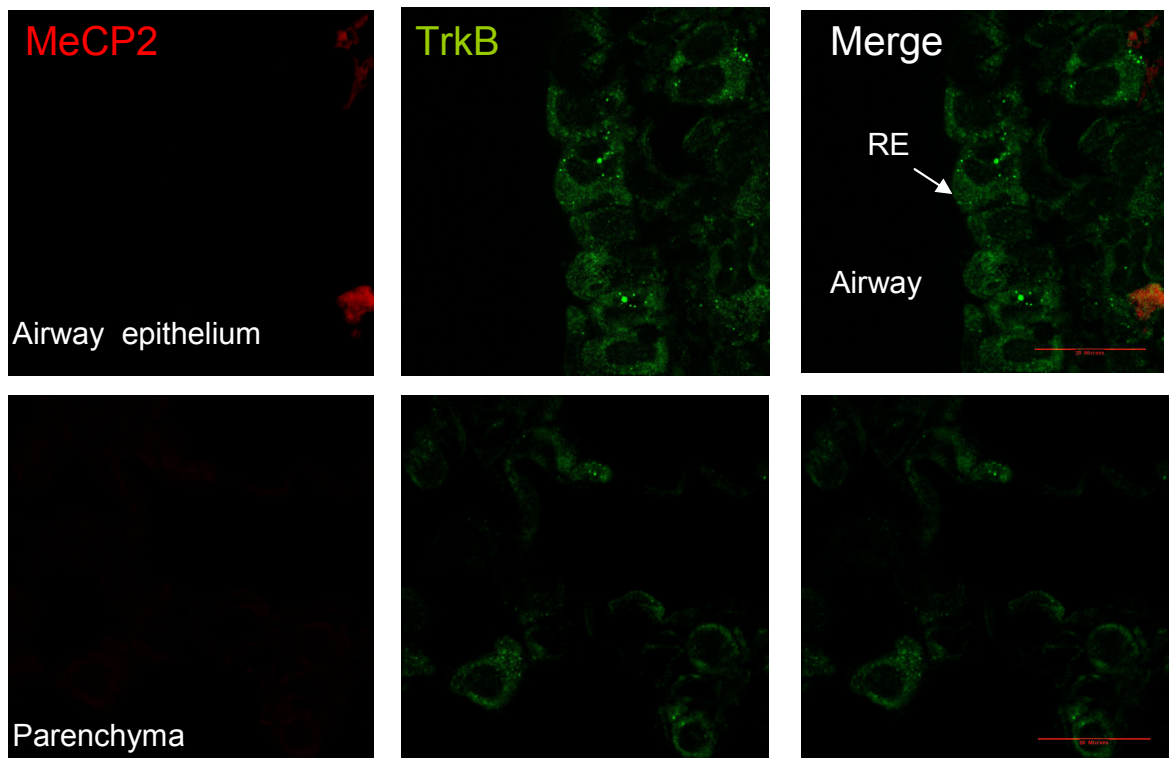


Fig 5-18 Single plane confocal image of MeCP2 and TrkB staining in *Stop/y* lung. TrkB staining was observed in both the epithelial cells of the airways and in the lung parenchyma. No MeCP2 positive staining was observed in the *Stop/y* animal.

TrkB expression was observed in the parenchyma and respiratory epithelium of the *Stop/y,cre-TM* animals (Fig 5-19). As seen in WT, the most intense TrkB positive staining was observed towards the apex of the cells of the respiratory epithelium.

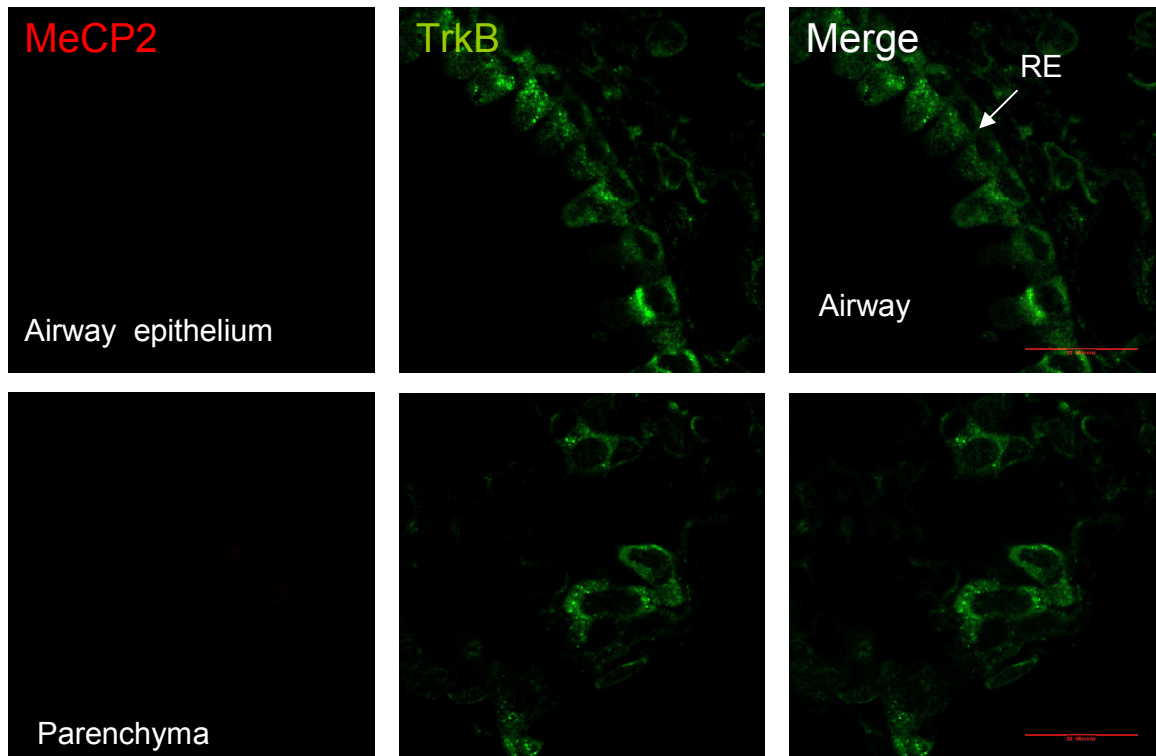


Fig 5-19 Single plane confocal images of MeCP2 and TrkB staining in *Stop/y,cre-TM* animal. RE – respiratory epithelium. MeCP2 staining was not found in the *Stop/ycre-TM* sections. TrkB positive staining was observed in both the epithelial cells of the airways and in the interstitial cells of the lung parenchyma.

In the *Stop/y,cre+TM* tissue, TrkB staining was observed in the respiratory epithelium and in the cells of the parenchyma (Fig 5-19). Some TrkB expressing cells of the respiratory epithelium and parenchyma exhibited positive MeCP2 staining in the nuclei (Fig 5-20, merge panel inserts A and C) while others did not show positive MeCP2 staining (Fig 5-20 merge panel insert B). Some cells appeared to show positive MeCP2 staining in the cytoplasm (Fig 5-20 merge panel insert D) however to confirm that staining was real and that positive results were not due to autofluorescence, control sections in which no primary antibody had been applied were imaged (Fig 5-20 control images). The same positive red staining of the cytoplasm was observed in the sections with no antibody applied. In both the green and red channel, autofluorescent red blood cells were observed. However, no positive TrkB staining was observed suggesting that TrkB staining obtained from slices incubated with the TrkB antibody was a true positive.

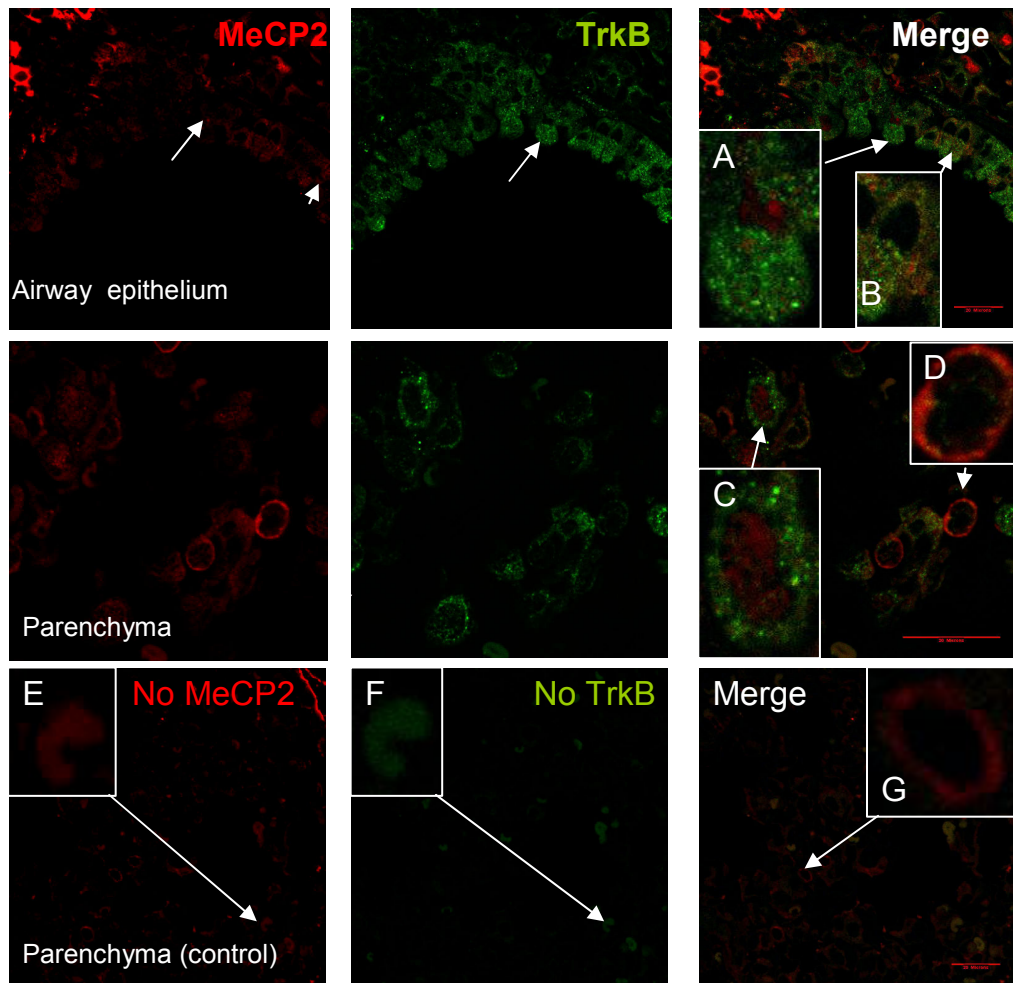


Fig 5-20 Single plane confocal image of MeCP2 and TrkB staining in *Stop/y,cre+TM* mice. **A** and **C** -illustrate what appeared to be positive MeCP2 staining in the nuclei of TrkB positive cells. **B** – shows a TrkB positive cell which was not MeCP2 positive. **D** – Cell within the parenchyma which appeared to show positive MeCP2 positive staining in the cytoplasm, however this was proven to be false negative as control section with no primary antibody applied also showed red staining in the cytoplasm of the cell (**G**). **E** and **F** – autofluorescent red blood cell. Scale bars = 20µm.

To observe whether or not the MeCP2 antibody was failing to bind in the lung tissue, images were taken from airway muscle tissue. MeCP2 positive staining was observed in the nuclei of the cells of the smooth muscle layer (Fig 5-21 lower panels) in *Stop/y,cre+TM* mice. Positive TrkB staining was also observed surrounding the MeCP2 positive nuclei. In control section (Fig 5-21 upper panels) where no primary antibody was applied, neither MeCP2 nor TrkB positive staining was observed.

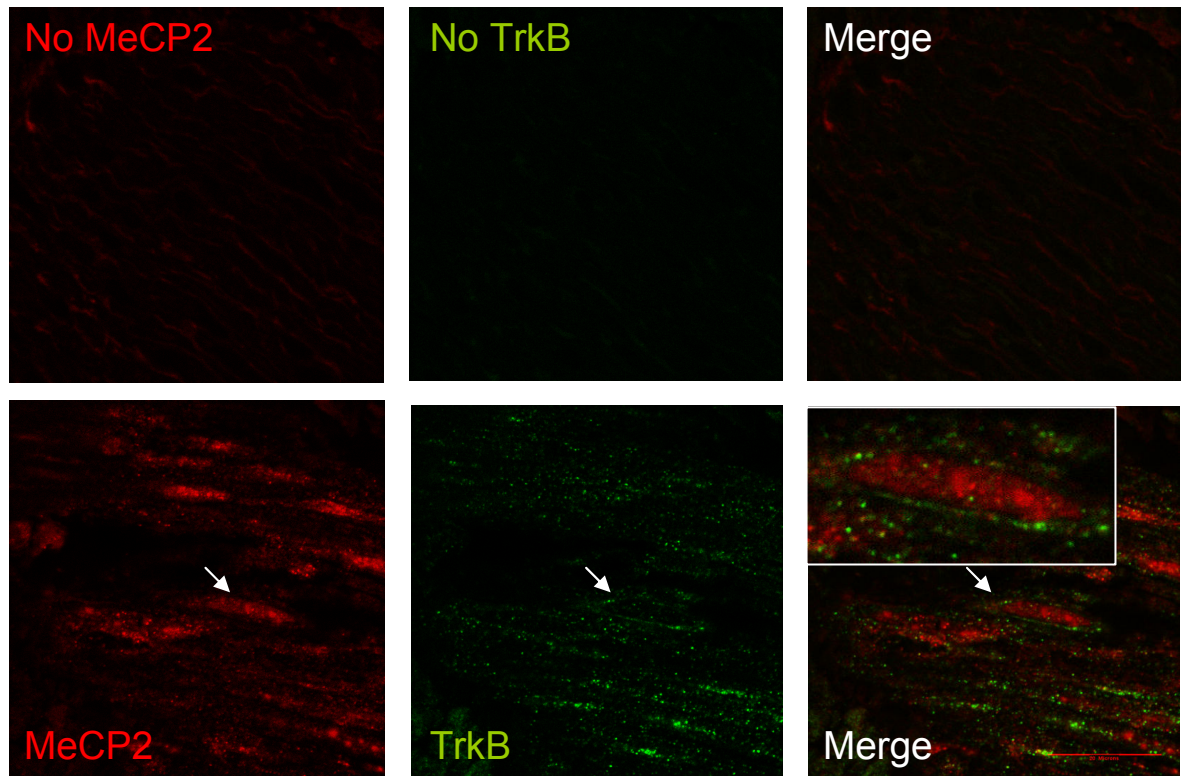


Fig 5-21 Single plane confocal images of MeCP2 and TrkB staining in *Stop/y,cre+TM* muscle layer. Upper panels show images taken from control sections in which no primary antibodies were applied. Neither MeCP2 nor TrkB positive staining was observed. Lower panels show images taken from sections incubated with MeCP2 and TrkB primary antibodies. Both MeCP2 and TrkB positive staining was observed in the airway muscle layer of the *stop/y,cre+TM* tissue. Scale bar = 20 μ m.

Since TrkB and MeCP2 immunofluorescent staining was weak, DAB staining was used to obtain clearer images of TrkB expression in order to assess the difference in TrkB expression between the genotypes.

TrkB expression is highlighted by brown deposits of staining (Fig 5-22). Positive TrkB was observed in the epithelial layer of the airways and also within the lung parenchyma (Fig 5-22 insert B). In WT, TrkB expression appeared evenly distributed throughout the parenchyma and TrkB staining appeared strongest at the apex of the respiratory epithelial cells (Fig 5-22 insert A). In *Stop/y* animals the most apparent TrkB staining also appeared to be at the apex of the cells of the respiratory epithelium (Fig 5-22 insert D). There were areas of darker

staining in the parenchyma of the *Stop/y* animals which may suggest greater TrkB expression (Fig 5-22 insert C). The DAB reaction was left to develop for the same period of time in all sections thus differences in staining are unlikely to be due to artefacts from the DAB reaction. In the *Stop/y,cre-TM* tissue, observation alone suggests that areas where the interalveolar septum is thickened exhibit increased amounts of TrkB expression, as indicated by the presence of brown punctate staining (Fig 5-22 insert E). The same was observed in the *Stop/y,cre+TM* tissue, with areas of increased tissue growth being characterised by greater TrkB expression than the WT (Fig 5-22 panel F). It cannot be ascertained from observation alone whether an increase in TrkB expression is the cause of the fibrosis-like tissue growth in the mutant animals, or whether the consolidation of the pulmonary tissue gives the impression of increased TrkB expression. Thus it would be of benefit in future studies to carry out mRNA analysis on the lung tissue to observe whether there are differences in the level of TrkB mRNA of WT and MeCP2 deficient mice.

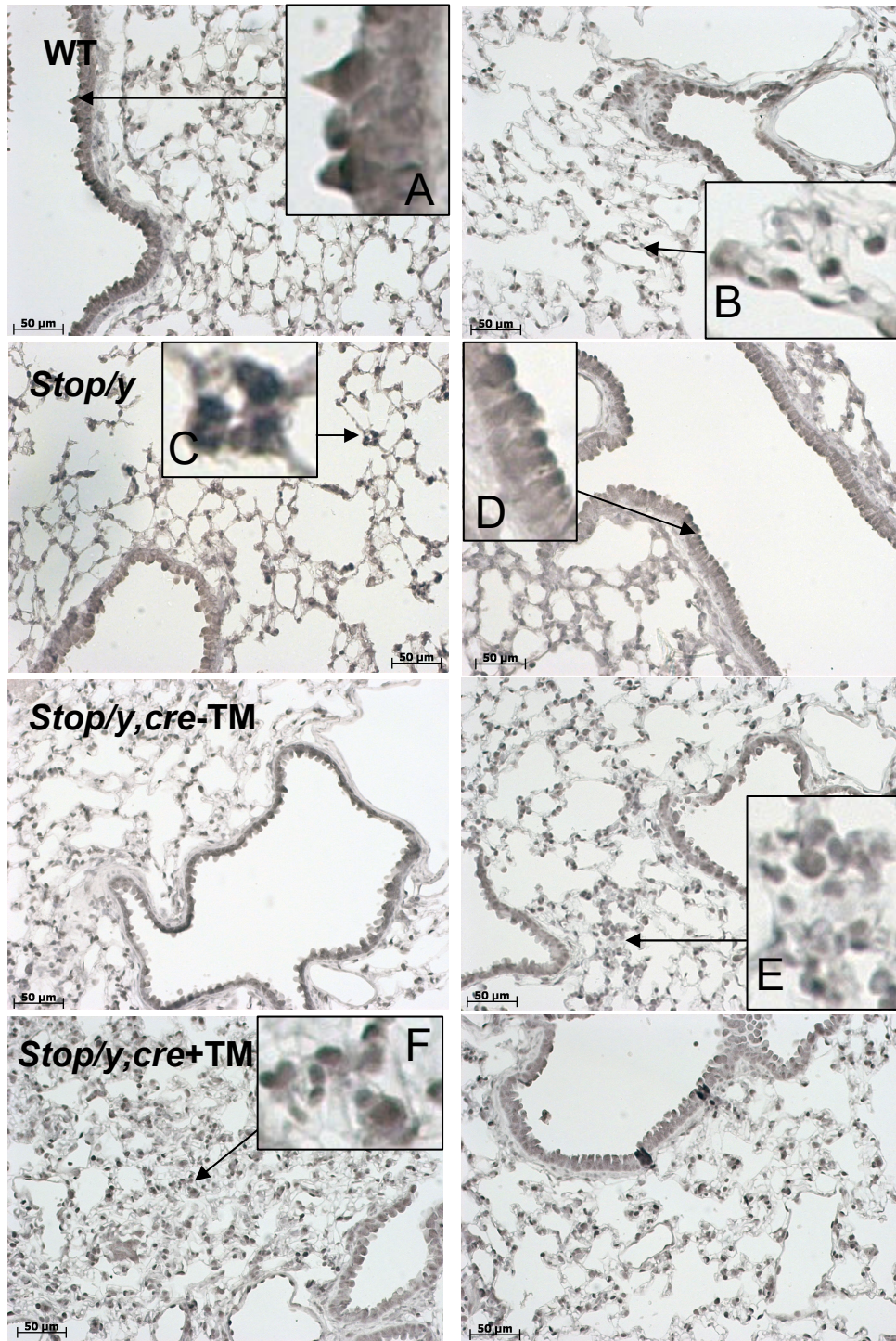


Fig 5-22 TrkB staining (DAB) of airways of WT, *Stop/y,cre-TM*, *Stop/y,cre+TM* and *Stop/y* males. Brown deposits indicate positive TrkB staining. WT animals exhibited positive TrkB staining in the parenchyma (B) and in respiratory epithelium. The strongest staining was observed at the apex of the epithelial cells (A). *Stop/y* tissue showed the strongest TrkB staining at the apex of the respiratory epithelial cells (D). TrkB expression appeared clustered in the parenchyma of the *Stop/y* tissue (C). Areas of thickened interalveolar septum in *Stop/y,cre-TM* and *Stop/y,cre+TM* tissue appeared characterised by increased amount of TrkB expression (E and F respectively). Scale bars = 50μm.

5.4 Discussion

5.4.1 Morphological Changes in MeCP2 Deficient Lungs

Preliminary H&E staining of the *Stop/y* animal which exhibited rale-like breathing and foaming at the mouth revealed an anomalous growth of tissue within the lung and an unknown substance gathering within the airway lumen (Fig 5-7), pathology similar to the fluid-filled dilated bronchioles observed in HRCT scans of human female RTT patients (De Felice, Guazzi et al. 2010). Future work would involve using stains to identify the cells present and ascertain whether the excessive growth is an immune or inflammatory response. PAS staining also indicated that there was a greater amount of mucin and glycoprotein within the *Stop/y* lung compared to the WT (Fig 5-10). Over production of surfactant and glycoproteins in the lung is observed in a rare lung disease known as alveolar proteinosis in which a build up of surfactant occurs in the alveoli and disturbs gas exchange. The disease is characterised by distal air spaces being filled with granular, eosinophilic material which stains positively with Periodic acid-schiff stain (PAS). An overproduction of surfactant may account for the foaming at the mouth which was also observed in some of the MeCP2 deficient tissue studied in this chapter however this cannot be confirmed without further PAS staining of *Stop/y*, *Stop/y,cre-TM* and *Stop/y,cre+TM* tissue. Future work may also involve staining lung tissue to quantify the number of type 2 pneumocytes. Comparison of the number of type 2 pneumocytes in MeCP2 deficient mice compared to WT may reveal whether an increase in this cell type is responsible for the excess mucin production and subsequent foaming at the mouth. Future investigation may also involve studying mucin secreting clara cells of the mouse respiratory tract using antibodies raised against clara cell secretory protein (CCSP). Over-production of mucus by clara cells could also contribute to the respiratory phenotype observed in the male MeCP2 deficient mice.

Staining of the *Stop/y*, *Stop/y,cre-TM* and *Stop/y,cre+TM* tissue mice with Masson's trichrome and Miller's elastin stain revealed that not all MeCP2 deficient lungs exhibited the same severity of pathology, and indeed those which presented an observable respiratory phenotype e.g. foaming at the mouth and rattling breath exhibited the most severe morphological changes in the lung.

Also, only 55% of the cases studied by De Felice et al., exhibited abnormal HRCT scans (De Felice *et al.*, 2010) which indicates that development of lung pathology is not a certainty in RTT syndrome. As shown in Fig 5-16, *Stop/y* animals that did not present rale-like breathing showed a greater behavioural score than animals that presented the severe respiratory phenotype. In contrast, *Stop/y,cre-TM* mice that presented rale-like breathing showed a greater behavioural score than those animals that did not present the rale-like phenotype. This suggests that a) the severity of the behavioural score may not reflect the severity of the respiratory phenotype and b) an increase in behavioural score does not predict the onset of rale-like breathing.

The data gathered in this study revealed that on average, the thickness of the respiratory epithelium did not differ significantly between the WT and MeCP2 deficient mice (Fig 6-12 plot A). However, observation of only animals which displayed rale-like breathing and foaming at the mouth revealed that there was a trend towards an increase in the thickness of the epithelium in MeCP2 deficient mice compared to WT. A thickening of the respiratory epithelium may be due to increased TrkB expression, which has been mentioned previously and will be discussed later in this chapter. Masson's trichrome staining revealed increased collagen deposits in the lungs of MeCP2 deficient mice compared to WT (Fig 5-11). Further study may involve using histological stains to differentiate between new and aged collagen deposits. Being able to estimate the stage at which the collagen deposits form may give further insight into the stage of development at which absence of MeCP2 in the lung begins to affect lung morphology.

It was also observed that the interalveolar septum was thicker in the MeCP2 deficient mice compared to the WT, significantly so in the *Stop/y,cre+TM* animals (Fig 5-13 plot A). The interalveolar septum is composed of two thin squamous epithelial layers between which lie capillaries and elastic and collagen fibres. The thin nature of the septum is necessary for the exchange of O₂ and CO₂. A thickening of the septum may lead to inadequate gas exchange within the lungs and this could lead to changes in partial pressures of gas within the blood which may contribute to some of the respiratory abnormalities observed in the mutant mice in chapter 3.

Sighing acts as a preventative measure against lung collapse (Reynolds, 1962), can improve gas exchange and lung volume in patients receiving ventilatory support for acute respiratory distress syndrome (Patroniti *et al.*, 2002) and serves to increase lung compliance and help prevent atelectasis (Glogowska *et al.*, 1972). Increased sighing behaviour in MeCP2 deficient males, which was reported in chapter 3, may occur in an attempt to 1) increase the lung compliance which has been compromised by the presence of increased collagen deposits (Fig 5-9) and 2) improve oxygenation which may have been compromised by the thickening of the interalveolar septum. The fact that the interalveolar septum is significantly thicker in *Stop/y,cre+TM* mice compared to WT (Fig 5-13) illustrates that reactivation of *Mecp2* may not be able to rescue the abnormal lung pathology which has formed. *Stop/y,cre+TM* mice showed a trend towards a thicker interalveolar septum than the *Stop/y,cre -TM* and *Stop/y* animals. One may expect that an absence of MeCP2 would have the same effect on each genotype i.e. each genotype would show the same amount of thickening of the interalveolar septum. However, it should be noted that the *Stop/y,cre +TM* animals tended to be older than the *Stop/y* and *Stop/y,cre -TM* animals at the time of perfusion thus the *Stop/y,cre +TM* mice may have had a longer period of time for the lung pathology to progress into the more severe state which was seen in Fig 5-11 and Fig 5-14. As with the respiratory epithelium, there was a trend towards a thicker interalveolar septum in the MeCP2 deficient mice that exhibited rale-like symptoms and foaming at the mouth compared to WT. This suggests that, perhaps as one would expect, a more severe lung pathology results in a more severe respiratory phenotype.

While comparison of the elastic fibres surrounding the airways showed no significant difference between the WT and mutant animals, observation of only the animals that exhibited the visible rale-like respiratory phenotype revealed that MeCP2 deficient mice had a trend towards an increased amount of elastin compared to the WT (Fig 5-15). From the images in Fig 5-14 it can also be noted that there were increased amounts of elastic fibres within the alveolar septum. An increase in the amount of elastin within the lung may serve to change the dynamic within the lung and alter lung compliance. Studies in *Mecp2^{-/+}* female mice indicate that lung compliance is not significantly different from the WT (Bissonnette & Knopp, 2006). However, this chapter makes use of a male model

in which MeCP2 is completely absent for the first few weeks of life whereas the female model utilised by Bissonnette et al will have MeCP2 present throughout life. The ubiquitous absence of MeCP2 may therefore have an effect on the lung of male MeCP2 deficient mice which is not recapitulated in the female model.

5.4.2 TrkB in the Lung

TrkB expression within the lung of WT and MeCP2 deficient mice was confirmed via both immunofluorescence and DAB reactions. TrkB was found to be expressed in both the epithelial cells of the airways and cells of the parenchyma. Fig 5-21 indicates that in *Stop/y,cre* +TM mice, cells in the smooth muscle layer surrounding the airways express TrkB and also express MeCP2. Previous studies of *Mecp2* reactivation have focused on *Mecp2* reactivation within the brain (Guy *et al.*, 2007) and as yet nothing is known about the level of *Mecp2* reactivation within the lung. MeCP2 has been shown to be expressed in the lung of *Stop/y,cre*+TM mice in this study (Fig 5.21) which indicates that *Mecp2* reactivation is occurring within this organ. However, no quantitative analysis has been performed thus the level of *Mecp2* reactivation in the lung remains unknown.

Autofluorescence within the lung can be an issue due to the autofluorescent nature of elastin. Since elastin content was shown to be increased in the MeCP2 deficient mice compared to WT, immunofluorescent detection of TrkB was problematic and DAB staining was utilised to overcome this issue. DAB staining revealed positive TrkB expression in all genotypes. In Fig 5-22 it appeared as though a greater amount of TrkB was expressed in MeCP2 deficient mice, particularly in areas where there appears to be a thickening of the interalveolar septum. However, it cannot be concluded from observation alone as to whether or not an increased amount of TrkB expression led to cell proliferation and thus a thickening of the interalveolar septum, or if another factor, such as infection, caused cell proliferation and the apparent increase in TrkB expression was secondary to this. 15 day old *TrkB* *-/-* mice, which express non functional TrkB, exhibit a thinner bronchial epithelium, larger air spaces and thinner blood vessel walls compared with WT (Garcia-Suarez *et al.*, 2009). As discussed in section 5.1.3, an overexpression NTRK2, the gene which encodes for the TrkB receptor,

was observed in the brains of RTT patients and MeCP2 deficient mice (Abuhatzira *et al.*, 2007) with a suggestion that over expression of the receptor may be a mechanism to compensate for the reduced levels of signalling molecule, BDNF. It could be hypothesised that an increase in the expression of TrkB which may arise from a reduced BDNF content in the MeCP2 deficient mice studied in this chapter may lead to changes opposing those observed in *TrkB* *-/-* mice i.e. thicker bronchial epithelium. It may be argued that an increase in TrkB receptor expression would have no such effect on the lung tissue as the fact still remains that in MeCP2 deficient mice BDNF (a ligand for TrkB) levels are reduced (Chang *et al.*, 2006a) and thus reduced signalling may balance out the increased receptor expression. However, TrkB can also be signalled by neurotrophin-4 (NT-4) and there is no evidence to suggest that a lack of MeCP2 has an impact on the level of this TrkB ligand.

TrkB expression is also shown to be enhanced in the airway epithelium of hypoxic rats (Sciesielski *et al.*, 2009). RTT patients and MeCP2 deficient mice often display lengthy apneas which may result in the animals developing hypoxic conditions within the body. Thus it could be hypothesised that MeCP2 deficient mice develop hypoxia as a results of apneic breathing and this may also serve to enhance TrkB expression, leading to morphological changes within the lung.

The immucytochemical processing of the lung tissue applied in this chapter was difficult to quantify and due to the fact that lung tissue was already paraffin embedded it was no longer possible to carry out mRNA analysis to compare levels of TrkB throughout the lungs of the various genotypes. This would be an experiment of great value for future studies. As mentioned, there exist two forms of the TrkB receptor, an active 145kDA protein and a truncated non-signalling 95 kDA protein. Studies so far suggest that in the human lung, both the full length and truncated isoforms of the TrkB receptor are expressed (Ricci *et al.*, 2004) whereas mice only express the truncated form (Hikawa *et al.*, 2002). The truncated form lacks cytoplasmic tyrosine kinase catalytic region and therefore does not signal in response to BDNF, so its role in the lung remains unknown. The TrkB antibody used in this study targeted both isoforms of the receptor and future studies may be aimed at investigating 1) which form(s) of

the TrkB receptor are expressed in the lung 2) if there is an increase in TrkB expression in MeCP2 deficient lungs, which form of the receptor is upregulated.

In conclusion, RTT syndrome has long been considered mainly as a neurological disorder but the fact that abnormal lung morphology has been proven in these male MeCP2 deficient mice and also in RTT patients (De Felice *et al.*, 2010) suggests that the respiratory abnormalities associated with RTT may not be solely the result of problems within neurons and neuronal networks.

**Chapter 6: Respiratory pattern of *Mecp2*^{+/-} mice
and investigation of possible underlying lung
pathology.**

6.1 Introduction

Many RTT studies are carried out using the male mouse model as these animals present a rapid onset of the RTT-like phenotype, displaying symptoms as young as 8 weeks old (Guy *et al.*, 2007). The phenotype develops more slowly, taking up to 6 months, in female mice heterozygous for a null mutation in *Mecp2* (*Mecp2*^{+/-}). As discussed in chapter 3, *MECP2* is an x-linked gene and is subject to X chromosome inactivation (XCI; see chapter 1 section 1.9.3). This results in females having a phenotype of varying severity due to the mosaic pattern of expression of the mutated *MeCP2* gene in cells. Male *MeCP2* deficient mice present a more homogeneous population since every cell will express the mutated *Mecp2* gene and this simplifies interpretation of data. However, *Mecp2*^{+/-} animals have a period of normal development followed by the appearance of RTT-like symptoms between 4-12 months of age (Guy *et al.*, 2001), a pattern of disease progression which is more similar to the human condition. The RTT like phenotype in *Mecp2*^{+/-} mice also tends to stabilise, resulting in animals that have a life span comparable to that of the WT (Guy *et al.*, 2007). Since the progression of the RTT-like phenotype in *Mecp2*^{+/-} female mice is more comparable to the human disease than *Mecp2*^{-/-}, and RTT is a predominantly female based disease affecting approximately 1 in 10,000 girls (Hagberg, 1985), it is of benefit to study the respiratory parameters in the female mouse model of the disease. The ventilatory response of *Mecp2*^{+/-} mice to hypercapnia does not differ significantly from the WT yet there are data to suggest that the hypoxic response of *Mecp2*^{+/-} animals is affected. At 5 months of age, *Mecp2*^{+/-} mice show a larger increase in V_e compared to WT after 1 minute of hypoxic exposure (Bissonnette & Knopp, 2006). It has been shown that *Mecp2*^{+/-} animals also display significantly reduced TH expression in the petrosal ganglion and adrenal medulla and a tendency towards reduced TH expression in the carotid bodies compared to WT (Roux *et al.*, 2008). Since TH expressing cells can be dopaminergic in nature, reduced TH expression would suggest a reduction in the ability to produce dopamine, a neurotransmitter known to have an inhibitory effect on the chemoafferent response (Bee & Pallot, 1995). Thus, reduced dopamine levels in the carotid bodies may explain the increased ventilatory response shown by *Mecp2*^{+/-} mice in response to hypoxia.

As mentioned in previous chapters, patients with RTT syndrome often experience respiratory abnormalities such as apneas and highly unstable breathing patterns with periods of breath holding and hyperventilation (Weese-Mayer *et al.*, 2006). The occurrence of apnea tends to be more frequent in *Mecp2^{+/-}* mice compared to WT (Abdala *et al.*, 2010) as is periodic breathing (Bissonnette & Knopp, 2008). Respiratory abnormalities were identified and quantified in the male model in chapter 3 but longitudinal study of the animals proved difficult as symptoms developed very quickly and many animals had to be euthanized thus reducing n numbers. As the female model tends to exhibit a slower progression of the RTT-like phenotype, a longitudinal study of the development of respiratory abnormalities was more feasible. Therefore this chapter aimed to investigate longitudinally the respiratory abnormalities of the *Mecp2^{+/-}* females before the onset and during the progression of the RTT-like symptoms using whole body plethysmography. As with the male model, it was of interest to ascertain whether the mice exhibited a disordered breathing pattern in normoxic conditions and how this breathing phenotype develops over time. The study also aimed to investigate whether the chemosensitive response of *Mecp2^{+/-}* mice is affected. This was achieved by exposing the *Mecp2^{+/-}* mice to varying intensities of hypercapnic (3%, 5% and 8% CO₂) and hypoxic (10% O₂) stimuli to observe the effect on respiratory output. The final aim was to look for evidence of pulmonary arterial hypertension in *Mecp2^{+/-}* animals.

As shown in chapter 5, the male MeCP2 mice were found to exhibit lung pathology which may have contributed towards the breathing abnormalities exhibited by the animals, and it was hypothesised that *Mecp2^{+/-}* mice may also have underlying lung pathology. Rats exposed to chronic hypoxia begin to develop muscularization of small pulmonary arteries (Hislop & Reid, 1976), which can lead to increased right ventricular pressure and right ventricular hypertrophy, which taken together can be an indication of pulmonary arterial hypertension (PAH). It is suggested that in RTT patients, hypoxemia can develop when subjects undergo apneic breathing (Southall *et al.*, 1988). As will be discussed further in this chapter, female *Mecp2^{+/-}* animals exhibited more frequent apnea than WT and as such may have been subject to hypoxemia. It could be hypothesised that these hypoxic conditions could lead to gradual development of PAH through the remodelling of the pulmonary vessels. Thus one

of the aims of this chapter was to carry out *in vivo* measurements of the three indices of pulmonary arterial hypertension; systolic right ventricular pressure (SRVP), ratio of the weight of the right ventricle compared to left ventricle plus septum (RV/LV+S) and the percentage of remodelled pulmonary blood vessels.

6.2 Methods

6.2.1 Female Mouse Model

See section 2.1.2 for more information regarding breeding. Mice were housed in cages containing a mixture of WT (n=7) and female heterozygotes (*Mecp2*^{+/-}; n=11), maintained on a 12 hour light/dark cycle and provided with food and water *ad libitum*. All experimental procedures were carried out under license from the UK Home Office and were subject to the Animals (Scientific Procedures) Act, 1986. During the progression of the experiment there was a spontaneous death in the WT animals. The animal had been noted as behaving quite erratically, post mortem analysis carried out by the on-site vet revealed no pathology. This resulted in Wt n=6

6.2.2 Behavioural Scoring

To monitor the progression of the RTT-like phenotype, animals were observed and scored behaviourally on a weekly basis using a 3 point scoring system created by Guy et al (2007) as described in chapter 2. The development of the phenotype in the female mice was slower and less variable than in the male mice. The 3 point scale would have been adequate for assessment of the female mice but the new 5 point scoring system (see chapter 2, section 2.2) was also implemented to observe whether adding more descriptors to the scoring system would yield more accurate tracking of the behavioural phenotype. Scoring was performed blind to the genotype and animals were scored from 8 wks to 32 wks old.

6.2.3 Respiratory Measurements

Breathing patterns during normoxia (21% O₂), hypercapnia (3%, 5% and 8% CO₂) and hypoxia (10% O₂) were measured *in vivo* using whole body plethysmography (see section 2.4). Recordings of WT (*n* = 6) and *Mecp2*^{+/-} (*n*=11) mice were taken at 5 week intervals, starting from 10 weeks to 32 weeks of age.

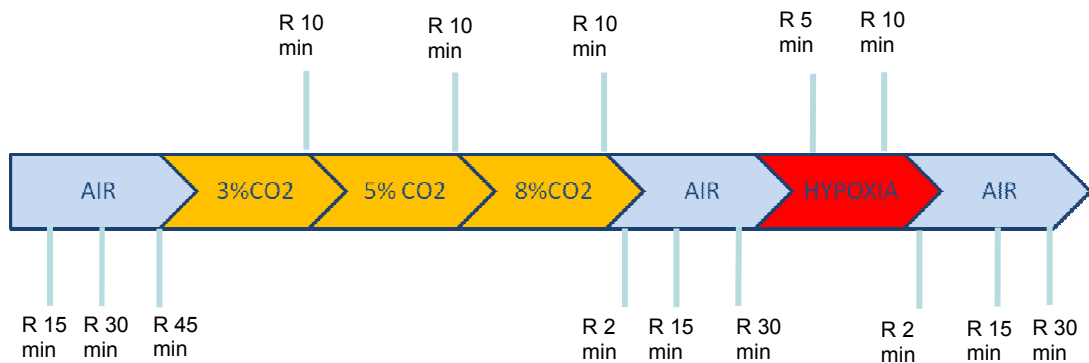


Fig 6-1 Protocol for measurement of respiratory parameters of *Mecp2*^{+/-} mice. Mice were allowed to habituate in normoxia for 45 min with recordings taken at 15, 30 and 45 min. Recordings were also taken after 10 min exposure to each of 3%, 5%, 8% CO₂. Post hypercapnic stimulus recordings taken in normoxia at 2 min, 15 min and 30 min before exposure to 10% O₂. Recordings were taken after 5 min and 10 min hypoxic exposure and post stimulus recordings made in normoxia at 2 min, 15 min and 30 min.

For each experimental session, mice were given 45 min to habituate to the chamber in normoxia, during which control recordings were made in at 15, 30 and 45 min time points. The chamber was then filled with 3% CO₂ (3% CO₂, 21% O₂, balanced N₂) for 10 min and a recording made at the end of the 10 min period. This was repeated for 5% (5% CO₂, 21% O₂, balanced N₂) and 8% CO₂ (8% CO₂, 21% O₂, balanced N₂). After exposure to hypercapnia, the chamber was flushed with air and recovery recordings made at 2, 15 and 30 min. The chamber was then filled with 10% O₂ (10% O₂, 5% CO₂, balanced N₂) and recordings made

after 5 min and 10 min hypoxic exposure. Following this, the chamber was flushed with air and recovery recordings made at 2, 15 and 30 min post hypoxic exposure. Each recording session was ~2 min; a calibration volume of 200 μ l was injected into the plethysmographic chamber towards the end of each recording session.

6.2.4 Respiratory Analysis

Respiratory data were sampled at 1000Hz, filtered at 0.01 Hz to remove DC components and analysed offline using Spike 2 (Spike2 software, Cambridge Instruments, UK). Movement distorts the plethysmographic signal and prevents reliable measurements, thus only data during periods of quiet breathing when the animal was still were analysed. Changes in respiratory frequency (Fr) were analysed on a breath by breath basis for each recording. As with the male mice in chapter 3, the number of apneas, sighs and “double breaths” were quantified (see section 2.4.2 for definition of respiratory characteristics).

6.2.5 PAH Analysis

PAH experiments were performed using 10-12 month old heterozygous *Mecp2*^{+/-} females (n=8) and wild-type (n=5) female littermates. Three indices of pulmonary arterial hypertension were assessed; *in vivo* measurement of right ventricular systolic pressure, ratio of the weight of the right ventricle to the left ventricle plus septum and quantification of the percentage of remodelled pulmonary blood vessels (see chapter 2 section 2.11 for methodology). Surgery was performed by colleague Margaret Nielsen (University of Glasgow, UK) and assisted by myself, lung tissue stained by David Russell (University of Glasgow, UK) and imaging/analysis of tissue performed by myself.

See section 2.11 for details regarding statistical analysis.

6.3 Results

6.3.1 Behavioural Score

Behavioural scoring was performed blind to the genotype. WT animals scored 0 throughout most of the study, scoring occasionally on the tremor characteristic which can be attributed to some WT animals being slightly nervous. *Mecp2*^{+/-} mice exhibited mild symptoms from 11 weeks old using the 3 point system (Fig 6-2 plot A), yet subtler symptoms which appeared at 9 wks old were picked up by the 5 point system (fig 6-2 plot B). This indicates that addition of descriptors in the behavioural scoring system allows RTT-like symptoms to be detected at an earlier stage. *Mecp2*^{+/-} females displayed an increasing severity of the RTT-like phenotype from 9-11 wks to 24 wks when the progression of the RTT-like symptoms slowed and a plateau was reached, as reported by (Guy, Hendrich et al. 2001).

It was noted that some of the *Mecp2*^{+/-} mice began to develop an obese phenotype, as had also been reported by Guy et al. The average weight of all the WT and the *Mecp2*^{+/-} mice were plotted at 10, 20 and 30 wks of age and no significant difference was found (fig 6-3, plot A, $p > 0.05$). There is no clear definition of obesity in animals but in the human, an individual is considered obese when body mass is 20-25% above ideal weight. Therefore, based on the final weight of the WT animals, the weight of *Mecp2*^{+/-} mice that had an end weight 25% greater than the WT (>40g) were plotted. The *Mecp2*^{+/-} mice were significantly heavier than the WT (fig 6-3 plot B) at 10 weeks (WT: 22.7±1.5g, *Mecp2*^{+/-}: 28.5±1.7g, $p < 0.05$), 20 weeks (WT: 29±3.7g, *Mecp2*^{+/-}: 37.5±1.7g, $p < 0.05$) and 30 weeks (WT: 30±2.4g, *Mecp2*^{+/-}: 45 ±1.4g, $p < 0.05$). There appeared to be no association between behavioural score and development of the obese phenotype (data not shown).

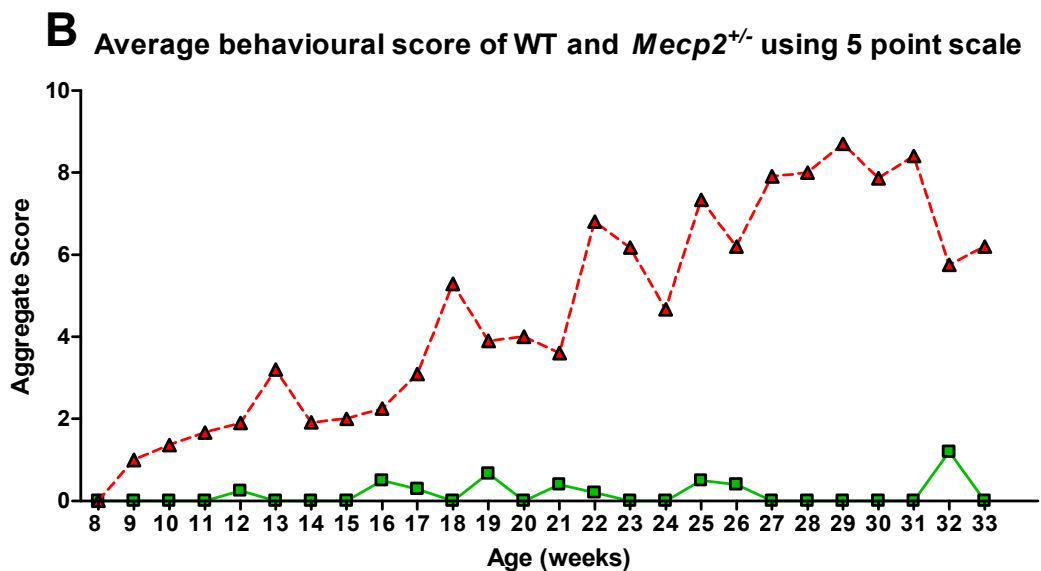
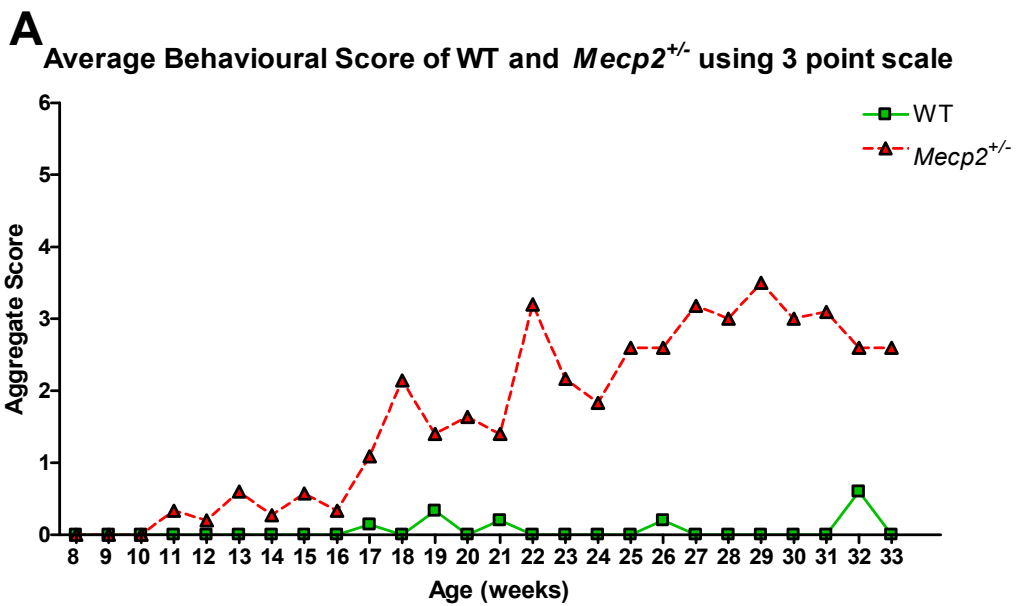
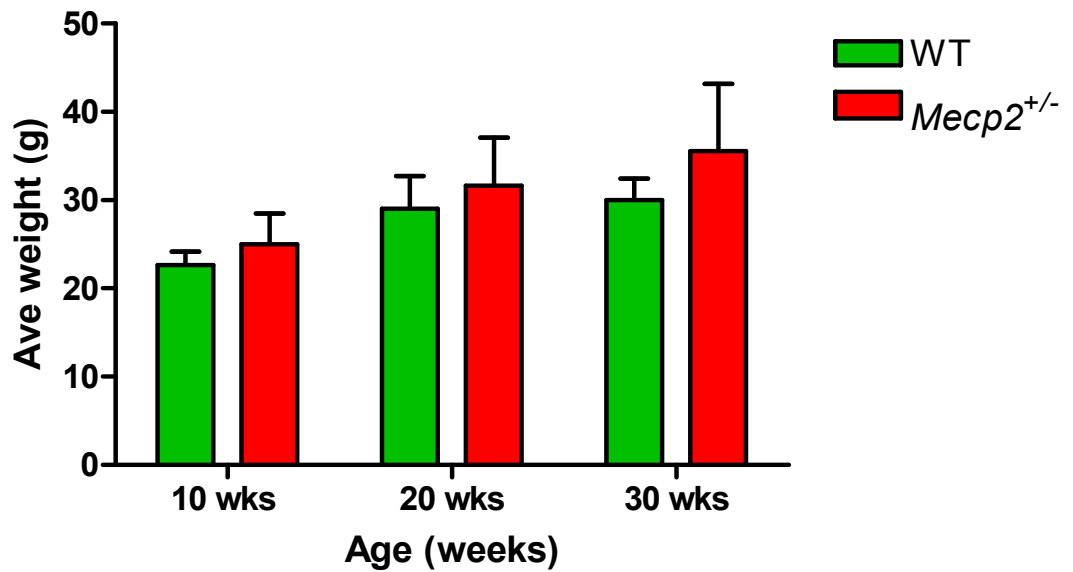


Fig 6-2 Plots to illustrate the average behavioural score of WT and *Mecp2*^{+/-} mice using 3 point and 5 point scales. **A** – 3 point scale. **B** – 5 point scale. Scoring began at 8 wks of age and ceased at 33 wks. Scoring was performed blind to the genotype. WT animals scored 0 throughout majority of the study, occasional scoring can be attributed to the tremor characteristic when animals were nervous. Symptoms were recorded in *Mecp2*^{+/-} animal at 8-9 wks using the 5 point scale yet score was not apparent until 10-11 wks using the 3 point scale.

A Average weight of WT vs *Mecp2*^{+/-} mice



B Average weight of WT vs *Mecp2*^{+/-} (obese)

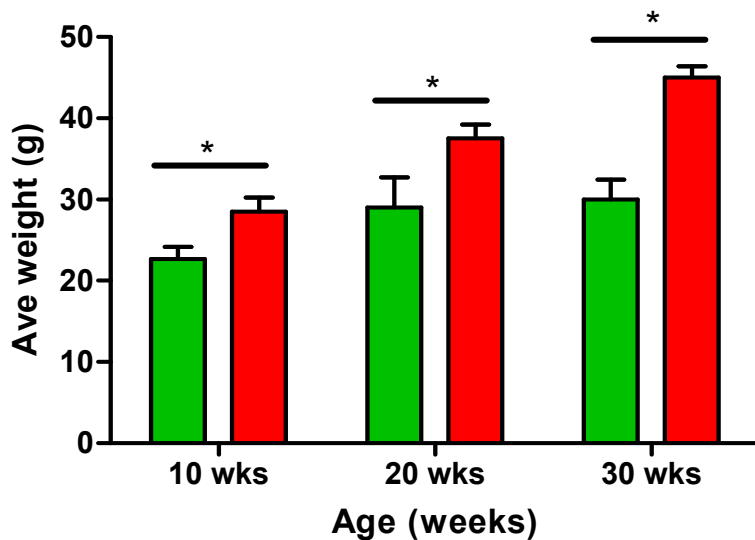


Fig 6-3 Plots to illustrate the average weight of WT and *Mecp2*^{+/-} mice. Human obesity classed a 20-25% above ideal weight. Looked at end weights and plotted only *Mecp2*^{+/-} mice who showed weight 25% greater than that of the WT (>40g). *Mecp2*^{+/-} in this category were found to be significantly heavier than the WT at 10 wks, 20 wks and 30 wks. Data presented as mean ± S.D. 2 way anova with Bonferroni post test. *p<0.05.

6.3.2 Respiratory Traces of *Mecp2*^{+/-} Animals

Respiratory traces of WT at 10 wks (Fig 6-4) showed a regular respiratory rhythm, an increase in respiratory frequency in response to hypercapnia, a mild increase in respiratory frequency in response to hypoxia and a return to baseline breathing when normoxic conditions were restored. *Mecp2*^{+/-} respiratory traces at 10 wks of age also showed a regular respiratory rhythm in air and an increase in respiratory frequency in response to hypercapnia. Respiratory abnormalities were present in the post hypercapnic normoxic periods, with evidence of sighing and apnea. Double breaths also became apparent during hypoxic exposure and apneas become apparent in the post hypoxic normoxic period. Respiratory traces taken at 19 wks (Fig 6-5) showed that the WT maintained a stable respiratory frequency in air and the same pattern of respiratory response to hypercapnia as was observed at 10 wks. The *Mecp2*^{+/-} trace was disordered in air and showed irregular respiratory frequency. Double breaths were also apparent in the *Mecp2*^{+/-} trace during hypoxic exposure and the respiratory frequency was disturbed at 15 min post hypoxia. Respiratory traces taken at 32 wks (Fig 6-6) showed that WT maintained the regular breathing pattern as had been observed at 10wks and 19 wks. The *Mecp2*^{+/-} breathing pattern was irregular in air, showing sighing and irregular respiratory frequency. Respiratory abnormalities were also apparent in the post hypercapnic recovery period with sighing and apnea both being prevalent. Double breaths were observed during hypoxic exposure and the respiratory frequency was notably greater than WT during hypoxic exposure. The post hypoxic periods in the *Mecp2*^{+/-} trace were interspersed with sighing and apnea and an irregular respiratory frequency.

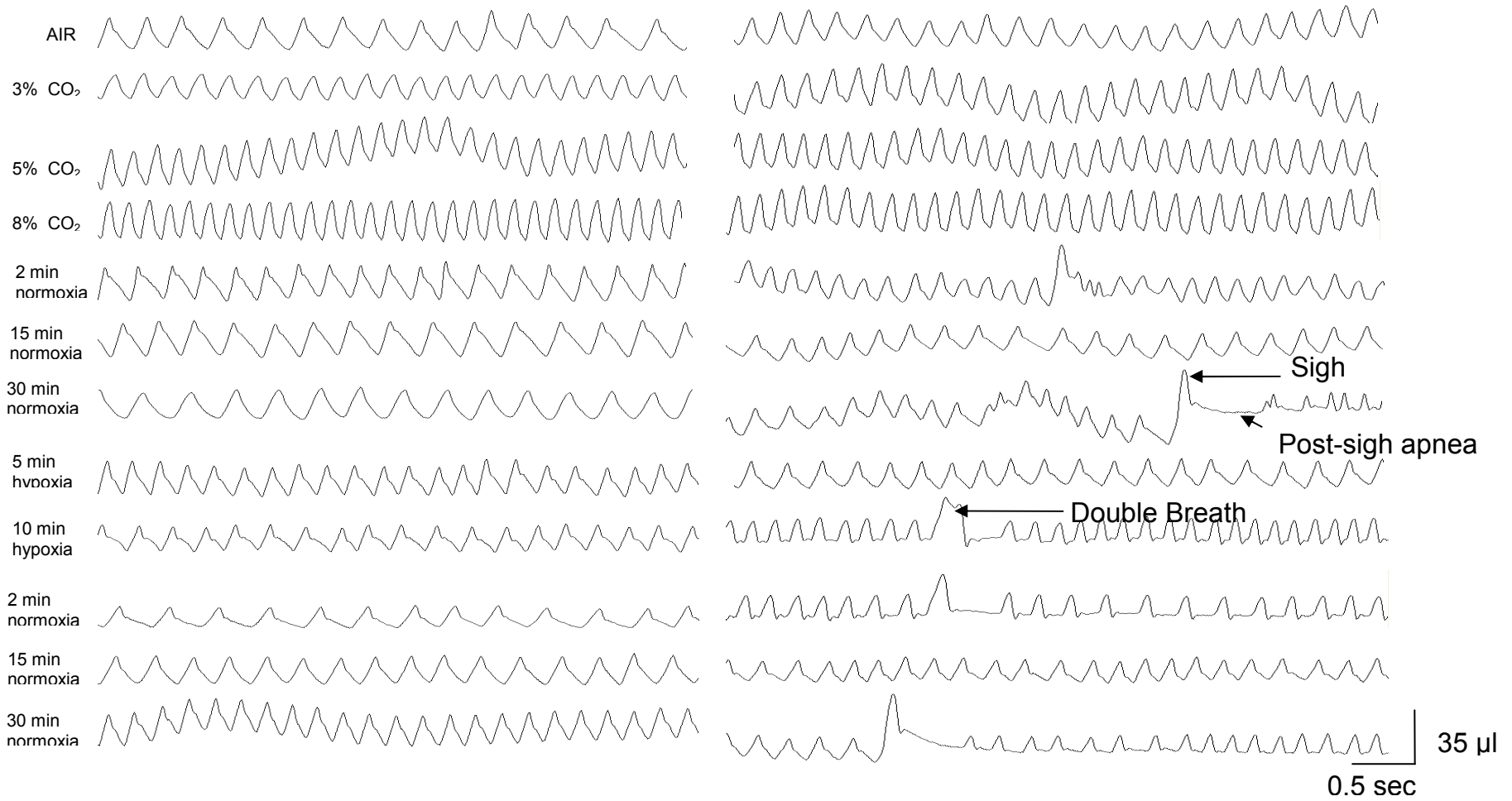


Fig 6-4 Respiratory traces of 10 wk old WT (left) and *Mecp2*^{+/-} (right) animals in normoxia, hypercapnia and hypoxia.

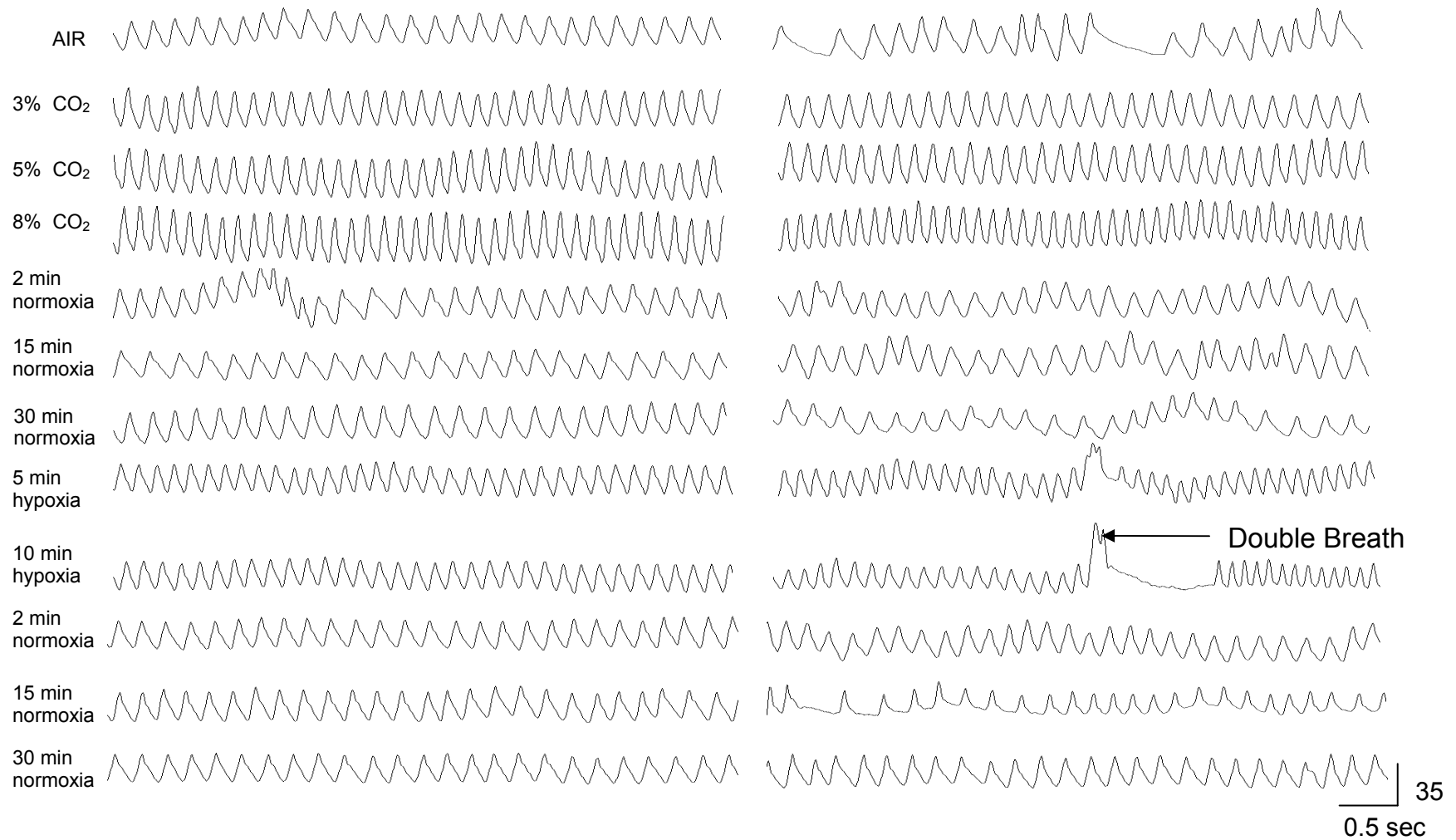


Fig 6-5 Respiratory traces of 19 wk old WT (left) and *Mecp2*^{+/-} (right) animals in normoxia, hypercapnia and hypoxia.

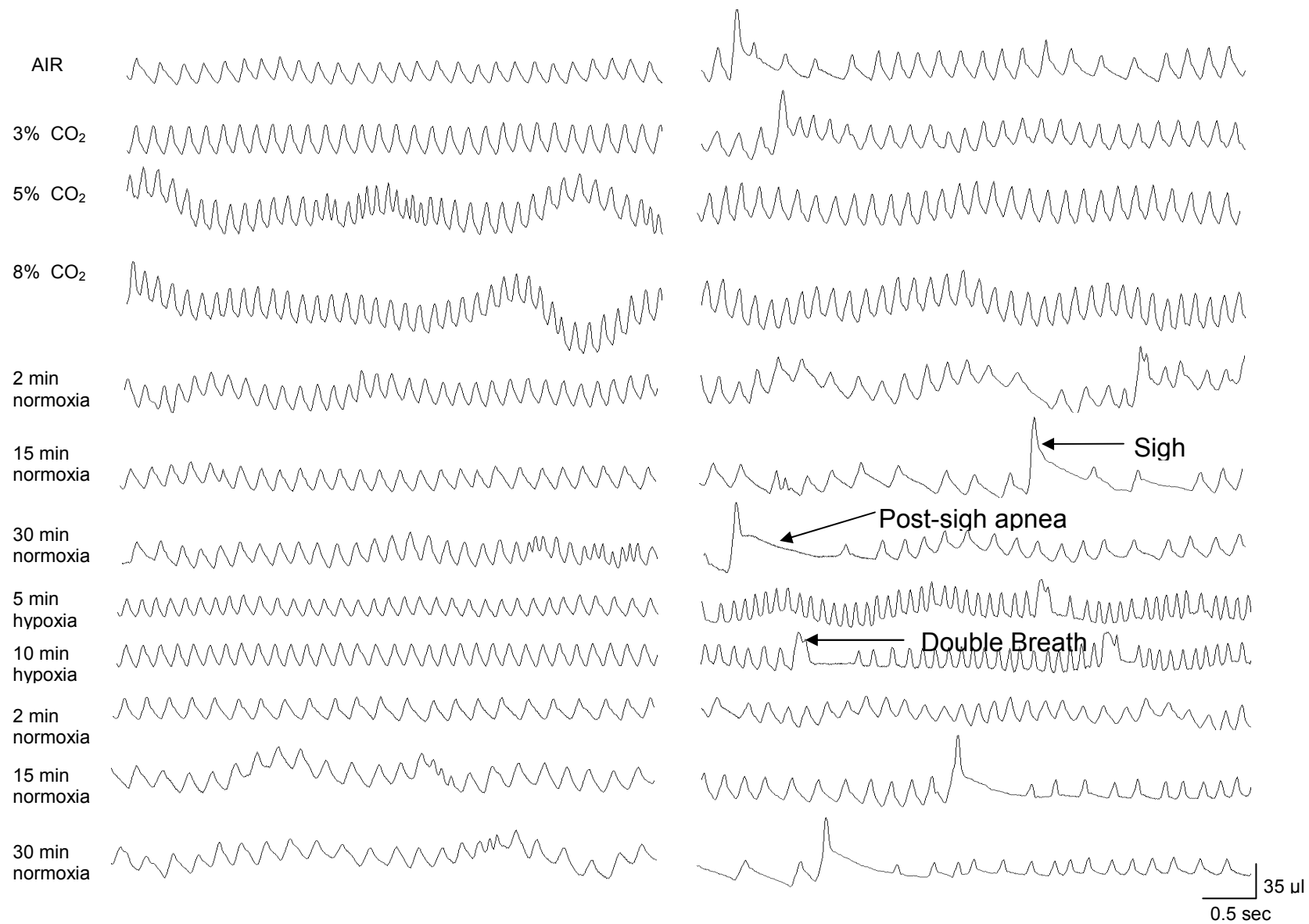


Fig 6-6 Respiratory traces of 32 wk old WT (left) and *Mecp2*^{+/-} (right) animals in normoxia, hypercapnia and hypoxia.

6.3.3 Quantifying Respiratory Abnormalities

At each week, WT animals showed a baseline respiratory frequency of approximately 200-250 bpm (Fig 6-7; 10 wks: 208 ± 28 bpm, 15 wks: 224 ± 35 bpm, 19 wks: 221 ± 25 bpm, 23 wks: 250 ± 36 bpm, 27 wks: 258 ± 27 bpm, 32 wks: 254 ± 22 bpm). WT animals showed an increase in average respiratory frequency in response to 3%, 5% and 8% CO₂ (e.g. 10 wks; 3% CO₂: 268 ± 38 bpm, 5% CO₂: 329 ± 38 bpm, 8% CO₂: 356 ± 19 bpm. 23 wks; 3% CO₂: 303 ± 36 bpm, 5% CO₂: 319 ± 19 bpm, 8% CO₂: 324 ± 40 bpm) and a subsequent decrease in frequency when normoxia was re-established (e.g. 10 wks; 2min: 230 ± 31 bpm, 15 min: 186 ± 22 bpm, 30 min: 179 ± 44 bpm. 23 wks; 2min: 234 ± 33 bpm, 15 min: 225 ± 35 bpm, 30 min: 219 ± 16 bpm). Compared to the average frequency observed at 30 min post hypercapnia, WT showed an increase in respiratory frequency after 5 min exposure to hypoxia (e.g. 10wks; 30 min post hypercap: 179 ± 43 bpm, 5 min hypoxia: 245 ± 21 bpm. 23 wks; 30 min post hypercap: 219 ± 16 bpm, 5 min hypoxia: 258 ± 39 bpm) however in some cases the respiratory frequency of WT animals after 5 min hypoxic exposure was lower than the average baseline respiratory frequency which was recorded at the beginning of the experiment (e.g. 27 wks; air(control): 258 ± 27 bpm, 5 min hypoxia: 248 ± 42 bpm). After 10 min hypoxic exposure, the average respiratory frequency of WT animals showed a trend towards a decrease (eg. 10wks; 5min hypoxia: 245 ± 21 bpm, 10 min hypoxia: 223 ± 29 bpm. 23 wks: 5 min hypoxia: 258 ± 39 bpm, 10 min hypoxia: 247 ± 53 bpm). Following hypoxic exposure, WT animals generally showed a trend towards a decrease in average respiratory frequency at 2 min , 15 min and 30 min (e.g. 23 wks; 2 min post hypoxia: 247 ± 38 bpm, 15 min post hypoxia: 236 ± 24 bpm, 30 min post hypoxia: 207 ± 55 bpm) however at 27 and 32 wks, WT mice showed a slight increase in average respiratory frequency at 30 min post hypoxia (27 wks; 15 min post hypoxia: 196 ± 35 bpm, 30 min post hypoxia: 204 ± 40 bpm. 32 wks; 15 min post hypoxia: 199 ± 21 bpm, 30 min post hypoxia: 227 ± 35 bpm).

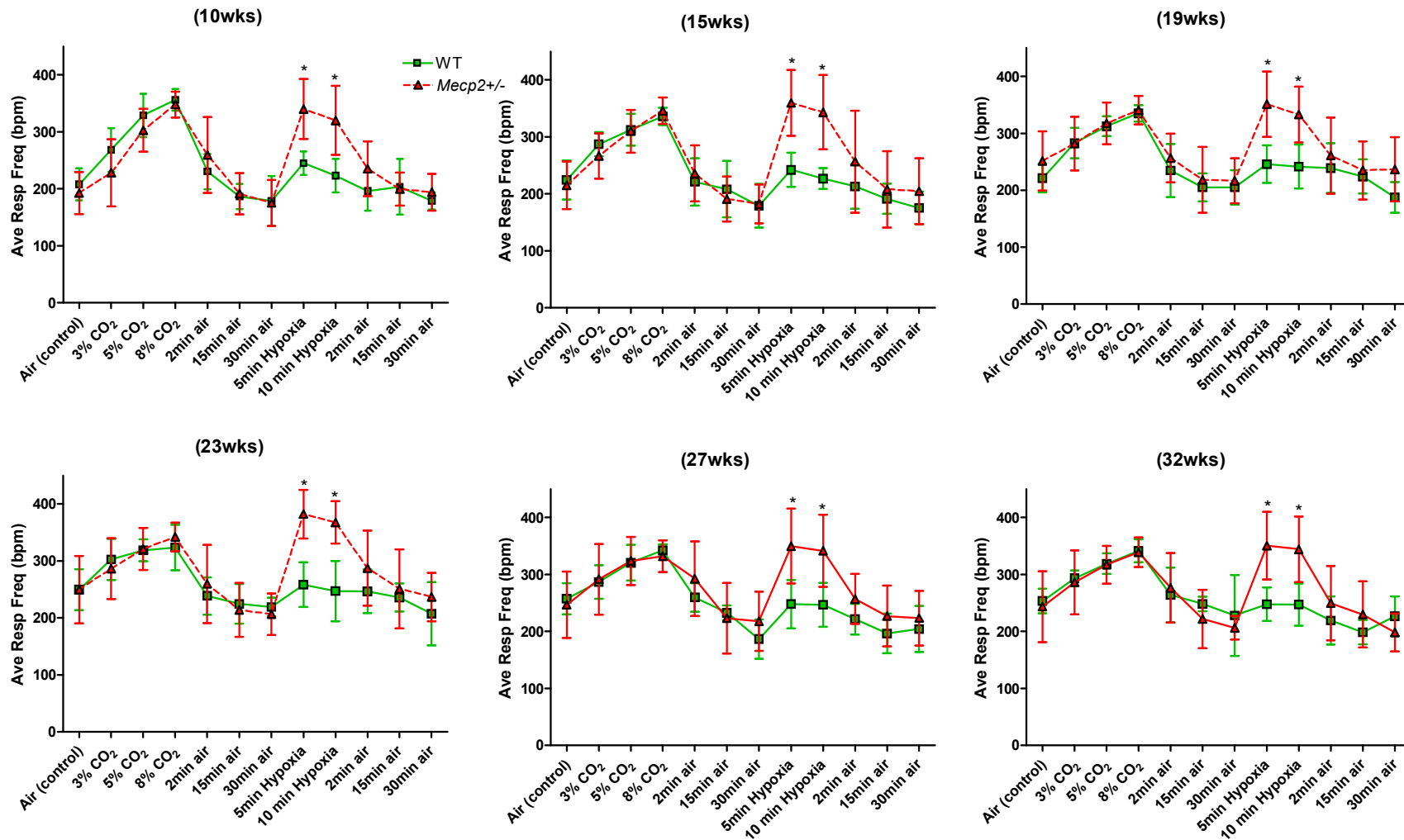


Fig 6-7 Plots to illustrate the average respiratory frequency of WT and *Mecp2*^{+/-} females under each respiratory stimulus. Data presented as mean \pm S.D. Two-way ANOVA assuming Gaussian distribution. Bonferroni post test. *p < 0.05

At each week, *Mecp2*^{+/-} animals had an average baseline respiratory frequency of which was not significantly different to WT (fig 6.7; 10 wks; air(control), *Mecp2*^{+/-}: 193±37bpm, WT: 208±28bpm. 23 wks; air(control), *Mecp2*^{+/-}: 250±59bpm, WT: 250±36bpm, p>0.05). *Mecp2*^{+/-} mice showed an increase in respiratory frequency compared to baseline when exposed to 3%, 5% and 8% CO₂ (e.g. 10 wks; 3% CO₂: 228±59bpm, 5% CO₂: 303±37bpm, 8% CO₂: 348±23bpm. 23 wks; 3% CO₂: 286±54bpm, 5% CO₂: 321±37bpm, 8% CO₂: 342±25bpm) which was not significantly different from the WT response (p>0.05). Post hypercapnia, *Mecp2*^{+/-} mice showed a decrease in respiratory frequency at 2 min, 15 min and 30 min (e.g. 10 wks; 2min: 259±67bpm, 15 min: 192±36bpm, 30 min: 175±40bpm. 23 wks; 2 min: 260±69bpm, 15 min: 214±47bpm, 30 min: 207±36bpm) which again was not significantly different from the WT response (P>0.05). Upon exposure to 10% O₂, *Mecp2*^{+/-} mice exhibited an increase in respiratory frequency compared to both 30 min post hypercapnia and the baseline frequency (e.g. 10 wks; 5 min hypoxia: 340±53bpm, 30 min post hypercapnia: 175±40bpm, air (control): 193±37bpm. 23 wks; 5 min hypoxia: 382±43bpm, 30 min post hypercapnia: 207±36bpm, air (control): 250±59bpm). The response of *Mecp2*^{+/-} mice to hypoxia was significantly greater than the WT at 5 min exposure (e.g. 10 wks; 5min exposure, WT: 245±21bpm, *Mecp2*^{+/-}: 340±53bpm, p<0.05) and at 10 min exposure (e.g. 10 wks; 10 min exposure, WT: 223±29bpm, *Mecp2*^{+/-}: 320±60bpm, p<0.05) in every week studied. *Mecp2*^{+/-} animals showed a decrease in respiratory frequency after normoxia was restored which was not significantly different from the WT (e.g. 10 wks; 2 min post hypoxia, *Mecp2*^{+/-}: 235±48bpm, WT: 196±34bpm. 15 min post hypoxia, *Mecp2*^{+/-}: 200±29bpm, WT: 204±49bpm, 30 min post hypoxia, *Mecp2*^{+/-}: 194±32bpm, WT: 179±15bpm.P>0.05).

It is of interest to note that the exaggerated response of *Mecp2*^{+/-} mice was noted as early as 10 weeks (fig 6-7), which precedes the development of the emergence of the behavioural phenotype as measured in the 3 point scale (fig 6-2). The 5 point scale suggests that at 10 weeks of age there exist mild behavioural symptoms.

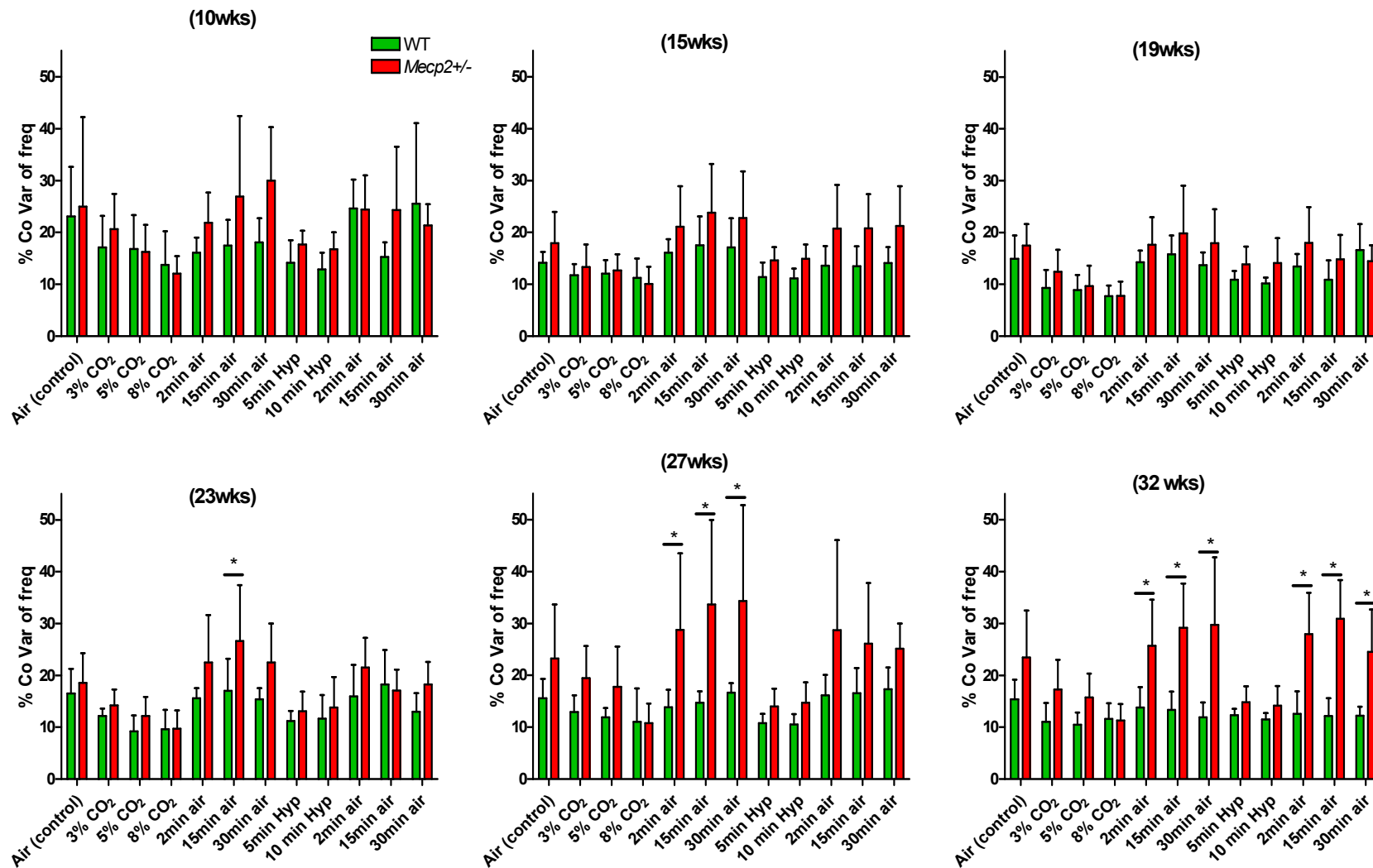


Fig 6-8 Plots to illustrate the coefficient of variation of the average respiratory frequency of WT and *Mecp2*^{+/-} females in normoxia, hypercapnia and hypoxia. Two-way anova assuming Gaussian distribution. Data presented as mean \pm S.D. Bonferroni post test; *p<0.05.

To highlight the variation in respiratory frequency, the coefficient of variation of the average respiratory frequency was calculated for each week (fig 6-8). In normoxic conditions, respiratory variability observed in WT mice was comparable from one week to the next (e.g. 10 wks; air (control): 23 ± 9.4 , 23 wks; air (control): 16.4 ± 4.7 % co var freq). WT show a trend towards a decrease in respiratory frequency in response to CO₂ and hypoxia with a trend towards an increase in variability in recovery periods. At 10, 15 and 19 wks, *Mecp2*^{+/-} females had a trend towards a greater degree of variability in the respiratory pattern compared to the WT during post hypercapnic (10wks; 2 min post hypercapnia, *Mecp2*^{+/-}: 21.9 ± 5.8 , WT: 16 ± 2.9 % co var freq. 15 min post hypercapnia, *Mecp2*^{+/-}: 26.9 ± 15.5 , WT: 17.5 ± 4.9 % co var freq. 30 min post hypercapnia, *Mecp2*^{+/-}: 29.9 ± 10.3 , WT: 18.1 ± 4.6 % co var. 15wks; 2 min post hypercapnia, *Mecp2*^{+/-}: 21 ± 7.8 , WT: 16 ± 2.6 % co var freq. 15 min post hypercapnia, *Mecp2*^{+/-}: 23.8 ± 9.4 , WT: 17.5 ± 5.6 % co var freq. 30 min post hypercapnia, *Mecp2*^{+/-}: 22.8 ± 8.9 , WT: 17.1 ± 5.6 % co var freq. 19wks; 2 min post hypercapnia, *Mecp2*^{+/-}: 17.6 ± 5.4 , WT: 14.2 ± 2.3 % co var freq. 15 min post hypercapnia, *Mecp2*^{+/-}: 19.8 ± 9.2 , WT: 15.8 ± 3.6 % co var freq. 30 min post hypercapnia, *Mecp2*^{+/-}: 17.9 ± 6.5 , WT: 13.7 ± 2.4 % co var freq). At 23 wks, *Mecp2*^{+/-} females had a significantly greater amount of variability in breathing compared to the WT in the 15 min post hypercapnic period (*Mecp2*^{+/-}: 26.6 ± 10.7 %co var of freq, WT: 17 ± 6.1 % co var freq, $p < 0.05$). The difference in variability between WT and *Mecp2*^{+/-} respiratory traces became more apparent as the animals aged. At 27 wks, the *Mecp2*^{+/-} mice had a significantly greater amount of variability in the respiratory trace compared to WT at 2min (*Mecp2*^{+/-}: 28.7 ± 14.8 , WT: 13.9 ± 3.4 %Co var freq, $p < 0.05$), 15min (*Mecp2*^{+/-}: 33.6 ± 16.3 , WT: 14.7 ± 2.3 % co var freq, $p < 0.05$) and 30 min (*Mecp2*^{+/-}: 34.3 ± 18.4 , WT: 16.7 ± 1.9 %co var, $p < 0.05$) post hypercapnia recovery periods. At 32 wks *Mecp2*^{+/-} animals had significantly more variable breathing patterns compared to WT during 2min (*Mecp2*^{+/-}: 25.7 ± 8.8 , WT: 13.8 ± 3.9 % co var freq, $p < 0.05$), 15 min (*Mecp2*^{+/-}: 29.1 ± 8.6 , WT: 13.3 ± 3.2 %co var freq, $p < 0.05$) and 30 min (*Mecp2*^{+/-}: 29.7 ± 13 , WT: 11.9 ± 2.8 %co var freq, $p < 0.05$) post hypercapnia recovery periods. At 32 wks *Mecp2*^{+/-} mice also displayed significantly more variance in breathing than the WT at 2 min (*Mecp2*^{+/-}: 27.9 ± 8 , WT: 12.6 ± 4.4 % co var freq, $p < 0.05$), 15 min (*Mecp2*^{+/-}: 30.9 ± 7.5 , WT: 12.1 ± 3.4 %co var freq, $p < 0.05$) and 30 min (*Mecp2*^{+/-}: 24.5 ± 8.2 , WT: 12.2 ± 1.7 % co var freq, $p < 0.05$) post hypoxic recovery.

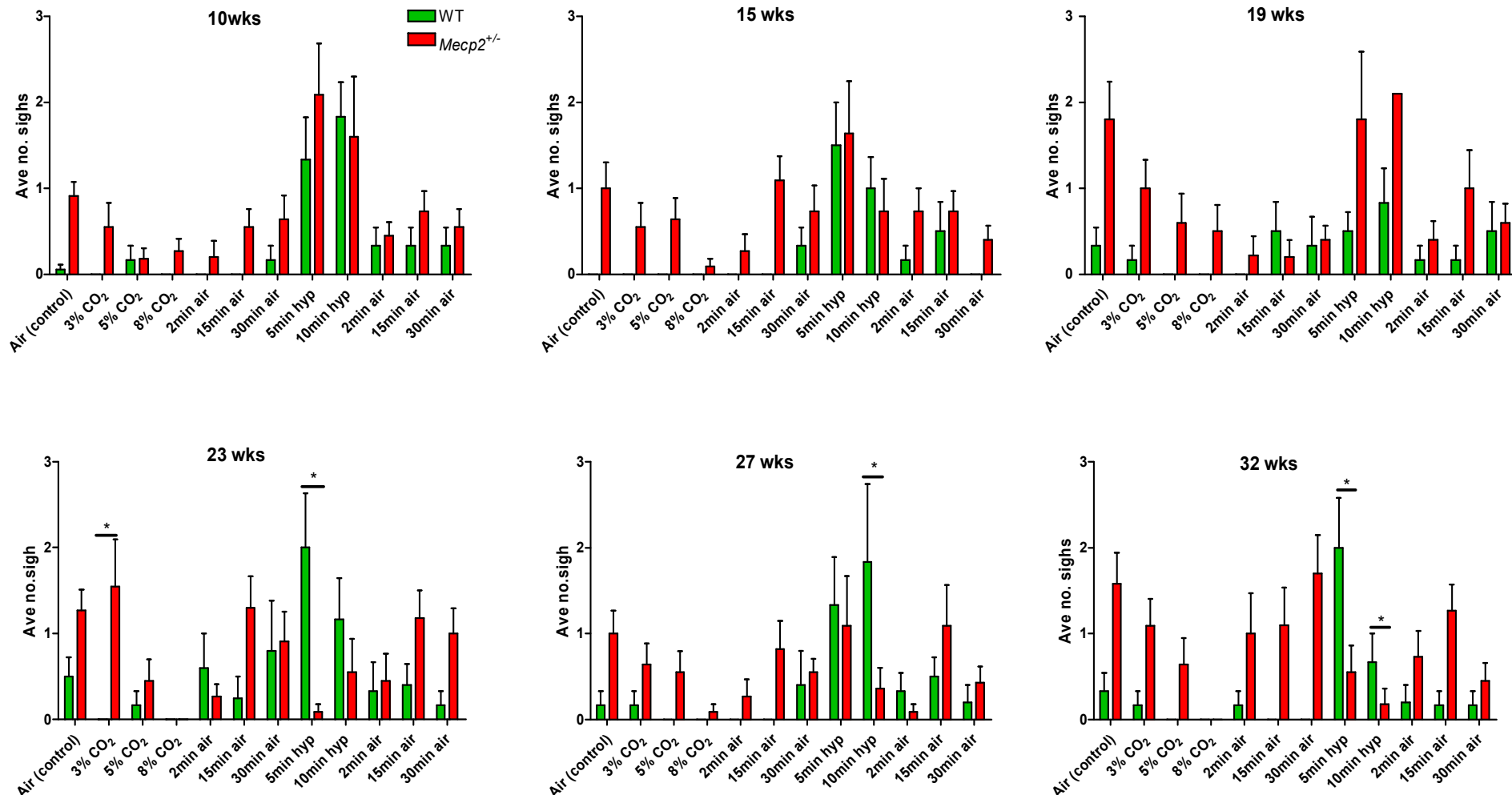


Fig 6-9 Plots illustrating the average number of sighs which occur per 2 min trace in WT and *Mecp2*^{+/-} mice in normoxia, hypercapnia and hypoxia. Data presented as mean ± S.D. Two-way anova assuming Gaussian distribution. Bonferroni post test; *p<0.05.

In air, WT mice exhibited one or fewer sighs per 2 min trace at each week studied (e.g. 10 wks; air (control): 0.1 ± 0.1 sighs. 23 wks; air (control): 0.5 ± 0.5 sighs; fig 6-9). At each week studied, WT animals showed an increase in the occurrence of sighing from baseline values when exposed to hypoxia (e.g. 10 wks; air (control): 0.1 ± 0.1 , 5 min hypoxia: 1.3 ± 1.2 , 10 min hypoxia: 1.8 ± 0.9 sighs. 23 wks; air (control): 0.5 ± 0.5 , 5 min hypoxia: 2 ± 1.5 , 10 min hypoxia: 1.2 ± 1.2 sighs). At all weeks studied, *Mecp2*^{+/-} mice exhibited a trend towards a greater occurrence of sighs compared to the WT in air (e.g. 10wks; air (control), *Mecp2*^{+/-}: 0.9 ± 0.5 , WT: 0.1 ± 0.1 sighs. 23 wks; air (control), *Mecp2*^{+/-}: 1.3 ± 0.8 , WT: 0.5 ± 0.5 sighs, $p > 0.05$). As was observed in WT, *Mecp2*^{+/-} mice exhibited an increased frequency of sighing compared to baseline when exposed to hypoxia at 10wks (baseline: 0.9 ± 0.5 , 5 min hypoxia: 2.1 ± 1.9 , 10 min hypoxia: 1.6 ± 2.3 sighs), 15wks (baseline: 1 ± 1 , 5 min hypoxia: $1.6 \pm 2.$, 10 min hypoxia: 0.7 ± 1.3 sighs) and 19 wks (baseline: 1.8 ± 1.4 , 5 min hypoxia: 1.8 ± 2.5 , 10 min hypoxia: 2.1 ± 2.6 sighs). However, at 23 wks *Mecp2*^{+/-} animals exhibited a reduction in the number of sighs compared to baseline when exposed to hypoxia (baseline: 1.3 ± 0.8 , 5 min hypoxia: 0.1 ± 0.3 , 10 min hypoxia: 0.6 ± 1.3). The occurrence of sighing in *Mecp2*^{+/-} mice from 23 wks onwards was also significantly less than WT when subjected to hypoxic exposure (23 wks: 5 min hypoxia, WT: 2 ± 1.5 , *Mecp2*^{+/-}: 0.1 ± 0.3 , $p < 0.05$. 10 min hypoxia, WT: 1.2 ± 1.2 , *Mecp2*^{+/-}: 0.6 ± 1.3 sighs, $p > 0.05$).

At all weeks studied, double breaths were rare in the WT animals (Fig 6-10), occurring only once or twice per 120 seconds. Double breaths showed a trend towards an increase in frequency in WT during hypoxic exposure (e.g. 15 wks; air: 0 double breaths, 5 min hypoxia: 1.33 ± 0.82 , 10 min hypoxia 1.5 ± 0.55 double breaths, $p > 0.05$). At all weeks studied, *Mecp2*^{+/-} mice had significantly more double breaths than the WT during the hypoxic stimulus (e.g. 15 wks; 5 min hypoxia, WT: 1.3 ± 0.8 , *Mecp2*^{+/-}: 6.9 ± 4.3 double breaths, $p < 0.05$. 10 min hypoxia, WT: 1.5 ± 0.5 , *Mecp2*^{+/-}: 5.1 ± 2.7 double breaths, $p < 0.05$). It is of interest to note that at each week, the number of double breaths showed a trend towards a decrease in *Mecp2*^{+/-} mice after 10 min of hypoxic exposure compared to 5 min of hypoxic exposure (e.g. 15 wks; 5 min hypoxia: 6.9 ± 4.3 , 10 min hypoxia: 5.1 ± 2.7 double breaths).

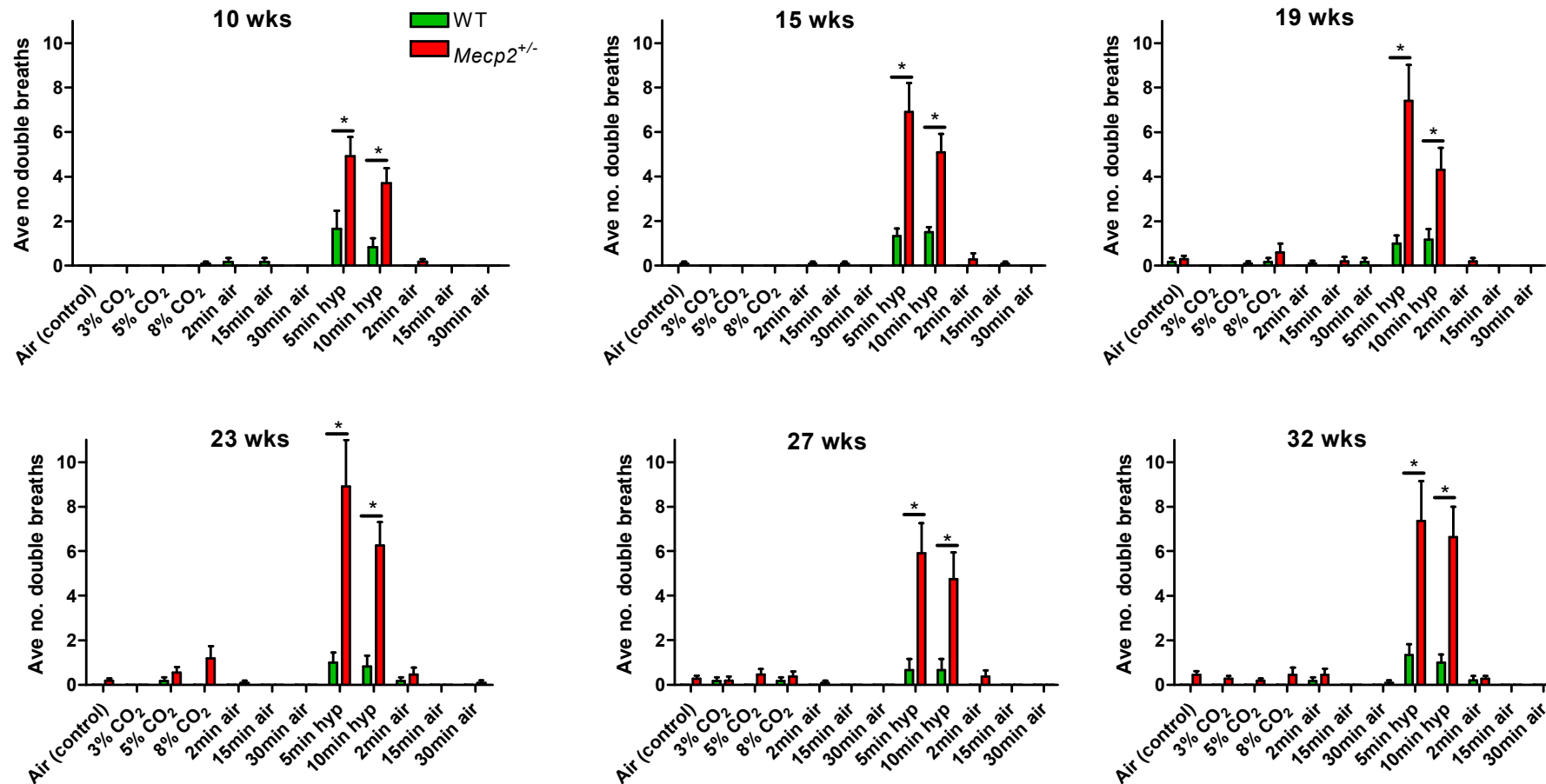


Fig 6-10 Average number of double breaths observed per 2min trace in WT and *Mecp2*^{+/-} females in air and during respiratory stimulus. Data is presented as mean \pm S.D. Two-way anova assuming Gaussian distribution. Bonferroni post test; * $p < 0.05$.

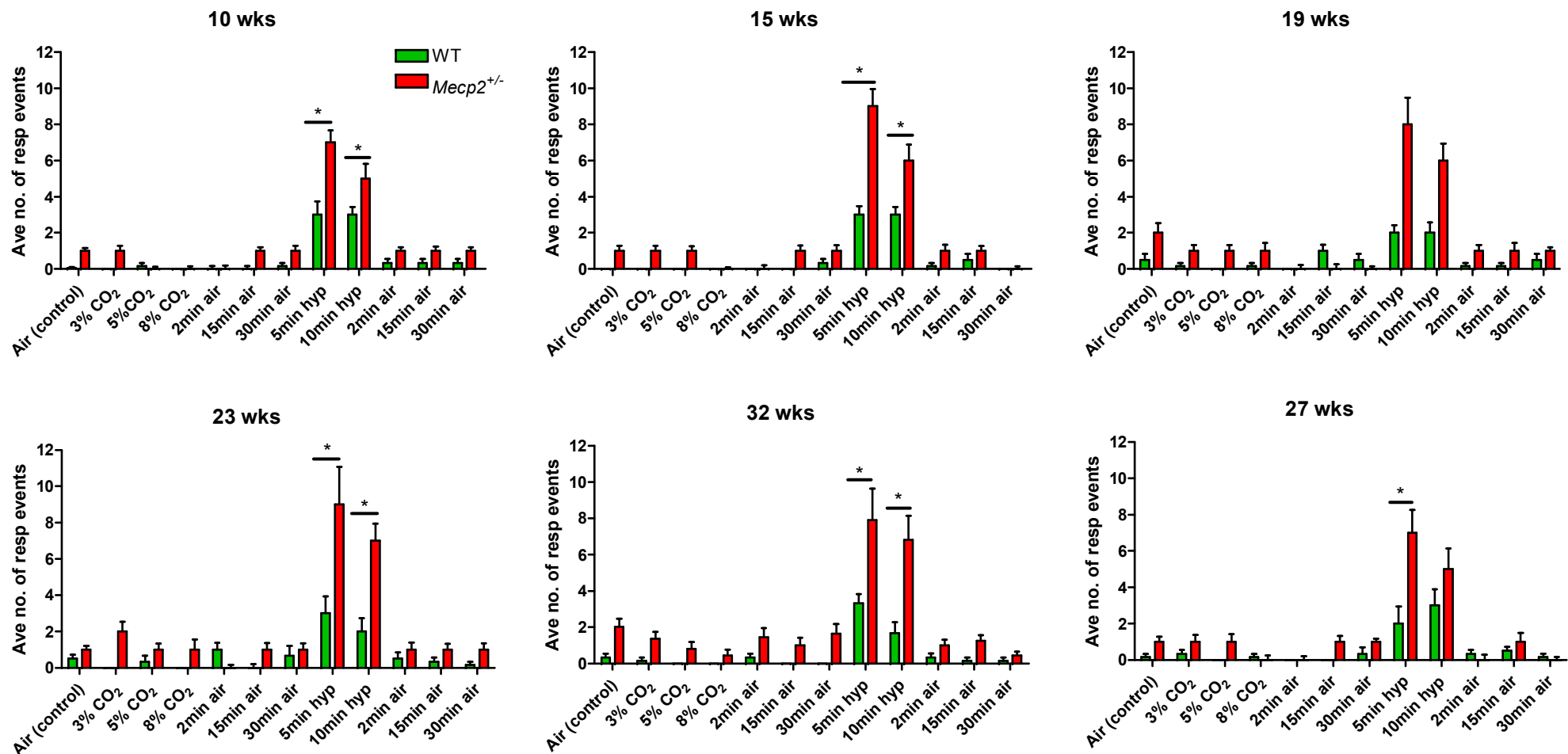


Fig 6-11 Average number of sighs and double breaths per 2min trace in WT and *Mecp2*^{+/-} females in normoxia, hypercapnia and hypoxia. Data is presented as mean ± S.D. Two-way anova assuming Gaussian distribution. Bonferroni post test; *p<0.05.

As mentioned above and illustrated in Figs 6-9 and 6-10, WT animals tended to show fewer sighs and double breaths compared to the *Mecp2*^{+/-} mice. Fig 6-11 shows that in hypoxic conditions, both the WT and *Mecp2*^{+/-} animals show an increase in sighs and double breaths compared to baseline values (e.g. 10 wks; WT air: 0.1±0.1, 5 min hypoxia: 3±1.8, 10 min hypoxia: 3±1 sighs/double breaths. *Mecp2*^{+/-}, air: 1±0.5, 5 min hypoxia: 7±2, 10 min hypoxia: 5±2.7 sighs/double breaths). In Fig 6-9, at 23 wks it was observed that *Mecp2*^{+/-} mice exhibited fewer sighs than WT during hypoxic exposure. However, Fig 6-11 shows that at each week studied, the *Mecp2*^{+/-} mice have more sighs and double breaths combined than WT when exposed to hypoxia. This suggests that the sighing profile of *Mecp2*^{+/-} animals changes at 23 wks to that of the double breath.

In all weeks studied, apneas in the WT mice were rare in normoxic, hypercapnic and hypoxic conditions with a maximum occurrence of 0.33±0.82 apneas per 2 min trace. Apneas were much more frequent in *Mecp2*^{+/-} mice than WT in normoxic condition (10 wks; WT: 0.33±0.82, *Mecp2*^{+/-}: 2.24±3.61 apneas per 2 min trace). As can be seen in Fig 6-12 the application of 3%, 5% and 8% CO₂ abolished the occurrence of apnea in the *Mecp2*^{+/-} mice. Apneas in the *Mecp2*^{+/-} mice were most apparent during the post hypercapnic recovery period (10 wks; air: 2.2±3.6 apneas, 2 min post hypercapnia: 0.4±0.8 apneas, 15 min post hypercapnia: 3.6±7.9 apneas, 30 min post hypercapnia: 4.8±8.5 apneas).

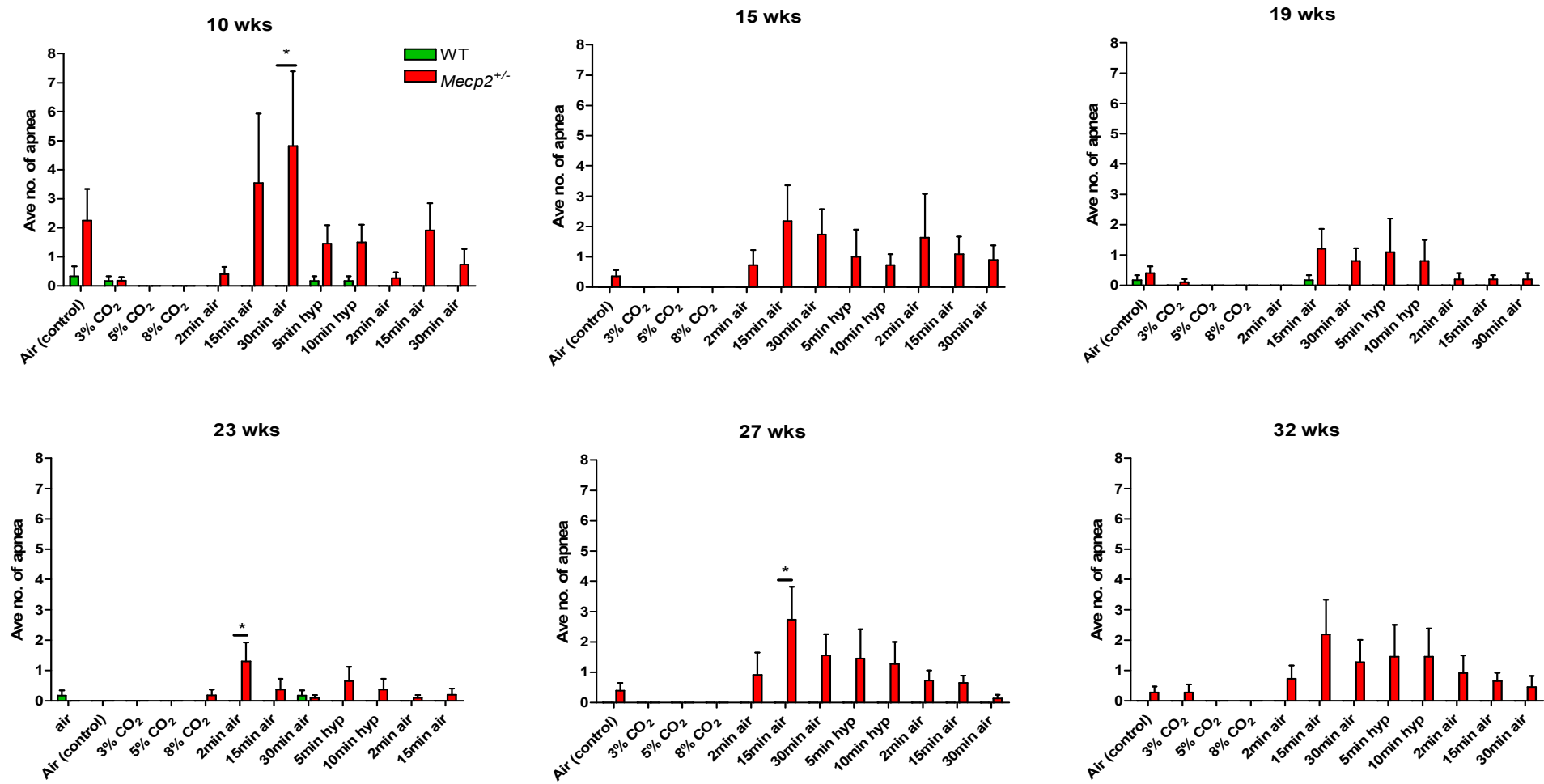


Fig 6-12 Average number of apneas observed per 2min trace in WT and *Mecp2*^{+/-} females under each respiratory stimulus. Two-way anova assuming Gaussian distribution. Bonferroni post test to look at row interaction ;* p<0.05

6.3.4 PAH analysis

Measurement of the right ventricular systolic pressure (RVSP; Fig 6-13 plot A) showed that there was no significant difference between WT and *Mecp2*^{+/-} mice (WT: 22.19±3.15, *Mecp2*^{+/-}: 24.09±2.67 mmHg, p<0.05). There was a trend towards an increased RV/LV+S ratio (Fig 6-13 plot C) yet statistical analysis revealed no significant difference between the two genotypes (WT: 0.19±0.02, *Mecp2*^{+/-}: 0.22±0.02 mmHg, p>0.05). There was also a trend towards a greater percentage of remodelled pulmonary blood vessels in *Mecp2*^{+/-} mice compared to WT (Fig 6-13 plot D) but this was not statistically significant (WT: 15.73±23.65, *Mecp2*^{+/-}: 40.61±19.67 mmHg, p>0.05). Systemic blood pressure (Fig 6-13 plot B) showed a trend towards an increase in *Mecp2*^{+/-} mice compared to WT (WT: 59.97±7.78, *Mecp2*^{+/-}: 71.97±12.04 mmHg, p>0.05).

The images in Fig 6-14 illustrate the difference between remodelled and non-remodelled pulmonary blood vessels of WT and *Mecp2*^{+/-} mice. WT mice exhibited a greater number of non-remodelled vessels compared to remodelled vessels. *Mecp2*^{+/-} tissue tended to have a higher percentage of remodelled pulmonary vessels. Remodelled vessels were characterised by muscularisation of the elastic lamina. Elastic fibres were also present in the alveolar tissue of the lung (Fig 6-14, white arrow) and appeared to be more abundant in *Mecp2*^{+/-} lung compared to WT.

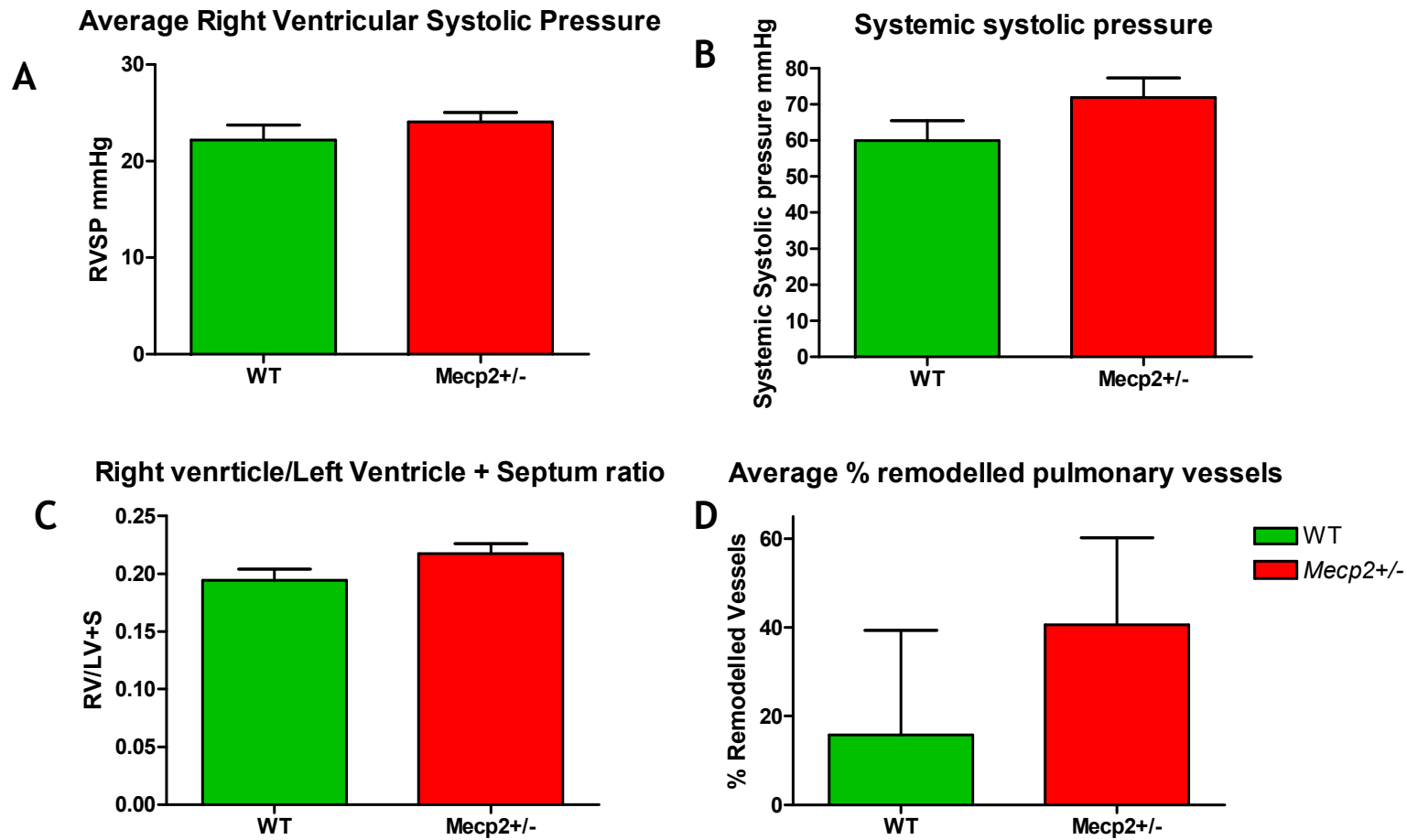


Fig 6-13 Plots to illustrate the measurement of indices of pulmonary arterial hypertension in WT (n=4) and *Mecp2*^{+/-} (n=8) mice. **A** – Average right ventricular systolic pressure (RVSP). **B** – systemic systolic pressure. **C** – Ratio of RV/LV+S, created by comparing the weight of the right ventricle (RV) with the left ventricle and septum (LV+S). **D** – The average percentage of remodelled pulmonary blood vessels with diameter <100µm. T-tests showed no significant difference between the genotypes in any of the parameters studied (p<0.05).

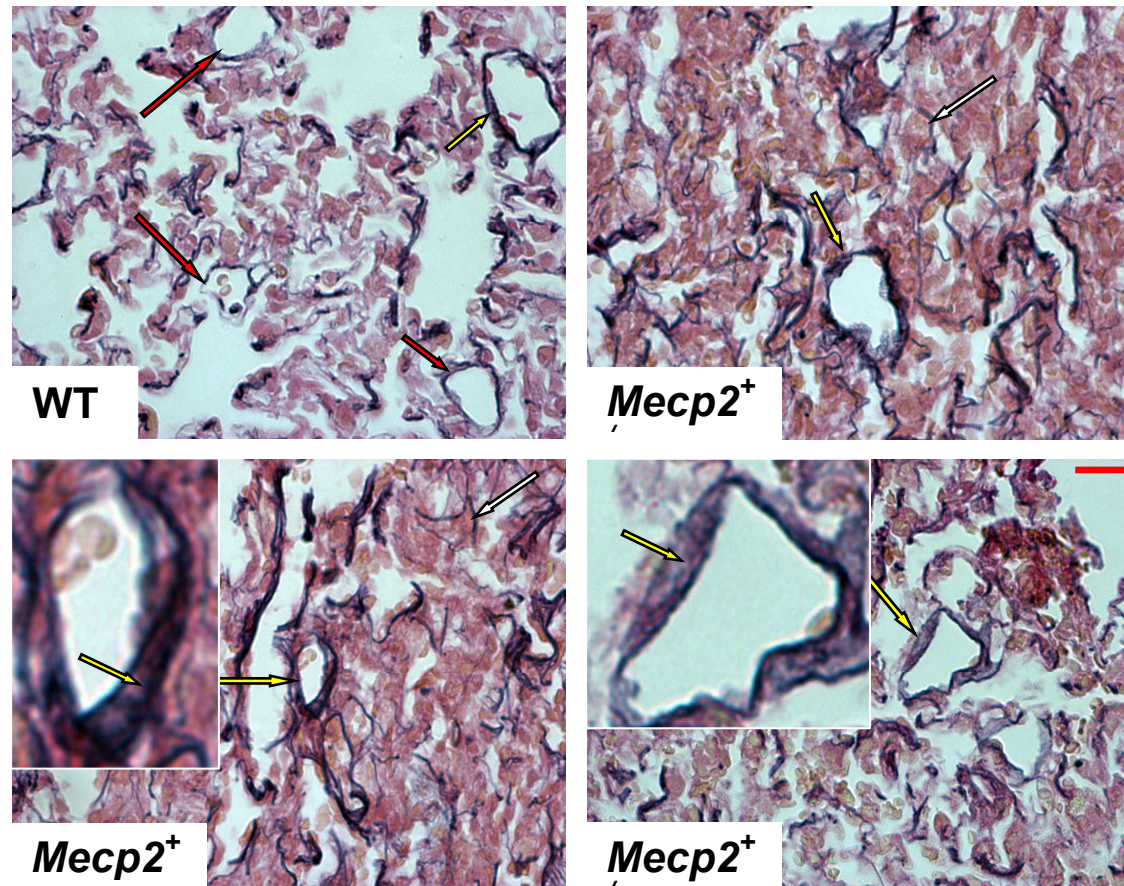


Fig 6-14 Light microscopy images of WT and *Mecp2*^{+/-} tissue stained with Miller's elastin stain and counterstained with Van Giesson's. Red arrows indicate non-remodeled blood vessel. Yellow arrows indicate remodeling of blood vessel as indicated by muscularisation of the elastic lamina surrounding the vessel (highlighted in the inserts in the lower panels). White arrow indicates elastin fibre. These fibres appeared to be more numerous in the *Mecp2*^{+/-} lung compared to WT. Scale bar = 20µm.

6.4 DISCUSSION

6.4.1 Behaviour

Development of the RTT-like phenotype in female heterozygous *Mecp2*^{+/-} mice is delayed compared to *Mecp2*^{-/y} male mice (Guy *et al.*, 2001). Whereas the *Stop/y* mice in chapter 3 exhibited symptoms from as young as 5 weeks old, WT and *Mecp2*^{+/-} animals were behaviourally similar from birth up to 5-8 weeks of age as previously reported (Bissonnette & Knopp, 2006). The RTT-like phenotype of the *Mecp2*^{+/-} females became apparent at 8-10 wks old and reached a plateau at about 24 wks of age (Fig 6-2). According to the 3 point scale used to score the *Mecp2*^{+/-} mice in this study (Fig 6-2 plot A), the animals showed behavioural symptoms at 11-13 wks of age which was earlier than was noted by Guy *et al.*, (2007). This could be due to the fact the mice studied by Guy *et al.* were maintained on a C57BL6 background whereas the females in this chapter were bred on the BALB/c background as it was found that this strain of mouse resulted in improved breeding. Also, there may be some variation in the way that each experimenter scores the behaviour of the animals which may account for the difference between the scores recorded in this study and those reported by Guy *et al.*, (2007).

The new 5 point scale that was devised illustrated that RTT-like symptoms became apparent from 9 wks of age (Fig 6-2 plot B), a week earlier than was described by the 3 point scale. This suggests that adding more descriptors to the scoring system improves detection of subtle changes in the behavioural phenotype. Many studies of the respiratory system of MeCP2 deficient mice do not score the phenotype of the animals as they develop (Viemari *et al.*, 2005; Voituron *et al.*, 2009). Scoring the animals behaviourally allows comparison between the appearance and development of the respiratory abnormalities and that of the behavioural phenotype. Observations can then be made as to whether respiratory abnormalities precede the behavioural phenotype or vice versa. Respiratory abnormalities including double breaths, apneas, sighing and an exaggerated ventilatory response to hypoxia all became apparent in the *Mecp2*^{+/-} mice from 10 wks of age, which precedes the onset of the severe RTT-like behavioural phenotype. These data may suggest that, from a clinical stand point, measuring respiratory parameters of RTT patients early on in life using

techniques such as plethysmography may prove useful in predicting and preparing for the onset of a more severe behavioural phenotype as the patient matures.

Whereas the first week of postnatal development in the mouse is usually likened to the first year of development in the human, the appearance and progression of the RTT like phenotype in the female mouse model corresponds more closely to the human RTT phenotype in real time rather than developmental time. The development of a more severe behavioural phenotype in the female mice occurred at about 4-6 months of age, and in the human the RTT phenotype begins to develop at approximately 6-18 months of age. The period of normal development in *Mecp2*^{+/-} mice which precedes the onset of the RTT phenotype indicates that MeCP2 may not be necessary for early development, but the delayed appearance of the phenotype suggests MeCP2 plays a key role in maintaining neuronal function during later stages of development (Guy, Gan et al. 2007; Gaultier, Bissonnette et al. 2008). It was also noted that some females developed an obese phenotype (Fig 6-3 plot B) as previously reported. This could be linked to reports of increase levels of leptin in Rett patients when compared to controls (Considine & Caro, 1997) given that there is a known positive correlation between leptin concentrations and BMI in humans (Blardi *et al.*, 2007). It is also hypothesised that decreased MeCP2 expression within the hypothalamus could affect the functioning of leptin, a key controller of energy homeostasis (Kerr *et al.*, 2008). However, the majority of Rett patients do not suffer obesity; rather they often display a stunted growth pattern. Leptin levels are increased during infections (Fantuzzi & Faggioni, 2000) and thus it is proposed that the increased leptin levels found in RTT patients are due to a chronic inflammatory state present in the patients which arise from common respiratory infections (Blardi *et al.*, 2007). As discussed in chapter 5, some of the male MeCP2 deficient mice had signs of lung pathology and it remains unknown as to whether this may be the result of a respiratory infection. It could be hypothesised that the obese phenotype exhibited by some of the *Mecp2*^{+/-} animals could be the result of increased leptin levels due to respiratory infection. However, there appeared to be no relationship between the obese phenotype of the mice and a more severe respiratory phenotype. Nor was the obese phenotype associated with a more severe behavioural score.

Data from PAH analyses revealed that *Mecp2*^{+/-} mice showed a trend towards an increased systemic blood pressure compared to WT (Fig 6-13 plot B). Since blood pressure is known to be increased by obesity, it could be that the rise in systemic blood pressure in *Mecp2*^{+/-} animals could be secondary to the obese phenotype exhibited.

6.4.2 The Hypercapnic and Hypoxic Response of *Mecp2*^{+/-} Mice

Exposure to hypoxia usually results in an initial increase in respiratory frequency due to signalling of the respiratory controllers by the carotid bodies. However, WT animals showed a surprisingly small respiratory response to hypoxic exposure at all weeks studied (Fig 6-4). This may be due to strain effects, as studies have shown C57BL6 mice do not show a significant increase in respiratory frequency compared to baseline when exposed to acute hypoxia (Ward *et al.*, 2007). Although the *Mecp2*^{+/-} mice in this study were maintained on a BALB/c background, the transgenic line was originally bred on a C57BL6 which may have some influence on the hypoxic response. Other research reveals that strain does not appear to affect the hypercapnic response and only has a bearing on the hypoxic response (Adachi *et al.*, 2006) which could account for the fact that the WT in this study have an increased respiratory frequency in response to hypercapnic exposure but a blunted respiratory response to hypoxia. *Mecp2*^{+/-} mice exhibited a rise in ventilation similar to that of the WT in response to 3%, 5% and 8% CO₂ exposure, a response also noted by Bissonette *et al.*, (2006) who observe that *Mecp2*^{+/-} mice exhibit an increase in ventilation (Ve) which is comparable to the WT when exposed to 3%, 5% and 7% CO₂. This indicates that the exaggerated response to hypoxia in *Mecp2*^{+/-} mice is controlled separately to the response to hypercapnia.

(Bissonnette & Knopp, 2006) describe an increase in ventilation of 5 months old *Mecp2*^{+/-} mice that exceeds WT in the first minute of exposure to a hypoxic (8% O₂) gas mixture. This group also reports that ventilation returns to control levels in WT and *Mecp2*^{+/-} animals in the fifth minute of hypoxic exposure, with *Mecp2*^{+/-} animals showing a lower Ve than WT. In contrast to this, data in this chapter illustrates that the exaggerated response to hypoxia compared to WT was maintained at both 5 min and 10 min hypoxia and respiratory frequency did not return to control level until 2 min post hypoxia recovery in air (Fig 6-7).The

Mecp2^{+/-} animals in this chapter demonstrated an exaggerated response to hypoxic stimuli compared to the WT from as early as 10 wks old (Fig 6-7). The same exaggerated response to hypoxia was also shown in *Mecp2*^{-/-} male mice compared to WT as early as post natal day 25 (Voituron *et al.*, 2009) data which suggest that MeCP2 deficiency leads to changes in the hypoxic response. Hypoxia is detected by the carotid body chemoreceptors which have inputs to the dorsal medulla, where activation of the respiratory network occurs to increase ventilation and restore normoxic conditions (Gaultier *et al.*, 2008). The altered response to hypoxia observed in the *Mecp2*^{+/-} mice in this chapter could be due to a problem with O₂ sensitivity of the carotid bodies. Application of dopamine onto carotid bodies causes a decrease in ventilatory response to hypoxia (Bee & Pallot, 1995) and blockade of dopamine autoreceptors results in increased chemoafferent activity and ventilation in anaesthetized cats (Iturriaga *et al.*, 1994). As TH is a marker of noradrenergic and dopaminergic neurons, it follows that a reduction in TH expression may also indicate reduced dopamine expression. Chapter 3 illustrated a decreased expression of TH expressing neurons in some adrenergic areas including the A1/C1 and A2/C2 of *Mecp2*^{-/-} mice. Thus, if the female mice also present a reduction in TH, a reduction in dopamine levels may also result which could account for the exaggerated response to hypoxia in the *Mecp2*^{+/-} animals. Indeed reduced TH expression has been reported in the petrosal ganglion and adrenal medulla of *Mecp2*^{+/-} mice, with a tendency towards reduction in the carotid body and superior cervical ganglion (Roux *et al.*, 2008). BDNF null mice also exhibit a loss of dopaminergic neurons of the petrosal ganglion (Erickson *et al.*, 2001), neurons which are important in the chemoafferent pathway. Since MeCP2 deficient mice are known to have reduced BDNF levels this may have a knock on effect on dopamine levels and could contribute to the exaggerated response to hypoxia.

The respiratory rhythm generating preBötC may be implicated in the response to hypoxia. Ward *et al.*, (2011) illustrate that *Mecp2*-null mice have exaggerated responses to 10% O₂ as do male mice which have a targeted removal of MeCP2 in HoxB1 tissues, tissues which may include the area of the preBötC. When MeCP2 is reintroduced to the HoxB1 tissues, there is a recovery of the hypoxic response and increases in ventilation when exposed to hypoxia become similar to WT. Also, rats with bilateral lesions to the preBötC have a disturbed respiratory

rhythm and an altered response to hypoxia with frequent apneas 2-7 min after exposure to 4.4% O₂ (Gray *et al.*, 2001) and NK1R knock out mice present a reduced response to hypoxia (Ptak *et al.*, 2002). Taken together, these data suggest that the preBötC may have an involvement in the hypoxic response, likely in integrating information from the peripheral chemoreceptors. In chapter 3, staining for NK1R in preBötC showed a trend towards reduced number of NK1 expressing neurons in MeCP2 deficient mice compared to WT. The n number in this study is low and therefore a robust conclusion can not be made from these data; however, if NK1R is reduced in the preBötC of *Mecp2*^{+/-} mice, this may contribute towards their altered response to hypoxia and increased respiratory variability. Further investigation is required at an anatomical level.

The methods applied in this chapter prevented blood gas sampling which may have provided a greater insight to the chemosensitivity of mutant animals. Since hypercapnia is defined as a blood gas level of 45mmHg CO₂, it would be of benefit to perform blood gas analysis of the animals during the experiments to check that the blood of each animal develops the same level of hypercapnia. If MeCP2 deficient mice are subject to periods of apnea and hyperventilation then these respiratory characteristics could affect blood gas levels and thus the blood of each animal may not develop a uniform level of hypercapnia or hypoxemia even when exposed to the same hypercapnic or hypoxic stimulus respectively.

6.4.3. Respiratory Variability and Maturity of Neurons

It is suggested that neurons can develop in the absence of MeCP2, given that RTT patients and MeCP2 deficient mice develop normally to begin with, but the cells produced may be functionally unstable (Guy *et al.*, 2001), indicated by the development of behavioural and respiratory phenotypes. Although respiratory abnormalities such as apnea and double breaths are present as early as 10 wks old in *Mecp2*^{+/-} females (Figs 6-10 and 6-12), the variability in the average respiratory frequency is not significantly different from WT at this age, highlighting a period of normal development in *Mecp2*^{+/-} animals. The variability in the respiratory pattern post hypercapnia and post hypoxia became significantly greater in *Mecp2*^{+/-} mice compared to WT from 23 wks onwards, indicating instability within the respiratory network. The symptoms of the RTT phenotype are not associated with neuronal death (Armstrong *et al.*, 1995; Roux

et al., 2007) implying instead that there may be a failure of neurons to reach maturity, indicated by the presence of reduced dendritic branching in the cerebral cortex (Armstrong *et al.*, 1995) and reduced neuronal size throughout the brains of RTT patients (Bauman *et al.*, 1995). The fact that respiratory variability becomes significantly greater in *Mecp2*^{+/-} compared to WT at 23 weeks onwards (Fig 6-8) may highlight a developmental stage at which neurons that lack MeCP2, and hence failed to reach maturity, become more important in the respiratory process and thus respiratory abnormalities become more apparent. The increase in post-stimulus respiratory variability at 23 wks onwards may also indicate functional instability of neuromodulator releasing neurons such as serotonergic neurons which are involved in both chemoreception and the stability of the respiratory rhythm. Functional instability of neurons may also affect neuron groups such as the nTS, an area responsible for integrating input from chemoreceptors and stretch receptors within the lung relaying the information to medullary centres, and also centres such as the preBötC complex which drives respiratory rhythm. MeCP2 has been shown to have an important role neuronal maintenance given that removal of MeCP2 from the neurons of adult mice leads to reduction in several synaptic proteins, a reduction in brain size and an increase in neuronal density (Minh *et al.*, 2012) and also recapitulates many of the behavioural deficits which develop in the absence of MeCP2 in early life (McGraw *et al.*, 2011).

6.4.4 Sighing and Double Breaths

As discussed in chapter 3, sighs are high amplitude breaths which are followed by a post-sigh apnoea (Fig 3-14; Voituron *et al.*, 2009). There are suggestions that sighs serve to increase lung compliance and prevent alectasis (Glogowska *et al.*, 1972), that they may act to reset respiratory controllers (Baldwin *et al.*, 2004) or that they have a role in triggering arousal from sleep (Franco *et al.*, 2003). Although their function is not well understood, sighing is considered to be a normal facet of respiratory activity. Previous work on *Mecp2* KO mice indicates that sighing may be characteristic of the breathing phenotype of RTT (Voituron *et al.*, 2010). As discussed in chapter 3, sighs are common in the neonate and young infant (Cross *et al.*, 1960) who both present under developed respiratory patterns, suggesting that sighing may be an indication of respiratory immaturity. In this study it was observed that sighs occurred more frequently in *Mecp2*^{+/-} mice

compared to WT (Fig 6-9) which could be an indication of an immature respiratory network. The frequency of sighing in *Mecp2*^{+/-} animals increased from 10 wks to 32 wks, highlighting how the lack of MeCP2 leads to an immaturity in the respiratory network which becomes increasingly apparent with age. Data in chapter 3 revealed that reactivation of MeCP2 in *Stop/y,cre* mice resulted in the reduction of sighing (Fig 3-10) implying again that a lack of MecP2 leads to immature or poorly maintained respiratory neurons and that reactivation of MeCP2 can rescue these underdeveloped neurons.

In cats, hypoxia and hypercapnia cause an increase in the occurrence of sighs (Cherniack *et al.*, 1981) and in anaesthetised rats hypoxia is thought to have a more profound effect on the frequency of sighing than hypercapnia (Bartlett Jr, 1971). The data in this chapter illustrates that hypoxia causes an increase in sigh frequency in *Mecp2*^{+/-} mice from 10 wks old to 23 wks old (Fig 6-9). There is an indication that chemoreception may play a key role in the control of sighing behaviour, as rats which have their carotid nerves severed no longer exhibit sighs (Bartlett Jr, 1971). The increased occurrence of sighing in the *Mecp2*^{+/-} females in response to hypoxia taken together with the exaggerated increase in respiratory frequency suggests an underlying deficit either in the detection of O₂ by the carotid bodies, or in the relaying of information from chemoreceptors such as the carotid bodies to respiratory controllers within the medulla. As previously discussed, Roux *et al* show that *Mecp2*^{+/-} mice have reduced TH expression compared to WT in the petrosal ganglion and adrenal medulla, areas which are important in the chemoafferent response. This reduction in TH expression may also suggest that the neurons in these chemoafferent regions are less able to produce dopamine, an important modulator of the chemoafferent response (Roux *et al.*, 2008).

The increased occurrence of sighing in MeCP2 deficient mice may be influenced by the level of neuromodulators within the respiratory network. NA releasing neurons have already been shown to be involved in the respiratory network, and it is known that there is reduced expression of TH, a marker for NA neurons, in the A1/C1 and A2/C2 of MeCP2 deficient male mice at one month and two months old respectively (Viemari *et al.*, 2005). This NA deficit which develops over time may result in reduced signalling to the respiratory network and could

account for the development of respiratory abnormalities. Also, there is evidence that breathing disturbances become more severe in MeCP2 deficient male mice at approximately 2 months old; the time point at which 5-HT system becomes disturbed (Viemari *et al.*, 2005). Future work may involve investigating the levels of bioamines such as NA and 5-HT in the female *Mecp2*^{+/-} animals to observe whether the female model develops the same neuromodulatory deficits as the male MeCP2 deficient model.

The preBötC is a site of respiratory rhythmogenesis and inspiratory control (Smith *et al.*, 1991) and as sighs are breaths with a large inspiratory amplitude, it can be suggested that the increase in sighing activity in *Mecp2*^{+/-} mice may also be driven by changes in the preBötC. However, sighing was shown to be increased in the *Mecp2*^{+/-} mice compared to WT as early as 10 wks old while the respiratory variability did not become significantly greater than the WT until 23 wks of age. If the preBötC was involved, one may have expected to see increased sighing behaviour and respiratory variability to become apparent at the same time point. Targeted ablation of NK1R expressing cells in the rat also had the effect of reducing sigh frequency (McKay *et al.*, 2005), which is in contradiction to the data shown in this chapter and chapter 3. This difference in results could be due to the fact that McKay *et al.* studied breathing patterns in the rat whereas this study makes use of mice. The group also studied the targeted ablation of only NK1 expressing cells whereas the mice in this study were bred with a ubiquitous deficiency in MeCP2 which could affect cells other than the NK1 expressing cells of the preBötC. For example, data in chapter 5 highlights morphological changes that occurred within the lungs of MeCP2 deficient mice, and structural changes within these key respiratory organs could have a bearing on the sigh profile of these animals. It is difficult to draw a conclusion as to the role of NK1 expressing neurons of the preBötC of *Mecp2*^{+/-} mice and their role in sigh frequency without analysis at the anatomical level.

As discussed above, sighs were more prevalent in *Mecp2*^{+/-} mice compared to WT during hypoxic exposure until 23 weeks of age, where WT mice began to exhibit more sighs than the *Mecp2*^{+/-}. However, observation of double breath frequency (Fig 6-10) indicated that at 23 wks there was an increase in the occurrence of double breaths in *Mecp2*^{+/-} than had been seen in previous weeks when exposed

to hypoxia. Fig 6-11 illustrates the occurrence of sighs and double breaths combined. This figure shows that the combination of breathing abnormalities (sighs and double breaths) was more common in the *Mecp2*^{+/-} animals compared to WT across all weeks studied. This reveals that at 23 weeks, the profile of respiratory abnormalities may change in the *Mecp2*^{+/-} animals to favour double breaths rather than sighing. A similar change was reported by Voituron et al., who illustrated that as male *Mecp2*^{-/-} mice aged, complex sighs (equivalent to double breaths) became more frequent than simple sighs (Voituron *et al.*, 2010). The sighing profile of humans changes with maturation, from biphasic sighs in neonates to simple sighs in adults (Qureshi *et al.*, 2009) which suggests a maturation step in the respiratory system is occurring. The fact that simple sighs change profile to that of double breaths at 23 weeks along with an increase in respiratory variability (Fig 6-8) suggests a possible failure of the respiratory system to maintain optimal function.

It was noted that the occurrence of double breaths, in normoxia in the male mice (chapter 3) and female model during the hypoxic stimulus, followed a rhythmic pattern. As previously discussed there are suggestions that sighs act to aid the resetting of respiratory controllers (Baldwin *et al.*, 2004). Thus it could be hypothesised that the rhythmic occurrence of double breaths in hypoxia are an attempt to reset respiratory rhythm generators.

6.4.5 Apnea

The results in Fig 6-8 demonstrated that the occurrence of apnea was greater in *Mecp2*^{+/-} mice than WT and that the frequency of apneas did not increase with age as was seen in both sighing and double breath behaviour. *In situ* studies of the arterially perfused brainstem-spinal cord prep reveal apneas are significantly more common in *Mecp2*^{+/-} mice than WT animals but the frequency of apnea is not affected by age (Abdala *et al.*, 2010). The same study indicates that application of a 5-HT_{1A} agonist reduces the number of apneas which occur in *Mecp2*^{+/-} animals. There is evidence to show that breathing disturbances become more severe in MeCP2 deficient mice at approximately 2 months old, the time point at which 5-HT system becomes disturbed (Viemari *et al.*, 2005). In chapter 3 it was shown that *Stop/y* males exhibited less 5-HT expressing cells than the WT and while no histology has been performed on the *Mecp2*^{+/-} mice in this study

it is known that 5-HT levels are reduced in the brains of RTT patients (Riederer *et al.*, 1985). In light of this data, it could be suggested that the increased occurrence of apnea in the *Mecp2*^{+/-} mice may result from a reduction in 5-HT expression and content.

The occurrence of apnea in *Mecp2*^{+/-} mice was generally suppressed during hypercapnic exposure and became more frequent during the 15 min post hypercapnic period (Fig 5-8). Similarly, *Mecp2*^{-y} mice exhibit transient apneas in the post hypercapnic period yet not during hypercapnic exposure (Voituron *et al.*, 2009). In contrast however, Voituron *et al.* observed a recovery of the respiratory parameters 10-15 min post stimulus whereas *Mecp2*^{+/-} mice in this study continued to display apnea even at 30 min post stimulus recovery (Fig 6-12). This difference in result may be due to the fact that Voituron *et al.* studied the occurrence of apnea in male mice with a complete absence of MeCP2 whereas the female mice in this study are heterozygous for a null mutation in *Mecp2* and expressed some amount of MeCP2 during development. Also, mice in this chapter were bred on a slightly different background compared to those studied by Voituron and background is known to influence the occurrence of spontaneous apnea in mice (Stettner *et al.*, 2008).

As mentioned previously, it can be hypothesised that the peripheral chemoreceptors are at fault in this model. If the chemoreceptors are unable to detect the changes in blood gases after hypercapnic exposure, the information relayed to the appropriate respiratory controllers may be incorrect and as such apneas still occur for up to 30 min following hypercapnic exposure.

The Locus Coeruleus (LC) contains noradrenergic neurons which display chemosensitive properties *in vitro* (Putnam *et al.*, 2004) and it has been shown that the number of TH expressing neurons in this area are reduced in MeCP2 null mice (Roux *et al.*, 2010). No histological analysis of the LC has been performed in this chapter but if a reduction in TH expression were to be found in the LC of *Mecp2*^{+/-} mice, this again may account for the variability that is seen in the respiratory pattern post hypercapnia.

Hypoxic exposure itself may contribute to the severity and occurrence of apnea. It has been shown that calcium transients are important in neuronal development (Spitzer *et al.*, 2002) and that the length and duration of these

signals can cause elongation or retraction of the neuronal processes. Hypoxia induces an increase in calcium transients which in turn promotes a retraction of neuronal processes (Mironov & Langohr, 2005) and in *Mecp2* KO mice it was found that there are fewer connections between neurons in the respiratory network and the rhythmic pattern was often interrupted by spontaneous and long lasting calcium increases (Mironov, 2009). *Mecp2*^{+/-} mice in this study present frequent apnea from 10 wks onwards and the hypoxia that could result from apneic breathing may lead to an increase in calcium transients, a subsequent retraction of the neuronal processes and as such a malformed and unstable network. An unstable respiratory network would also account for the increased occurrence of sighing and double breath behaviour which is also observed in the *Mecp2*^{+/-} animals.

Furthermore, studies in *Mecp2*^{-/y} mice revealed an increased susceptibility of hippocampal slices to hypoxia (Fischer *et al.*, 2009) with more recent investigations on rhythmically active *Mecp2*^{-/y} brainstem slices demonstrating that hypoxia induced depression spreading into the area of the pre-Bötzinger lead to cessation of respiratory activity (Kron *et al.*, 2011). It could be proposed that if the same susceptibility exists in *Mecp2*^{+/-} mice, then the depression of pre-Bötzinger activity could be contributing to the increased occurrence of apnea in these mice compared to WT.

6.4.6 PAH

PAH is a disease state thought to result from an imbalance between vasodilation and vasoconstriction of pulmonary vasculature. As was previously discussed, it was hypothesised that hypoxic episodes resulting from frequent apnoea in *Mecp2*^{+/-} mice may lead to structural remodelling of the blood vessels, which ultimately leads to an increase in pulmonary arterial pressure and right ventricular hypertrophy which taken together are indices of PAH. Hypoxia-induced vasoconstriction of the pulmonary vessels is mediated by factors such as endothelin and 5-HT (Dumas *et al.*, 1999). 5-HT is known to promote smooth muscle cell hyperplasia in bovine tissue (Lee *et al.*, 1994) and also act as a mitogen, a promoter of cell division, in rat pulmonary arteries (Pitt *et al.*, 1994). The fact that increased plasma levels of 5-HT are found in primary pulmonary hypertension patients (Hervé *et al.*, 1995) indicates that an increase in the level of 5-HT expression could perhaps affect the progression of the PAH

disease state. However, data from chapter 4 suggests that there was a trend towards a decrease in 5-HT expression in certain medullary areas of MeCP2 deficient mice, and previous studies have reported a deficit in 5-HT levels associated with an MeCP2 deficit in both mice (Viemari *et al.*, 2005) and RTT patients (Riederer *et al.*, 1985), which makes this an unlikely hypothesis. Reports suggest that it may not be the level of 5-HT itself which is a determinant of PAH, given that selective serotonin reuptake inhibitors (SSRIs) lead to an increase in 5-HT levels but are not associated with the development of PAH (Marcos *et al.*, 2003). One hypothesis is that exposure to chronic hypoxia results in an increased expression of the serotonin transporter 5-HTT (Eddahibi *et al.*, 1999), and the activity of this transporter may lead to the remodelling of pulmonary vasculature given that 5-HTT^{-/-} mice have reduced levels of pulmonary remodelling compared to WT following hypoxic exposure (Eddahibi *et al.*, 2000). Future work may involve monitoring the blood gases of the female mice when exhibiting periods of apnea to monitor if hypoxaemia does develop and to what extent. Also, mRNA analysis of the lung tissue may prove useful in comparing the levels of 5-HTT expression in WT and *Mecp2*^{+/-} mice to observe whether or not this may be the mechanism by which vascular remodelling occurs.

Other factors may also be involved in the progression of the PAH phenotype. Prostacyclin is a known vasodilator and production requires the enzyme prostacyclin synthase. BDNF has been shown to increase the production of this enzyme in cerebral arteries of rabbits (Santhanam *et al.*), suggesting that this neurotrophic factor may play an indirect role in the modulation of vascular tone. BDNF levels are known to be reduced in MeCP2 deficient mice (Chang *et al.*, 2006b) which could result in a reduced level of prostacyclin. Such a change in the level of this vasodilator may lead to an imbalance of vasodilation/vasoconstriction and could ultimately lead to or enhance the progression of PAH. Indeed, it has been shown that the small arteries of patients suffering severe pulmonary hypertension exhibit reduced levels of prostacyclin synthase compared to controls (TUDER *et al.*, 1999).

Observation of WT and *Mecp2*^{+/-} lung tissue showed that *Mecp2*^{+/-} animals tended to have more positive elastin staining in the parenchyma compared to WT. Primary pulmonary hypertension (PPH) is rare, with pulmonary arterial

hypertension more commonly occurring secondary to conditions such as chronic obstructive lung disease and interstitial fibrosis. The increased elastin deposits observed in *Mecp2*^{+/-} animals may indicate the development of a fibrosis-like pathology. A similar thickening of interalveolar tissue was also observed in MeCP2 deficient male mice in chapter 5. Future work may thus involve more extensive histological staining of the lung e.g. application of Masson's trichrome stain to highlight collagen deposits, to look for changes in other morphological aspects of the female lung which may suggest the presence of another disease state to which PAH may be secondary.

To conclude, although statistical analysis showed no significant difference between WT and *Mecp2*^{+/-} animals, this thesis presents a novel finding that all three indices of PAH (sRVP, RV/LV+S and percentage remodelling) showed a trend towards an increase in *Mecp2*^{+/-} mice which may indicate early development of the PAH disease state. Future work may involve a) studying a larger sample size of *Mecp2*^{+/-} animals for signs of PAH and b) carrying out PAH analysis at various time points to observe when the onset of the disease state occurs.

Chapter 7: Final Discussion

Sudden death with unexplained cause is frequently associated with RTT syndrome, and previous reports show that up to 26% of the population of RTT patients fall into this category (Kerr *et al.*, 1997). It has been suggested that respiratory abnormalities may be a contributing factor in the sudden death of RTT patients thus it is of great importance that a better understanding of the mechanisms which underlie these abnormalities is obtained. The studies presented in this thesis have suggested that the respiratory abnormalities presented in MeCP2 deficient mouse models of RTT syndrome may be due to a combination of neuromodulatory and chemosensitive deficits, along with morphological changes within the lung.

7.1 Behavioural Phenotype of Male and Female Model

As has been discussed in previous chapters, RTT syndrome is predominantly a female disorder yet a large proportion of RTT based research makes use of the male mouse model because it presents a more homogeneous population of animals. This thesis brings together data from both male and female mouse models of RTT syndrome, allowing comparisons to be made of behaviour and progression of the RTT-like phenotype. Behaviourally, the male model developed symptoms at a much younger age than females, with symptoms appearing as young as 6 weeks old. The progression of the phenotype was also more rapid in the male MeCP2 deficient mice, with animals showing an increase in behavioural score over a matter of days whereas females exhibited a progression in the behavioural phenotype over weeks. The rapid onset of symptoms in the male mice led to the development of a new behavioural score which involved adding more descriptors to the 3 point score created by Guy *et al.* (Guy *et al.*, 2007). Adding more descriptors to the scale and scoring animals 3 times each week highlighted the variability in behavioural score both within an animal and between different animals in the MeCP2 deficient male population. The speed at which the phenotype progressed differed vastly from one animal to the next. Some of the male MeCP2 deficient mice developed the RTT-like phenotype at a younger age than was expected and as result some animals had to be excluded from the study. One reason for this rapid onset of symptoms may be that the RTT-like phenotype was stress induced as a result of transportation from the breeding centre (Oxfordshire, England) to the research facility (Glasgow, Scotland). There is evidence to suggest that MeCP2 deficient mice may be more

prone to stress and anxiety, with deletion of MeCP2 in Sim-1 (single minded homolog 1) expressing neurons of the hippocampus resulting in animals spending less time in the centre of the open field test compared to WT controls, an indication of anxious behaviour. The total time spent moving was comparable between the WT and MeCP2 deficient animals, indicating that the reduced amount of time spent in the centre of the open field test was not due to lethargy or reduced movement of the MeCP2 deficient mice (Fyffe *et al.*, 2008). Removal of MeCP2 from the amygdala, the emotional processing centre, yields mice which spend less time in the open arms and significantly more time in the closed arms of the elevated plus maze compared to WT controls (Adachi *et al.*, 2009). Furthermore, in the *Mecp2*^{308/y} model, in which mice express a truncated form of MeCP2, animals show increased corticosterone releasing hormone (CRH) and increased corticosterone levels compared to WT which may account for their reported anxious behaviour (McGill *et al.*, 2006). Since the male model used in this thesis presented a ubiquitous absence of MeCP2, it is feasible that all of the areas targeted in the models above could be affected.

Stress leads to the release of CRH by the hypothalamus which in turn stimulates production of adrenocorticotrophic hormone (ACTH). This hormone causes the adrenal cortex to produce glucocorticoids, such as corticosterone in the rodent or cortisol in humans, which bind to glucocorticoid receptors to activate or repress genes (Reichardt & Schutz, 1998). Normally, the negative feedback of glucocorticoids on the hypothalamus and pituitary means the stress response is transient, however, it has been reported that RTT patients have increased levels of urinary cortisol (Motil *et al.*, 2006) indicating a misregulation of the stress response and a lack of negative feedback. Oral treatment of *Mecp2*^{-/y} mice with corticosterone leads to a decreased life span, while *Mecp2*^{+/-} females show an earlier onset of hindlimb claspings and tremor (Braun *et al.*), behavioural characteristics which are used to indicate the onset of the RTT-like syndrome. Thus, if the male MeCP2 deficient mice studied in this thesis were subjected to stress during the transportation process, subsequent increases in cortisol levels may result in the early onset of the RTT like phenotype and could account for the short lifespan that was shown by some of the MeCP2 deficient mice. Treatment of *Mecp2*^{-/y} mice with the glucocorticoid receptor antagonist RU486 leads to a later onset of hindlimb claspings (Braun *et al.*), suggesting that

suppression of the stress response can slow the development of the phenotype. Other studies have shown that in normal conditions the basal levels of cortisol are not elevated in *Mecp2*-null mice, yet glucocorticoid inducible genes such as *Sgk* (Nuber *et al.*, 2005) and *Fkbp5* (Nuber *et al.*, 2005; Chahrour *et al.*, 2008b), a gene that has been implicated in post traumatic stress disorder (Binder *et al.*, 2008), are upregulated before and after onset of neurological symptoms in the *Mecp2*^{-/-} model which suggests that MeCP2 may directly modulate *Fkbp5* and *Sgk* gene expression. Taken together, these data suggest that a misregulation of the stress response exists in MeCP2 deficient mice and that inappropriate glucocorticoid signalling could enhance the progression of the RTT like phenotype. Further evidence to strengthen this hypothesis is found in the female mice studied in this thesis. These mice did not undergo the long transportation from the breeding centre to the research facility as these animals were bred in house. The development of the RTT like phenotype was only variable in the respect that not all of the female mice developed the same level of behavioural score. This is to be expected as the female model presents a mosaic pattern of MeCP2 expression and thus the phenotype is subject to skewing.

The stress level of experimental animals is an important point to consider particularly when studying respiratory behaviour. Stress will undoubtedly affect the respiratory output of the animals and as such it is imperative that animals are properly habituated, even more so in animals which are prone to increased stress responses. A recent study has indeed shown that breathing irregularities in *Mecp2* deficient mice may be enhanced if the animal is stressed. The study revealed that exposing *Mecp2* deficient mice to a stress inducing odour resulted in an increase in breathing irregularities compared to the WT controls (Ren *et al.*, 2012). Furthermore, following treatment with a corticotrophin-releasing factor antagonist there was no significant difference between the respiratory regularity of WT and *Mecp2* deficient mice, indicating that the stress response may play a role in the respiratory pattern of *Mecp2* deficient mice. Episodes of stress and anxiety are often common among RTT patients (Sansom *et al.*, 1993), perhaps due to misregulation of the stress response by MeCP2, and thus could account for some of the respiratory abnormalities observed in these patients. Another observation is that corticosteroids are sometimes used as anti-epileptic drugs (Gupta & Appleton, 2005), and epilepsy can often be a feature of the RTT

phenotype. The data discussed above suggest that oral application of corticosterone to MeCP2 deficient rodents leads to a decreased life span and quicker onset of the RTT phenotype (Braun *et al.*, 2012). Thus, it could be hypothesised that care must be taken when considering administration of corticosteroids in the treatment of RTT-based epileptic seizures because increased levels of corticosteroids may worsen other facets of the RTT phenotype.

Another point to consider is that corticosteroids are known to induce osteoporosis. RTT patients have been reported as having low bone density and reduced bone formation (Roende *et al.*; Budden & Gunness, 2003; Roende *et al.*, 2011). Whether or not this reduced bone density is related to treatment with anti-epilepsy drugs is debatable; however, since bone density is known to be reduced in some RTT patients who did not receive anti-epilepsy treatment, then caution must be used when considering the application of osteoporosis-inducing drugs to treat other facets of the RTT phenotype.

With regards to the female *Mecp2*^{+/-} mice, although the animals exhibited the same behavioural phenotype as the male model e.g. hindlimb claspings, tremor, the progression of the RTT-like phenotype was more comparable from one animal to the next than had been seen in the male mice. It was also noted that some females developed an obese phenotype (Fig 6-3 plot B) as was reported by Guy *et al.* (Guy *et al.*, 2007). This phenotype was not observed in the male MeCP2 deficient mice, but this may be due to the fact that female mice had a longer lifespan than males and as such the obese phenotype had longer to develop.

Obesity is not usually seen in typical RTT patients, but may be associated with non typical RTTs. One young boy with a frameshift mutation in *MECP2* was reported as having an obese phenotype (Kleefstra *et al.*, 2002). A study of female patients with preserved speech variant RTT syndrome reported that 6 out of 18 had an overweight and often obese phenotype (Zappella *et al.*, 2001). The obese phenotype of MeCP2 deficient females could be attributed to several factors. There is evidence that application of corticosterone not only affects phenotypic characteristics such as hindlimb claspings and tremor, but MeCP2 deficient mice that receive the treatment also develop increased fat deposits

(Braun *et al.*, 2012). Since MeCP2 deficient mice have been shown to have an increased stress response i.e. a greater release of cortisol, the obese phenotype could be secondary to the increased level of circulating glucocorticoids. However, studies of the circulating levels of glucocorticoids in an *Mecp2*-null model suggests that there are no such increases in serum glucocorticosteroids (Nuber *et al.*, 2005).

It has also been shown that mice with *Mecp2* knocked out in only Sim-1 expressing neurons had increased levels of leptin compared to control at 42 wks old (Fyffe *et al.*, 2008). Leptin levels were normal at 6 wks which suggests that it is not an increase in leptin levels which results in the obese phenotype but instead the increased fat deposits acquired by mice through hyperphagia then lead to increased leptin levels. It is also hypothesised that decreased *Mecp2* expression within the hypothalamus could affect the functioning of leptin, a key controller of energy homeostasis (Kerr *et al.*, 2008) which may account for the obese phenotype observed in the *Mecp2*^{+/-} mice. Leptin concentrations are known to be positively correlated with BMI in humans (Blardi *et al.*, 2007) and thus the increase in body mass of female MeCP2 deficient mice could be linked to reports of increased levels of leptin in RTT patients when compared to controls (Considine & Caro, 1997). However, the majority of RTT patients do not suffer obesity; rather they often display a stunted growth pattern. The increases in leptin levels are thus thought to be due to the chronic inflammatory state present in the patients which arise from common respiratory infections (Blardi *et al.*, 2007), as leptin levels are shown to be increased during infections (Fantuzzi & Faggioni, 2000). As discussed in chapter 5, some of the male *Mecp2* deficient mice had signs of lung pathology and it remains unknown as to whether this may be the result of a respiratory infection. It could be hypothesised that the obese phenotype exhibited by some of the *Mecp2*^{+/-} animals could be the result of similar lung pathology and increased leptin levels due to respiratory infection. However, the obese phenotype of the *Mecp2*^{+/-} mice did not appear to be associated with a more severe respiratory phenotype. Nor was the obese phenotype associated with a more severe behavioural score.

7.2 MeCP2 and Maturation

The period of normal development which occurs in MeCP2 deficient mice prior to the onset of the RTT-like phenotype indicates that MeCP2 may not be necessary for early development, but the delayed appearance of the phenotype suggests that MeCP2 plays a key role in maintaining neuronal function during later stages of development (Guy, Gan et al. 2007; Gaultier, Bissonnette et al. 2008).

MeCP2 does not appear to affect the differentiation of early precursors but expression of MeCP2 increases with neuronal maturation (Kishi & Macklis, 2004) indicating its importance in adulthood. Studies have shown that knocking out MeCP2 in the adult recapitulates the behavioural phenotype observed in mice which undergo germ line knock out (McGraw *et al.*, 2011). MeCP2 has been implicated in the maturation of neurons given that RTT patients tend to have smaller heads and reduced brain size compared to controls (Armstrong *et al.*, 1999). With no evidence of cell death found in these smaller brains and evidence of reduced neuronal size (Bauman *et al.*, 1995), it can be hypothesised that neurons have failed to mature in the absence of MeCP2. Reduced brain size and reduced dendritic branching are also features which are observed in the brains of mice which have had MeCP2 removed in adulthood (Minh *et al.*, 2012), highlighting the importance of MeCP2 in neuronal maintenance.

Mecp2 KO mice exhibit fewer connections between neurons (Mironov, 2009) which could result in the presence of underdeveloped respiratory networks. Neonates, which have a much less developed respiratory network compared to adults, exhibit a variable respiratory pattern often characterised with frequent sighs (Cross *et al.*, 1960). The fact that MeCP2 deficient males studied in this thesis exhibited an increase in the number of sighs (Fig 3-15) and an increase in respiratory frequency (Fig 3-8) compared to WT during development implies a degree of immaturity exists within the respiratory network. The period of normal development which precedes the onset of sighing and increase in respiratory frequency in MeCP2 deficient mice suggests that respiratory activity can initially occur normally in the absence of MeCP2. This may indicate that the respiratory rhythm generators of MeCP2 mice are in tact, but a lack of data from staining of the preBötC and RTN rhythm generating regions in chapter 4 means a solid conclusion cannot be drawn.

In this thesis, the term double breath was used to define a respiratory behaviour which resembled two large amplitude inspirations separated by incomplete expiration. Another group report a similar breathing phenotype but refer to it as “complex sighing” (Voituron *et al.*, 2010) and report that as mice grow older, complex sighs become more apparent in the *Mecp2*^{-/y} compared to WT. The results in chapter 3 and chapter 6 illustrate that double breaths are more apparent in mice lacking MeCP2 than the WT (Fig 3-14, Fig 6-8). In the male model, the frequency of double breaths also increased as the animals aged and RTT-like behavioural phenotype progressed. It is interesting to note that prior to the onset of changes in respiratory frequency (T-1 to 2, Fig 3-8), double breaths were already more apparent in mice lacking MeCP2 than in the WT (Fig 3-19). As discussed in chapter 3, the increased frequency of double breaths which precede changes in respiratory frequency may act as an indicator of a more severe breathing phenotype to follow. These data agree with the suggestion of Voituron *et al.* (2010) that non-invasive assessment of breathing patterns early on in RTT patients, using methods such as plethysmography, could prove useful in predicting the onset of more severe respiratory abnormalities.

The combination of sighs and double breaths was more common in *Mecp2*^{+/-} animals compared to WT across all weeks studied. However, at 23 weeks the profile of respiratory abnormalities changed in the *Mecp2*^{+/-} animals to favour double breaths rather than sighs. A similar change was reported by Voituron *et al.*, who illustrated that as *Mecp2*^{-/y} mice aged, complex sighs (which appear to be equivalent to what is termed as “double breaths” in this thesis) became more frequent than simple sighs (Voituron *et al.*, 2010). The sighing profile of humans normally changes during maturation, from biphasic sighs in neonates to simple sighs in adults (Qureshi *et al.*, 2009). The fact that sighs change profile to that of double breaths at 23 weeks along with an increase in post stimulus respiratory variability (Fig 6-5) almost implies regression of the respiratory system and a failure in maturation.

Reactivation of *Mecp2* in the male MeCP2 deficient mice resulted in a reduction of the respiratory frequency, a trend towards a reduction in the number of sighs in air and also a transient reduction in the number of double breaths. This suggests that some of the changes in the respiratory network that occur in the absence of MeCP2 are not irreversible, and again that it is likely that the

reactivation of *Mecp2* allows neurons to mature to the appropriate level to execute adequate respiratory control. However, the fact that double breaths start to become apparent a few weeks following *Mecp2* reactivation (Fig 3-19) indicates that a) this particular respiratory characteristic is controlled by circuits separate to those which control sighing and respiratory frequency and b) some irreversible changes have occurred in the network which means that this respiratory phenotype persists even after the reactivation of *Mecp2*. Another explanation for the persistence of respiratory abnormalities may be that application of TM only removes the stop cassette in approx 80% of neurons (Guy *et al.*, 2007). *Mecp2* is not reactivated in every cell and therefore a small MeCP2 deficiency remains.

It has been shown in this thesis that there was a general trend towards a reduction in the number of cells expressing 5-HT and TH in MeCP2 male deficient mice compared to WT. This may indicate that MeCP2 is critical in the maintenance of neuromodulatory neurons such as NA and 5-HT expressing neurons.

7.3 MeCP2 and Neuromodulation

Since the NA system continues to mature postnatally, it could be hypothesised that the absence of MeCP2 affects the development and maintenance of the NA system. The male MeCP2 deficient mice studied in chapter 3 showed a trend towards a reduced number of TH expressing neurons in the A2/C2 and the A1/C1 regions compared to WT (Fig 4-21). Since neurons in these adrenergic areas are thought to be involved in modulating frequency and stability of the respiratory pattern (Hilaire *et al.*, 1990; Zanella *et al.*, 2006), a reduction in the number of TH neurons may account for the variable breathing pattern that was reported in chapter 3. This reduction in the number of TH expressing neurons agrees with previous studies of *Mecp2*^{-y} mice which found a reduction in TH expression in the A2/C2 region at one month old and the A1/C1 at 2 months old (Viemari *et al.*, 2005). Variability in the duration of the respiratory cycle also became apparent as NA deficits developed. In this thesis, the immunocytochemical analysis of the brainstem of MeCP2 deficient male mice was not carried out at various developmental time points and so it cannot be concluded at which stage the trend toward reduced TH expression became apparent. However, what is

novel about the work presented in this thesis is the ability to reactivate the *Mecp2* gene and to observe whether or not transcription of MeCP2 is able to rescue the deficit in bioamine expression. Fig 4-21 plot A illustrates that *Stop/y,cre+TM* mice, animals that underwent *Mecp2* reactivation, exhibited a trend towards fewer TH positive cells than WT and *Stop/y* mice. This may initially suggest that *Stop/y,cre* and *Stop/y* mice did not develop the same deficit in TH and thus *Stop/y* animals do not act as an appropriate control. However, *Stop/y* mice were younger than WT and *Stop/y,cre +TM* mice by approximately 10 weeks at the time of perfusion due to the rapid onset of symptoms and their inability to be rescued by *Mecp2* reactivation. It has been reported that number of NA neurons in certain noradrenergic areas decreases as mice age (Tatton 1991) and that the number of TH expressing neurons in the A1/C1 and A2/C2 regions is larger in neonates than in adult mice (Hilaire, 2006). Therefore, *Stop/y,cre +TM* mice may appear to have fewer TH positive neurons compared to WT, but it may be that the neurons of the *Stop/y* mice would have shown the same reduction in TH expression as *Stop/y,cre +TM* mice if they had survived to an older age.

Fig 4-21 also shows that even though the average number of MeCP2 expressing cells in the *Stop/y,cre +TM* mice were reduced compared to WT (plot C), the average number of TH positive neurons which also express MeCP2 was not significantly different between the WT and *Stop/y,cre +TM* genotypes. Furthermore, in *Stop/y,cre +TM* mice, 50-60% of MeCP2 positive neurons also expressed TH whereas in the WT only 20-40% of MeCP2 neurons also expressed TH. This suggests that out of the few neurons that re-expressed MeCP2 in *Stop/y,cre +TM* mice, a large proportion were associated with TH expression and thus reactivation of *Mecp2* appeared to favour noradrenergic neurons. However, reactivation of *Mecp2* in *Stop/y,cre +TM* mice did not restore the level of TH expression to that of WT (Fig 4-21 plot A). This may indicate that a) reactivation of *Mecp2* is not an adequate method of restoring noradrenergic signalling in MeCP2 deficient mice and thus may not be an appropriate avenue to pursue in a clinical setting or b) the 80% cassette deletion in this model does not yield sufficient MeCP2 expression to rescue the deficit in TH expression.

The reduction in the number of TH positive cells in MeCP2 deficient mice is thought to be due to a change in the cell phenotype rather than as a result of

cell death, as no evidence of apoptosis is found in the A1/C1 and A2/C2 regions of MeCP2 deficient mice (Roux *et al.*, 2007). Research indicates that in *Mecp2*^{-/y} mice there may be deficient expression of TH and dopamine beta hydroxylase (Zhang *et al.*, 2010a), enzymes which are important in the synthesis of noradrenaline. It has been shown that application of NA uptake inhibitor Desipramine for 2 weeks in MeCP2 deficient mice results in a reduction in the number of apneas (Roux *et al.*, 2007). This suggests that although MeCP2 deficient mice present a reduction in TH expressing neurons, those that remain may be functionally capable of restoring respiratory parameters with the aid of pharmacological intervention. However, results from another study revealed that the level of NA within the medulla was reduced in *Mecp2*^{-/y} mice after treatment with Desipramine (Zanella *et al.*, 2008) which may indicate that the recovery of respiratory parameters may not be due to a restoration of NA content in the brain but of NA mediated systems in the periphery.

Noradrenergic signalling is not the only area to be considered in the management of RTT syndrome. Neither Pet-1 conditional knock out mice (which only have MeCP2 removed from serotonergic cells) nor TH-conditional knock out mice (which have MeCP2 removed from adrenergic cells) present a particular breathing phenotype as seen in *Mecp2*^{-/y} mice (Samaco *et al.*, 2009). It is likely that the respiratory abnormalities which result from a deficiency of MeCP2 are due to insufficient noradrenergic and serotonergic neuromodulation alone.

There is evidence to show that breathing disturbances become more severe in MeCP2 deficient mice at approximately 2 months old, the time point at which 5-HT system becomes disturbed (Viemari *et al.*, 2005). *In situ* studies of the arterially perfused brainstem-spinal cord prep reveal apneas are significantly more common in *Mecp2*^{-/+} mice than WT animals but the frequency of apnea is not affected by age (Abdala *et al.*, 2010). Data in chapter 6 build on this result by showing that *in vivo*, apnea in *MeCP2*^{+/-} mice are also more common than in WT (Fig 6-8) and that frequency of apnea does not increase with age. Abdala *et al.* show that application of a 5-HT_{1A} agonist reduces the number of apneas which occur in *Mecp2*^{-/+} animals, indicating that increasing 5-HT signalling may help to alleviate this particular respiratory characteristic (Abdala *et al.*, 2010). In chapter 3 it was shown that *Stop/y* males exhibited a trend towards fewer 5-HT expressing cells than the WT and while no histology has been performed on

the *Mecp2*^{-/+} mice in this thesis, it is known that 5-HT levels are reduced in the brains of *Mecp2*-null mice (Ide *et al.*, 2005) and in RTT patients (Riederer *et al.*, 1985). In light of these data, it could be suggested that the increased occurrence of apnea in the *Mecp2*^{+/-} mice may result from a reduction in 5-HT expression. As was discussed with regards to TH, the reduction in 5-HT positive cells is probably due to a loss of cell phenotype rather than cell death. There is evidence of a reduction in tryptophan hydroxylase 2 levels, the enzyme needed for production of 5-HT, in *Mecp2*-null mice (Samaco *et al.*, 2009).

A reduction in the number of 5-HT expressing neurons may have a profound impact on the respiratory pattern given that Pet-1 KO mice have a 70-80% loss of 5-HT neurons in the CNS (Hendricks *et al.*, 2003) and at neonatal stages show an increased variability in respiratory output compared to WT animals. Pet-1 KO mice also fail to achieve the maturation step seen at post natal day 4.5 in the WT mice, when the breathing patterns becomes stabilised (Erickson *et al.*, 2007). It has been previously discussed that MeCP2 is important in proper maturation of neurons, and it could be hypothesised that a deficit in MeCP2 and in 5-HT could have a cumulative effect on the maturation of neurons involved in the respiratory network.

After reactivation of *Mecp2*, respiratory frequency is reduced (Fig 3-8) yet sighs and apnea still persist. The number of 5-HT neurons in *Stop/y,cre*+TM mice does not return to WT level. The persistence of a reduced number of 5-HT neurons in the MeCP2 deficient mice even after *Mecp2* has been reactivated (Fig 3-9) may account for the degree of variability that still remains within the breathing pattern of *Stop/y,cre* +TM mice and also for the persistence of apneas (Fig 3-22). As was observed with TH expression, levels of MeCP2 expression in *Stop/y,cre* +TM mice were lower than WT. While 80-100% of 5-HT expressing cells of the WT animal also expressed MeCP2, only 60-80% of 5-HT cells in the *Stop/y,cre* +TM mice expressed MeCP2. Also, the percentage of MeCP2 expressing neurons which were associated with 5-HT was comparable between the WT and *Stop/y,cre* +TM mice. This indicates that *Mecp2* reactivation was not occurring as favourably in 5-HT regions as was seen in noradrenergic regions.

The data in this thesis have not conclusively established in which cells *Mecp2* is reactivated, and previous studies have shown that restoring *Mecp2* in one

specific location within the brain i.e. the forebrain, is not able to rescue the RTT-like phenotype of MeCP2 deficient mice (Alvarez-Saavedra *et al.*, 2007). The fact that double breaths began to reoccur in *Stop/y,cre* male mice in the weeks following *Mecp2* reactivation may indicate that MeCP2 has not been restored to an area of the brain which is key in controlling this part of the respiratory phenotype. Another hypothesis is that not enough *Mecp2* is reactivated, with cassette deletion being only 80% effective. Future work may involve gene therapy and targeted delivery of MeCP2 to TH and 5-HT expressing neurons, whether through the use of viral vectors or other methods. Research has shown a decrease in motor deterioration and rescue of motor activity in using adenovirus to deliver a construct driving *Mecp2* expression in the striatum of MeCP2 null mice (Kosai *et al.*, 2005). However, as MeCP2 has global functions, restoration of MeCP2 expression in neuromodulatory areas alone may not be sufficient to restore respiratory patterns to WT level. Also, care must be taken, particularly in light of the *Mecp2*^{+/-} model which already expresses some amount of MeCP2, that MeCP2 does not become over expressed. The effects of over expressing MeCP2 can be as detrimental as the absence of MeCP2, with studies overexpressing MeCP2 in post mitotic neurons leading to severe motor dysfunction in mice (Luikenhuis *et al.*, 2004).

7.4 Chemosensitivity – Response to hypoxia and hypercapnia

Both male and female models studied in this thesis were found to exhibit an abnormal chemosensitive response. Four weeks prior to gene reactivation, the respiratory response of *Stop/y,cre* mice to hypercapnic exposure was similar to that of the WT (Fig 3-10). However, at the point of TM treatment *Stop/y,cre* animals exhibited an abnormal response to CO₂ exposure, with a reduction in respiratory frequency in contrast to the increased respiratory frequency exhibited by WT animals. This suggests that a period of normal development occurs within MeCP2 deficient mice, but as the animals mature the absence of MeCP2 and subsequent neuronal immaturity becomes apparent in the abnormal chemosensitive response. LC neurons have been implicated in the chemosensitive response, with more than 80% of the neurons in this area being activated by hypercapnia or acidic pH (Putnam *et al.*, 2004). The number of TH expressing neurons is also known to be reduced in MeCP2 deficient mice (Viemari

et al., 2005). Studies have shown that *in vivo*, MeCP2 null mice have a reduced ventilatory response to mild hypercapnic stimuli yet maintain a response to more severe hypercapnic stimulus, with *in vitro* data indicating a reduced sensitivity of LC neurons to CO₂ (Zhang *et al.*). Fig 4-21 plot A illustrates that there was a trend towards fewer TH expressing neurons in the LC compared to WT which may account for the lack of response to CO₂. Reactivation of *Mecp2* did not restore the number of TH positive neurons in the LC to WT level which may account for the persistence of the abnormal hypercapnic response in *Stop/y,cre* mice

Females showed a similar increase in respiratory frequency in response to CO₂ as WT and initially this may indicate that the presence of MeCP2, albeit at a reduced level compared to WT, allowed the chemosensitive networks to develop properly. However, Fig 6-12 shows that apneas tended to be most prevalent at 15 min post hypercapnic stimulus, suggesting an inability of the respiratory network to restore normal breathing following hypercapnic exposure. There may exist a fault within the chemosensory network such as a) inadequate detection of the changes in blood gases after hypercapnic exposure or b) incorrect relaying of information to the appropriate respiratory controllers.

Hypoxic exposure may contribute to the severity and occurrence of apnea. Calcium transients are important in neuronal development (Spitzer *et al.*, 2002) and the length and duration of these signals can cause elongation or retraction of the neuronal processes. Hypoxia induces an increase in calcium transients which in turn promotes a retraction of neuronal processes (Mironov & Langohr, 2005) and in *Mecp2* KO mice it was found that there are fewer connections between neurons in the respiratory network and the rhythmic pattern was often interrupted by spontaneous and long lasting calcium increases (Mironov, 2009). *Mecp2*^{-/+} mice in this study presented frequent apnea from 10 weeks onwards. With a lack of respiratory activity, a hypoxic state may develop within the animal leading to an increase in calcium transients. Subsequent retraction of the neuronal processes would lead to a malformed and unstable network which could account for the increased occurrence of sighing and double breaths which is also observed in the *Mecp2*^{-/+} animals.

Mecp2^{-y} mice have also been shown to have abnormal breathing post hypoxia and post hypercapnia, characterised by apnea and variable rhythm (Voituron *et al.*, 2009). In agreement with this, Fig 3-22 indicates that *Stop/y,cre* mice exhibited apnea after hypercapnic stimuli. A novel part of this thesis again was the ability to reactivate *Mecp2* and observe how this influences various respiratory parameters. It was observed that post hypercapnic apneas persisted in *Stop/y,cre* mice following *Mecp2* reactivation which indicates that perhaps some irreversible change has occurred in the respiratory network as a result of the initial absence of *Mecp2*. However, it should be noted that the data regarding the rescue *Stop/y,cre* animal in this case was based on n=1 so no conclusive results can be drawn.

We have novel data to show that reactivation of *Mecp2* restores the respiratory frequency yet after TM treatment and *MeCP2* reactivation, it was noted that the *Stop/y,cre* mice still had an abnormal response to hypercapnic stimuli (Fig 3-12 and 3-13). This indicates again that changes in chemosensitivity which may have occurred due to the lack of *MeCP2* may actually have led to some permanent changes in the chemosensitive response.

There is an indication that sighs could potentially be driven by the chemosensitive response. Rats which have had their carotid nerves severed no longer exhibit sighs (Bartlett Jr, 1971) and in the cat, local application of cyanide to excite the carotid bodies induces sighing activity (Glogowska *et al.*, 1972). In cats, hypoxia and hypercapnia were both shown to cause an increase in the occurrence of sighs (Cherniack *et al.*, 1981) but in the male *MeCP2* deficient mice in this chapter the frequency of sighs did not seem to be affected by hypercapnic exposure (Fig 3-16 and 3-17). Previous studies have indicated that in anaesthetised rats hypoxia has a greater effect on the frequency of sighing than hypercapnia (Bartlett Jr, 1971). Data collected from the *Mecp2*^{+/-} females in this thesis illustrated that hypoxia caused an increase in sigh frequency from 10 wks old to 23 wks of age (Fig 6-8). The ventilatory response to hypoxia was also exaggerated compared to WT across all weeks studied (Fig 6-4). Male *MeCP2* deficient mice in this thesis were not subjected to hypoxic stimulus due to the fact that the mortality rate was high in this group and it was proposed that the mutant animals that had a severe behavioural score may not be able to cope with this respiratory stimulus. However, previous studies have indicated an

exaggerated response to hypoxia in *Mecp2*^{-/-} male mice compared to WT as early as post natal day 25 (Voituron *et al.*, 2009). The altered response to hypoxia observed in the *Mecp2*^{+/-} mice could be due to a problem with O₂ sensitivity of the carotid bodies, since these chemoreceptors are sensitive to changes in O₂ and have inputs to the dorsal medulla, where activation of the respiratory network occurs to increase ventilation and restore normoxic conditions (Gaultier *et al.*, 2008). Application of dopamine onto carotid bodies causes a decrease in ventilatory response to hypoxia (Bee & Pallot, 1995) and blockade of dopamine autoreceptors results in increased chemoafferent activity and ventilation in anaesthetized cats (Iturriaga *et al.*, 1994). Thus, a reduction in dopamine levels in *Mecp2*^{+/-} animals may account for the exaggerated response to hypoxia. TH acts as a marker for noradrenergic and dopaminergic neurons. Thus it follows that a reduction in TH expression may also indicate reduced dopamine expression in MeCP2 deficient mice. Although TH expression has not been quantified in the *Mecp2*^{+/-} mice in this thesis, Roux *et al.* show that *Mecp2*^{+/-} mice have reduced TH expression compared to WT in the petrosal ganglion and adrenal medulla, areas which are important in the chemoafferent response (Roux *et al.*, 2008). This reduction in TH expression may suggest that the neurons in these chemoafferent regions are less able to produce dopamine, an important modulator of the chemoafferent response. BDNF null mice also exhibit a loss of dopaminergic neurons of the petrosal ganglion (Erickson *et al.*, 2001), neurons which are important in the chemoafferent pathway. Since MeCP2 deficient mice are known to have reduced BDNF levels this may have a knock on effect on dopamine levels and could contribute to the exaggerated response to hypoxia.

It was noted that female WT mice in this study showed an increased respiratory frequency in response to hypercapnic exposure but a blunted respiratory response to hypoxia. There is evidence to suggest that there may be a genetic influence on respiratory response (Tankersley *et al.*, 1994). Strain does not appear to affect the hypercapnic response but does have a bearing on the hypoxic response. For example, after exposure to 8% O₂, a greater increase in respiratory frequency was seen in the A/J strain than C57BL6 (Adachi *et al.*, 2006). Thus the apparent blunted response may be accounted for by the background onto which the mice were bred.

Although much RTT based research focuses on the neurological aspect of the disease, another factor to consider in the appearance of respiratory abnormalities is the contribution of systemic pathologies.

7.5 Lung Pathology

MeCP2 has been shown to be highly expressed within the lung (Shahbazian *et al.*, 2002b) and studies of female classic RTT patients, those with loss of function mutation in *MECP2*, indicated that 55% of the cases studied exhibited abnormal HRCT scans of the lung (De Felice *et al.*, 2010). In the same way, not all of the MeCP2 deficient male mice studied in chapter 3 exhibited pulmonary abnormalities, yet some began to exhibit foaming at the mouth and a rale-like rattling within the chest. Histological staining of the lung tissue revealed that some animals presented more severe morphological changes within the lung than others. Generally, those which had exhibited the most severe observable respiratory phenotype i.e. foaming at the mouth exhibited the most severe lung pathology. These findings lie in agreement with reports from De Felice who found that the severity of the pulmonary abnormalities differed from one patient to the next. In the RTT patients it was found that subjects with pulmonary lesions were older than those who did not present lesions and also that the likelihood of finding pulmonary abnormalities was greater in patients above the age of 11.

De Felice report a thickening of the bronchial walls in eight out of 15 female RTT patients (De Felice *et al.*, 2010) and data in this thesis (chapter 5) indicate a trend towards thickening of the elastic fibres surrounding the airways of MeCP2 deficient male mice (Fig 5-15). A trend towards a thickening of the interalveolar septum was also observed in MeCP2 deficient mice (Fig 5-13). These changes in the morphology of the lung may account for the increased occurrence of sighing that was observed in the MeCP2 deficient mice, given that sighs have been proposed to increase lung compliance and thus prevention of aelectasis (Glogowska *et al.*, 1972). Previous work on *Mecp2* KO mice has indicated that sighing may be characteristic of the breathing phenotype of RTT (Voituron *et al.*, 2010). Although there was a trend towards a reduction in the number of sighs post *Mecp2* reactivation, sighs were not abolished and continued to occur at a higher frequency than was seen in WT. This indicates that the

reduction of sighing is likely to be due to maturation of respiratory networks in the brainstem, yet the persistence of sighing behaviour after *Mecp2* has been reactivated may be accounted for by the underlying lung pathology.

Furthermore, thickening of the interalveolar septum may indicate that the diffusion barrier between alveoli and capillaries could be thickened in MeCP2 deficient mice. This is likely to result in a disturbance in the exchange of gases within the lung. Blood gas measurements were not made in the MeCP2 male deficient mice, but De Felice reports that a reduction in PaO₂ and also a ventilation-perfusion mismatch was found in the females that had abnormal HRCT scans (De Felice *et al.*, 2010). Previous studies of RTT patients by the same group also indicate a ventilation-perfusion mismatch (De Felice *et al.*, 2009). Due to the invasive nature of the technique, lung biopsies of the RTT patients were not available for histological analysis. The advantage of the studies presented in this thesis are that the animal model can be used to study the respiratory abnormalities *in vivo* and tissue can subsequently be removed and processed to investigate the possible influence of pulmonary abnormalities on respiratory behaviour.

The fact that the WT animals did not present any lung abnormalities suggests that the absence of MeCP2 has an effect on pulmonary maintenance, but whether this is a direct or indirect effect remains unknown. MeCP2 is thought to be a transcriptional repressor of BDNF (Chen *et al.*, 2003), the signalling molecule for the TrkB receptor. TrkB mRNA is found in adult human lung tissue (Yamamoto *et al.*, 1996; Ricci *et al.*, 2004) and these receptors are thought to play an important role in the developing mouse lung. Fifteen day old *TrkB* *-/-* mice, which express a non functional form of TrkB, exhibit a thinner bronchial epithelium, larger air spaces and thinner blood vessel walls than WT and also changes in the morphology of type 2 pneumocytes (Garcia-Suarez *et al.*, 2009). Since BDNF levels are reduced in MeCP2 deficient mice (Chang *et al.*, 2006b) it was hypothesised that an upregulation of TrkB may occur to compensate for the lack of signalling molecule. Upregulation of the receptor may then lead to cell proliferation and could account for the pulmonary lesions observed in the MeCP2 deficient mice. Also, *in vivo* studies indicate that in rats, TrkB expression is higher in the lungs of hypoxic rats compared to normoxic controls which led to increased contractility of the airways (Sciesielski *et al.*, 2009). If the male

MeCP2 deficient mice share the ventilation perfusion mismatch reported in the female RTT patients, then hypoxic conditions may develop within the body which could also enhance TrkB expression. Although the presence of TrkB was confirmed in both WT and MeCP2 deficient animals, data regarding the upregulation of the receptor was not conclusive and as the tissue had already been paraffin embedded, mRNA analysis was not feasible. Future work may involve carrying out mRNA analysis to quantify the level of TrkB expression in MeCP2 deficient lungs.

While reactivation of *Mecp2* was able to restore some respiratory parameters such as respiratory frequency, it was not able to reverse the morphological changes within the lungs of MeCP2 deficient animals. The persistence of lung pathology as a result of a deficiency in MeCP2 may be clinically important, as many pharmacological approaches to managing RTT so far have had a neurological focus. Investigation and treatment of underlying pulmonary abnormalities may serve to improve the respiratory phenotype of RTT patients, however methods by which this can be achieved non-invasively may prove difficult. Also, data in chapter 5 shows that a severe behavioural score in MeCP2 deficient mice did not guarantee the onset of rale-like breathing and severe morphological changes within the lung. Thus, it may be difficult to determine which RTT patients are at risk of developing pulmonary abnormalities and a large scale screening process is unlikely to be a feasible approach.

Novel data presented in this thesis indicates for the first time that morphological changes occur within the lung of MeCP2 male deficient animals which a) may underlie respiratory abnormalities and b) which are not rescued by reactivation of *Mecp2*.

With evidence of lung pathology in the male MeCP2 deficient model and reports of abnormalities in the lungs of female RTT patients (De Felice *et al.*, 2010) it was hypothesised that MeCP2 deficient females may also present pulmonary abnormalities. Investigation of three indices of pulmonary arterial hypertension (sRVP, RV/LV+S and pulmonary remodelling) revealed a trend towards an increase in the values recorded in *Mecp2*^{+/-} animals compared to WT (Figs 6-13 and 6-14). Remodelling of the airways and subsequent increases in RVP and right ventricular hypertrophy may result from hypoxic exposure. Chronic hypoxic

exposure results in an increased expression of the serotonin transporter 5-HTT by rat pulmonary arterial smooth muscle cells (Eddahibi *et al.*, 1999). Increased activity of 5-HTT may lead to the remodelling of pulmonary vasculature given that 5-HTT^{-/-} mice have reduced levels of pulmonary remodelling compared to WT following hypoxic exposure (Eddahibi *et al.*, 2000). The female MeCP2 deficient mice in this thesis trended towards an increased number of apneas compared to WT, and apneic breathing can lead to hypoxic conditions within the blood (Southall *et al.*, 1988). Thus, repeated hypoxic exposure may occur in *Mecp2*^{+/-} animals which could lead to remodelling of the pulmonary vasculature and development of PAH. It is common for PAH to develop secondary to other disease states including interstitial fibrosis. In chapter 5, data shows areas of fibrosis-like growth within MeCP2 deficient male lung tissue (Figs 5-7 and 5-8). Although the morphology of the female lung was not studied to the same extent, images of Miller's elastin stained *Mecp2*^{+/-} tissue (Fig 6-14) showed that more fibrous and elastin deposits were observed compare to WT. Whether or not this change in morphology can be defined as fibrosis requires further investigation, however it was apparent that the morphology of the *Mecp2*^{+/-} tissue was markedly different to WT. Thus, it could be hypothesised that the indication of PAH in *Mecp2*^{+/-} mice may be secondary to another, as yet undefined, disease state. As with the MeCP2 deficient males, the novel data presented in this thesis suggests that the respiratory abnormalities suffered by MeCP2 deficient animals may not stem solely from neurological problems, but that peripheral systems may also be a contributing factor.

Appendix 1

Methodology for the preparation of solutions used in perfusion and processing of tissue described in chapter 2.

1L of 4% Paraformaldehyde

400ml distilled water heated in 1L volumetric flask before addition of 40g paraformaldehyde (using gloves and on fume bench). Solution mixed until paraformaldehyde powder began to dissolve. NaOH added drop by drop until all paraformaldehyde powder dissolved and solution became clear. Solution was then filtered through two filter papers into another 1L volumetric flask. 500ml of 0.2M Phosphate Buffer added to the volumetric flask and topped up to 1 litre with distilled water. Solution then transferred into a one-litre bag ready for perfusion.

30% Sucrose solution

Dissolved 30 g sucrose into 100ml of distilled water

0.2M Phosphate buffer (PB)

Weighed out 17.47g of Sodium di-hydrogen phosphate (NaH_2PO_4), 40.75g di-sodium hydrogen phosphate (NaHPO_4) and added to 2L of distilled water.

0.3M Phosphate buffer saline (PBS)

1800mls distilled water + 200mls 0.2 PB+72g NaCl

Phosphate buffer saline + Triton X-100 (0.3%PBST)

500ml 0.3PBS + 1.5ml Triton

0.01M Citrate Buffer

3.84g anhydrous citric acid added to 1800ml distilled water. pH of solution was adjusted to pH 6.0 using NaOH and made up to 2L with distilled water.

Tris Buffered Saline (TBS)

Mixed 605g Tris(hydroxymethyl)aminomethane (Tris) and 876g NaCl in some distilled water in a conical flask on the stirrer until dissolved. Transferred solution to 10L container and made up to 8L with distilled water. Checked pH (in fume hood with gloves) and added HCl accordingly until pH around 8 (approx 250ml. Made up to around 9.5L with distilled water and checked pH. Added HCl until pH 7.4.

TBS Tween (TBST)

1ml Tween dissolved in 1L TBS

NGS/TBS/BSA solution

1g bovine serum albumin dissolved in 16 ml TBS and 4 ml normal goat serum.

List of References

- Abdala APL, Dutschmann M, Bissonnette JM & Paton JFR. (2010). Correction of respiratory disorders in a mouse model of Rett syndrome. *Proc Natl Acad Sci U S A* **107**, 18208-18213.
- Abuhatzira L, Makedonski K, Kaufman Y, Razin A & Shemer R. (2007). MeCP2 Deficiency in the Brain Decreases BDNF Levels by REST/CoREST-Mediated Repression and Increases TRKB Production. *Epigenetics* **2**, 214-222.
- Adachi M, Autry AE, Covington HE, 3rd & Monteggia LM. (2009). MeCP2-mediated transcription repression in the basolateral amygdala may underlie heightened anxiety in a mouse model of Rett syndrome. *J Neurosci* **29**, 4218-4227.
- Adachi T, Ogawa H, Okabe S, Kitamuro T, Kikuchi Y, Shibahara S, Shirato K & Hida W. (2006). Mice with Blunted Hypoxic Ventilatory Response are Susceptible to Respiratory Disturbance during Hypoxia. *The Tohoku Journal of Experimental Medicine* **209**, 125-134.
- Alvarez-Saavedra M, Saez MA, Kang D, Zoghbi HY & Young JL. (2007). Cell-specific expression of wild-type MeCP2 in mouse models of Rett syndrome yields insight about pathogenesis. *Hum Mol Genet* **16**, 2315-2325.
- Amiel J, Dubreuil V, Ramanantsoa N, Fortin G, Gallego J, Brunet JF & Goridis C. (2009). PHOX2B in respiratory control: Lessons from congenital central hypoventilation syndrome and its mouse models. *Respiratory Physiology & Neurobiology* **168**, 125-132.
- Amir RE, Van den Veyver IB, Schultz R, Malicki DM, Tran CQ, Dahle EJ, Philippi A, Timar L, Percy AK, Motil KJ, Lichtarge O, Smith EO, Glaze DG & Zoghbi HY. (2000). Influence of mutation type and X chromosome inactivation on Rett syndrome phenotypes. *Annals of Neurology* **47**, 670-679.
- Amir RE, Van den Veyver IB, Wan M, Tran CQ, Francke U & Zoghbi HY. (1999a). Rett syndrome is caused by mutations in X-linked MECP2, encoding methyl-CpG-binding protein 2. *Nature Genetics* **23**, 185-188.
- Amir RE & Zoghbi HY. (2000). Rett syndrome: Methyl-CpG-binding protein 2 mutations and phenotype-genotype correlations. *American Journal of Medical Genetics* **97**, 147-152.
- Ariani F, Hayek G, Rondinella D, Artuso R, Mencarelli MA, Spanhol-Rosseto A, Pollazzon M, Buoni S, Spiga O, Ricciardi S, Meloni I, Longo I, Mari F, Broccoli V, Zappella M & Renieri A. (2008). FOXP1 is responsible for the congenital variant of Rett syndrome. *American Journal of Human Genetics* **83**, 89-93.
- Armstrong D, Dunn JK, Antalffy B & Trivedi R. (1995). Selective dendritic alterations in the cortex of Rett syndrome. *J Neuropathol Exp Neurol* **54**, 195-201.

- Armstrong DD, Dunn JK, Schultz RJ, Herbert DA, Glaze DG & Motil KJ. (1999). Organ growth in Rett syndrome: A postmortem examination analysis. *Pediatric Neurology* **20**, 125-129.
- Asaka Y, Jugloff DG, Zhang L, Eubanks JH & Fitzsimonds RM. (2006). Hippocampal synaptic plasticity is impaired in the Mecp2-null mouse model of Rett syndrome. *Neurobiol Dis* **21**, 217-227.
- Bago M, Marson L & Dean C. (2002). Serotonergic projections to the rostroventrolateral medulla from midbrain and raphe nuclei. *Brain Res* **945**, 249-258.
- Baldwin DN, Suki B, Pillow JJ, Roiha HL, Minocchieri S & Frey U. (2004). Effect of sighs on breathing memory and dynamics in healthy infants. *Journal of Applied Physiology* **97**, 1830-1839.
- Balkowiec A & Katz DM. (1998). Brain-derived neurotrophic factor is required for normal development of the central respiratory rhythm in mice. *J Physiol* **510 (Pt 2)**, 527-533.
- Balkowiec A & Katz DM. (2000). Activity-dependent release of endogenous brain-derived neurotrophic factor from primary sensory neurons detected by ELISA in situ. *Journal of Neuroscience* **20**, 7417-7423.
- Balkowiec A & Katz DM. (2002). Cellular mechanisms regulating activity-dependent release of native brain-derived neurotrophic factor from hippocampal neurons. *Journal of Neuroscience* **22**, 10399-10407.
- Ballas N, Liou DT, Grunseich C & Mandel G. (2009). Non-cell autonomous influence of MeCP2-deficient glia on neuronal dendritic morphology. *Nature Neuroscience* **12**, 311-317.
- Bartlett Jr D. (1971). Origin and regulation of spontaneous deep breaths. *Respiration Physiology* **12**, 230-238.
- Bauman ML, Kemper TL & Arin DM. (1995). Microscopic observations of the brain in Rett syndrome. *Neuropediatrics* **26**, 105-108.
- Bee D & Pallot DJ. (1995). Acute hypoxic ventilation, carotid body cell division, and dopamine content during early hypoxia in rats. *Journal of Applied Physiology* **79**, 1504-1511.
- Bennett FM & Tenney SM. (1982). Comparative mechanics of mammalian respiratory system. *Respiration Physiology* **49**, 131-140.
- Bernard DG, Li A & Nattie EE. (1996). Evidence for central chemoreception in the midline raphe. *J Appl Physiol* **80**, 108-115.
- Bert P. (1868). Changements de pression de l'air dans la poitrine pendant les deux temps de l'acte respiratoire. *C R Soc Biol* **22-23**.

- Biancardi V, Bicego KC, Almeida MC & Gargaglioni LH. (2008). Locus coeruleus noradrenergic neurons and CO₂ drive to breathing. *Pflugers Arch* **455**, 1119-1128.
- Bianchi AL, Denavit-saubie M & Champagnat J. (1995). Central Control of Breathing in Mammals - Neuronal Circuitry, Membrane-Properties, and Neurotransmitters. *Physiological Reviews* **75**, 1-45.
- Binder EB, Bradley RG, Liu W, Epstein MP, Deveau TC, Mercer KB, Tang Y, Gillespie CF, Heim CM, Nemeroff CB, Schwartz AC, Cubells JF & Ressler KJ. (2008). Association of FKBP5 polymorphisms and childhood abuse with risk of posttraumatic stress disorder symptoms in adults. *Jama-Journal of the American Medical Association* **299**, 1291-1305.
- Bissonnette JM & Knopp SJ. (2006). Separate respiratory phenotypes in methyl-CpG-binding protein 2 (Mecp2) deficient mice. *Pediatr Res* **59**, 513-518.
- Bissonnette JM & Knopp SJ. (2008). Effect of inspired oxygen on periodic breathing in methyl-CpG-binding protein 2 (Mecp2) deficient mice. *Journal of Applied Physiology* **104**, 198-204.
- Blain GM, Smith CA, Henderson KS & Dempsey JA. (2010). Peripheral chemoreceptors determine the respiratory sensitivity of central chemoreceptors to CO₂. *Journal of Physiology-London* **588**, 2455-2471.
- Blanchi B & Sieweke MH. (2005). Mutations of brainstem transcription factors and central respiratory disorders. *Trends in Molecular Medicine* **11**, 23-30.
- Bardi P, de Lalla A, Ambrogio T, Zappella M, Cevenini G, Ceccatelli L, Auteri A & Hayek J. (2007). Rett Syndrome and Plasma Leptin Levels. *The Journal of Pediatrics* **150**, 37-39.
- Bouvier J, Autran S, Dehorter N, Katz DM, Champagnat J, Fortin G & Thoby-Brisson M. (2008). Brain-derived neurotrophic factor enhances fetal respiratory rhythm frequency in the mouse preBotzinger complex in vitro. *Eur J Neurosci* **28**, 510-520.
- Bouvier J, Autran S, Fortin G, Champagnat J & Thoby-Brisson M. (2006). Acute role of the brain-derived neurotrophic factor (BDNF) on the respiratory neural network activity in mice in vitro. *J Physiol Paris* **100**, 290-296.
- Bradley SR, Pieribone VA, Wang W, Severson CA, Jacobs RA & Richerson GB. (2002). Chemosensitive serotonergic neurons are closely associated with large medullary arteries. *Nat Neurosci* **5**, 401-402.
- Braun S, Kottwitz D & Nuber UA. Pharmacological interference with the glucocorticoid system influences symptoms and lifespan in a mouse model of Rett syndrome. *Human Molecular Genetics* **21**, 1673-1680.
- Budden SS & Gunniss ME. (2003). Possible mechanisms of osteopenia in Rett syndrome: Bone histomorphometric studies. *Journal of Child Neurology* **18**, 698-702.

- Cajal SR. (1909). *Histologie du Système Nerveux de l'Homme et des Vertébrés* Maloine, Paris.
- Chahrour M, Jung SY, Shaw C, Zhou X, Wong STC, Qin J & Zoghbi HY. (2008a). MeCP2, a Key Contributor to Neurological Disease, Activates and Represses Transcription. *Science* **320**, 1224-1229.
- Chandler SP, Guschin D, Landsberger N & Wolffe AP. (1999). The methyl-CpG binding transcriptional repressor MeCP2 stably associates with nucleosomal DNA. *Biochemistry* **38**, 7008-7018.
- Chang Q, Khare G, Dani V, Nelson S & Jaenisch R. (2006a). The disease progression of Mecp2 mutant mice is affected by the level of BDNF expression. *Neuron* **49**, 341-348.
- Chapin JL. (1954). Ventilatory response of the unrestrained and unanesthetized hamster to CO₂. *Am J Physiol* **179**, 146-148.
- Chen RZ, Akbarian S, Tudor M & Jaenisch R. (2001). Deficiency of methyl-CpG binding protein-2 in CNS neurons results in a Rett-like phenotype in mice. *Nat Genet* **27**, 327-331.
- Chen WG, Chang Q, Lin Y, Meissner A, West AE, Griffith EC, Jaenisch R & Greenberg ME. (2003). Derepression of BDNF transcription involves calcium-dependent phosphorylation of MeCP2. *Science* **302**, 885-889.
- Cherniack NS, von Euler C, Glogowska M & Homma I. (1981). Characteristics and rate of occurrence of spontaneous and provoked augmented breaths. *Acta Physiol Scand* **111**, 349-360.
- Cirignotta F, Lugaresi E, Montagna P, Opitz JM & Reynolds JF. (1986). Breathing impairment in rett syndrome. *American Journal of Medical Genetics* **25**, 167-173.
- Coates EL, Li AH & Nattie EE. (1993). Widespread Sites of Brain-Stem Ventilatory Chemoreceptors. *Journal of Applied Physiology* **75**, 5-14.
- Collins AL, Levenson JM, Vilaythong AP, Richman R, Armstrong DL, Noebels JL, David Sweatt J & Zoghbi HY. (2004). Mild overexpression of MeCP2 causes a progressive neurological disorder in mice. *Hum Mol Genet* **13**, 2679-2689.
- Considine RV & Caro JF. (1997). Leptin and the regulation of body weight. *Int J Biochem Cell Biol* **29**, 1255-1272.
- Cross KW, Klaus M, Tooley WH & Weisser K. (1960). The response of the newborn baby to inflation of the lungs. *J Physiol* **151**, 551-565.
- Curtis AR, Headland S, Lindsay S, Thomas NS, Boye E, Kamakari S, Roustan P, Anvret M, Wahlstrom J, McCarthy G & et al. (1993). X chromosome linkage studies in familial Rett syndrome. *Hum Genet* **90**, 551-555.

- Dani VS, Chang Q, Maffei A, Turrigiano GG, Jaenisch R & Nelson SB. (2005). Reduced cortical activity due to a shift in the balance between excitation and inhibition in a mouse model of Rett syndrome. *Proc Natl Acad Sci U S A* **102**, 12560-12565.
- Dauger S, Pattyn A, Lofaso F, Gaultier C, Goridis C, Gallego J & Brunet JF. (2003). Phox2b controls the development of peripheral chemoreceptors and afferent visceral pathways. *Development* **130**, 6635-6642.
- De Felice C, Ciccoli L, Leoncini S, Signorini C, Rossi M, Vannuccini L, Guazzi G, Latini G, Comporti M, Valacchi G & Hayek J. (2009). Systemic oxidative stress in classic Rett syndrome. *Free Radical Biology and Medicine* **47**, 440-448.
- De Felice C, Guazzi G, Rossi M, Ciccoli L, Signorini C, Leoncini S, Tonni G, Latini G, Valacchi G & Hayek J. (2010). Unrecognized Lung Disease in Classic Rett Syndrome A Physiologic and High-Resolution CT Imaging Study. *Chest* **138**, 386-392.
- De Felipe C, Herrero JF, O'Brien JA, Palmer JA, Doyle CA, Smith AJ, Laird JM, Belmonte C, Cervero F & Hunt SP. (1998). Altered nociception, analgesia and aggression in mice lacking the receptor for substance P. *Nature* **392**, 394-397.
- Deguchi K, Antalffy BA, Twohill LJ, Chakraborty S, Glaze DG & Armstrong DD. (2000). Substance P immunoreactivity in Rett syndrome. *Pediatr Neurol* **22**, 259-266.
- Del Negro CA, Morgado-Valle C, Hayes JA, Mackay DD, Pace RW, Crowder EA & Feldman JL. (2005). Sodium and calcium current-mediated pacemaker neurons and respiratory rhythm generation. *J Neurosci* **25**, 446-453.
- Ding Y-Q, Marklund U, Yuan W, Yin J, Wegman L, Ericson J, Deneris E, Johnson RL & Chen Z-F. (2003). Lmx1b is essential for the development of serotonergic neurons. *Nat Neurosci* **6**, 933-938.
- Drorbaug JE & Fenn WO. (1955). A BAROMETRIC METHOD FOR MEASURING VENTILATION IN NEWBORN INFANTS. *Pediatrics* **16**, 81-87.
- Dubreuil V, Ramanantsoa N, Trochet D, Vaubourg V, Amiel J, Gallego J, Brunet JF & Goridis C. (2008). A human mutation in Phox2b causes lack of CO₂ chemosensitivity, fatal central apnea, and specific loss of parafacial neurons. *Proc Natl Acad Sci U S A* **105**, 1067-1072.
- Dumas JP, Bardou M, Goirand F & Dumas M. (1999). Hypoxic pulmonary vasoconstriction. *General Pharmacology: The Vascular System* **33**, 289-297.
- Dutschmann M & Herbert H. (2006). The Kolliker-Fuse nucleus gates the postinspiratory phase of the respiratory cycle to control inspiratory off-switch and upper airway resistance in rat. *European Journal of Neuroscience* **24**, 1071-1084.

- Eddahibi S, Fabre V, Boni C, Martres MP, Raffestin B, Hamon M & Adnot S. (1999). Induction of Serotonin Transporter by Hypoxia in Pulmonary Vascular Smooth Muscle Cells. *Circulation Research* **84**, 329-336.
- Eddahibi S, Hanoun N, Lanfumey L, Lesch KP, Raffestin B, Hamon M & Adnot S. (2000). Attenuated hypoxic pulmonary hypertension in mice lacking the 5-hydroxytryptamine transporter gene. *The Journal of Clinical Investigation* **105**, 1555-1562.
- Elian M & Rudolf ND. (1991). EEG and respiration in Rett syndrome. *Acta Neurol Scand* **83**, 123-128.
- Erickson JT, Brosenitsch TA & Katz DM. (2001). Brain-derived neurotrophic factor and glial cell line-derived neurotrophic factor are required simultaneously for survival of dopaminergic primary sensory neurons in vivo. *J Neurosci* **21**, 581-589.
- Erickson JT, Conover JC, Borday V, Champagnat J, Barbacid M, Yancopoulos G & Katz DM. (1996). Mice lacking brain-derived neurotrophic factor exhibit visceral sensory neuron losses distinct from mice lacking NT4 and display a severe developmental deficit in control of breathing. *J Neurosci* **16**, 5361-5371.
- Erickson JT, Shafer G, Rossetti MD, Wilson CG & Deneris ES. (2007). Arrest of 5HT neuron differentiation delays respiratory maturation and impairs neonatal homeostatic responses to environmental challenges. *Respiratory Physiology & Neurobiology* **159**, 85-101.
- Evans JC, Archer HL, Colley JP, Ravn K, Nielsen JB, Kerr A, Williams E, Christodoulou J, Gecz J, Jardine PE, Wright MJ, Pilz DT, Lazarou L, Cooper DN, Sampson JR, Butler R, Whatley SD & Clarke AJ. (2005). Early onset seizures and Rett-like features associated with mutations in CDKL5. *Eur J Hum Genet* **13**, 1113-1120.
- Fantuzzi G & Faggioni R. (2000). Leptin in the regulation of immunity, inflammation, and hematopoiesis. *Journal of Leukocyte Biology* **68**, 437-446.
- Feldman JL & Del Negro CA. (2006). Looking for inspiration: new perspectives on respiratory rhythm. *Nature Reviews Neuroscience* **7**, 232-242.
- Feldman JL, Mitchell GS & Nattie EE. (2003). Breathing: rhythmicity, plasticity, chemosensitivity. *Annu Rev Neurosci* **26**, 239-266.
- Feldman JL & Smith JC. (1989). Cellular mechanisms underlying modulation of breathing pattern in mammals. *Ann N Y Acad Sci* **563**, 114-130.
- Felten DL & Crutcher KA. (1979). Neuronal-vascular relationships in the raphe nuclei, locus coeruleus, and substantia nigra in primates. *The American journal of anatomy* **155**, 467-481.
- Fischer M, Reuter J, Gerich FJ, Hildebrandt B, Hagele S, Katschinski D & Muller M. (2009). Enhanced Hypoxia Susceptibility in Hippocampal Slices From a

- Mouse Model of Rett Syndrome. *Journal of Neurophysiology* **101**, 1016-1032.
- Foltz CJ & Ullman-Cullere M. (1999). Guidelines for assessing the health and condition of mice. *Lab Animal* **28**, 28-32.
- Fortin G & Thoby-Brisson M. (2009). Embryonic emergence of the respiratory rhythm generator. *Respir Physiol Neurobiol* **168**, 86-91.
- Fujii M, Umezawa K & Arata A. (2004). Dopaminergic modulation on respiratory rhythm in rat brainstem-spinal cord preparation. *Neurosci Res* **50**, 355-359.
- Fyffe SL, Neul JL, Samaco RC, Chao HT, Ben-Shachar S, Moretti P, McGill BE, Goulding EH, Sullivan E, Tecott LH & Zoghbi HY. (2008). Deletion of *Mecp2* in *Sim1*-expressing neurons reveals a critical role for MeCP2 in feeding behavior, aggression, and the response to stress. *Neuron* **59**, 947-958.
- Garcia-Suarez O, Perez-Pinera P, Laura R, Germana A, Esteban I, Cabo R, Silos-Santiago I, Cobo JL & Vega JA. (2009). TrkB is necessary for the normal development of the lung. *Respiratory Physiology & Neurobiology* **167**, 281-291.
- Gaultier C, Bissonnette J & Hilaire G. (2008). Possible role of bioaminergic systems in the respiratory disorders of Rett syndrome
Genetic Basis for Respiratory Control Disorders. pp. 271-289. Springer US.
- Gaultier C & Gallego J. (2008). Neural control of breathing: insights from genetic mouse models. *Journal of Applied Physiology* **104**, 1522-1530.
- Gemelli T, Berton O, Nelson ED, Perrotti LI, Jaenisch R & Monteggia LM. (2006). Postnatal loss of methyl-CpG binding protein 2 in the Forebrain is sufficient to mediate behavioral aspects of Rett syndrome in mice. *Biological Psychiatry* **59**, 468-476.
- Gesell R, Bricker J & Magee C. (1936). Structural and functional organization of the central mechanism controlling breathing. *American Journal of Physiology* **117**, 423-452.
- Ghosh A, Carnahan J & Greenberg M. (1994). Requirement for BDNF in activity-dependent survival of cortical neurons. *Science* **263**, 1618-1623.
- Giacometti E, Luikenhuis S, Beard C & Jaenisch R. (2007). Partial rescue of MeCP2 deficiency by postnatal activation of MeCP2. *Proc Natl Acad Sci U S A* **104**, 1931-1936.
- Glogowska M, Richardson PS, Widdicombe JG & Winning AJ. (1972). The role of the vagus nerves, peripheral chemoreceptors and other afferent pathways in the genesis of augmented breaths in cats and rabbits. *Respiration Physiology* **16**, 179-196.

- Goyal M, O'Riordan MA & Wiznitzer M. (2004). Effect of topiramate on seizures and respiratory dysrhythmia in Rett syndrome. *J Child Neurol* **19**, 588-591.
- Gray PA, Janczewski WA, Mellen N, McCrimmon DR & Feldman JL. (2001). Normal breathing requires preBotzinger complex neurokinin-1 receptor-expressing neurons. *Nat Neurosci* **4**, 927-930.
- Gray PA, Rekling JC, Bocchiario CM & Feldman JL. (1999). Modulation of respiratory frequency by peptidergic input to rhythmogenic neurons in the preBotzinger complex. *Science* **286**, 1566-1568.
- Gupta R & Appleton R. (2005). Corticosteroids in the management of the paediatric epilepsies. *Archives of Disease in Childhood* **90**, 379-384.
- Guy J, Gan J, Selfridge J, Cobb S & Bird A. (2007). Reversal of neurological defects in a mouse model of Rett syndrome. *Science* **315**, 1143-1147.
- Guy J, Hendrich B, Holmes M, Martin JE & Bird A. (2001). A mouse Mecp2-null mutation causes neurological symptoms that mimic Rett syndrome. *Nat Genet* **27**, 322-326.
- Guyenet PG, Bayliss DA, Mulkey DK, Stornetta RL, Moreira TS & Takakura AT. (2008). The retrotrapezoid nucleus and central chemoreception. *Adv Exp Med Biol* **605**, 327-332.
- Guyenet PG, Mulkey DK, Stornetta RL & Bayliss DA. (2005a). Regulation of ventral surface chemoreceptors by the central respiratory pattern generator. *J Neurosci* **25**, 8938-8947.
- Guyenet PG, Sevigny CP, Weston MC & Stornetta RL. (2002). Neurokinin-1 receptor-expressing cells of the ventral respiratory group are functionally heterogeneous and predominantly glutamatergic. *Journal of Neuroscience* **22**, 3806-3816.
- Guyenet PG, Stornetta RL, Bayliss DA & Mulkey DK. (2005b). Retrotrapezoid nucleus: a litmus test for the identification of central chemoreceptors. *Exp Physiol* **90**, 247-253; discussion 253-247.
- Haas RH, Dixon SD, Sartoris DJ & Hennessy MJ. (1997). Osteopenia in Rett syndrome. *The Journal of Pediatrics* **131**, 771-774.
- Hagberg B. (1985). Rett's Syndrome: Prevalence and Impact on Progressive Severe Mental Retardation in Girls. *Acta Pædiatrica* **74**, 405-408.
- Hagberg B, Aicardi J, Dias K & Ramos O. (1983). A progressive syndrome of autism, dementia, ataxia, and loss of purposeful hand use in girls: Rett's syndrome: report of 35 cases. *Ann Neurol* **14**, 471-479.
- Hagberg B & Hagberg G. (1997). Rett syndrome: epidemiology and geographical variability. *Eur Child Adolesc Psychiatry* **6 Suppl 1**, 5-7.

- Haldane JS & Priestley JG. (1905). The regulation of the lung-ventilation. *J Physiol* **32**, 225-266.
- Hayashi F & Lipski J. (1992). The role of inhibitory amino acids in control of respiratory motor output in an arterially perfused rat. *Respiration Physiology* **89**, 47-63.
- Hendricks T, Francis N, Fyodorov D & Deneris ES. (1999). The ETS Domain Factor Pet-1 Is an Early and Precise Marker of Central Serotonin Neurons and Interacts with a Conserved Element in Serotonergic Genes. *The Journal of Neuroscience* **19**, 10348-10356.
- Hendricks TJ, Fyodorov DV, Wegman LJ, Lelutiu NB, Pehek EA, Yamamoto B, Silver J, Weeber EJ, Sweatt JD & Deneris ES. (2003). Pet-1 ETS gene plays a critical role in 5-HT neuron development and is required for normal anxiety-like and aggressive behavior. *Neuron* **37**, 233-247.
- Hervé P, Launay J-M, Scrobohaci M-L, Brenot F, Simonneau G, Petitpretz P, Poubeau P, Cerrina J, Duroux P & Drouet L. (1995). Increased plasma serotonin in primary pulmonary hypertension. *The American Journal of Medicine* **99**, 249-254.
- Hikawa S, Kobayashi H, Hikawa N, Kusakabe T, Hiruma H, Takenaka T, Tomita T & Kawakami T. (2002). Expression of neurotrophins and their receptors in peripheral lung cells of mice. *Histochemistry and Cell Biology* **118**, 51-58.
- Hilaire G. (2006). Endogenous noradrenaline affects the maturation and function of the respiratory network: Possible implication for SIDS. *Autonomic Neuroscience-Basic & Clinical* **126**, 320-331.
- Hilaire G, Monteau R & Errchidi S. (1989). Possible Modulation of the Medullary Respiratory Rhythm Generator by the Noradrenergic-A5 Area - an Invitro Study in the Newborn Rat. *Brain Res* **485**, 325-332.
- Hilaire G, Monteau R, Gauthier P, Rega P & Morin D. (1990). Functional significance of the dorsal respiratory group in adult and newborn rats: in vivo and in vitro studies. *Neuroscience Letters* **111**, 133-138.
- Hilaire G, Viemari JC, Coulon P, Simonneau M & Bevençut M. (2004). Modulation of the respiratory rhythm generator by the pontine noradrenergic A5 and A6 groups in rodents. *Respir Physiol Neurobiol* **143**, 187-197.
- Hislop A & Reid L. (1976). New findings in pulmonary arteries of rats with hypoxia-induced pulmonary hypertension. *Br J Exp Pathol* **57**, 542-554.
- Hodges MR & Richerson GB. (2008). Contributions of 5-HT neurons to respiratory control: neuromodulatory and trophic effects. *Respir Physiol Neurobiol* **164**, 222-232.
- Hodges MR, Wehner M, Aungst J, Smith JC & Richerson GB. (2009). Transgenic Mice Lacking Serotonin Neurons Have Severe Apnea and High Mortality during Development. *Journal of Neuroscience* **29**, 10341-10349.

- Holtman JR, Jr. (1988). Immunohistochemical localization of serotonin- and substance P-containing fibers around respiratory muscle motoneurons in the nucleus ambiguus of the cat. *Neuroscience* **26**, 169-178.
- Ide S, Itoh M & Goto Y. (2005). Defect in normal developmental increase of the brain biogenic amine concentrations in the mecp2-null mouse. *Neurosci Lett* **386**, 14-17.
- Irvin C & Bates J. (2003). Measuring the lung function in the mouse: the challenge of size. *Respiratory Research* **4**, 4.
- Iturriaga R, Larrañán C & Zapata P. (1994). Effects of dopaminergic blockade upon carotid chemosensory activity and its hypoxia-induced excitation. *Brain Res* **663**, 145-154.
- Jacobs BL & Fornal CA. (1991). Activity of brain serotonergic neurons in the behaving animal. *Pharmacol Rev* **43**, 563-578.
- Jacquin TD, Borday V, SchneiderMaunoury S, Topilko P, Ghilini G, Kato F, Charnay P & Champagnat J. (1996). Reorganization of pontine rhythmogenic neuronal networks in Krox-20 knockout mice. *Neuron* **17**, 747-758.
- Janczewski WA & Feldman JL. (2006). Distinct rhythm generators for inspiration and expiration in the juvenile rat. *J Physiol* **570**, 407-420.
- Janczewski WA, Onimaru H, Homma I & Feldman JL. (2002). Opioid-resistant respiratory pathway from the preinspiratory neurones to abdominal muscles: in vivo and in vitro study in the newborn rat. *J Physiol* **545**, 1017-1026.
- Johnson SM, Koshiya N & Smith JC. (2001). Isolation of the kernel for respiratory rhythm generation in a novel preparation: The pre-Botzinger complex "island". *Journal of Neurophysiology* **85**, 1772-1776.
- Johnson SM, Smith JC & Feldman JL. (1996). Modulation of respiratory rhythm in vitro: role of Gi/o protein-mediated mechanisms. *Journal of Applied Physiology* **80**, 2120-2133.
- Johnston MV, Jeon OH, Pevsner J, Blue ME & Naidu S. (2001). Neurobiology of Rett syndrome: a genetic disorder of synapse development. *Brain Dev* **23 Suppl 1**, S206-213.
- Jones PL, Veenstra GJC, Wade PA, Vermaak D, Kass SU, Landsberger N, Strouboulis J & Wolffe AP. (1998). Methylated DNA and MeCP2 recruit histone deacetylase to repress transcription. *Nature Genetics* **19**, 187-191.
- Julu POO, Kerr AM, Apartopoulos F, Al-Rawas S, Engerstrom IW, Engerstrom L, Jamal GA & Hansen S. (2001). Characterisation of breathing and associated central autonomic dysfunction in the Rett disorder. *Archives of Disease in Childhood* **85**, 29-37.

- Kachidian P, Poulat P, Marlier L & Privat A. (1991). Immunohistochemical evidence for the coexistence of substance P, thyrotropin-releasing hormone, GABA, methionine-enkephalin, and leucin-enkephalin in the serotonergic neurons of the caudal raphe nuclei: a dual labeling in the rat. *J Neurosci Res* **30**, 521-530.
- Katz DM. (2005). Regulation of respiratory neuron development by neurotrophic and transcriptional signaling mechanisms. *Respir Physiol Neurobiol* **149**, 99-109.
- Katz DM & Balkowiec A. (1997). New insights into the ontogeny of breathing from genetically engineered mice. *Curr Opin Pulm Med* **3**, 433-439.
- Kerr AM, Armstrong DD, Prescott RJ, Doyle D & Kearney DL. (1997). Rett syndrome: analysis of deaths in the British survey. *Eur Child Adolesc Psychiatry* **6 Suppl 1**, 71-74.
- Kerr B, Alvarez-Saavedra Ma, SÃ¡ez MA, Saona A & Young JI. (2008). Defective body-weight regulation, motor control and abnormal social interactions in *Mecp2* hypomorphic mice. *Human Molecular Genetics* **17**, 1707-1717.
- Kishi N & Macklis JD. (2004). MECP2 is progressively expressed in post-migratory neurons and is involved in neuronal maturation rather than cell fate decisions. *Molecular and Cellular Neuroscience* **27**, 306-321.
- Kleefstra T, Yntema HG, Oudakker AR, Romein T, Sistermans E, Nillessen W, Van Bokhoven H, De Vries BBA & Hamel BCJ. (2002). De novo MECP2 frameshift mutation in a boy with moderate mental retardation, obesity and gynaecomastia. *Clinical Genetics* **61**, 359-362.
- Kosai, Kusaga, Isagai, Hirata, S N, Y M, T T, S T & T M. (2005). 58. Rett Syndrome Is Reversible and Treatable by MeCP2 Gene Therapy into the Striatum in Mice. *Mol Ther* **11**, 24-24.
- Krause KL, Forster HV, Davis SE, Kiner T, Bonis JM, Pan LG & Qian B. (2009). Focal acidosis in the pre-Botzinger complex area of awake goats induces a mild tachypnea. *J Appl Physiol* **106**, 241-250.
- Kron M, Zimmermann JL, Dutschmann M, Funke F & Muller M. (2011). Altered responses of MeCP2-deficient mouse brain stem to severe hypoxia. *Journal of Neurophysiology* **105**, 3067-3079.
- Lahiri S, Mokashi A, Mulligan E & Nishino T. (1981). Comparison of aortic and carotid chemoreceptor responses to hypercapnia and hypoxia. *Journal of Applied Physiology* **51**, 55-61.
- Lalley PM. (2008). Opioidergic and dopaminergic modulation of respiration. *Respir Physiol Neurobiol* **164**, 160-167.
- Lalley PM, Bischoff AM & Richter DW. (1994). Serotonin 1A-receptor activation suppresses respiratory apneusis in the cat. *Neurosci Lett* **172**, 59-62.

- Lalley PM, Bischoff AM, Schwarzacher SW & Richter DW. (1995). 5-HT₂ receptor-controlled modulation of medullary respiratory neurones in the cat. *J Physiol* **487** (Pt 3), 653-661.
- Lang M, Wither RG, Brotchie JM, Wu CP, Zhang L & Eubanks JH. (2013). Selective preservation of MeCP2 in catecholaminergic cells is sufficient to improve the behavioral phenotype of male and female *Mecp2*-deficient mice. *Human Molecular Genetics* **22**, 358-371.
- Lawson EE, Waldrop TG & Eldridge FL. (1979). Naloxone enhances respiratory output in cats. *J Appl Physiol* **47**, 1105-1111.
- Lee SL, Wang WW, Lanzillo JJ & Fanburg BL. (1994). SEROTONIN PRODUCES BOTH HYPERPLASIA AND HYPERTROPHY OF BOVINE PULMONARY-ARTERY SMOOTH-MUSCLE CELLS IN CULTURE. *American Journal of Physiology* **266**, L46-L52.
- Legallois M. (1813). *Experiments on the Principles of Life*. Thomas, Philadelphia.
- Leonard H, Thomson M, Bower C, Fyfe S & Constantinou J. (1995). Skeletal abnormalities in Rett syndrome: Increasing evidence for dysmorphogenetic defects. *American Journal of Medical Genetics* **58**, 282-285.
- Li A, Randall M & Nattie EE. (1999). CO₂ microdialysis in retrotrapezoid nucleus of the rat increases breathing in wakefulness but not in sleep. *Journal of Applied Physiology* **87**, 910-919.
- Liu YY, Ju G & Wong-Riley MT. (2001). Distribution and colocalization of neurotransmitters and receptors in the pre-Botzinger complex of rats. *J Appl Physiol* **91**, 1387-1395.
- Loeschcke HH. (1982). Central chemosensitivity and the reaction theory. *J Physiol* **332**, 1-24.
- Luikenhuis S, Giacometti E, Beard CF & Jaenisch R. (2004). Expression of MeCP2 in postmitotic neurons rescues Rett syndrome in mice. *Proc Natl Acad Sci U S A* **101**, 6033-6038.
- Lumsden T. (1923). Observations on the respiratory centres in the cat. *Journal of Physiology-London* **57**, 153-160.
- MacLean MR, Deuchar GA, Hicks MN, Morecroft I, Shen S, Sheward J, Colston J, Loughlin L, Nilsen M, Dempsey Y & Harmar A. (2004). Overexpression of the 5-Hydroxytryptamine Transporter Gene. *Circulation* **109**, 2150-2155.
- Malan A. (1973). Ventilation measured by body plethysmography in hibernating mammals and in poikilotherms. *Respiration Physiology* **17**, 32-44.
- Marcos E, Adnot S, Pham MH, Nosjean A, Raffestin B, Hamon M & Eddahibi S. (2003). Serotonin Transporter Inhibitors Protect against Hypoxic Pulmonary Hypertension. *American Journal of Respiratory and Critical Care Medicine* **168**, 487-493.

- Marcus CL, Carroll JL, McColley SA, Loughlin GM, Curtis S, Pyzik P & Naidu S. (1994). Polysomnographic characteristics of patients with Rett syndrome. *J Pediatr* **125**, 218-224.
- Marder E & Calabrese RL. (1996). Principles of rhythmic motor pattern generation. *Physiol Rev* **76**, 687-717.
- Matsuishi T, Nagamitsu S, Yamashita Y, Murakami Y, Kimura A, Sakai T, Shoji H, Kato H & Percy AK. (1997). Decreased cerebrospinal fluid levels of substance P in patients with Rett syndrome. *Ann Neurol* **42**, 978-981.
- McGill BE, Bundle SF, Yaylaoglu MB, Carson JP, Thaller C & Zoghbi HY. (2006). Enhanced anxiety and stress-induced corticosterone release are associated with increased Crh expression in a mouse model of Rett syndrome. *Proc Natl Acad Sci U S A* **103**, 18267-18272.
- McGraw CM, Samaco RC & Zoghbi HY. (2011). Adult Neural Function Requires MeCP2. *Science* **333**, 186-186.
- McKay LC & Feldman JL. (2008). Unilateral ablation of pre-Botzinger complex disrupts breathing during sleep but not wakefulness. *Am J Respir Crit Care Med* **178**, 89-95.
- McKay LC, Janczewski WA & Feldman JL. (2005). Sleep-disordered breathing after targeted ablation of preBotzinger complex neurons. *Nat Neurosci* **8**, 1142-1144.
- Mellen NM, Janczewski WA, Bocchiaro CM & Feldman JL. (2003). Opioid-induced quantal slowing reveals dual networks for respiratory rhythm generation. *Neuron* **37**, 821-826.
- Mencarelli MA, Spanhol-Rosseto A, Artuso R, Rondinella D, De Filippis R, Bahi-Buisson N, Nectoux J, Rubinsztajn R, Bienvenu T, Moncla A, Chabrol B, Villard L, Krumina Z, Armstrong J, Roche A, Pineda M, Gak E, Mari F, Ariani F & Renieri A. (2010). Novel FOXP1 mutations associated with the congenital variant of Rett syndrome. *Journal of Medical Genetics* **47**, 49-53.
- Miescher-Rusch F. (1885). Bemerkungen zur Lehre von der Athembewegungen *Arch Anat Physiol Physiol Abt* **6**.
- Minh VCN, Du F, Felice CA, Shan XW, Nigam A, Mandel G, Robinson JK & Ballas N. (2012). MeCP2 Is Critical for Maintaining Mature Neuronal Networks and Global Brain Anatomy during Late Stages of Postnatal Brain Development and in the Mature Adult Brain. *Journal of Neuroscience* **32**, 10021-10034.
- Mironov S. (2009). Respiratory Circuits: Function, Mechanisms, Topology, and Pathology. *Neuroscientist* **15**, 194-208.
- Mironov SL & Langohr K. (2005). Mechanisms of Na⁺ and Ca²⁺ influx into respiratory neurons during hypoxia. *Neuropharmacology* **48**, 1056-1065.

- Morin X, Cremer H, Hirsch M-R, Kapur RP, Goridis C & Brunet J-Fo. (1997). Defects in Sensory and Autonomic Ganglia and Absence of Locus Coeruleus in Mice Deficient for the Homeobox Gene *Phox2a*. *Neuron* **18**, 411-423.
- Mortola JP. (2001). *Respiratory Physiology of Newborn Mammals: A Comparative Perspective* The John Hopkins University Press, Baltimore, Maryland.
- Motil KJ, Schultz RJ, Abrams S, Ellis KJ & Glaze DG. (2006). Fractional calcium absorption is increased in girls with Rett syndrome. *Journal of Pediatric Gastroenterology and Nutrition* **42**, 419-426.
- Mulkey DK, Rosin DL, West G, Takakura AC, Moreira TS, Bayliss DA & Guyenet PG. (2007). Serotonergic neurons activate chemosensitive retrotrapezoid nucleus neurons by a pH-independent mechanism. *J Neurosci* **27**, 14128-14138.
- Mulkey DK, Stornetta RL, Weston MC, Simmons JR, Parker A, Bayliss DA & Guyenet PG. (2004). Respiratory control by ventral surface chemoreceptor neurons in rats. *Nat Neurosci* **7**, 1360-1369.
- Nagarajan N, Quast C, Boxall AR, Shahid M & Rosenmund C. (2001). Mechanism and impact of allosteric AMPA receptor modulation by the ampakine CX546. *Neuropharmacology* **41**, 650-663.
- Nan X, Ng HH, Johnson CA, Laherty CD, Turner BM, Eisenman RN & Bird A. (1998). Transcriptional repression by the methyl-CpG-binding protein MeCP2 involves a histone deacetylase complex. *Nature* **393**, 386-389.
- Nan XS, Tate P, Li E & Bird A. (1996). DNA methylation specifies chromosomal localization of MeCP2. *Molecular and Cellular Biology* **16**, 414-421.
- Nattie E. (2006). Why do we have both peripheral and central chemoreceptors? *Journal of Applied Physiology* **100**, 9-10.
- Nuber UA, Kriaucionis S, Roloff TC, Guy J, Selfridge J, Steinhoff C, Schulz R, Lipkowitz B, Ropers HH, Holmes MC & Bird A. (2005). Up-regulation of glucocorticoid-regulated genes in a mouse model of Rett syndrome. *Human Molecular Genetics* **14**, 2247-2256.
- O'Connor RD, Zayzafoon M, Farach-Carson MC & Schanen NC. (2009). *Mecp2* deficiency decreases bone formation and reduces bone volume in a rodent model of Rett syndrome. *Bone* **45**, 346-356.
- Ogier M & Katz DM. (2008). Breathing dysfunction in Rett syndrome: understanding epigenetic regulation of the respiratory network. *Respir Physiol Neurobiol* **164**, 55-63.
- Ogier M, Wang H, Hong E, Wang Q, Greenberg ME & Katz DM. (2007). Brain-derived neurotrophic factor expression and respiratory function improve after ampakine treatment in a mouse model of Rett syndrome. *J Neurosci* **27**, 10912-10917.

- Onimaru H & Homma I. (2003). A novel functional neuron group for respiratory rhythm generation in the ventral medulla. *J Neurosci* **23**, 1478-1486.
- Onimaru H & Homma I. (2008). Two modes of respiratory rhythm generation in the newborn rat brainstem-spinal cord preparation. *Adv Exp Med Biol* **605**, 104-108.
- Onimaru H, Ikeda K & Kawakami K. (2008). CO₂-Sensitive Preinspiratory Neurons of the Parafacial Respiratory Group Express Phox2b in the Neonatal Rat. *Journal of Neuroscience* **28**, 12845-12850.
- Onimaru H, Shamoto A & Homma I. (1998). Modulation of respiratory rhythm by 5-HT in the brainstem-spinal cord preparation from newborn rat. *Pflugers Arch* **435**, 485-494.
- Patroniti N, Foti G, Cortinovis B, Maggioni E, Bigatello LM, Cereda M & Pesenti A. (2002). Sigh improves gas exchange and lung volume in patients with acute respiratory distress syndrome undergoing pressure support ventilation. *Anesthesiology* **96**, 788-794.
- Paxinos G & Franklin K. (2001). *The Mouse Brain in Stereotaxic Coordinates, Deluxe Second Edition (with CD-ROM)*. {Academic Press}.
- Pena F & Ramirez JM. (2002). Endogenous activation of serotonin-2A receptors is required for respiratory rhythm generation in vitro. *J Neurosci* **22**, 11055-11064.
- Pitt BR, Weng WL, Steve AR, Blakely RD, Reynolds I & Davies P. (1994). Serotonin Increases DNA-Synthesis in Rat Proximal and Distal Pulmonary Vascular Smooth-Muscle Cells in Culture. *American Journal of Physiology* **266**, L178-L186.
- Ptak K, Burnet H, Blanchi B, Sieweke M, De Felipe C, Hunt SP, Monteau R & Hilaire G. (2002). The murine neurokinin NK1 receptor gene contributes to the adult hypoxic facilitation of ventilation. *Eur J Neurosci* **16**, 2245-2252.
- Ptak K, Yamanishi T, Aungst J, Milescu LS, Zhang R, Richerson GB & Smith JC. (2009). Raphe neurons stimulate respiratory circuit activity by multiple mechanisms via endogenously released serotonin and substance P. *J Neurosci* **29**, 3720-3737.
- Putnam RW, Filosa JA & Ritucci NA. (2004). Cellular mechanisms involved in CO₂ and acid signaling in chemosensitive neurons. *Am J Physiol Cell Physiol* **287**, C1493-1526.
- Qureshi M, Khalil M, Kwiatkowski K & Alvaro RE. (2009). Morphology of sighs and their role in the control of breathing in preterm infants, term infants and adults. *Neonatology* **96**, 43-49.
- Ramocki MB, Tavyev YJ & Peters SU. (2010). The MECP2 Duplication Syndrome. *American Journal of Medical Genetics Part A* **152A**, 1079-1088.

- Reichardt HM & Schütz G. (1998). Glucocorticoid signalling-multiple variations of a common theme. *Molecular and Cellular Endocrinology* **146**, 1-6.
- Rekling JC & Feldman JL. (1998). PreBotzinger complex and pacemaker neurons: hypothesized site and kernel for respiratory rhythm generation. *Annu Rev Physiol* **60**, 385-405.
- Ren J, Ding XQ, Funk GD & Greer JJ. (2012). Anxiety-Related Mechanisms of Respiratory Dysfunction in a Mouse Model of Rett Syndrome. *Journal of Neuroscience* **32**, 17230-17240.
- Reynolds LB. (1962). Characteristics of an inspiration-augmenting reflex in anesthetized cats. *Journal of Applied Physiology* **17**, 683-688.
- Ricci A, Felici L, Mariotta S, Mannino F, Schmid G, Terzano C, Cardillo G, Amenta F & Bronzetti E. (2004). Neurotrophin and Neurotrophin Receptor Protein Expression in the Human Lung. *American Journal of Respiratory Cell and Molecular Biology* **30**, 12-19.
- Richerson GB. (1995b). Response to CO₂ of neurons in the rostral ventral medulla in vitro. *Journal of Neurophysiology* **73**, 933-944.
- Richerson GB. (2004). Serotonergic neurons as carbon dioxide sensors that maintain pH homeostasis. *Nat Rev Neurosci* **5**, 449-461.
- Richter DW. (1996). *Neural regulation of respiration: Rhythmogenesis and afferent control*. Springer-Verlag; Springer-Verlag New York, Inc.
- Richter DW, Manzke T, Wilken B & Ponimaskin E. (2003). Serotonin receptors: guardians of stable breathing. *Trends in Molecular Medicine* **9**, 542-548.
- Riederer P, Brucke T, Sofic E, Kienzl E, Schnecker K, Schay V, Kruzik P, Killian W & Rett A. (1985). Neurochemical aspects of the Rett syndrome. *Brain Dev* **7**, 351-360.
- Riederer P, Weiser M, Wichart I, Schmidt B, Killian W & Rett A. (1986). Preliminary brain autopsy findings in progredient Rett syndrome. *Am J Med Genet Suppl* **1**, 305-315.
- Robinson L, Guy J, McKay L, Brockett E, Spike RC, Selfridge J, De Sousa D, Merusi C, Riedel G, Bird A & Cobb SR. (2012). Morphological and functional reversal of phenotypes in a mouse model of Rett syndrome. *Brain*.
- Roende G, Ravn K, Fuglsang K, Andersen H, Nielsen JB, Brondum-Nielsen K & Jensen JEB. (2011). DXA Measurements in Rett Syndrome Reveal Small Bones With Low Bone Mass. *Journal of Bone and Mineral Research* **26**, 2280-2286.
- Rohdin M, Fernell E, Eriksson M, Albage M, Lagercrantz H & Katz-Salamon M. (2007). Disturbances in cardiorespiratory function during day and night in Rett syndrome. *Pediatric Neurology* **37**, 338-344.
- Rolando S. (1985). Rett syndrome: report of eight cases. *Brain Dev* **7**, 290-296.

- Roux J-C, Dura E & Villard L. (2008). Tyrosine hydroxylase deficit in the chemoafferent and the sympathoadrenergic pathways of the *Mecp2* deficient mouse. *Neuroscience Letters* **447**, 82-86.
- Roux JC, Dura E, Moncla A, Mancini J & Villard L. (2007). Treatment with desipramine improves breathing and survival in a mouse model for Rett syndrome. *Eur J Neurosci* **25**, 1915-1922.
- Roux JC, Panayotis N, Dura E & Villard L. (2010). Progressive Noradrenergic Deficits in the Locus Coeruleus of *Mecp2* Deficient Mice. *Journal of Neuroscience Research* **88**, 1500-1509.
- Samaco RC, Fryer JD, Ren J, Fyffe S, Chao HT, Sun YL, Greer JJ, Zoghbi HY & Neul JL. (2008). A partial loss of function allele of Methyl-CpG-binding protein 2 predicts a human neurodevelopmental syndrome. *Human Molecular Genetics* **17**, 1718-1727.
- Samaco RC, Hogart A & LaSalle JM. (2005). Epigenetic overlap in autism-spectrum neurodevelopmental disorders: MECP2 deficiency causes reduced expression of UBE3A and GABRB3. *Hum Mol Genet* **14**, 483-492.
- Samaco RC, Mandel-Brehm C, Chao HT, Ward CS, Fyffe-Maricich SL, Ren J, Hyland K, Thaller C, Maricich SM, Humphreys P, Greer JJ, Percy A, Glaze DG, Zoghbi HY & Neul JL. (2009). Loss of MeCP2 in aminergic neurons causes cell-autonomous defects in neurotransmitter synthesis and specific behavioral abnormalities. *Proc Natl Acad Sci U S A* **106**, 21966-21971.
- Samaco RC & Neul JL. (2011). Complexities of Rett syndrome and MeCP2. *J Neurosci* **31**, 7951-7959.
- Sansom D, Krishnan VHR, Corbett J & Kerr A. (1993). Emotional and Behavioral-Aspects of Rett Syndrome. *Developmental Medicine and Child Neurology* **35**, 340-345.
- Santhanam AVR, Smith LA & Katusic ZS. Brain-Derived Neurotrophic Factor Stimulates Production of Prostacyclin in Cerebral Arteries / Supplemental Data. *Stroke* **41**, 350-356.
- Sapru HN & Krieger AJ. (1977). Carotid and aortic chemoreceptor function in the rat. *Journal of Applied Physiology* **42**, 344-348.
- Schanen NC, Dahle EJ, Capozzoli F, Holm VA, Zoghbi HY & Francke U. (1997). A new Rett syndrome family consistent with X-linked inheritance expands the X chromosome exclusion map. *Am J Hum Genet* **61**, 634-641.
- Schneider-Maunoury S, Topilko P, Seitanidou T, Levi G, Cohen-Tannoudji M, Pournin S, Babinet C & Charnay P. (1993). Disruption of *Krox-20* results in alteration of rhombomeres 3 and 5 in the developing hindbrain. *Cell* **75**, 1199-1214.
- Sciesielski LK, Paliege A, Martinka P & Scholz H. (2009). Enhanced pulmonary expression of the TrkB neurotrophin receptor in hypoxic rats is associated

with increased acetylcholine-induced airway contractility. *Acta Physiologica* **197**, 253-264.

- Shahbazian M, Young J, Yuva-Paylor L, Spencer C, Antalffy B, Noebels J, Armstrong D, Paylor R & Zoghbi H. (2002a). Mice with truncated MeCP2 recapitulate many Rett syndrome features and display hyperacetylation of histone H3. *Neuron* **35**, 243-254.
- Shahbazian MD, Antalffy B, Armstrong DL & Zoghbi HY. (2002b). Insight into Rett syndrome: MeCP2 levels display tissue- and cell-specific differences and correlate with neuronal maturation. *Hum Mol Genet* **11**, 115-124.
- Shahbazian MD & Zoghbi HY. (2001). Molecular genetics of Rett syndrome and clinical spectrum of MECP2 mutations. *Curr Opin Neurol* **14**, 171-176.
- Shao XM & Feldman JL. (1997). Respiratory rhythm generation and synaptic inhibition of expiratory neurons in pre-Botzinger complex: differential roles of glycinergic and GABAergic neural transmission. *J Neurophysiol* **77**, 1853-1860.
- Skene PJ, Illingworth RS, Webb S, Kerr ARW, James KD, Turner DJ, Andrews R & Bird AP. (2010). Neuronal MeCP2 Is Expressed at Near Histone-Octamer Levels and Globally Alters the Chromatin State. *Molecular Cell* **37**, 457-468.
- Smith JC, Abdala AP, Rybak IA & Paton JF. (2009). Structural and functional architecture of respiratory networks in the mammalian brainstem. *Philos Trans R Soc Lond B Biol Sci* **364**, 2577-2587.
- Smith JC, Ellenberger HH, Ballanyi K, Richter DW & Feldman JL. (1991). Pre-Botzinger complex: a brainstem region that may generate respiratory rhythm in mammals. *Science* **254**, 726-729.
- Smith JC, Morrison DE, Ellenberger HH, Otto MR & Feldman JL. (1989). Brainstem projections to the major respiratory neuron populations in the medulla of the cat. *J Comp Neurol* **281**, 69-96.
- Southall DP, Kerr AM, Tirosh E, Amos P, Lang MH & Stephenson JB. (1988). Hyperventilation in the awake state: potentially treatable component of Rett syndrome. *Archives of Disease in Childhood* **63**, 1039-1048.
- Spitzer NC, Kingston PA, Manning TJ & Conklin MW. (2002). Outside and in: development of neuronal excitability. *Curr Opin Neurobiol* **12**, 315-323.
- Stettner GM, Huppke P, Brendel C, Richter DW, Gartner J & Dutschmann M. (2007). Breathing dysfunctions associated with impaired control of postinspiratory activity in Mecp2-/-y knockout mice. *J Physiol* **579**, 863-876.
- Stettner GM, Zanella Sb, Huppke P, Gartner J, Hilaire Gr & Dutschmann M. (2008). Spontaneous central apneas occur in the C57BL/6J mouse strain. *Respiratory Physiology & Neurobiology* **160**, 21-27.

- Stornetta RL, Moreira TS, Takakura AC, Kang BJ, Chang DA, West GH, Brunet JF, Mulkey DK, Bayliss DA & Guyenet PG. (2006). Expression of Phox2b by brainstem neurons involved in chemosensory integration in the adult rat. *J Neurosci* **26**, 10305-10314.
- Stornetta RL, Rosin DL, Wang H, Sevigny CP, Weston MC & Guyenet PG. (2003). A group of glutamatergic interneurons expressing high levels of both neurokinin-1 receptors and somatostatin identifies the region of the pre-Botzinger complex. *Journal of Comparative Neurology* **455**, 499-512.
- Sun YE & Wu H. (2006). The ups and downs of BDNF in Rett syndrome. *Neuron* **49**, 321-323.
- Swanson LW. (1976). The locus coeruleus: A cytoarchitectonic, golgi and immunohistochemical study in the albino rat. *Brain Res* **110**, 39-56.
- Takakura AC, Moreira TS, Colombari E, West GH, Stornetta RL & Guyenet PG. (2006). Peripheral chemoreceptor inputs to retrotrapezoid nucleus (RTN) CO₂-sensitive neurons in rats. *J Physiol* **572**, 503-523.
- Tankersley CG, Fitzgerald RS & Kleeberger SR. (1994). Differential control of ventilation among inbred strains of mice. *American Journal of Physiology - Regulatory, Integrative and Comparative Physiology* **267**, R1371-R1377.
- Thoby-Brisson M, Cauli B, Champagnat J, Fortin G & Katz DM. (2003). Expression of functional tyrosine kinase B receptors by rhythmically active respiratory neurons in the pre-Botzinger complex of neonatal mice. *Journal of Neuroscience* **23**, 7685-7689.
- Thoby-Brisson M & Ramirez JM. (2001). Identification of two types of inspiratory pacemaker neurons in the isolated respiratory neural network of mice. *J Neurophysiol* **86**, 104-112.
- Thoby-Brisson M, Trinh JB, Champagnat J & Fortin G. (2005). Emergence of the pre-Botzinger respiratory rhythm generator in the mouse embryo. *J Neurosci* **25**, 4307-4318.
- TUDER RM, COOL CD, GERACI MW, WANG J, ABMAN SH, WRIGHT L, BADESCH D & VOELKEL NF. (1999). Prostacyclin Synthase Expression Is Decreased in Lungs from Patients with Severe Pulmonary Hypertension. *American Journal of Respiratory and Critical Care Medicine* **159**, 1925-1932.
- Viemari JC, Bevengut M, Burnet H, Coulon P, Pequignot JM, Tiveron MC & Hilaire G. (2004). Phox2a gene, A6 neurons, and noradrenaline are essential for development of normal respiratory rhythm in mice. *Journal of Neuroscience* **24**, 928-937.
- Viemari JC, Roux JC, Tryba AK, Saywell V, Burnet H, Pena F, Zanella S, Bevengut M, Barthelemy-Requin M, Herzing LB, Moncla A, Mancini J, Ramirez JM, Villard L & Hilaire G. (2005). Mecp2 deficiency disrupts norepinephrine and respiratory systems in mice. *J Neurosci* **25**, 11521-11530.

- Voituron N & Hilaire G. (2011). The benzodiazepine Midazolam mitigates the breathing defects of *Mecp2*-deficient mice. *Respiratory Physiology & Neurobiology* **177**, 56-60.
- Voituron N, Zanella S, Menuet C, Dutschmann M & Hilaire G. (2009). Early breathing defects after moderate hypoxia or hypercapnia in a mouse model of Rett syndrome. *Respir Physiol Neurobiol* **168**, 109-118.
- Voituron N, Zanella S, Menuet C, Lajard AM, Dutschmann M & Hilaire G. (2010). Early abnormalities of post-sigh breathing in a mouse model of Rett syndrome. *Respir Physiol Neurobiol* **170**, 173-182.
- Voss MD, De Castro D, Lipski J, Pilowsky PM & Jiang C. (1990). Serotonin immunoreactive boutons form close appositions with respiratory neurons of the dorsal respiratory group in the cat. *J Comp Neurol* **295**, 208-218.
- Wade PA. (2004). Dynamic regulation of DNA methylation coupled transcriptional repression: BDNF regulation by MeCP2. *BioEssays* **26**, 217-220.
- Wan M, Lee SS, Zhang X, Houwink-Manville I, Song HR, Amir RE, Budden S, Naidu S, Pereira JL, Lo IF, Zoghbi HY, Schanen NC & Francke U. (1999). Rett syndrome and beyond: recurrent spontaneous and familial MECP2 mutations at CpG hotspots. *Am J Hum Genet* **65**, 1520-1529.
- Wang H, Chan SA, Ogier M, Hellard D, Wang Q, Smith C & Katz DM. (2006). Dysregulation of brain-derived neurotrophic factor expression and neurosecretory function in *Mecp2* null mice. *J Neurosci* **26**, 10911-10915.
- Wang W, Tiwari JK, Bradley SR, Zaykin RV & Richerson GB. (2001). Acidosis-stimulated neurons of the medullary raphe are serotonergic. *J Neurophysiol* **85**, 2224-2235.
- Ward CS, Arvide EM, Huang TW, Yoo J, Noebels JL & Neul JL. (2011). MeCP2 Is Critical within HoxB1-Derived Tissues of Mice for Normal Lifespan. *Journal of Neuroscience* **31**, 10359-10370.
- Ward NL, Moore E, Noon K, Spassil N, Keenan E, Ivanco TL & LaManna JC. (2007). Cerebral angiogenic factors, angiogenesis, and physiological response to chronic hypoxia differ among four commonly used mouse strains. *Journal of Applied Physiology* **102**, 1927-1935.
- Weaving LS, Christodoulou J, Williamson SL, Friend KL, McKenzie OL, Archer H, Evans J, Clarke A, Pelka GJ, Tam PP, Watson C, Lahooti H, Ellaway CJ, Bennetts B, Leonard H & Gecz J. (2004). Mutations of CDKL5 cause a severe neurodevelopmental disorder with infantile spasms and mental retardation. *Am J Hum Genet* **75**, 1079-1093.
- Weese-Mayer DE, Lieske SP, Boothby CM, Kenny AS, Bennett HL, Silvestri JM & Ramirez JM. (2006). Autonomic nervous system dysregulation: Breathing and heart rate perturbation during wakefulness in young girls with Rett syndrome. *Pediatric Research* **60**, 443-449.

- Wenninger JM, Pan LG, Klum L, Leekley T, Bastastic J, Hodges MR, Feroah TR, Davis S & Forster HV. (2004). Large lesions in the pre-Botzinger complex area eliminate eupneic respiratory rhythm in awake goats. *Journal of Applied Physiology* **97**, 1629-1636.
- Wong-Riley MT & Liu Q. (2005). Neurochemical development of brain stem nuclei involved in the control of respiration. *Respir Physiol Neurobiol* **149**, 83-98.
- Yamamoto M, Sobue G, Yamamoto K & Mitsuma T. (1996). Expression of mRNAs for neurotrophic factors (NGF, BDNF, NT-3, and GDNF) and their receptors (p75^{sup} and ngfr, TrkA, TrkB, and TrkC) in the adult human peripheral nervous system and nonneural tissues. *Neurochemical Research* **21**, 929-938.
- Yamamoto Y, Onimaru H & Homma I. (1992). Effect of substance P on respiratory rhythm and pre-inspiratory neurons in the ventrolateral structure of rostral medulla oblongata: an in vitro study. *Brain Res* **599**, 272-276.
- Yamauchi M, Ocak H, Dostal J, Jacono FJ, Loparo KA & Strohl KP. (2008). Post-sigh breathing behavior and spontaneous pauses in the C57BL/6J (B6) mouse. *Respir Physiol Neurobiol* **162**, 117-125.
- Yasui DH, Peddada S, Bieda MC, Vallero RO, Hogart A, Nagarajan RP, Thatcher KN, Farnham PJ & LaSalle JM. (2007). Integrated epigenomic analyses of neuronal MeCP2 reveal a role for long-range interaction with active genes. *Proc Natl Acad Sci U S A* **104**, 19416-19421.
- Young JI, Hong EP, Castle JC, Crespo-Barreto J, Bowman AB, Rose MF, Kang D, Richman R, Johnson JM, Berget S & Zoghbi HY. (2005). Regulation of RNA splicing by the methylation-dependent transcriptional repressor methyl-CpG binding protein 2. *Proc Natl Acad Sci U S A* **102**, 17551-17558.
- Zanella S, Roux JC, Viemari JC & Hilaire G. (2006). Possible modulation of the mouse respiratory rhythm generator by A1/C1 neurones. *Respiratory Physiology & Neurobiology* **153**, 126-138.
- Zanella Sb, Mebarek S, Lajard A-M, Picard N, Dutschmann M & Hilaire Gr. (2008). Oral treatment with desipramine improves breathing and life span in Rett syndrome mouse model. *Respiratory Physiology & Neurobiology* **160**, 116-121.
- Zappella M, Meloni I, Longo I, Hayek G & Renieri A. (2001). Preserved speech variants of the Rett syndrome: molecular and clinical analysis. *Am J Med Genet* **104**, 14-22.
- Zhang XL, Su J, Rojas A & Jiang C. (2010a). Pontine norepinephrine defects in Mecp2-null mice involve deficient expression of dopamine beta-hydroxylase but not a loss of catecholaminergic neurons. *Biochemical and Biophysical Research Communications* **394**, 285-290.

- Zhang XL, Su JD, Cui NR, Gai HY, Wu ZY & Jiang C. (2011). The disruption of central CO₂ chemosensitivity in a mouse model of Rett syndrome. *American Journal of Physiology-Cell Physiology* **301**, C729-C738.
- Zhang ZW, Zak JD & Liu H. (2010b). MeCP2 Is Required for Normal Development of GABAergic Circuits in the Thalamus. *Journal of Neurophysiology* **103**, 2470-2481.
- Zhao ZQ, Scott M, Chiechio S, Wang JS, Renner KJ, Gereau RWt, Johnson RL, Deneris ES & Chen ZF. (2006). Lmx1b is required for maintenance of central serotonergic neurons and mice lacking central serotonergic system exhibit normal locomotor activity. *J Neurosci* **26**, 12781-12788.
- Zoghbi HY, Percy AK, Glaze DG, Butler IJ & Riccardi VM. (1985). Reduction of biogenic amine levels in the Rett syndrome. *N Engl J Med* **313**, 921-924.